

Aus dem Institut für Phytopathologie
Der Christian-Albrechts-Universität zu Kiel

On the Evolution of Quantitative Disease Resistance to Necrotrophic Fungal Pathogens in Solanum species.

Dissertation
Zur Erlangung des Doktorgrades
Der Agrar- und Ernährungswissenschaftlichen Fakultät
der Christian-Albrechts-Universität zu Kiel

vorgelegt von

M. Sc. Severin Johannes Einspanier
aus Freising
Kiel, 2025

Dekan Prof. Dr. Tim Diekötter

1. Berichterstatter: Prof. Dr. Remco Stam
2. Berichterstatter: Prof. Dr. Silvio Waschina

Tag der mündlichen Prüfung: 02. Juli 2025

Veröffentlicht mit Genehmigung der Agrar- und Ernährungswissenschaftlichen Fakultät der
Christian-Albrechts Universität zu Kiel.

Zusammenfassung

Nekrotrophe Pathogene wie der Generalist *Sclerotinia sclerotiorum* stellen weltweit eine Bedrohung für zahlreiche Nutzpflanzen dar. Durch das Fehlen vollständiger Resistenzen sind Züchter auf quantitative Krankheitsresistenz (QDR) angewiesen. Dabei handelt es sich um eine unvollständige, aber breit wirksame Krankheits-Toleranz. Jedoch ist die QDR-Zucht nicht immer hinreichend erfolgreich u.a. aufgrund unbekannter regulatorische Faktoren auf Seiten der Wirtspflanze. Entsprechend ist es von großer Bedeutung, die Regulation von QDR sowie deren Evolution zu verstehen um Züchtungsstrategien zu verbessern.

In dieser Arbeit habe ich die QDR-Diversität wilder Tomatenpopulationen gegenüber *S. sclerotiorum* charakterisiert. Dabei habe ich eine erstaunliche Vielfalt an QDR-Mechanismen, darunter Infektionshäufigkeit, Verzögerungsphase und Läsionsverdopplungszeit (LDT) beobachtet, sowohl zwischen als auch innerhalb der Arten. Mittels Hochdurchsatz-Phänotypisierung konnte ich zudem nachweisen, dass diese drei Parameter unabhängig voneinander sind. Dies könnte darauf hindeuten, dass QDR von unabhängigen biologischen Prozesse beeinflusst wird.

Durch differentielle Genexpressionsanalysen und verschiedene Netzwerkanalysen konnte ich zeigen, dass basale und stark artspezifische genregulatorische Netzwerke (GRNs) die LDT-vermittelte QDR kontrollieren. Dabei beobachtete ich, dass der konservierte Transkriptionsfaktor NAC29 in *Solanum pennellii* eine neue Rolle in der QDR spielt. Obwohl NAC29 in allen fünf untersuchten Arten vorhanden ist, wird dessen Expression nur in *S. pennellii* nach einer Infektion induziert und geht „neue“ Interaktionen mit abwehrrelevanten Zielgenen ein.

Zudem konnte ich zeigen, dass die verlängerte Latenzphase eines resistenten *S. pennellii*-Genotyps durch eine erhöhte basale Genexpression eines WRKY6-assoziierten GRNs sowie von Rezeptorgen bestimmt wird. Diese erhöhte basale Expression könnte eine frühere und gezieltere Abwehrreaktion ermöglichen und so die Infektion verzögern.

Diese Studie zeigt, dass komplexe regulatorische Umstrukturierungen QDR zugrunde liegen, wobei die Dauer der Verzögerungsphase und LDT unabhängig durch den Wirt kontrolliert werden. Evolutionsanalysen verdeutlichen die Rolle von Paralog-Diversifikation in QDR. Es

ist daher naheliegend, dass ähnliche QDR-Niveaus durch die konvergente Evolution solcher Netzwerke entstehen können, vermutlich getrieben durch genetische Drift. Die Einblicke dieser Thesis verbessern unser Verständnis darüber, wie QDR-Mechanismen reguliert werden und unterstützt dabei die Entwicklung von Zucht-Strategien für eine effektivere QDR-Züchtung.

Summary

Generalist necrotrophic pathogens like *Sclerotinia sclerotiorum* threaten many crops worldwide. The absence of complete resistance has driven breeders to rely on quantitative disease resistance (QDR), an incomplete yet broad-range plant defence. However, challenges in linking QDR loci to phenotypes highlight how poorly host regulatory factors are understood. Unravelling the evolution and complexity of QDR networks is crucial for improving resistance breeding strategies. In this thesis, I characterised the QDR diversity of wild tomato populations against *S. sclerotiorum*. I observed an astonishing diversity of the QDR mechanisms, including infection frequency, lag phase duration, and lesion doubling time (LDT), among and within different species. Using high-throughput phenotyping, I found no correlation between either of the three mechanisms, suggesting the existence of independent biological processes determining QDR.

I investigated the shifts in gene expression of genotypes spanning an LDT gradient. Using differential gene expression analysis and different types of network analysis, I observed that basal and highly species-specific gene regulatory networks (GRN) determine LDT-driven QDR. I showed that the conserved NAC29 transcription factor co-opted a role in QDR in *Solanum pennellii*. Although NAC29 is conserved across all five species, it is only induced upon infection in *S. pennellii* and is linked to defence-related downstream genes, indicating GRN rewiring.

Using longitudinal gene expression profiling, I observed prolonged lag-phase duration in an *S. pennellii* genotype which is most likely driven by elevated basal gene expression of a WRKY6-associated GRN and receptor genes. Elevated basal expression might facilitate an earlier and more targeted defence response, delaying fungal infection.

This study demonstrates that complex regulatory rewiring underlies QDR, with lag-phase duration and lesion doubling time (LDT) controlled independently by the host. Evolutionary analysis highlights the role of paralog diversification, followed by lineage-specific co-option into QDR-related gene regulatory networks. I propose that similar levels of QDR may arise through the convergent evolution of these networks, likely driven by genetic drift. These insights improve our understanding of how QDR mechanisms are regulated and evolve, thereby supporting the development of pre-breeding strategies for more effective QDR-focused breeding programs.

Table of content

Zusammenfassung	I
Summary	III
Table of content.....	IV
Acknowledgements	1
Abbreviations	2
Introduction	4
Wild Germplasm as a Source of New Breeding Material	4
Wild Solanum Species	4
The Solanum Species Selected for Analysis	5
Necrotrophic Pathogens Pose a Threat to the Global Food Production	7
<i>Sclerotinia sclerotiorum</i> as a Model for Research	8
Quantitative Disease Resistance Against Generalist Pathogens	8
Gene Network Evolution.....	9
Gene Regulatory Networks: Mapping the Blueprint of Regulatory Complexity.....	10
Mechanisms of Gene Regulatory Network Rewiring	11
The Evolution of GRNs Underlying Complex Traits	11
Aim of this Study	13
Publication 1.....	16
Publication 2.....	44
Publication 3.....	100
General Discussion and Outlook.....	148
QDR Diversity in Wild Pathosystems.....	148
An Extended Model of QDR.....	148

Infection frequency	149
Lag Phase Duration	149
Lesion Growth Rate	150
Implications of the QDR Model	152
The Evolution of QDR-Networks	153
Regulatory Divergence Drives Functional Convergence	153
Paralog Divergence as a Driver of Convergent Evolution	153
Regulatory Divergence, Genetic Drift, and the Emergence of QDR	156
Conclusion.....	157
Implications and Outlook	157
Supplementary Information.....	159
Publication bibliography	160
Declarations of co-authorship	168

Acknowledgements

I would not have been able to complete the work in this thesis without the support of many incredible people.

My deepest gratitude goes to my doctoral advisor, Prof. Dr. Remco Stam, whose guidance and insight shaped this project and my personal and scientific growth. His ingenuity, trust, and the freedom to pursue my ideas allowed me to explore, develop, and thrive. I deeply valued the scientific rigour, constructive criticism, and loyalty throughout our collaboration. My appreciation also belongs to the members of the examiner's board.

I am especially thankful to Dr. Felix Hoheneder, who opened my eyes to the beautiful world of plant pathology. I am very thankful for the years we spent together in the field. I sincerely appreciate Chris, my companion throughout the PhD journey. His intellectual, technical, and emotional support was indispensable; this work would not have been possible without him.

I also thank my office mates and friends, Wilken and Gonne, for countless discussions, shared beers, and open ears. My heartfelt thanks go to Johanna and Hendrik for their fresh perspectives, support through challenging moments, and steadfast friendship. I deeply enjoyed our time together and valued every exchange, scientific or otherwise.

Heartfelt thanks to all the students I had the privilege of working with, especially Lilly and Ellen, whose unwavering support in the greenhouse over the years was invaluable to our group. I'm also grateful to Antonia, Roy, and Gideon for their dedication and tireless help, and to my Master's students Sina, Charlott, Raffael, Swapnil, and Oscar for trusting me as a supervisor, and for the great moments we shared along the way.

Many thanks to all the phyto-colleagues at AG Stam and AC for creating such a supportive and joyful working atmosphere. I especially want to thank Bettina and Susanne for keeping the wet lab running smoothly and for their invaluable help with RNA isolation and other experimental work.

To my family, especially my parents and brother, thank you for your endless support, love, and encouragement throughout my life. I deeply appreciate Hannah, who carried me through the last years, cared for me in every way, and never failed to brighten my days.

Abbreviations

Avr	Avirulence Gene
Cf	<i>Cladosporium fulvum</i> Resistance Gene
cis-elements	non-coding DNA that regulates the transcription of adjacent genes
CWR	Crop Wild Relatives
DAMPs	Damage-Associated Molecular Patterns
dpi	Days past inoculation
GRN	Gene Regulatory Network
hpi	Hours past inoculation
IF	Infection Frequency
LDT	Lesion Doubling Time
MAPK	Mitogen-Activated Protein Kinase
OA	Oxalic acid
PAMPs	Pathogen-Associated Molecular Patterns
PR	Pathogenesis-Related (Protein)
PTI	Pattern-Triggered Immunity
QDR	Quantitative Disease Resistance
R-gene	Resistance Gene (dominant, complete resistance)
RLK	Receptor-Like Kinase
RLP	Receptor-Like Protein
ROS	Reactive Oxygen Species
SNP	Single Nucleotide Polymorphism
TAI	Transcript Age Index
TDI	Transcript Divergence Index
TF	Transcription Factor
TIR-NBS-LRR	Toll/Interleukin-1 Receptor-Nucleotide-Binding Site-Leucine-Rich Repeat (Resistance Protein Class)
trans-elements	coding DNA sequences for upstream regulatory genes (TFs)
WGCNA	Weighted Gene Co-expression Network Analysis
WRKY	WRKY Transcription Factor Family



Introduction

Introduction

The domestication of crop plants is a central component of human development and is widely considered a cultural achievement (Purugganan and Fuller 2009). Ever since, the optimisation of crop properties has been the main goal of plant breeders, aiming to increase productivity, flavour, shelf life, nutritional value, or suitability in production systems (such as synchronous ripening or inhibition of seed shattering, Purugganan and Fuller 2009). One major aspect of plant breeding is the development of germplasm that resists many environmental stresses, like abiotic stresses (e.g., drought or salt stress), but also against biotic stresses: plant diseases.

Wild Germplasm as a Source of New Breeding Material

Agricultural and horticultural production systems typically consist of genetically uniform plant populations, ensuring homogenous development and uniform plant traits, both of which are vital for large-scale production. Although all modern crops are initially derived from wild species, domestication followed by intensive selection poses strong bottlenecks in genetic diversity (Tanksley and McCouch 1997). The use of crop wild relatives (CWRs), therefore, depicts a valuable resource for introducing genomic novelty and valuable traits into modern elite cultivars (Bohra et al. 2022; Krug et al. 2023). McCouch (2004) argued that plant breeding (and ultimately the world's food supply) heavily relies on an equilibrium of new ideas (originated from wild germplasm) and high-performing, field-proven resources. Accordingly, McCouch points out that the potential in CWRs does not just lie in genes, providing new traits. Besides the reintroduction of alleles lost due to domestication, the overall context determining phenotypic plasticity responding to different environmental characteristics (specifically pointing at biological redundancy and pleiotropy) illustrates the relevance of CWRs in modern breeding (Tanksley and McCouch 1997). Recent studies showed that increasing crop diversity and genomic asynchrony stabilise agricultural systems and increase tolerance to sharp harvest losses (Renard and Tilman 2019; Egli et al. 2020). Indeed, modelling indicates that compensatory effects from diverse crop plants account for one-third of global yield, a contribution on par with irrigation-driven yield variability (Ray et al. 2015).

Wild *Solanum* Species

To facilitate the implementation of beneficial traits from CWRs, breeders and researchers need to infer the phenotypic and genomic trait diversity of wild ecosystems. Mapping phenotypic

plasticity to genomic features has been a major focus of pre-breeding programs and crop improvement in general. In tomatoes, this field of research was pioneered by Charles M. Rick, who was the first to sample, document and breed with wild populations (Rick and Butler, 1956). The growing availability of high-throughput sequencing technology has accelerated research on CWRs, in particular on wild tomato species (e.g., *S. lycopersicoides*, *S. chilense*, *S. pennellii*, or *S. habrochaites*, Bolger et al. 2014; Powell et al. 2022; Munir et al. 2016; Silva-Arias et al. 2025; Alonge et al. 2020; Bohra et al. 2022; Krug et al. 2023). As one of the most species-rich angiosperm genera, wild tomatoes exhibit remarkable morphological diversity and extensive genetic variation, comprising valuable resources among wild relatives for plant breeding and evolutionary studies (fig. 1, Peralta et al. 2008). The high Andes region, the primary centre of origin for *Solanum* species, is recognised as one of the world's biodiversity hotspots, exhibiting among the highest rates of species diversification ever recorded (Schluter and Pennell 2017). Studies have shown that the net diversification rate in this region exceeds that of other evolutionary hotspots, likely driven by the harsh environmental conditions that necessitate rapid habitat adaptation (Madriñán et al. 2013). Population genomic studies have characterised the role of habitat adaptation in *Solanum* divergence. Despite having similar genetic backgrounds, closely related *Solanum* species can exhibit different variances in the fitness effects of deleterious mutations, indicating that environmental conditions significantly shape their genetic diversity (Tellier et al. 2011). This is further supported by findings describing that environmental variables might determine the divergence or specification of wild *Solanum* species (Nakazato et al. 2010).

The *Solanum* Species Selected for Analysis

Building on these reports, I will focus on five tomato CWRs: *Solanum chilense*, *S. habrochaites*, *S. lycopersicoides*, *S. pimpinellifolium* and *S. pennellii*. These CWRs exhibit substantial morphological and genomic diversity and were subject to research on stress tolerance before (fig. 1, Peralta et al. 2008; Li et al. 2023; Alonge et al. 2020). Generally, all wild tomatoes in this study originate in western South America, with *S. pennellii*, *S. chilense*, and *S. lycopersicoides* primarily found in high-elevation desert regions with extreme aridity. Within these habitats, the plants are typically found in small islands of vegetation, known as *lomas*, which mainly capture humidity from sea air (Peralta et al. 2008). The repertoire of stress tolerance varies between the species and their respective accessions/populations. For example, *S. chilense* and *S. habrochaites* show increased abiotic stress tolerance against drought or low temperatures/freezing (Nosenko et al. 2016; Munir et al. 2016). In contrast, several salt and

drought tolerance quantitative trait loci (QTLs) were found in *S. pennellii* introgression lines (ILs), like the ILs 2-5, 7-4-1 or 9-1 (Bolger et al. 2014). Despite showing considerable abiotic stress tolerance, the focal CWRs harbour significant variability against biotic stresses. This is illustrated by previous research on *S. chilense*, showing significant phenotypic variation in resistance against multiple pathogenic fungi, including *Phytophthora infestans*, *Alternaria solani*, and *Fusarium spp.* (Stam et al. 2017). This is further supported by findings illustrating strong genotype-to-genotype interactions between *Alternaria spp.* and *Solanum* genotypes (Schmey et al. 2023). Other studies have highlighted significant phenotypic variability in *S. habrochaites* and *S. lycopersicoides* accessions regarding their degree of resistance to *B. cinerea* (Finkers et al. 2007; Miao et al. 2022; Chen et al. 2015; Davis et al. 2009). This facilitated the identification of *B. cinerea* resistance QTLs, such as the *S. habrochaites* loci *Rbcq1*, *Rbcq2* or *Rbcq4a*, and first gene-level characterisations including the *S. habrochaites* OSCA gene family (Finkers et al. 2007; Davis et al. 2009). However, the best-documented examples of resistance introduced from CWRs into domestic tomato cultivars involve major resistance genes (*R*-genes). One prominent example is the I-3 resistance gene from *S. pennellii*, which confers monogenic resistance against *F. oxysporium* f. sp. *lycopersici* (Scott and Jones 1989). The major resistance genes Cf-2 and Cf-9, originally from *S. pimpinellifolium*, provide full resistance against the biotrophic pathogen *Cladosporium fulvum* and have been successfully introgressed into domestic tomato germplasm (Thomas et al. 1997; Thomas et al. 1998; Jones et al. 1994). Another major *C. fulvum* resistance gene, Cf-4, was introgressed from *S. habrochaites* (Thomas et al. 1997). Kahlon et al. (2020) observed significant intraspecific variation in *S. chilense*'s ability to recognise the *C. fulvum* avirulence effectors Avr4 and Avr9. The authors conclude that major R-gene-mediated resistance exhibits significant diversity, likely driven by a complex genetic interplay shaping resistance polymorphism.

Although an increasing number of alleles and QTLs originating from CWRs have been characterised and introduced into elite cultivars, breeders and researchers have criticised their underperformance. Generally, phenotypic stability and genotype-to-phenotype translation are impeded, possibly due to epistatic effects, hence underestimating the genomic background of individuals in diverse populations (Sackton and Hartl 2016; Alonge et al. 2020; Bedinger et al. 2011). The underlying mechanisms will be part of this investigation.

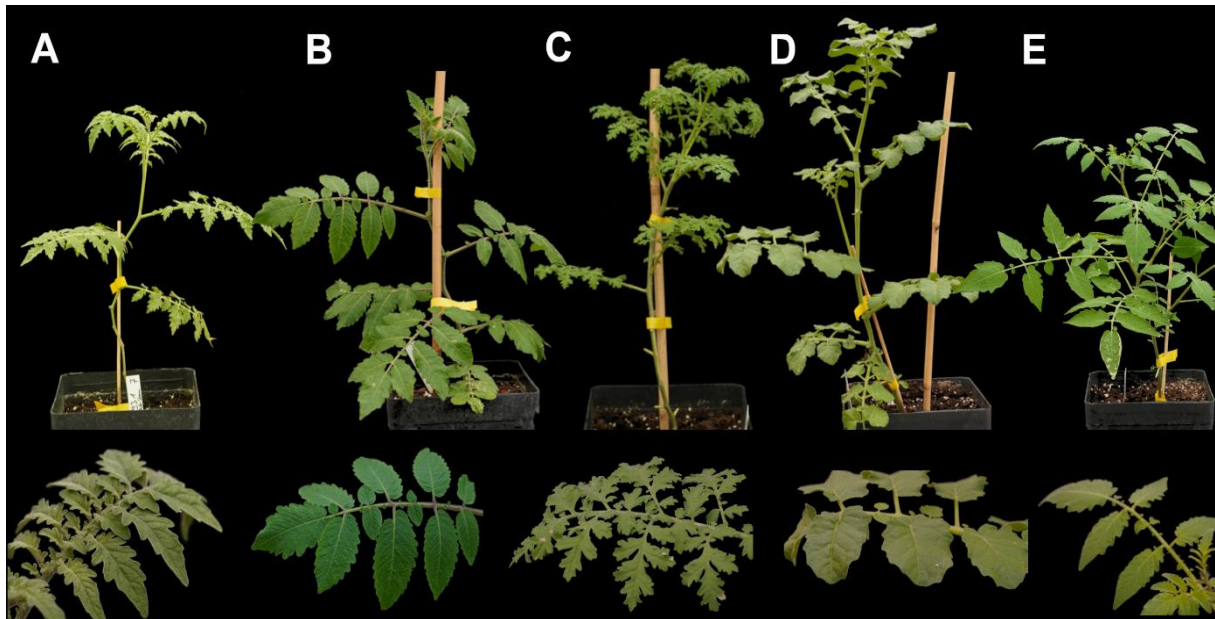


Figure 1: The wild tomato species used in this study exhibit significant morphological diversity. A) *Solanum chilense*, B) *S. habrochaites*, C) *S. lycopersicoides*, D) *S. pennellii*, and E) *S. pimpinellifolium*. The top panels show juvenile plants and the lower panels show representative leaves of each species.

Necrotrophic Pathogens Pose a Threat to the Global Food Production

Infection with plant pathogenic organisms like fungi or oomycetes leads to various plant diseases (Oliver et al. 2024). Although there is increasing evidence for more complexity, plant pathogens are commonly divided into three groups based on their lifestyle: necrotrophs, hemibiotrophs and biotrophs. Necrotrophic organisms feed from dead plant tissue and actively kill the plant cells to acquire nutrients. In contrast, biotrophic pathogens rely on living host cells. They are mostly obligately dependent on the host organism, keeping the host alive by the secretion of effectors to trigger a feed exchange (Liao et al. 2022; Oliver et al. 2024). The pathogen lifestyle is a consequence of its strategy for infection, as necrotrophs use molecules like cell wall degrading enzymes or oxalic acid to manipulate its host or induce cell death (Rowe et al. 2010). Against the common assumption that necrotrophic pathogens follow a simplistic strategy of killing cells, it is clear that those organisms face multiple challenges during colonisation and evolved distinct mechanisms to escape host defence (Doehlemann et al. 2017). While some necrotrophic pathogens, such as *Alternaria* spp. secrete host-specific toxins conferring host-specificity; generalist pathogens developed mechanisms to facilitate the colonisation of a wide array of host plants. The most commonly known generalist necrotrophs are *Sclerotinia sclerotiorum* and *Botrytis cinerea*, both being pathogenic on more than 400 documented hosts (Derbyshire et al. 2022; Newman and Derbyshire 2020). Recent research indicates that generalist pathogens maintain this generalism by high functional redundancy and degeneracy, reducing selective pressure on individual pathways. Despite a considerable fitness

cost, functional redundancies, possibly underlying diversifying selection, enable necrotrophic pathogens to infect a wide diversity of host species effectively (Derbyshire and Raffaele 2023; Stukenbrock and McDonald 2009; Rowe and Kliebenstein 2007).

***Sclerotinia sclerotiorum* as a Model for Research**

S. sclerotiorum is a cosmopolitan necrotrophic fungal pathogen causing devastating plant diseases on more than 400 host plants, including the destructive disease Sclerotinia stem rot on oilseed rape (Boland and Hall 1994). In oilseed rape, the estimated yearly yield loss is about 10-20%, while reports from tomatoes documented yield losses of up to 50% (Mazumdar 2021). Infection begins with the germination of sexual ascospores or mycelial growth, both originating from long-lived sclerotia (Mazumdar 2021; Oliver et al. 2024). The fungus penetrates host tissues using appressoria and employs a highly coordinated infection strategy involving the secretion of cell wall-degrading enzymes, small proteins (so-called effectors) and oxalic acid to manipulate host defences (Williams et al. 2011; Doehlemann et al. 2017). During the early phase of infection (< 24 hpi), *S. sclerotiorum* secretes effector proteins, like ITL, which dampens ethylene and salicylic acid-mediated defence responses, as well as oxalic acid to weaken the host's pathogen recognition and reactive oxygen species (ROS) homeostasis (Ding et al. 2021; Seifbarghi et al. 2017; Derbyshire et al. 2019; Derbyshire et al. 2022). After the initial phase of infection, *S. sclerotiorum* changes towards a necrotrophic lifestyle, releasing toxins and hydrolytic enzymes (e.g., cellulases, proteases, pectinases), and cell-death inducing effectors, like NEP1, or NEP2 to facilitate colonisation, often triggering programmed cell death (Mbengue et al. 2016; Williams et al. 2011). Ultimately, *S. sclerotiorum* kills the host and completes its disease cycle by forming new sclerotia within dead plant tissues. The new sclerotia then remain dormant in the soil.

Quantitative Disease Resistance Against Generalist Pathogens

To date, no complete form of resistance against generalist necrotrophic pathogens like *B. cinerea* or *S. sclerotiorum* has been found. This is in contrast to the broad availability of dominant *R*-genes against biotrophic pathogens, which confer complete resistance by triggering a hypersensitive response (Wang et al. 2019; Mbengue et al. 2016; Oliver et al. 2024). Consequently, resistance breeding heavily relies on quantitative disease resistance (QDR). QDR is defined as a partial, non-complete form of resistance. The degree of resistance follows a continuous distribution over a polymorph population from susceptible to mostly resistant genotypes, which contrasts the binomial distribution found for *R*-gene-mediated resistance

phenotypes. Accordingly, QDR is controlled by many small-effect loci, possibly via a highly interlinked gene network (Corwin and Kliebenstein 2017; Roux et al. 2014; Derbyshire et al. 2022). The nuanced nature of QDR phenotypes and QDR loci adds significant complexity to the functional and genomic characterisation of QDR. It has been hypothesised that the interconnected structure of QDR likely arises from multiple independent genetic properties of QDR loci, including pleiotropic effects on morphology, roles in signal integration, involvement in metabolic pathways, and the modulation of weak or partial resistance genes (Poland et al. 2009). It was further proposed that the continuous distribution of heritable phenotypes might result from the interaction of genetic loci (Wang et al. 2019). QDR is commonly used in breeding and traced to QTLs (St.Clair 2010). Also, genome-wide association studies can be useful in characterising potential candidate loci. In a recent study, Lin et al. (2024) screened 322 oilseed rape accessions and identified a mitogen-activated kinase (BnaA07.MKK9) conferring an advantage of 30 % increased QDR. Yet this study reflects one of the strongest QDR loci as most QTLs are observed, with less than 10 % explaining observed phenotypic variance (Wang et al. 2019). Although the underlying genomic features appear highly complex, evolutionary analysis showed that the most durable resistance relies on many minor genes (Brown 2015; Poland et al. 2009). Using a network-based approach in wild pathosystems, Barrett et al. (2015) demonstrated that broad-spectrum resistance typically arises through partial rather than complete resistance. The authors hypothesised that this phenomenon reflects evolutionary trade-offs between resistance breadth and intensity. Yet, targeted breeding for QDR displays a valuable tool for resistance breeding.

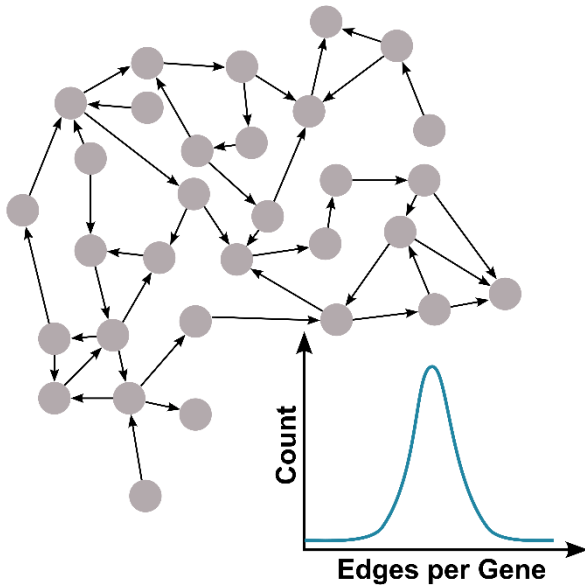
Gene Network Evolution

Single gene-for-gene interactions alone cannot fully explain the phenotypic complexity underlying QDR, underscoring the importance of investigating broader gene regulatory networks (GRNs) and their evolution (Kahlon and Stam 2021; McDonald and Reed 2023). Recent studies highlight how network approaches can effectively capture the polymorphic nature and evolutionary dynamics of complex traits. For example, Kahlon et al. (2020) demonstrated how complex receptor polymorphisms determine QDR diversity in *S. chilense* against *C. fulvum*. However, missing genotype-to-phenotype links can be explained by shifts in gene regulatory networks.

Gene Regulatory Networks: Mapping the Blueprint of Regulatory Complexity

Regulatory variation is a major driver of phenotypic diversity (Thompson et al. 2015). Hierarchical regulatory interactions mostly depend on the interaction of a transcription factor (TF) and its target genes. Because regulatory genes control and are controlled by many other genes, their interactions form a complex, interconnected network called gene regulatory networks (GRNs, Erwin and Davidson 2009). It is known that most GRNs approximate a scale-free topology, meaning that most genes have only a few connections, while a small number of key genes act as central “hubs” or “kernels” with many connections (fig. 2, Broido and Clauset 2019; Nicolau and Schoenauer 2009; Babu et al. 2004; Ouma et al. 2018). Another fundamental property of GRNs is their modularity, which reflects self-contained entities of interacting components (sub-networks) rather than all interactions of all genes (Thompson et al. 2015). GRNs can be further broken down into sub-modules, which are determined by *cis*- or *trans*-regulatory elements and provide a more granular dependency structure (Hatileberg and Hinman 2021).

Random, Non-Hierarchical Network Topology



Modular scale-free Network Topology

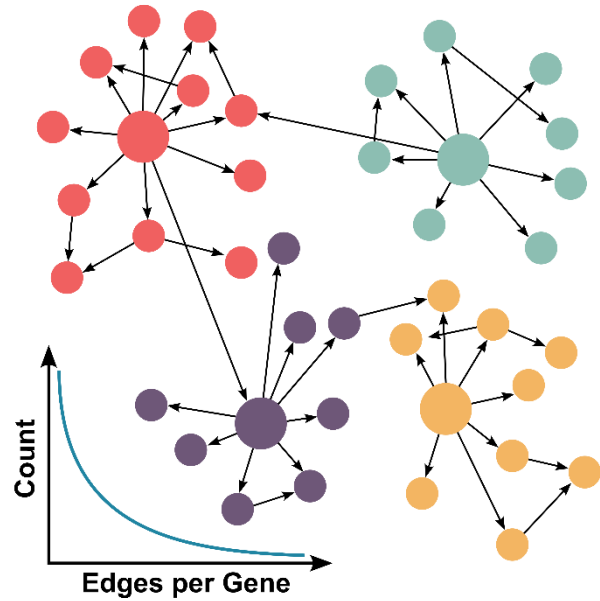


Figure 2: Exemplary structure of a random network and a modular scale-free network topology as models for gene regulatory networks. The density plots show the distribution of edge counts per gene for each network. Node colours indicate module membership, while larger nodes represent hub genes. Adapted from Petit (2024).

Mechanisms of Gene Regulatory Network Rewiring

Due to their multi-layered architecture, GRN topology can be altered by multiple processes. Small changes to genomic DNA, like mutations of single base pairs, single nucleotide polymorphism (SNP), and insertion or deletion of sequences, can change the regulatory landscape (Erwin and Davidson 2009). The impact of these mutations depends on their genomic context: *cis*-regulatory changes (e.g., promotor mutations) mostly affect single genes, while *trans*-regulatory changes (e.g., mutations in transcription factors) can influence all downstream targets (Hatleberg and Hinman 2021). Such modifications typically alter the network topology of sub-networks by changing specific gene-to-gene relationships. In contrast, large-scale events like gene or genome duplication or rearrangements can reshape the GRN landscape. Duplications, in particular, may lead to functional redundancy, neofunctionalisation (co-optation) or subfunctionalisation with potentially strong phenotypic effects (Conant and Wolfe 2008). It is important to note that the impact of DNA sequence changes on GRNs depends heavily on their genomic location and the context of other genetic changes within the genome and network (Erwin and Davidson 2009). While the mechanisms driving GRN rewiring are relatively well understood, predicting how specific genomic alterations affect the regulatory landscape and resulting phenotypes remains a major challenge. This might originate from the pleiotropic and epistatic effects inherent to GRNs, reflecting their highly interconnected and quantitative nature (Mackay and Anholt 2024).

The Evolution of GRNs Underlying Complex Traits

Regulatory divergence is often a critical first step towards phenotypic change and the evolution of new traits/adaptation. For instance, despite no detectable genomic changes, *Ralstonia solanacearum* clones exhibited significant regulatory rewiring and enhanced adaptation to the resistant host after 300 serial host passages (Gopalan-Nair et al. 2021). Similarly, Szymański et al. (2020) demonstrated that regulatory plasticity, rather than genomic sequence variation, plays a major role in *B. cinerea* resistance of tomato ILs. Yet it is unclear how complex regulatory networks evolve, as exemplified by the ongoing debate about the role of adaptive selection vs. genetic drift in GRN evolution (Lynch 2007; Thompson et al. 2015; Hill et al. 2021; Houle and Rossoni 2022). Since Wilkins' (2007) initial observations of gene network diversification in morphological evolution, the relationship between network position and evolutionary pressure has been the subject of fundamental research in model organisms. However, many studies focussed on the role of mutation on *cis*- or *trans* sequences in adaptive evolution (Stern and

Orgogozo 2009). Phenotypic variability may arise from divergent regulatory networks, where different nodes and edges evolve at varying rates across GRNs and sub-networks or modules (Kahlon and Stam 2021; Davidson and Erwin 2006). This is especially evident when comparing hub genes to peripheral genes. While GRNs often exhibit a bow-tie structure (few hub genes integrate many inputs and control downstream targets), these hubs are highly vulnerable to genetic changes (McDonald and Reed 2023). Although major sub-modules (kernels, hubs) are thought to be under evolutionary constraint, recent evidence indicates that regulatory shifts within these hubs may facilitate more rapid adaptation (Erwin and Davidson 2009; Wei et al. 2024).

The modularity of GRNs may allow phenotypic changes without disrupting the remaining system (Espinosa-Soto 2018). It is unclear how pleiotropic modules (like potential QDR modules) with overlapping/redundant functions evolve; perhaps one might compensate for another's specialisation. Due to experimental and analytical complexity, research on GRN evolution of complex quantitative phenotypes remains sparse (McDonald and Reed 2023; Mackay and Anholt 2024). The low number of scientific reports on GRN-based analysis of QDR-evolution also illustrates this. Recent findings illustrate that phenotypic plasticity (hence pleiotropy) underlies a species-specific connectivity landscape in GRNs and their subnetworks (Ouma et al. 2018). As shown by the , a comprehensive understanding of QDR-GRN evolution is missing, yet it will significantly influence breeding for QDR and, ultimately, management of disease epidemics (Barrett et al. 2015).

Aim of this Study

Research in plant-parasite interaction aims to identify and characterise mechanisms driving host resistance or pathogen virulence. The new conceptual understanding will be used to develop future elite cultivars. In this dissertation, I will focus on the quantitative disease resistance of wild tomato species against *Sclerotinia sclerotiorum*. This research primarily aims to explore the mechanisms that influence the diversity and evolution of QDR in this model system.

The main objective of this research is to compare the regulatory responses to necrotrophic fungi in five different *Solanum* species. Through this comparison, I aim to uncover general principles that govern the diversification of these responses across multiple evolutionary scales, encompassing both intraspecific and interspecific variation. This will enable me to gain insights into the mechanistic fundament of QDR. Based on this, I defined three key research questions to guide our experimental investigation.

1) QDR-Phenotyping

Do wild tomato species exhibit distinct QDR phenotypes, and do divergent or shared defence strategies drive these?

Hypothesis: Wild tomato species exhibit distinct QDR phenotypes, each employing species-specific defence strategies shaped by unique phenotypic mechanisms.

Methodology: To address the research question, I used a camera-based high-resolution phenotyping system. I screened up to ten accessions of four wild tomato species infected with *S. sclerotiorum*, with a temporal resolution of 10 min. This enabled me to characterise the QDR of the tested plant accession and define distinct mechanisms driving QDR.

2) Evolution of QDR

Are the gene networks underpinning QDR evolutionarily diversified across evolutionary scales?

Hypothesis: Enhanced QDR phenotypes arise from complex gene networks shaped by lineage-specific network evolution.

Methodology: I identified genotypes of contrasting LDT-mediated QDR of five host species based on the findings of publication 1. Then, I conducted an RNAseq experiment to unravel the regulatory response during the lesion growth phase. I then performed different network analysis

methods (weighted gene coregulation and regulatory network analyses). I applied phylotranscriptomics to unravel the evolutionary mechanisms driving QDR among five *Solanum* species.

3) Longitudinal regulation of QDR

How does the temporal (longitudinal) variation in gene expression influence the degree of QDR?

Hypothesis: Longitudinal variation in gene expression can alter the degree of QDR, indicating that timing and preformation of regulatory elements are crucial determinants of resistance.

Methodology: Similar to the previous research question, I identified candidate genotypes based on publication 1. I then performed a time-series experiment to characterise regulatory changes over time. Here, I used a hyperspectral camera system to identify photosynthetic stress alongside. I further applied differential gene expression analysis and gene regulatory network analysis to identify regulatory patterns.

Publication 1



Publication 1

Title: High-Resolution Disease Phenotyping Reveals Distinct Resistance Mechanisms of Tomato Crop Wild Relatives against *Sclerotinia sclerotiorum*

Manuscript published after peer review in Plant Phenomics

Severin Einspanier, Christopher Tominello-Ramirez, Mario Hasler, Adelin Barbacci, Sylvain Raffaele, Remco Stam. High-Resolution Disease Phenotyping Reveals Distinct Resistance Mechanisms of Tomato Crop Wild Relatives against *Sclerotinia sclerotiorum*. *Plant Phenomics*. 2024;6:0214.DOI:10.34133/plantphenomics.0214

Contributions: I designed and conducted all experiments, analysed and visualised data, and wrote the manuscript.

RESEARCH ARTICLE

High-Resolution Disease Phenotyping Reveals Distinct Resistance Mechanisms of Tomato Crop Wild Relatives against *Sclerotinia sclerotiorum*

Severin Einspanier¹, Christopher Tominello-Ramirez¹, Mario Hasler², Adelín Barbacci³, Sylvain Raffaele³, and Remco Stam^{1*}

¹Department of Phytopathology and Crop Protection, Institute of Phytopathology, Faculty of Agricultural and Nutritional Sciences, Christian-Albrechts-University, 24118 Kiel, Germany. ²Lehrfach Variationsstatistik, Faculty of Agricultural and Nutritional Sciences, Christian-Albrechts-University, Kiel, 24118 Kiel, Germany. ³Laboratoire des Interactions Plantes Microorganismes Environnement (LIPME), INRAE, CNRS, Castanet Tolosan Cedex, France.

*Address correspondence to: Remco.Stam@phytomed.uni-kiel.de

Besides the well-understood qualitative disease resistance, plants possess a more complex quantitative form of resistance: quantitative disease resistance (QDR). QDR is commonly defined as a partial but more durable form of resistance and, therefore, might display a valuable target for resistance breeding. The characterization of QDR phenotypes, especially of wild crop relatives, displays a bottleneck in deciphering QDR's genomic and regulatory background. Moreover, the relationship between QDR parameters, such as infection frequency, lag-phase duration, and lesion growth rate, remains elusive. High hurdles for applying modern phenotyping technology, such as the low availability of phenotyping facilities or complex data analysis, further dampen progress in understanding QDR. Here, we applied a low-cost (<1.000 €) phenotyping system to measure lesion growth dynamics of wild tomato species (e.g., *Solanum pennellii* or *Solanum pimpinellifolium*). We provide insight into QDR diversity of wild populations and derive specific QDR mechanisms and their cross-talk. We show how temporally continuous observations are required to dissect end-point severity into functional resistance mechanisms. The results of our study show how QDR can be maintained by facilitating different defense mechanisms during host–parasite interaction and that the capacity of the QDR toolbox highly depends on the host's genetic context. We anticipate that the present findings display a valuable resource for more targeted functional characterization of the processes involved in QDR. Moreover, we show how modest phenotyping technology can be leveraged to help answer highly relevant biological questions.

Citation: Einspanier S, Tominello-Ramirez C, Hasler M, Barbacci A, Raffaele S, Stam R. High-Resolution Disease Phenotyping Reveals Distinct Resistance Mechanisms of Tomato Crop Wild Relatives against *Sclerotinia sclerotiorum*. *Plant Phenomics* 2024;6:Article 0214. <https://doi.org/10.34133/plantphenomics.0214>

Submitted 2 May 2024
Accepted 19 June 2024
Published 5 August 2024

Copyright © 2024 Severin Einspanier et al. Exclusive licensee Nanjing Agricultural University. No claim to original U.S. Government Works. Distributed under a Creative Commons Attribution License 4.0 (CC BY 4.0).

Introduction

Quantitative disease resistance in plants

Plant resistance is commonly divided into 2 concepts with fundamental differences: qualitative and quantitative resistance [1,2]. While qualitative disease resistance provides a highly effective race-specific resistance, quantitative disease resistance (QDR) is a broad-range yet incomplete resistance [2,3]. Qualitative resistance is driven by major race-specific resistance genes (R-genes). They often lead to complete and easily observable resistance and were the dominant research focus for disease resistance breeding programs. However, reports of R-genes losing their efficacy against pathogens have increased recently, and major resistance genes have not been identified for many so-called necrotrophic plant pathogens, like *Botrytis cinerea* or *Sclerotinia sclerotiorum* [3–7]. Commonly, degrees of QDR cannot be divided into discrete

classes. Quantitative resistance phenotypes are continuously distributed and can only be explained by highly integrated, polygenic regulatory mechanisms [8]. Moreover, QDR can manifest itself in several ways, ranging from differences in infection frequency (IF) on the leaf or delayed onset of infection to stalled lesion growth. Numerous studies documented wide distributions of QDR phenotypes against necrotrophic pathogens in both natural and domesticated plant populations, yet the relations of different QDR phenotypes have not yet been studied in detail [1–3,8–12]. Recent reports summarized the diversity in functional QDR, arguing that QDR might be influenced by many independent components such as regulation as a pleiotropic side effect, weak R-genes, involvement in defense signal transduction, or *cis/trans*-regulatory mechanisms [1,2]. Indeed, many QTLs that influence some degree of QDR have been identified [8,13,14]. Linkage of such QTLs or the underlying loci to exact resistance features, like the lag-phase duration, will be one of the future challenges

that would allow understanding and utilizing QDR in pathogen resistance breeding.

Phenotyping technology and approaches to quantify QDR

The functional characterization of QDR highly depends on precisely measured phenotypes [2,15]. However, the experimental design required to assess QDR phenotypes over entire plant or pathogen populations quickly exceeds the limits of traditional, manual scoring methods and calls for more sophisticated phenotyping technology. The increasing availability of sensor technology (e.g., RGB, multi- or hyperspectral sensors) and analytical methods (e.g., deep-learning or artificial intelligence algorithms) recently have strengthened the attention to plant phenotyping [16]. Many studies have shown how imaging technology can be used not only to determine plant phenotypes like plant height, nutritional status, or water-use efficiency but also to assist breeder's decisions [14,17,18]. Moreover, several reviews recently summarized the potential of modern sensor technology and related software in quantifying phenotypes of host-parasite interactions on multiple levels [19–24]. Even advanced applications, like in-field phenotyping or assessing complex features in non-standardized conditions, are possible due to deep-learning models like “PLPNet” or “ResNet-9” [25–27]. However, large phenotyping platforms also have limitations. High-end systems often collect a multitude of 3D scanning images or images in multiple spectral wavelengths. Analysis of these data is computationally intensive and often requires very specific knowledge. Thus, such technologies might overwhelm (non-data-science) researchers with high amounts of complex datasets as substantial skills are required to derive easy-to-interpret insights relevant to answering biological research questions [28]. A second challenge lies in adapting an established phenotyping system for various pathosystems, i.e., different crops or pathogens [22,29]. Lastly, most high-end phenotyping systems have very high investment and running costs and thus are less available. Combined with the aforementioned low flexibility, this further limits their use and application in the broad spectrum of plant pathology, where quick and easy screening of QDR in a large panel of plants is one of the main objectives. Recent developments, however, enable researchers to use the generally available consumer-level technology and build low-cost phenotyping platforms like the “Navatron” [30]. In this study, we show the usefulness of such systems in unraveling QDR dynamics in crop wild relatives.

Wild tomato populations as a reservoir of potential QDR loci against major pathogens

The domestic tomato (*Solanum lycopersicum*) is a major food crop of global importance [31]. However, plant pathogens, including the necrotroph *S. sclerotiorum* or species from the genus *Alternaria*, commonly threaten tomato production worldwide [32–35]. Host resistance and fungicides are the standard tools to protect tomatoes against these pathogens. However, strong selection pressure caused by R-genes or fungicides and higher-than-expected pathogen diversity in the field result in losing fungicide efficacy or plant resistance against such species [36–40]. Therefore, highly diverse wild populations are an invaluable source of desirable alleles in breeding, as crosses between wild and domestic can lead to increased performance and stress

tolerance [41]. Integrating phenotyping with screening of genetically highly diverse wild resources will help characterize novel alleles for QDR breeding [42].

Wild tomato species originated from several radiation events and can generally be classified into 4 groups within the so-called section *Lycopersicon*, containing a total of 15 species and 2 species in the section *Lycopersicoides* [43]. All species have adapted to specific habitats ranging from the edge of the Atacama desert to the Andes, where they withstand diverse (a)biotic stresses. Evolutionary analyses show that different species and populations have evolved drought or salt stress tolerance, as well as adaptation to cold stress [44–48]. Previous studies have also shown substantial variation in susceptibility and resistance of wild *Solanum* spp. against various pathogens but often relied on manual or single time-point disease assessments, thus lacking the temporal resolution and statistical power to describe QDR mechanisms confidently [38,49,50]. In light of the variation of QDR already shown, wild tomato species are perfectly suited for quantification of QDR mechanisms as proof of principle. Moreover, defining whether specific QDR mechanisms play major roles in resistance will generate much-needed insights into the biology of QDR to help design future durable resistance breeding projects against major pathogens.

S. sclerotiorum is a necrotrophic pathogen that can infect hundreds of host species, including important crops such as rapeseed and tomato [30,51,52]. On vegetables, including tomatoes, infection with *S. sclerotiorum* can cause tremendous yield loss due to collapsing stems or damaged fruits [53,54]. Infection in the field can happen through air-dispersed ascospores or via myceliogenic germination of its overwintering structures in the soil, the so-called sclerotia [32,52]. In experimental conditions, mycelial inoculation procedures are commonly used, as the preparation of ascospores can display a major challenge [55–59]. No complete form of resistance against the generalist *S. sclerotiorum* has been characterized; therefore, resistance breeding relies on QDR as the source of new alleles [32,52,55,57,60].

In the present work, we build on a low-budget image-based phenotyping system [30] to derive high-resolution time-resolved disease phenotypes and dissect them into 3 distinct QDR mechanisms. We show the potential of this system by characterizing the natural diversity of QDR phenotypes of wild *Solanum* species and, therefore, provide insights into the mechanisms underlying QDR against the generalist pathogen *S. sclerotiorum*. We use this system as a model to address whether QDR is always represented by a similar mechanism, i.e., IF or lag-phase duration, and show that the orchestration of different QDR mechanisms affects the overall QDR on a genotype-specific basis. Accordingly, we argue that the different host species have evolved specific mechanisms to maintain a defined degree of QDR.

Materials and Methods

Experimental design

We screened multiple accessions of 4 wild tomato species (*S. pennellii*, *S. lycopersicoides*, *S. habrochaites*, and *S. lycopersicoides*) with a detached-leaf assay. All accessions of the same species were tested as one batch for up to 5 independent repetitions. To facilitate comparability between batches, *S. lycopersicum* cv. C32 was used as a control in every experiment. A schematic of the experimental procedures is displayed in Fig. 1.

S. sclerotiorum inoculum preparation

For inoculation experiments, the *S. sclerotiorum* isolate 1980 or the OAH1:GFP (green fluorescent protein) isolate (for microscopic analysis only, [61]) was used. The fungus was alternately cultivated on potato dextrose agar (Sigma-Aldrich) and solid malic acid medium [62] at approximately 25 °C in the dark. Four 1-cm pieces of *S. sclerotiorum* inoculum were used to inoculate 100 ml of potato dextrose broth. After 4 days of incubation on a rotary shaker (24 °C, 120 rpm), a fungal mycelium suspension was generated: for this, the medium was mixed 2 times using a dispenser (IKA T25) for 10 s at 24,000 rpm. The mixture was then vacuum-filtrated through cheesecloth, and the remaining liquid was concentrated to an optical density (OD) of 1. For the negative control, fungal tissue was removed from the solution by centrifugation, and the supernatant was autoclaved. Tween 20 was used as a surfactant. Per leaf, one drop (10 µl) of inoculum was used.

Plant growing conditions

Wild tomato germplasm was obtained from the C. M. Rick Tomato Genetics Resource Center of the University of California, Davis (TGRC UC-Davis, <http://tgrc.ucdavis.edu/>) (see Table S5). The species were selected to include genetically diverse species within the section *Lycopersicon* and a species from the section *Lycopersicoides* (Fig. 2). All plants were grown at the greenhouse facility of the Department of Phytopathology and Crop Protection, Institute of Phytopathology, Faculty

of Agricultural and Nutritional Sciences, Christian Albrechts University, Kiel, Germany. Following seed surface sterilization using 2.75% hypochlorite (15 min incubation followed by washing twice with dH₂O), seeds were sown in the substrate (STENDER C700, Germany) and cultivated in a growth chamber (21 °C, 65% rH, 16 h of 450 photosynthetically active radiation [PAR]). From the 3-leaf stage on, plants were cultivated in standard greenhouse conditions with supplement light (approximately 16 h/day, 15 to 25 °C at 50% to 70% rH). Plants were fertilized via the irrigation system (monthly, 1% Sagaphos Blue, Germany). Plants were propagated using cuttings (Chryzotop Grün 0.25%) and regularly screened for virus infection.

Detached leaf assay

Detached leaf assays were conducted to measure QDR of a diverse panel of wild *Solanaceae* plants. A custom phenotyping system was adapted [30]. A 50 cm × 70 cm PMMA tray was filled with 8 layers of blue tissue paper and flooded with 700 ml of sterile dH₂O. Plant leaves were placed abaxial side up onto

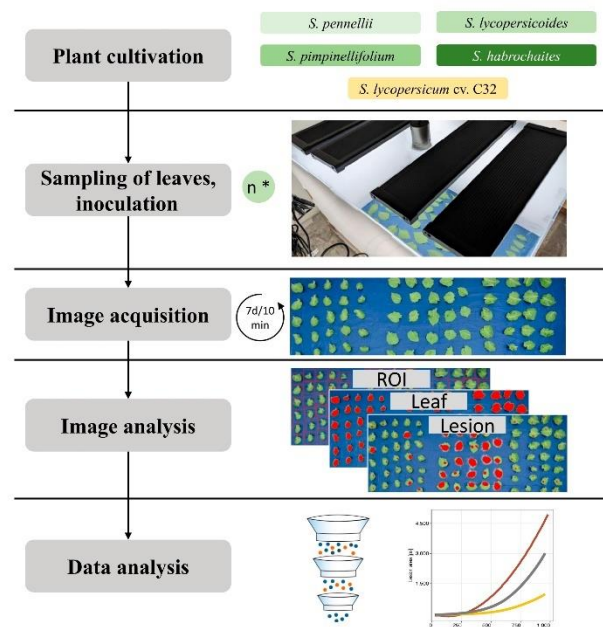


Fig. 1. Overview of the high-throughput phenotyping assay. We cultivated 36 accessions from 4 wild tomato species (*S. pennellii*, *S. habrochaites*, *S. pimpinellifolium*, and *S. lycopersicoides*) and the domestic tomato cultivar “C32” in a greenhouse for detached-leaf assays. We harvested single leaves, inoculated using a *Sclerotinia sclerotiorum* mycelial suspension and placed them in the phenotyping boxes. Every 10 min, we captured images of the leaves for the duration of 1 week. We then manually defined regions of interest for each leaf and set thresholds for the feature classes “leaf”, “background”, and “lesion” in the HSV color scheme. Finally, we performed image analysis on all images, collected and filtered the data, and conducted further analytical steps to quantify the lesion development over time.

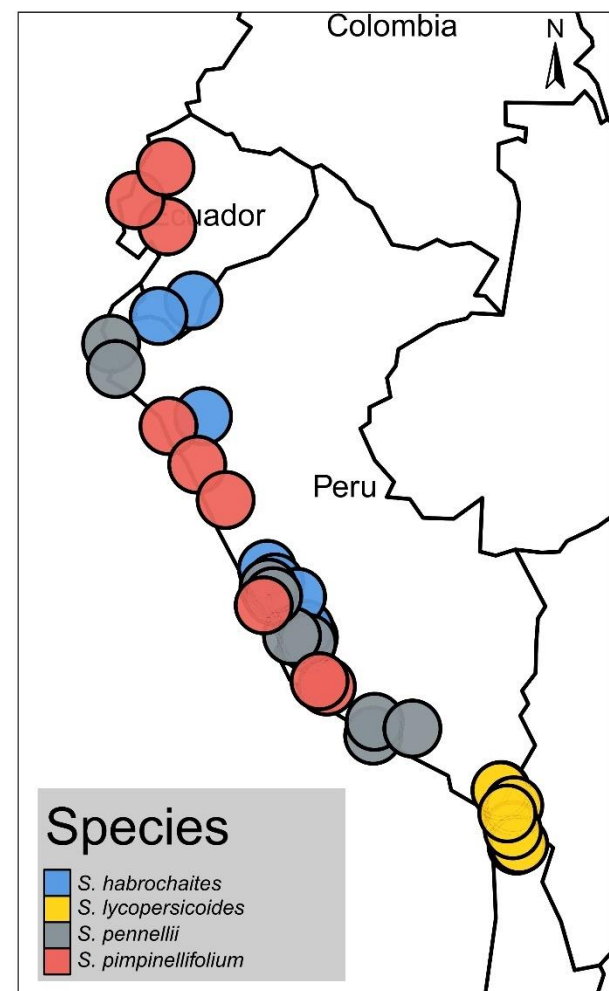


Fig. 2. Sampling localities of wild tomato accessions used in this study. Seed material of all wild tomato accessions was provided from C. M. Rick Tomato Genetics Resource Center of the University of California, Davis (TGRC UC-Davis, <http://tgrc.ucdavis.edu/>). Individual dots represent the geographical origin of each accession.

the tissue and inoculated with 10 µl of mock/*S. sclerotiorum* suspension. Next, the tray is covered with a custom hood. The boxes were placed inside a growth chamber (24 °C) and incubated for 7 days. The assay was independently repeated 5 times. We used a representative set of 3 experiments for all further analysis. We tested potential border effects on the resistance parameters and found no statistically significant impact of leaf position on the measured parameters. Consequently, the leaves were not spatially randomized on the tray.

Phenotyping platform

High-resolution images were acquired using RGB cameras (Yealink UVC30) mounted on the box. Cameras were controlled using Raspberry Pi microcomputers or desktop PCs running headless Ubuntu22. A cron daemon launched the image-acquisition script every 10 min. Plant lights also briefly (1 s) illuminate during nighttime for image capture to enable images in the dark while maintaining circadian rhythm. This was achieved by using the “Shelly Plus Plug S” wifi plug (Fig. S1).

Image analysis

We adapted the “navautron” software package (<https://github.com/A02I01/Navautron>). The image analysis involved manually defining regions of interest (ROIs) using ImageJ (ImageJ Version 1.530). Further, HSV thresholds were optimized individually per box. For this, “assess_noChl.py” was used, and an overlay was generated in Gimp (Version 2.10). Once binary masks represented the respective feature classes (leaf_healthy, leaf_diseased, and background), the whole dataset was evaluated using the “infest.py” script. Segmentation was iterated and classified pixel was counted. The analysis includes functions from the python3 (Version 3.11.4) libraries “numpy” (Version 1.25.2), “opencv” (Version 4.8.1.78), “plantcv” (Version 4.0.1), and “scikit-image” (Version 0.22.0). The plantcv function “dilate” was used to remove leaf edges containing shadows with $ksize = 9$, $i = 1$ [63]. To improve thresholding accuracy (e.g., filling holes) on the lesion, an index filter was applied [ndimage.generic_filter(mask, threshold, size = 3, mode = “constant”)] with a condition to overwrite pixels deviating from the value of the majority of the surrounding pixels. $np.sum(mask)$ was used to quantify the number of pixels in each feature class (lesion and leaf). Code and scripts can be found at https://github.com/seveein/QDR_Wild_Tomatoes.

Microscopy analysis

Plant leaves were harvested and inoculated under standard conditions as described before but with either a GFP-expressing *S. sclerotiorum* strain, the *S. sclerotiorum* wild-type 1980, or the mock suspension. The leaves were evaluated at 12-h intervals using a Zeiss Discovery V20 stereomicroscope under bright light and fluorescent illumination (Zeiss HXP120). Images were taken using an AxioCam MRc camera.

Statistical analysis

An interactive R-script (R-Version 4.3.2, R-Studio 2023.12.1+402) was utilized to extract lag-phase duration and lesion doubling time (LDT) to quantify resistance characteristics [30]. Each leaf’s lesion size over time was fitted against a 4-degree polynomial regression. The fit to the measured data point was reviewed for each sample. LDT and lag phase were determined based on a segmented regression analysis, expecting 2 linear

phases: first, a linear phase during the lag period (no symptom development), and second, a linear log growth (symptom) during the exponential growth phase. The period prior to the lesion growth (LDT) is considered the lag phase, while the LDT represents the log(slope) of the linear growing curve in this area.

A 2-tier filtering pipeline was developed to increase accuracy and remove artifacts from the dataset. First, time points with leaf-size outliers were trimmed by removing 2.5% of the individual reads. Next, individual leaves with unexpectedly high variability in leaf area were excluded from the dataset. Therefore, samples with $sd(leaf) > 10\%$ of the $mean(leaf)$ were removed from the dataset using a simple tidyverse (v. 2.0.0) pipeline.

As a measure of symptom development over time, the area under the disease progress curve (AUDPC) was calculated using the R-package agricolae (v. 1.3-6). General statistical analysis and visualization were conducted in RStudio (R-Version 4.3.2, R-Studio 2023.12.1+402 [64]) and the packages tidyverse [65], ggplot2 [66], ggpubr [67], and agricolae [68]. AUDPC is defined with i = time and y_i = symptom severity at time i as [68]:

$$AUDPC = \sum_{i=1}^N \frac{(y_i + y_{i+1}) \times (i - 1)}{2} \quad (1)$$

For continuous variables (lag-phase duration, LDT, AUDPC, and tt100), a statistical model based on a generalized least squares model was defined [69]. In contrast, a generalized linear model was defined for binomial values (IF, 100%/f) [70]. These models included genotype and start date (without interaction effect).

The residuals corresponding to the continuous values were assumed to be approximately normally distributed and heteroscedastic concerning the different genotypes. These assumptions are based on a graphical residual analysis (Figs. S8 and S9). Based on these models, a pseudo R^2 was calculated [71], and an analysis of variance (ANOVA) was conducted, followed by multiple contrast tests [72,73]. User-defined contrast matrices were used (a) to compare the species’ means with each other and (b) to compare the population means within their specific species with the corresponding species’ mean. The individual leaf area was previously found to have no significant influence on lesion area; therefore, it was not included in our statistical model [74]. A linear mixed-effects model was used to determine the relationship between AUDPC and predictors such as genotype, lag-phase duration, and LDT. Random intercepts were specified per start date to account for experimental repetitions.

Based on this model, fixed-effect values were extracted and used to predict AUDPC per genotype _{$i=1,2,3$} in relation to varying lag and LDT values.

$$AUDPC_i = Intercept_i + Coefficient_{lag_i} \times lag + Coefficient_{LDT_i} \times LDT + Coefficient_{lag_i \times LDT_i} \times lag \times LDT \quad (2)$$

The associated R-codes can be found at https://github.com/seveein/phenotyping_QDR_Wild_Tomatoes.

Results

Wild tomato species carry different levels of quantitative resistance against *S. sclerotiorum* depending on defense parameters

We investigated the phenotypic diversity in QDR in 4 wild tomato species (*S. habrochaites*, *S. lycopersicoides*, *S. pennellii*, and *S. pimpinellifolium*) against the *S. sclerotiorum* isolate 1980 [13]. We used the “Navatron” automated phenotyping system for continuous image acquisition and applied a threshold-based segmentation algorithm to extract phenotypic data (Fig. S1). Hence, we calculated different QDR parameters such as IF, lag-phase duration, LDT, or AUDPC to quantify temporal dynamics of infection (Fig. 3). High variability between experimental runs with wild tomatoes has been described before [6,49,74]. To account for this, we applied a generalized least squares model (glms, continuous variables) and a generalized linear model (glm, discrete variables) for statistical analysis [69]. Overall, we discovered a great diversity of resistance phenotypes among the tested plant species. We found no 100% resistant accessions (Fig. S4). We observed a significant difference in lag-phase duration among plant species, which we define as the time from infection until the first symptoms appear (see Fig. 3A, C, and D). For instance, *S. pimpinellifolium* showed the shortest time from inoculation until lesion development (adjusted mean = 36.2 h). In contrast, *S. habrochaites* and *S. pennellii* displayed a significantly prolonged lag phase (both approximately 59 h) (see Table S1). Using segmented regression analysis, we determined the speed of lesion growth on individual leaves of the panel. The fastest-growing lesions were found on the species *S. pimpinellifolium* and *S. pennellii*. Lesions on *S. pennellii* and *S. pimpinellifolium* leaves doubled in size within approximately 11 h [6.56 log(LDT) and 6.55 log(LDT), respectively], while lesions on *S. habrochaites* and *S. lycopersicoides* spread significantly slower. Those lesions expanded with an average rate of approximately 7.7 log(LDT), corresponding to roughly 36 h (*S. habrochaites*) and 41 h (*S. lycopersicoides*) (see Table S2). Moreover, we observed that the success of disease establishment (IF) depends highly on the host species. We identified a significantly lower infection rate on *S. habrochaites* (corrected IF estimate 80 %), whereas *S. lycopersicoides* and *S. pennellii* displayed significantly higher IF (~93% and 95%, respectively) (Fig. 3B).

Individual QDR measures show different levels of intraspecific variation and conservation on *S. pennellii* and *S. lycopersicoides* accessions

To assess the within-species diversity of QDR phenotypes, we tested different accessions of each represented species. We collected phenotypic data from 7 *S. lycopersicoides* and 9 *S. pennellii* populations (Fig. 4), as well as 8 populations of *S. habrochaites* and 10 populations of the species *S. pimpinellifolium* (Figs. S2 and S3). In particular, the comparison of *S. lycopersicoides* and *S. pennellii* highlights that QDR diversity differs between species. We observed that the (adjusted) mean duration of the lag phase on different *S. pennellii* accessions ranged from 1.59 days (38 h, LA1809) to 2.86 days (68 h, LA1303) (Fig. 4A and C). Using a generalized least squares model, we identified accessions with a significantly shorter lag phase than the grand mean of the species (LA1809 and LA2657). In contrast, the accessions LA1656 and LA1303 displayed a significantly longer lag phase

(2.75 days [66 h] and 2.86 days [68 h], respectively) (Fig. 4A and C). Next, we observed a significantly shorter overall lag-phase duration of *S. lycopersicoides* accessions than *S. pennellii*. Accordingly, the first symptoms appeared after 1.3 days (31 h, LA2772) and the latest appeared at 1.83 days after inoculation (43 h, LA1966). The overall time till initial symptom development was more conserved; only 2 *S. lycopersicoides* accessions deviated significantly from the grand mean, being more susceptible than the overall species level (LA2776 and LA2772) (Fig. 4B and D). Similarly, we found a lack of variation in lag-phase duration in the populations of *S. pimpinellifolium*. At the same time, *S. habrochaites* accessions displayed a wider variability of lag-phase phenotypes (Fig. S2 and Table S3).

Next, we analyzed the variability of the lesion growth rate between accessions of each species using the logarithmic LDT. We observed that all tested *S. pennellii* accessions displayed an average LDT ranging from 5.84 h (LA1303) to 13.07 h (LA2963). Five accessions (LA1809, LA1282, LA2719, LA2657, and LA1303) have a significantly faster lesion development than the grand mean (LDT < 11 h). The populations LA2963 and LA1941 displayed a significantly longer LDT (13.07 and 9.8 h, respectively) (Fig. 4E and G). Generally, we found that symptoms of *S. lycopersicoides* grew significantly slower (observed range: 14.9 h to 40 h). However, we still observed a significant within-species variability. For instance, symptoms on leaves of the accession LA2951 doubled within $\text{lsmean} = 7.88 \log(\text{LDT})$ (approximately 44 h), while lesions of LA2777 expanded much faster at $\text{lsmean} = 6.8 \log(\text{LDT})$ (15 h, Fig. 4F and H). We observed a high variability among the accessions for *S. pennellii* and *S. lycopersicoides*, mostly deviating from the species mean in LDT with high significance. Interestingly, the LDT on *S. habrochaites* and *S. pimpinellifolium* appeared much more conserved between the accessions, as only a few samples significantly differed from the grand mean (Fig. S3 and Table S4).

Disease resistance measures are not linked and characterize distinct components of QDR

To test whether fungal infection is directly linked to delayed lesion growth, we conducted microscopy assays using a GFP-tagged *S. sclerotiorum* mutant of the *S. sclerotiorum* isolate 1980 [75]. We selected 2 accessions from *S. pennellii* with significantly altered lag-phase duration. At 72 h post inoculation (hpi), freshly developed mycelium was observed on leaves of the *S. pennellii* accession with the shortest lag-phase duration (LA1809). In contrast, on the less susceptible accession LA1303, the first fungal structures started growing at 96 hpi (Fig. S7). Fluorescent microscopy imaging showed that fungal mycelial structures were always accompanied by clear formation of necrotic lesions but cannot be observed prior to visual lesion development (Fig. 5C and Fig. S7). Thus, this shows that a longer lag phase does not represent any latent or biotrophic infection and that IF and lag-phase duration are likely uncoupled phenomena.

We performed a correlation analysis to consolidate the relationship between the QDR parameters further. First, we tested the overall relation of lsmean LDT and $\text{lsmean lag-phase duration}$ by pooling all accessions of all species. We found that LDT and lag phase were independent ($R = 0.14$), with no significant relationship ($P = 0.42$) (Fig. S5). We also tested the correlation between QDR mechanisms at the species level. We found only minor linear relationships between LDT and lag phase for the 4 tested species. However, we found a weak, significant negative

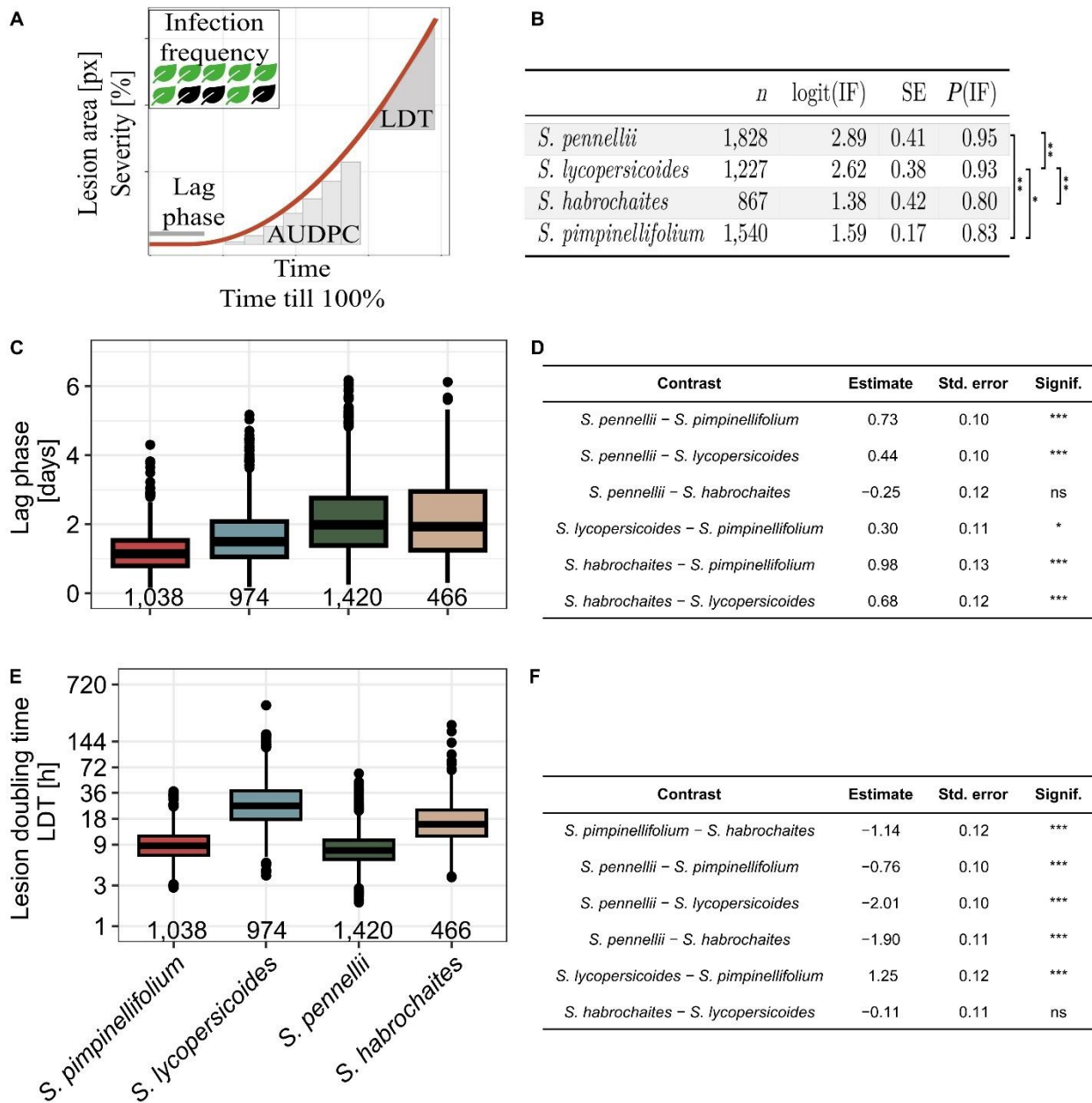


Fig. 3. Wild tomato species possess a broad diversity of resistance against *S. sclerotiorum*. (A) Exemplary illustration of different QDR parameters used in this study. The infection frequency is defined as the percentage of leaves showing a lesion after 7 days of incubation. The lag phase is defined as the time till first visual symptoms appear. We used a segmented regression analysis to determine the lag phase's end mathematically. The absolute lesion size is represented as pixel counts, whereas normalization against leaf area results in symptom severity. The area under the disease progress curve (AUDPC) is defined as the integral area under the severity curve, which depicts the severity over time. As a measure of the lesion spread, the lesion doubling time (LDT) describes the time till a lesion doubles its size. The time till a lesion covers 100% of a leaf is described by tt100%. (B) The infection frequency of *S. sclerotiorum* inoculum differs significantly between the host species. The table shows a meta-analysis of pooled accessions collected from 3 independent experiments. (C) Time till lesion formation (in days). The number on the x-axis indicates the count of individual leaves tested. (D) Statistical analysis of pairwise differences in lag-phase duration between the tested wild tomato species. Values are displayed in days and derived from a generalized least squares model. (E) Lesion growth rate during the exponential growth phase hours, plotted on a log scale. The number on the x-axis indicates the count of individual leaves tested. Raw values are plotted. (F) Statistical analysis of pairwise differences between the tested wild tomato species regarding lesion doubling time. Values are displayed as log(LDT[h]). Levels of significance are displayed as *** $P < 0.001$, ** $P < 0.01$, * $P < 0.05$, $P < 0.1$.

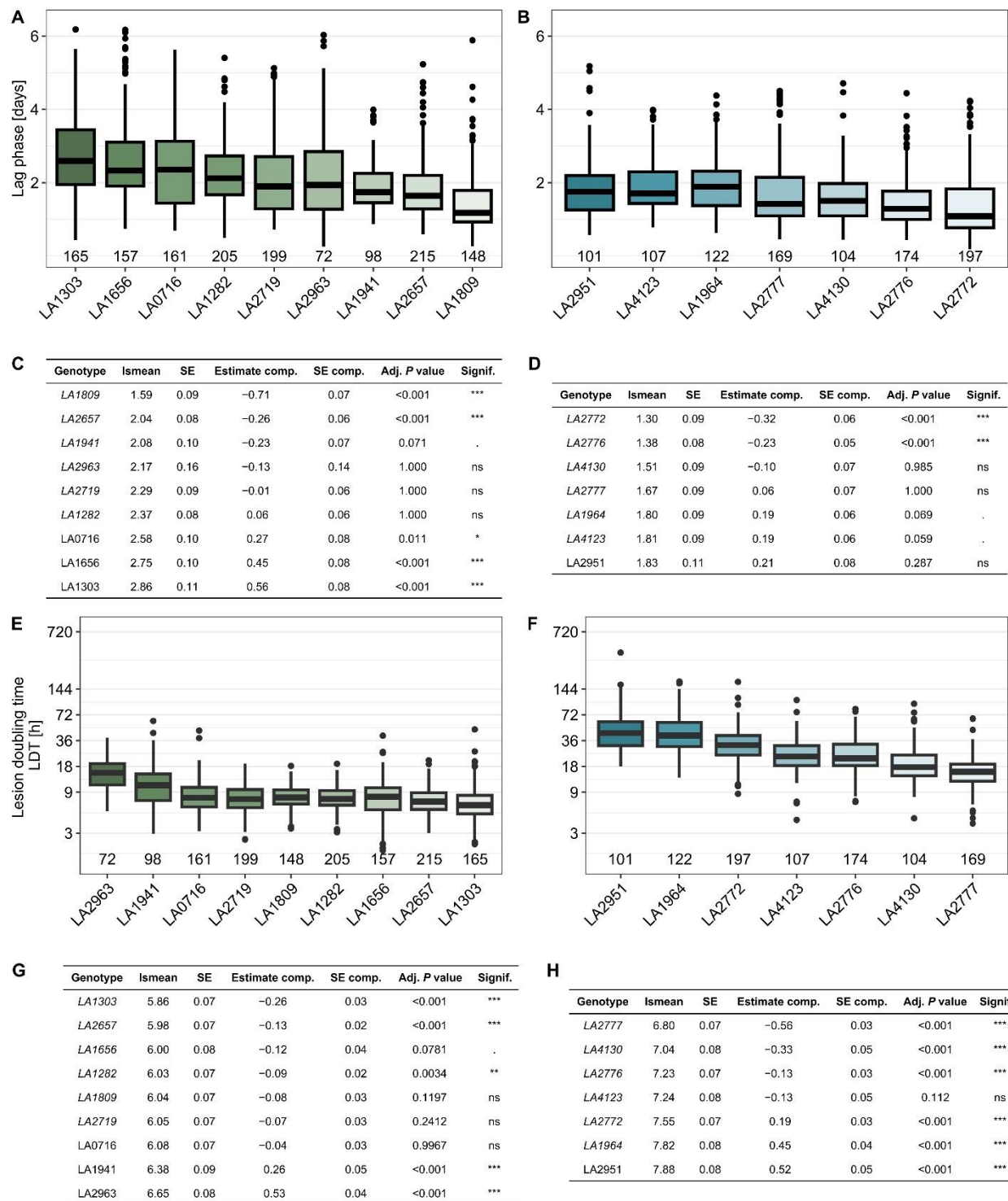


Fig. 4. QDR parameters show different levels of variation depending on the host species (*S. pennellii* and *S. lycopersicoides*). (A) The lag-phase duration (in days after infection) of *S. sclerotiorum* infection on *S. pennellii* accessions displays a higher level of intraspecific diversity than on accessions of *S. lycopersicoides* (B). (C and D) Variation statistics of the lag-phase duration contrasting each accession with the grand mean per species [*S. pennellii* (C); *S. lycopersicoides* (D)]. Estimates are displayed in days after inoculation. (E and F) The lesion doubling time (in hours) of *S. sclerotiorum* infection on *S. pennellii* accessions is lower than on *S. lycopersicoides*. (G) Variation statistics of LDT on *S. pennellii* and (H) *S. lycopersicoides*. Ismean values and SE indicate the adjusted mean and SE per population. Estimate comp., SE comp. and P values describe pairwise statistics of each accession against the grand mean. The numbers on the x-axis in panels A, B, E, and F indicate the count of individual leaves tested. Levels of significance are displayed as *** $P < 0.001$, ** $P < 0.01$, * $P < 0.05$, $P < 0.1$.

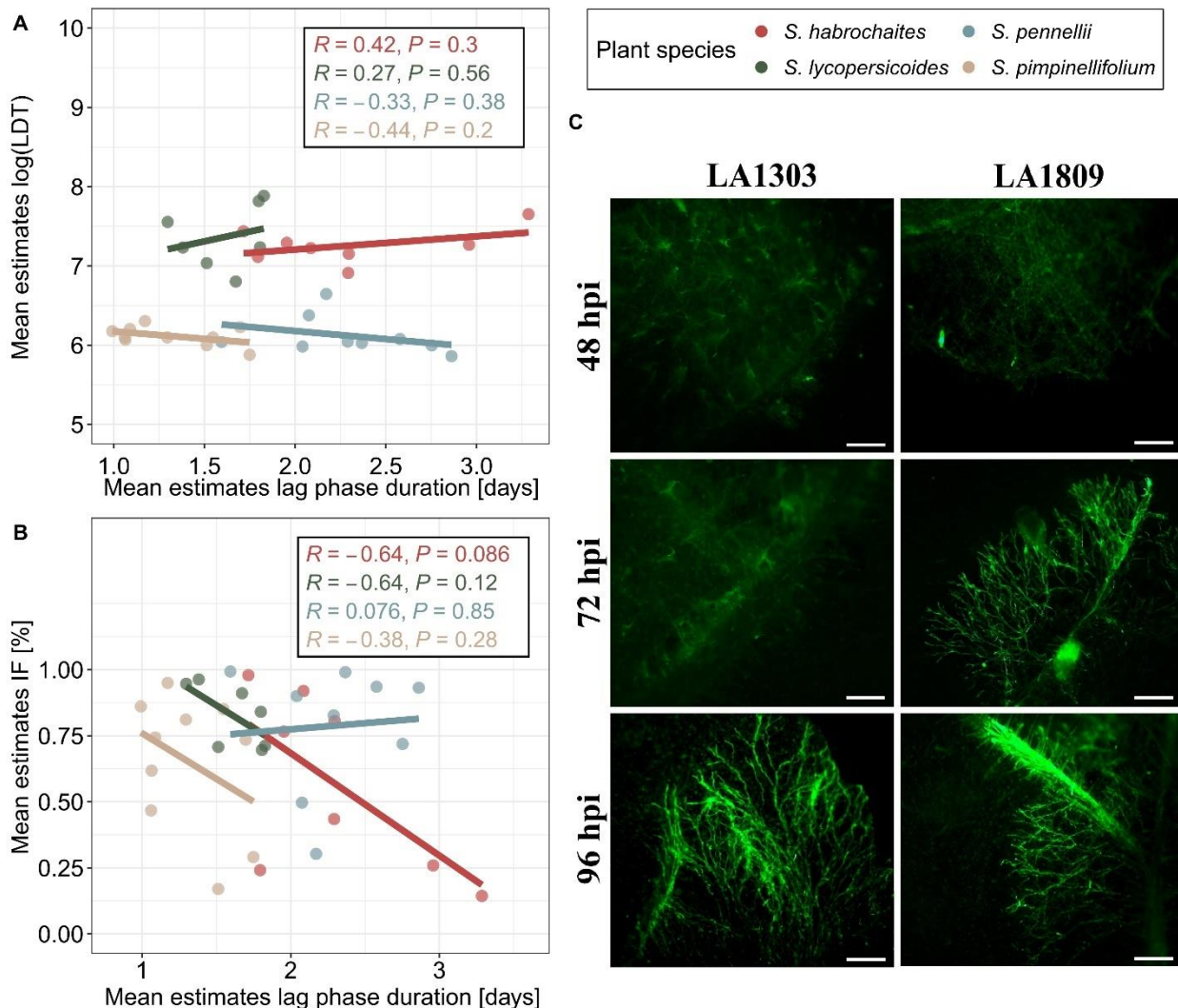


Fig. 5. Different QDR parameters are independent from each other. (A) Pearson correlation analysis of LDT and lag-phase duration. Dots represent the least squares of each accession. (B) Pearson correlation analysis between the infection frequency and lag-phase duration. Dots represent infection frequency adjusted per-accession estimates from glm/gls. (C) The lag-phase duration of *Ss1980:GFP* infection on *S. pennellii* genotypes is reflected in fungal growth dynamics. Images show a representative selection of 10 biological replicates. The scale bar indicates 500 μm .

correlation between IF and the duration of the lag phase (lsmean) in *S. habrochaites* ($R = -0.64$, $p = 0.086$) (Fig. 5A and B). For the remaining species, no significant correlation was found. We did not find a single host accession with high levels of resistance in both LDT and lag-phase duration.

Severity analysis reveals distinct resistance phenotypes against *S. sclerotiorum* within a single species

For an in-depth analysis of disease severity, we selected 3 *S. pennellii* accessions with similar leaf sizes: LA1282, LA1809, and LA1941 (Fig. 6A). While symptoms developed on most of the leaves, the impact of infection is highly dependent on the respective accession (see Fig. 6B). Accession LA1941 shows a significantly lower IF (~51%) and a significantly lower rate of fully infected leaves than LA1809 (approximately 11% vs. approximately 41%) or LA1282 (approximately 33%, Fig. 6C).

We further found differences regarding the speed of lesion growth over time between the genotypes. While lesions on LA1282 and LA1941 reached 100% severity within 6.5 to 7 days, we observed that symptoms on LA1809 reached the point of saturation significantly faster (after approximately 5 days, Fig. 7). This is also reflected by significantly increased AUDPC values of LA1809 (AUDPC approximately 250). In LA1282, we measured not only a lower AUDPC compared to LA1809 (Fig. 6E), but also an insignificant difference in the rate of fully infected leaves (Fig. 6C). This could hint toward a delayed but explosive lesion growth on LA1282 (Fig. 7).

The moderation of QDR parameters is genotype-dependent

Next, we used a linear mixed-effect model (lme) to test which of the factors have the strongest effects on disease severity on

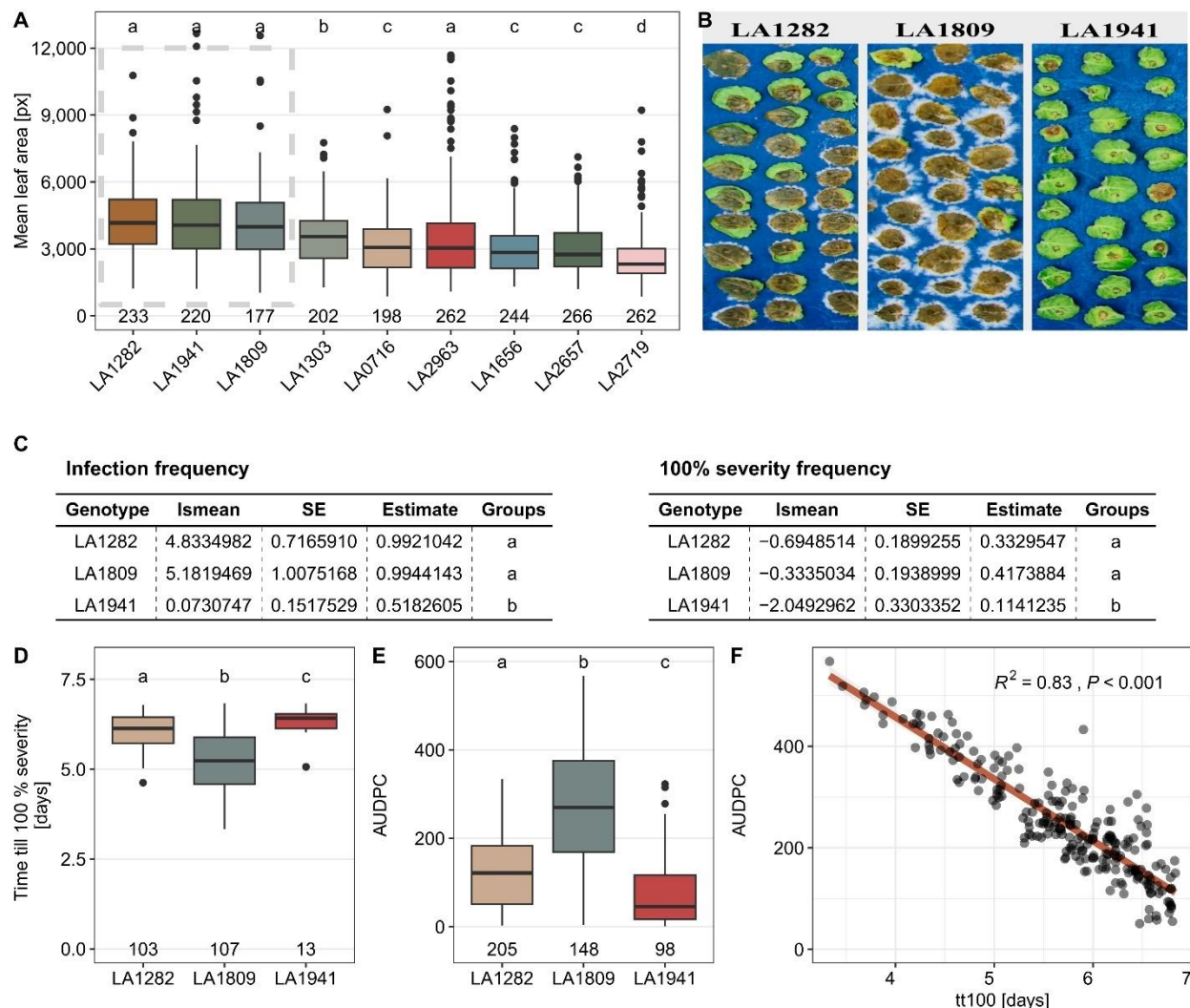


Fig. 6. *S. pennellii* accession LA1941 harbors a significantly elevated level of quantitative resistance against *S. sclerotiorum*. (A) Mean leaf area of *S. pennellii* accessions quantified during infection experiments. The data of 3 independent experiments are shown. HSD test was performed to identify cluster with similar leaf size. Selected plants with similar leaf size are indicated by the box. (B) Exemplary images of *S. sclerotiorum* infections on the *S. pennellii* populations LA1282, LA1809, and LA1941 at 7 days post-inoculation. (C) Statistical analysis of infection frequency (IF) and frequency of fully infected leaves at the end of experiment. “Ismean” represents the estimate as logits, while “estimate” represents the estimated probability. (D) Comparison of time till lesion saturation of *S. sclerotiorum* on *S. pennellii* genotypes. (E) Area under disease progress curve (AUDPC) of 3 *S. pennellii* populations with similar leaf size. Wilcoxon test was performed for levels of significance. Time series data from previous experiments was used. (F) Pearson correlation analysis of tt100 vs. AUDPC. The numbers at the base of all boxplots represent individual leaves tested. All statistics were calculated using a glm/gls with custom contrast matrices. Compact letter displays were determined using the package “multcompLetters” with a threshold of $P < 0.05$.

those accessions (*S. pennellii* LA1282, LA1809, and LA1941). Following the ANOVA, we found a significant influence of most tested variables (genotype, lag phase, and LDT) on the AUDPC (Table). Strikingly, we found that the genomic background of the tested plants is insufficient to explain the observed diversity in AUDPC. In other words, we observe a significant relationship between lag, LDT, and their interaction with the genotype. Because of this, we extracted the fixed-effect estimates from the lme and generated predictor functions for the AUDPC of each genotype. Then, we modeled the AUDPC using high-confidence lag and LDT values from previous observations (see Fig. 3C and D). We observed the highly variable influence of lag-phase duration, LDT, and their interaction on the AUDPC

(Fig. 8). Strikingly, we found that variation of the LDT has almost no influence on the AUDPC of LA1809 besides the generally elevated severity level (Fig. 8). Further, we found that only a prolonged lag-phase duration might contribute to an increased potential for lower severity in LA1809 (Fig. 8). However, the influence of longer lag phase is reduced with increasing LDT. For leaves of the accessions LA1282 and LA1941, we found a stronger combined effect of lag-phase and LDT on the severity. More specifically, a prolonged lag phase might lead to a small reduction of the symptom severity on LA1282 while reducing the AUDPC on LA1941 more rapidly. Further, we observe that a prolonged LDT reduced symptom severity in both LA1282 and LA1941.

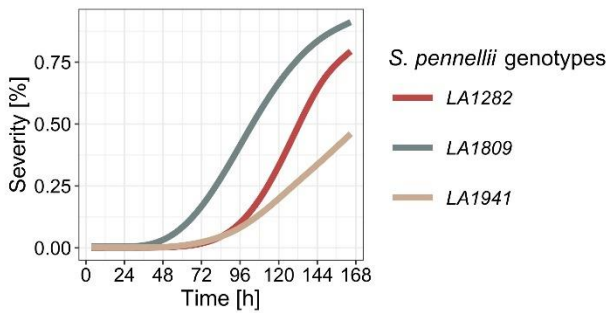


Fig. 7. Exemplary growth curve of 3 *S. pennellii* accessions with different resistance levels against *S. sclerotiorum*. Shown is the mean symptom severity of each accession as share of leaf area over the period of 7 days. The experiment was independently repeated 3 times. $n_{LA1282} = 205$, $n_{LA1809} = 148$, $n_{LA1941} = 98$.

Table. Statistical analysis of the effects of genotype, lag-phase duration, LDT, and their interactions on disease severity (AUDPC) of the *S. pennellii* accessions LA1282, LA1809, and LA1941. Results of an analysis of variance (ANOVA) based on a linear mixed-effects model are shown.

	numDF	denDF	F value	P value
Intercept	1	437	136.8	<0.001
Genotype	2	437	211.34	<0.001
Lag	1	437	251.68	<0.001
LDT	1	437	90.41	<0.001
Genotype:Lag	2	437	8.54	<0.001
Genotype:LDT	2	437	2.32	0.099
Lag:LDT	1	437	21.91	<0.001
Genotype:Lag:LDT	2	437	3.3	0.038

Discussion

QDR against *S. sclerotiorum* is highly diverse in *Solanum* spp.

Wild tomato species have been screened for quantitative resistance phenotypes against many diseases, including Tomato brown rugose fruit virus, *Phytophthora infestans*, *Alternaria solani*, *Fusarium* spp., or *B. cinerea* [8,49,50,74,76–79]. However, high hurdles in characterizing QDR on a phenotypic level limit detailed insights into the functional role of QDR against necrotrophic pathogens. This was mostly due to the lack of affordable high-throughput phenotyping facilities [1,2,5,8,80]. Here, we present a unique dataset of high-resolution QDR phenotypes against *S. sclerotiorum* on a diverse set of wild *Solanum* species derived from a low-budget phenotyping setup, using detached leaf infections. There are potential disadvantages to using detached leaf assays, i.e., the lack of feedback mechanisms between leaf and root/shoot, which could make plants more susceptible if this feedback plays a role in amplifying the defense signal, or more susceptible if this feedback provides susceptibility factors or nutrients for the pathogen. The immense gain in efficiency in both experimental setup and data analysis, together with the fact that detached leaf assays have been used successfully in tomato and with *S. sclerotiorum* and other necrotrophic leaf pathogens, justifies the decision to develop our methods for detached leaves [30,49,50,74,78]. In total, we tested almost 7,000 leaves over the duration of 7 days with approximately 1,000 measurements each, resulting in approximately 7 million data points. We used this unique dataset to characterize the lesion development of infected leaves and applied advanced statistical analysis methods to extract more specific descriptors for QDR, such as lag phase, LDT, or AUDPC [30]. Because of this system's scale and temporal resolution, we generated novel insights into the phenomena contributing to QDR.

Interspecific QDR phenotypes follow a wide distribution

As expected, we observed a diverse range of disease phenotypes, as demonstrated in previous studies [6,49,78]. None of the tested

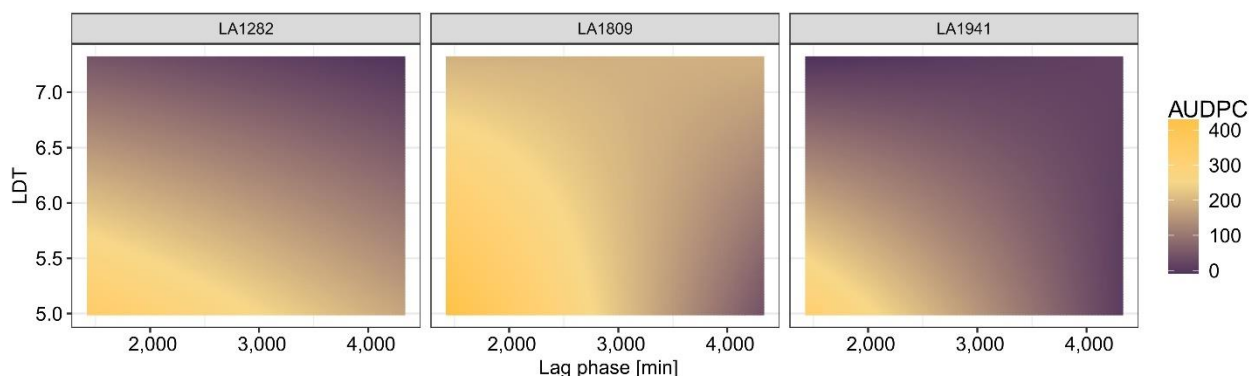


Fig. 8. The crosstalk of lag-phase duration and LDT is highly genotype-dependent and specifically determines the symptom severity. We used the *S. pennellii* accessions LA1282, LA1809, and LA1941 to test for the genotype-dependent relationship between lag and LDT. Therefore, we extracted the estimates for the factors LDT and lag per each genotype from an ANOVA based on a generalized least square model (Table 1). The per-genotype AUDPC was modeled using the extracted estimates over a range of values representing the plausible range of lag/LDT values. Crosses represent the observed mean AUDPC (Fig. 6E).

accessions carried complete resistance against *S. sclerotiorum*, although we found a wide distribution of infection phenotypes. Also, no high “universal” level of partial resistance or tolerance among multiple QDR parameters was found, as none of the species harbors significant advantages in multiple measures (IF, lag phase, or LDT). Complete resistance against *S. sclerotiorum* is rarely found in cultivated crops [32,52,60,81]. We provide evidence that the time till the emergence of the first lesions (lag phase) is highly variable within and between host species, with only *S. lycopersicoides* showing a rather conserved lag-phase duration (Fig. 4B). Interestingly, Barbacci et al. [30] reported that in *Arabidopsis thaliana*, the lag-phase duration is mostly influenced by the *S. sclerotiorum* isolate rather than the host accession. The comparably low genetic diversity of the host may have influenced the observed range of QDRs. Standing genetic variation is considered much higher in (predominantly) outcrossing *Solanum* species than in inbreeding *A. thaliana* accessions [82]. Accordingly, we assume that the influence of genetic features on the lag-phase duration depends on the specific genomic background of the host plant species. However, fungal influences on pathogenesis cannot be ignored, as the concept of the “extended phenotype”, describing the interaction of both genomes, i.e., a genotype \times genotype (G \times G) interaction for host and pathogen, for one phenotype, is well established [37,83]. Furthermore, quantitative host resistance features have been described to interact with the pathogen's genotype as described for camalexin-associated resistance [50,84].

QDR phenotypes also differ on the intraspecific level but at varying degrees

High variability of QDR phenotypes among genotypes of the same plant species has been reported on multiple hosts before [6,30,49,74,85,86]. We show that the degree of variability depends on the host species and the respective resistance parameter. Whereas LDT is rather stable among *S. pimpinellifolium* accessions, it is highly variable on *S. lycopersicoides* accessions (see Fig. 4 and Fig. S3). The specific forms of QDR phenotypes might hint at independent regulatory mechanisms and different evolutionary backgrounds with relatively recent developments, leading to genetic variation, rather than conserved QDR mechanisms. Host adaptation to natural habitats and its influence on disease resistance has been studied before [87,88]. Adaptation might explain disease phenotypes as most *S. lycopersicoides* accessions show significantly prolonged LDT. The habitat of *S. lycopersicoides* faces much more rain than the other species, leading to higher chances of successful infection events than in relatively dry habitats, thus requiring mechanisms to fight established infections. In contrast, drought-resistant *S. pennellii* has high capabilities in delaying infection events, while it lacks defense efficacy once an infection is established (Fig. 3), similar to the *S. chilense* desert population losing resistance against the fungus *Passalora fulva* [46,87,89]. However, to truly test these hypotheses, significantly higher sample sizes and infections under natural conditions would be required, possibly paired with screenings of the morphological properties of the species to assess the pleiotropic influence of habitat adaptation on QDR, e.g., via cuticle thickness or stomata density.

QDR and genotype \times genotype \times environment interactions

S. pennellii accession LA0716 was characterized as relatively resistant against *B. cinerea*, while this genotype is highly susceptible

to *S. sclerotiorum* (Fig. S6) [6]. Also in *S. chilense*, QDR phenotypes vary between the pathogen, suggesting the presence of pathogen-specific regulatory mechanisms [78]. However, the pathogen diversity tested in such studies might greatly affect the observed degree of resistance. A study with *Phytophthora infestans* on 85 *S. chilense* accessions showed that the relative differences in resistance phenotypes between individuals were mainly determined by the plant genotype, with modest effects of pathogen isolate used [49]. In contrast, large-scale screenings of infections with different *B. cinerea* isolates showed a clear genotype \times genotype (G \times G) effect both on panels of wild and domesticated tomatoes and on *A. thaliana* [37,50,74,90,91]. In addition, we have shown in *S. chilense* that QDR phenotypes, like the IF, can be correlated with the phytohormone ethylene [92]. Knowing that such phytohormonal regulation is also affected by abiotic, environmental (E) factors like temperature, humidity, and light availability, we propose that QDR polymorphism is implemented in a complex signaling network affected by G \times G \times E interactions [1,5,93,94].

QDR is determined by the interplay of QDR mechanisms

QDR is commonly defined as a highly interconnected regulatory network with an integrated, pleiotropic role in general plant metabolism [1]. Therefore, the linkage of different defense mechanisms, like IF and lag-phase duration, could be a good perspective for resistance breeding. However, we did not observe strong correlations between QDR parameters and did not find a species or accession with a universal high resistance level for all tested parameters. Disconnected QDR parameters have been reported before: *Xanthomonas axanopodis* mutants showed increased IF but a reduced lesion growth rate on cassava and *B. cinerea* showed unconnected IF and lesion expansion rates on wild tomatoes [6,95]. We used the presented phenotyping platform to show that the moderation or cross-talk between defense mechanisms is genotype-specific and differs even between accessions of the same species (Fig. 8). Based on these findings, we propose a model for QDR against necrotrophic pathogens involving 3 genetically distinct mechanisms: (a) prohibition of initial infection, (b) retardation of disease outbreaks, and (c) deceleration of ongoing infections.

Disease severity is specifically determined by genotype-dependent moderation of QDR mechanisms

We used 3 differently severely infected *S. pennellii* genotypes to describe the influence of 2 of the QDR mechanisms (retardation and deceleration of symptom development) on overall symptom severity. Interestingly, the different accessions possess diverse capabilities in moderating the QDR mechanisms, as our model-based approach indicates contrasting roles of LDT and lag-phase duration. In *A. thaliana*, it was shown that lesion traits, like lesion size or shape, are also controlled by genetically distinct mechanisms [90]. Previous work showed that defense-associated hormone responses greatly differ between different wild tomato accessions and even within the same population. In *S. chilense*, ethylene responses could only be linked to IF in one population but not in others [92]. Therefore, we argue that the orchestration of QDR measures highly depends on the specific genetic background, and future studies should determine the complex interplay between various QDR-regulating mechanisms [94].

In this study, we used a new phenotyping platform to derive different QDR-related phenotypes. The low cost and high flexibility of the system allowed us to screen a big set of diverse plants relatively fast, and therefore, we identified new genotypes with distinct QDR properties. Accordingly, we characterized accessions and species with beneficial properties as significantly longer lag-phase duration (*S. pennellii*, LA1303 and LA1656) or prolonged LDT (*S. lycopersicoides*, LA2951 and LA1964). Accordingly, we suggest that *S. pennellii* accessions are specialized in delaying lesion development, whereas *S. lycopersicoides* accessions are more capable of slowing down the spread of established lesions. Follow-up research is needed to identify the genes underlying these differences. Moreover, the influence of increasing lack of nutrition during the time of the experiment must be critically evaluated to exclude starvation-induced loss of resistance. The resolution of the present dataset will enhance the ability to predict distinct defense phases, facilitating more targeted sampling mechanisms for transcriptomic or metabolomic analysis. This can help breed durable resistance in tomato crops with delayed and less severe symptoms without inducing strong evolutionary pressure. The sustainability of major R-gene-mediated resistance (including pyramiding of such) has regularly been questioned [4,96]. Facilitating the concept of QDR is proposed to thwart the arms race between plant hosts and pathogens. QDR phenotypes specifically tolerate disease to a certain extent without applying a strong bottleneck onto the pathogen population [14]. Our findings provide major insights into the architecture of QDR mechanisms and will help in the targeted functional characterization of QDR. By disentangling end-point QDR phenotypes into discrete resistance mechanisms, the functional characterization of genetic features controlling QDR will become much more targeted. Based on this study, the factors influencing the level of QDR can be explained in much more detail.

Acknowledgments

We gratefully acknowledge Hendrik Seide, Lilly Gieseler, and Ellen Krohn for their technical support and Dr. Farooq Ahmad for his insightful feedback and discussions while writing the manuscript. We also thank the TGRC at UC Davis (USA) for seed material.

Funding: This work was partly funded by the DFG (STA1547/6 and SFB924) and the ANR (ANR-21-CE20-30) for the collaborative project ResiDEvo. Exchange visits were supported by the DAAD and the Partenariat Hubert Curien programme of Campus France.

Author contributions: R.S. and S.R. conceived this study. S.E. planned and performed the experiments. A.B. and C.T.-R. developed the image analysis pipeline. S.E. conducted all analytical steps and produced the figures. M.H. developed the statistical tests and models. S.E. and R.S. wrote the manuscript. All authors read and approved the final manuscript.

Competing interests: The authors declare that they have no competing interests.

Data Availability

Additional data can be found in the Supplementary Materials. All scripts used for this study as well as input data are available at https://github.com/seveein/phenotyping_QDR_Wild_Tomatoes.

Supplementary Materials

Figs. S1 to S9
Tables S1 to S5

References

- Poland JA, Balint-Kurti PJ, Wisser RJ, Pratt RC, Nelson RJ. Shades of gray: The world of quantitative disease resistance. *Trends Plant Sci.* 2009;14(1):21–29.
- Roux F, Voisin D, Badet T, Balagué C, Barlet X, Huard-Chauveau C, Roby D, Raffaele S. Resistance to phytopathogens *e tutti quanti*: Placing plant quantitative disease resistance on the map: Quantitative disease resistance in plants. *Mol Plant Pathol.* 2014;15(5):427–432.
- Mbengue M, Navaud O, Peyraud R, Barascud M, Badet T, Vincent R, Barbacci A, Raffaele S. Emerging trends in molecular interactions between plants and the broad host range fungal pathogens *Botrytis cinerea* and *Sclerotinia sclerotiorum*. *Front Plant Sci.* 2016;7:422.
- Brown JKM. Durable resistance of crops to disease: A Darwinian perspective. *Annu Rev Phytopathol.* 2015;53:513–539.
- Gou M, Balint-Kurti P, Xu M, Yang Q. Quantitative disease resistance: Multifaceted players in plant defense. *J Integr Plant Biol.* 2023;65(2):594–610.
- ten Have A, van Berloo R, Lindhout P, van Kan JAL. Partial stem and leaf resistance against the fungal pathogen *Botrytis cinerea* in wild relatives of tomato. *Eur J Plant Pathol.* 2007;117:153–166.
- Tian L, Li J, Xu Y, Qiu Y, Zhang Y, Li X. A MAP kinase cascade broadly regulates the lifestyle of *Sclerotinia sclerotiorum* and can be targeted by HIGS for disease control. *Plant J.* 2023;118(2):324–344.
- Corwin JA, Kliebenstein DJ. Quantitative resistance: More than just perception of a pathogen. *Plant Cell.* 2017;29(4):655–665.
- Boudhrioua C, Bastien M, Torkamaneh D, Belzile F. Genome-wide association mapping of *Sclerotinia sclerotiorum* resistance in soybean using whole-genome resequencing data. *BMC Plant Biol.* 2020;20(1):195.
- Frey LA, Vleugels T, Ruttink T, Schubiger FX, Pégard M, Skot L, Grieder C, Studer B, Roldán-Ruiz I, Kölliker R. Phenotypic variation and quantitative trait loci for resistance to southern anthracnose and clover rot in red clover. *Theor Appl Genet.* 2022;135(12):4337–4349.
- Fusari CM, Di Rienzo JA, Trogia C, Nishinakamasu V, Moreno MV, Maringolo C, Quiroz F, Álvarez D, Escande A, Hopp E, et al. Association mapping in sunflower for sclerotinia head rot resistance. *BMC Plant Biol.* 2012;12:93.
- Wu J, Cai G, Tu J, Li L, Liu S, Luo X, Zhou L, Fan C, Zhou Y. Identification of QTLs for resistance to *Sclerotinia* stem rot and BnC.IGMT5.A as a candidate gene of the major resistant QTL SRC6 in *Brassica napus*. *PLoS One.* 2013;8(7):Article e67740.
- Derbyshire M, Denton-Giles M, Hegedus D, Seifbarghy S, Rollins J, Van Kan J, Seidl MF, Faino L, Mbengue M, Navaud O, et al. The complete genome sequence of the phytopathogenic fungus *Sclerotinia sclerotiorum* reveals insights into the genome architecture of broad host range pathogens. *Genome Biol Evol.* 2017;9(3):593–618.
- Willoquet L, Savary S, Yuen J. Multiscale phenotyping and decision strategies in breeding for resistance. *Trends Plant Sci.* 2017;22(5):420–432.

15. Dracatos PM, Lück S, Douchkov DK. Diversifying resistance mechanisms in cereal crops using microphenomics. *Plant Phenomics*. 2023;5:0023.
16. Walsh JJ, Mangina E, Negrão S. Advancements in imaging sensors and AI for plant stress detection: A systematic literature review. *Plant Phenomics*. 2024;6:0153.
17. Fahlgren N, Feldman M, Gehan MA, Wilson MS, Shyu C, Bryant DW, Hill ST, McEntee CJ, Warnasooriya SN, Kumar I, et al. A versatile phenotyping system and analytics platform reveals diverse temporal responses to water availability in *Setaria*. *Mol Plant*. 2015;8(10):1520–1535.
18. Watt M, Fiorani F, Usadel B, Rascher U, Muller O, Schurr U. Phenotyping: New windows into the plant for breeders. *Annu Rev Plant Biol*. 2020;71:689–712.
19. Bock CH, Barbedo JGA, Del Ponte EM, Bohnenkamp D, Mahlein A-K. From visual estimates to fully automated sensor-based measurements of plant disease severity: Status and challenges for improving accuracy. *Phytopathol Res*. 2020;2:9.
20. Mahlein A-K. Plant disease detection by imaging sensors—Parallels and specific demands for precision agriculture and plant phenotyping. *Plant Dis*. 2016;100(2):241–251.
21. Mahlein A-K, Kuska MT, Thomas S, Wahabzada M, Behmann J, Rascher U, Kersting K. Quantitative and qualitative phenotyping of disease resistance of crops by hyperspectral sensors: Seamless interlocking of phytopathology, sensors, and machine learning is needed! *Curr Opin Plant Biol*. 2019;50:156–162.
22. Mutka AM, Bart RS. Image-based phenotyping of plant disease symptoms. *Front Plant Sci*. 2015;5:734.
23. Simko I, Jimenez-Berni JA, Sirault XRR. Phenomic approaches and tools for phytopathologists. *Phytopathology*. 2017;107(1):6–17.
24. Tanner F, Tonn S, de Wit J, Van den Ackerveken G, Berger B, Plett D. Sensor-based phenotyping of above-ground plant-pathogen interactions. *Plant Methods*. 2022;18(1):35.
25. Anim-Ayeko AO, Schillaci C, Lipani A. Automatic blight disease detection in potato (*Solanum tuberosum* L.) and tomato (*Solanum lycopersicum*, L. 1753) plants using deep learning. *Smart Agric Technol*. 2023;4:100178.
26. Kuska MT, Heim RHJ, Geedicke I, Gold KM, Brugger A, Paulus S. Digital plant pathology: A foundation and guide to modern agriculture. *J Plant Dis Prot*. 2022;129(3):457–468.
27. Tang Z, He X, Zhou G, Chen A, Wang Y, Li L, Hu Y. A precise image-based tomato leaf disease detection approach using PLPNet. *Plant Phenomics*. 2023;5:0042.
28. Kersting K, Bauckhage C, Wahabzada M, Mahlein A-K, Steiner U, Oerke E-C, Römer C, Plümer L. Feeding the world with big data: Uncovering spectral characteristics and dynamics of stressed plants. In: Lässig J, Kersting K, Morik K, editors. *Computational sustainability*. Cham: Springer International Publishing; 2016. p. 99–120.
29. Poorter H, Hummel GM, Nagel KA, Fiorani F, Von Gillhaussen P, Virnich O, Schurr U, Postma JA, Van De Zedde R, Wiese-Klinkenberg A. Pitfalls and potential of high-throughput plant phenotyping platforms. *Front Plant Sci*. 2023;14:1233794.
30. Barbacci A, Navaud O, Mbengue M, Barascud M, Godiard L, Khafif M, Lacaze A, Raffaele S. Rapid identification of an Arabidopsis NLR gene as a candidate conferring susceptibility to *Sclerotinia sclerotiorum* using time-resolved automated phenotyping. *Plant J*. 2020;103(2):903–917.
31. FAO. Agricultural production statistics 2000–2022. FAO. 2023. <https://doi.org/https://doi.org/10.4060/cc9205en>
32. Bolton MD, Thomma BPHJ, Nelson BD. *Sclerotinia sclerotiorum* (lib.) de Bary: Biology and molecular traits of a cosmopolitan pathogen. *Mol Plant Pathol*. 2006;7(1):1–16.
33. Foolad MR, Merk HL, Ashrafi H. Genetics, genomics and breeding of late blight and early blight resistance in tomato. *Crit Rev Plant Sci*. 2008;27(2):75–107.
34. Schmey T, Tominello-Ramirez CS, Brune C, Stam R. *Alternaria* diseases on potato and tomato. *Mol Plant Pathol*. 2024;25(3):Article e13435.
35. Zalom FG. Pests, endangered pesticides and processing tomatoes. *Acta Hort*. 2003;223–233.
36. Einspanier S, Susanto T, Metz N, Wolters PJ, Vleeshouwers VGAA, Lankinen A, Liljeroth E, Landschoot S, Ivanović Ž, Hüchelhoven R, et al. Whole-genome sequencing elucidates the species-wide diversity and evolution of fungicide resistance in the early blight pathogen *Alternaria solani*. *Evol Appl*. 2022;15(10):1605–1620.
37. Rowe HC, Kliebenstein DJ. All mold is not alike: The importance of intraspecific diversity in necrotrophic plant pathogens. *PLoS Pathog*. 2010;6(3):Article e1000759.
38. Schmey T, Small C, Einspanier S, Hoyoz LM, Ali T, Gamboa S, Mamani B, Sepulveda GC, Thines M, Stam R. Small-spored *Alternaria* spp. (section *Alternaria*) are common pathogens on wild tomato species. *Environ Microbiol*. 2023;25(10):1830–1846.
39. Silva RA, Lehner MS, Paula Júnior TJ, Mizubuti ESG. Fungicide sensitivity of isolates of *Sclerotinia sclerotiorum* from different hosts and regions in Brazil and phenotypic instability of thiophanate-methyl resistant isolates. *Trop Plant Pathol*. 2024;49:93–103.
40. Wang Q, Mao Y, Li S, Li T, Wang J, Zhou M, Duan Y. Molecular mechanism of *Sclerotinia sclerotiorum* resistance to succinate dehydrogenase inhibitor fungicides. *J Agric Food Chem*. 2022;70(23):7039–7048.
41. Bolger A, Scossa F, Bolger ME, Lanz C, Maumus F, Tohge T, Quesneville H, Alseekh S, Sørensen I, Lichtenstein G, et al. The genome of the stress-tolerant wild tomato species *Solanum pennellii*. *Nat Genet*. 2014;46(9):1034–1038.
42. Rebetzke GJ, Jimenez-Berni J, Fischer RA, Deery DM, Smith DJ. Review: High-throughput phenotyping to enhance the use of crop genetic resources. *Plant Sci*. 2019;282:40–48.
43. Pease JB, Haak DC, Hahn MW, Moyle LC. Phylogenomics reveals three sources of adaptive variation during a rapid radiation. *PLoS Biol*. 2016;14(2):Article e1002379.
44. Böndel KB, Lainer H, Nosenko T, Mboup M, Tellier A, Stephan W. North–south colonization associated with local adaptation of the wild tomato species *Solanum chilense*. *Mol Biol Evol*. 2015;32(11):2932–2943.
45. Fischer I, Camus-Kulandaivelu L, Allal F, Stephan W. Adaptation to drought in two wild tomato species: The evolution of the *Asr* gene family. *New Phytol*. 2011;190(4):1032–1044.
46. Kahn TL, Fender SE, Bray EA, O'Connell MA. Characterization of expression of drought- and abscisic acid-regulated tomato genes in the drought-resistant species *Lycopersicon pennellii*. *Plant Physiol*. 1993;103(2):597–605.
47. Nosenko T, Böndel KB, Kumpfmüller G, Stephan W. Adaptation to low temperatures in the wild tomato species *Solanum chilense*. *Mol Ecol*. 2016;25(12):2853–2869.

48. Stam R, Nosenko T, Hörger AC, Stephan W, Seidel M, Kuhn JMM, Haberer G, Tellier A. The de novo reference genome and transcriptome assemblies of the wild tomato species *Solanum chilense* highlights birth and death of NLR genes between tomato species. *G3*. 2019;9(12):3933–3941.
49. Kahlon PS, Verin M, Hükelhoven R, Stam R. Quantitative resistance differences between and within natural populations of *Solanum chilense* against the oomycete pathogen *Phytophthora infestans*. *Ecol Evol*. 2021;11(12):7768–7778.
50. Soltis NE, Atwell S, Shi G, Fordyce R, Gwinner R, Gao D, Shafi A, Kliebenstein DJ. Interactions of tomato and *Botrytis cinerea* genetic diversity: Parsing the contributions of host differentiation, domestication, and pathogen variation. *Plant Cell*. 2019;31(2):502–519.
51. Boland GJ, Hall R. Index of plant hosts of *Sclerotinia sclerotiorum*. *Can J Plant Pathol*. 1994;16(2):93–108.
52. Derbyshire MC, Denton-Giles M. The control of sclerotinia stem rot on oilseed rape (*Brassica napus*): Current practices and future opportunities. *Plant Pathol*. 2016;65(6):859–877.
53. Mazumdar P. Sclerotinia stem rot in tomato: A review on biology, pathogenicity, disease management and future research priorities. *J Plant Dis Prot*. 2021;128:1403–1431.
54. O'Sullivan CA, Belt K, Thatcher LF. Tackling control of a cosmopolitan phytopathogen: *Sclerotinia*. *Front Plant Sci*. 2021;12:Article 707509.
55. Chen J, Ullah C, Giddings Vassão D, Reichelt M, Gershenzon J, Hammerbacher A. *Sclerotinia sclerotiorum* infection triggers changes in primary and secondary metabolism in *Arabidopsis thaliana*. *Phytopathology*. 2021;111(3):559–569.
56. Sucher J, Mbengue M, Dresen A, Barascud M, Didelon M, Barbacci A, Raffaele S. Phylotranscriptomics of the Pentapetalae reveals frequent regulatory variation in plant local responses to the fungal pathogen *Sclerotinia sclerotiorum*. *Plant Cell*. 2020;32(6):1820–1844.
57. Uloth MB, You MP, Finnegan PM, Banga SS, Banga SK, Sandhu PS, Yi H, Salisbury PA, Barbeti MJ. New sources of resistance to *Sclerotinia sclerotiorum* for crucifer crops. *Field Crop Res*. 2013;154:40–52.
58. Wei D, Mei J, Fu Y, Disi JO, Li J, Qian W. Quantitative trait loci analyses for resistance to *Sclerotinia sclerotiorum* and flowering time in *Brassica napus*. *Mol Breed*. 2014;34:1797–1804.
59. Williams B, Kabbage M, Kim H-J, Britt R, Dickman MB. Tipping the balance: *Sclerotinia sclerotiorum* secreted oxalic acid suppresses host defenses by manipulating the host redox environment. *PLoS Pathog*. 2011;7(6):Article e1002107.
60. Wang Z, Ma L-Y, Cao J, Li Y-L, Ding L-N, Zhu K-M, Yang Y-H, Tan X-L. Recent advances in mechanisms of plant defense to *Sclerotinia sclerotiorum*. *Front Plant Sci*. 2019;10:1314.
61. Badet T, Voisin D, Mbengue M, Barascud M, Sucher J, Sadon P, Balagué C, Roby D, Raffaele S. Parallel evolution of the POQR prolyl oligo peptidase gene conferring plant quantitative disease resistance. *PLoS Genet*. 2017;13(12):Article e1007143.
62. Li R, Rimmer R, Buchwaldt L, Sharpe AG, Séguin-Swartz G, Coutu C, Hegedus DD. Interaction of *Sclerotinia sclerotiorum* with a resistant *Brassica napus* cultivar: Expressed sequence tag analysis identifies genes associated with fungal pathogenesis. *Fungal Genet Biol*. 2004;41(8):735–753.
63. Gehan MA, Fahlgren N, Abbasi A, Berry JC, Callen ST, Chavez L, Doust AN, Feldman MJ, Gilbert KB, Hodge JG, et al. PlantCV v2: Image analysis software for high-throughput plant phenotyping. *PeerJ*. 2017;5:Article e4088.
64. R Core Team. *R: A language and environment for statistical computing*. Vienna (Austria): R Foundation for Statistical Computing; 2022. <https://www.R-project.org/>.
65. Wickham H, Averick M, Bryan J, Chang W, McGowan LD, François R, Grolemund G, Hayes A, Henry L, Hester J, et al. Welcome to the tidyverse. *J Open Source Softw*. 2019;4(43):1686.
66. Wickham H. *ggplot2*. New York (NY): Springer New York; 2009. <https://doi.org/https://doi.org/10.1007/978-0-387-98141-3>
67. Kassambara A. *ggpubr: “ggplot2” Based Publication Ready Plots*. 2023. <https://CRAN.R-project.org/package=ggpubr>
68. de Mendiburu F, Yaseen M. *Agricolae: Statistical procedures for agricultural research*; 2020. <https://CRAN.R-project.org/package=agricolae>
69. Carroll RJ, Ruppert D. *Transformation and weighting in regression*. New York: Chapman and Hall; 1988.
70. McCullagh P, Nelder JA. *Generalized linear models*. 2nd ed. [Nachdr.]. London: Chapman & Hall; 1999.
71. Nakagawa S, Schielzeth H. A general and simple method for obtaining R^2 from generalized linear mixed-effects models. *Methods Ecol Evol*. 2013;4(2):133–142.
72. Bretz F, Hothorn T, Westfall P. *Multiple comparisons using R*. 0 ed. Chapman and Hall/CRC; 2016.
73. Hothorn T, Bretz F, Westfall P. Simultaneous inference in general parametric models. *Biom J*. 2008;50(3):346–363.
74. Caseys C, Shi G, Soltis N, Gwinner R, Corwin J, Atwell S, Kliebenstein DJ. Quantitative interactions: The disease outcome of *Botrytis cinerea* across the plant kingdom. *G3*. 2021;11(8):jkab175.
75. Badet T, Léger O, Barascud M, Voisin D, Sadon P, Vincent R, Le Ru A, Balagué C, Roby D, Raffaele S. Expression polymorphism at the *ARPC4* locus links the actin cytoskeleton with quantitative disease resistance to *Sclerotinia sclerotiorum* in *Arabidopsis thaliana*. *New Phytol*. 2019;222(1):480–496.
76. Foolad R, Zhang P, Khan AA, Niño-Liu D, Lin Y. Identification of QTLs for early blight (*Alternaria solani*) resistance in tomato using backcross populations of a *Lycopersicon esculentum* × *L. hirsutum* cross. *Theor Appl Genet*. 2002;104(6-7):945–958.
77. Kabas A, Fidan H, Kucukaydin H, Atan HN. Screening of wild tomato species and interspecific hybrids for resistance/tolerance to tomato brown rugose fruit virus (ToBRFV). *Chil J Agric Res*. 2022;82(1):189–196.
78. Stam R, Scheikl D, Tellier A. The wild tomato species *Solanum chilense* shows variation in pathogen resistance between geographically distinct populations. *PeerJ*. 2017;5:Article e2910.
79. Zhang LP, Lin GY, Niño-Liu D, Foolad MR. Mapping QTLs conferring early blight (*Alternaria solani*) resistance in a *Lycopersicon esculentum* × *L. hirsutum* cross by selective genotyping. *Mol Breed*. 2003;12(1):3–19.
80. Méline V, Caldwell DL, Kim B, Khangura RS, Baireddy S, Yang C, Sparks EE, Dilkes B, Delp EJ, Iyer-Pascuzzi AS. Image-based assessment of plant disease progression identifies new genetic loci for resistance to *Ralstonia solanacearum* in tomato. *Plant J*. 2023;113(5):887–903.
81. Ding L-N, Li T, Guo X-J, Li M, Liu X-Y, Cao J, Tan X-L. Sclerotinia stem rot resistance in rapeseed: Recent progress and future prospects. *J Agric Food Chem*. 2021;69(10):2965–2978.
82. Peralta IE, Spooner DM, Knapp S. Taxonomy of wild tomatoes and their relatives (*Solanum* sect. *Lycopersicoides*, sect

- Juglandifolia*, sect *Lycopersicon*; Solanaceae). *Am Soc Plant Taxonomists*. 2008;84:186.
83. Lambrechts L, Fellous S, Koella JC. Coevolutionary interactions between host and parasite genotypes. *Trends Parasitol*. 2006;22(1):12–16.
 84. Pedras MSC, Hossain S, Snitynsky RB. Detoxification of cruciferous phytoalexins in *Botrytis cinerea*: Spontaneous dimerization of a camalexin metabolite. *Phytochemistry*. 2011;72(2-3):199–206.
 85. Chauhan S, Katoch S, Sharma SK, Sharma PN, Rana JC, Singh K, Singh M. Screening and identification of resistant sources against *Sclerotinia sclerotiorum* causing white mold disease in common bean. *Crop Sci*. 2020;60(4):1986–1996.
 86. Yanar Y, Miller SA. Resistance of pepper cultivars and accessions of *capsicum* spp. to *Sclerotinia sclerotiorum*. *Plant Dis*. 2003;87(3):303–307.
 87. Kahlon PS, Seta SM, Zander G, Scheikl D, Hükelhoven R, Joosten MHAJ, Stam R. Population studies of the wild tomato species *Solanum chilense* reveal geographically structured major gene-mediated pathogen resistance. *Proc Biol Sci*. 2020;287(1941):20202723.
 88. Stam R, Silva-Arias GA, Tellier A. Subsets of NLR genes show differential signatures of adaptation during colonization of new habitats. *New Phytol*. 2019;224(1):367–379.
 89. Rick CM. Potential genetic resources in tomato species: Clues from observations in native habitats. In: Srb AM, editor. *Genes, enzymes and populations*. Boston (MA): Springer US; 1973. p. 255–269.
 90. Fordyce RF, Soltis NE, Caseys C, Gwinner R, Corwin JA, Atwell S, Copeland D, Feusier J, Subedy A, Eshbaugh R, et al. Digital imaging combined with genome-wide association mapping links loci to plant-pathogen interaction traits. *Plant Physiol*. 2018;178(3):1406–1422.
 91. Soltis NE, Caseys C, Zhang W, Corwin JA, Atwell S, Kliebenstein DJ. Pathogen genetic control of transcriptome variation in the *Arabidopsis thaliana*–*Botrytis cinerea* pathosystem. *Genetics*. 2020;215(1):253–266.
 92. Kahlon PS, Förner A, Muser M, Oubounyt M, Gigl M, Hammerl R, Baumbach J, Hükelhoven R, Dawid C, Stam R. Laminarin-triggered defence responses are geographically dependent in natural populations of *Solanum chilense*. *J Exp Bot*. 2023;74(10):erad087.
 93. Altmann M, Altmann S, Rodriguez PA, Weller B, Elorduy Vergara L, Palme J, Marín-de La Rosa N, Sauer M, Wenig M, Villacéja-Aguilar JA, et al. Extensive signal integration by the phytohormone protein network. *Nature*. 2020;583(7815):271–276.
 94. Kahlon PS, Stam R. Polymorphisms in plants to restrict losses to pathogens: From gene family expansions to complex network evolution. *Curr Opin Plant Biol*. 2021;62:Article 102040.
 95. Mutka AM, Fentress SJ, Sher JW, Berry JC, Pretz C, Nusinow DA, Bart R. Quantitative, image-based phenotyping methods provide insight into spatial and temporal dimensions of plant disease. *Plant Physiol*. 2016;172(2):650–660.
 96. Stam R, McDonald BA. When resistance gene pyramids are not durable—The role of pathogen diversity: R-gene pyramid durability and pathogen diversity. *Mol Plant Pathol*. 2018;19(3):521–524.

Supplementary Materials for:

High-resolution disease phenotyping reveals distinct resistance mechanisms of wild tomato crop wild relatives against *Sclerotinia sclerotiorum*

Short title: Wild tomatoes harbour unique QDR mechanisms

In: Plant Phenomics

Authors

Severin Einspanier¹, Christopher Tominello-Ramirez¹, Mario Hasler², Adelin Barbacci³, Sylvain Raffaele³, Remco Stam^{1*}

¹ Department of Phytopathology and Crop Protection, Institute of Phytopathology, Faculty of Agricultural and Nutritional Sciences, Christian Albrechts University, Kiel, Germany

² Lehrfach Variationsstatistik, Faculty of Agricultural and Nutritional Sciences, Christian-Albrechts-University of Kiel, Hermann-Rodewald-Straße 9, 24118 Kiel, Germany

³ Laboratoire des Interactions Plantes Microorganismes Environnement (LIPME), INRAE, CNRS, Castanet Tolosan Cedex, France.

* Address correspondence to: Remco.Stam@phytomed.uni-kiel.de

Supplementary Material

Tables

Suppl. Table 1 Estimate Means lag-phase duration per species.

Suppl. Table 2: Estimate Means LDT

Suppl. Table 3: Grand Mean contrasts lag

Suppl. Table 4: Grand Mean contrasts LDT

Suppl. Table 5: *Solanum* accessions used in this study

Figures

Suppl. Figure 1: Exemplary schematic of the “navautron” phenotyping platform.

Suppl. Figure 2: Lag-phase duration shows different levels of variation depending on the host species.

Suppl. Figure 3: LDT shows different levels of variation depending on the host species.

Suppl. Figure 4: Per-accession infection frequency estimates. Values derived from a glm on three independent repetitions.

Suppl. Figure 5: Correlation analysis between Infection frequency estimates and LDT.

Suppl. Figure 6: Pooled correlation analysis of all accessions.

Suppl. Figure 7: Bright light microscopy images of *S. sclerotiorum* infections on two *S. pennellii* accessions with different lag phase durations.

Suppl. Figure 8: Residual plot of lag-phase duration values.

Suppl. Figure 9: Residual plot of LDT values.

Tables

Suppl. Table 1: Estimate Means lag-phase duration per species.

Species	Lag estimate [h]	std.error [h]
<i>S. habrochaites</i>	59.74	3.10
<i>S. lycopersicoides</i>	43.32	2.71
<i>S. pennellii</i>	59.87	2.71
<i>S. pimpinellifolium</i>	36.22	0.89

Suppl. Table 2: Estimate Means LDT

Species	LDT-estimate [h]	std.error [h]
<i>S. habrochaites</i>	36.85	0.02
<i>S. lycopersicoides</i>	41.13	0.02
<i>S. pennellii</i>	11.80	0.02
<i>S. pimpinellifolium</i>	11.77	0.02

Suppl. Table 3: Grand Mean contrasts lag

Species	Accession	estimate (h)	std.error	statistic	adj.p.value	signif
<i>S. habrochaites</i>	LA1721	-13.9805	3.2319	-0.0721	0.0006	***
<i>S. habrochaites</i>	LA2167	-12.0752	3.2768	-0.0614	0.0078	**
<i>S. habrochaites</i>	LA1559	-8.2475	2.3949	-0.0574	0.0191	*
<i>S. habrochaites</i>	LA1731	-5.0888	3.3181	-0.0256	0.9840	ns
<i>S. habrochaites</i>	LA2128	-0.1378	5.7960	-0.0004	1.0000	ns
<i>S. habrochaites</i>	LA2409	-0.0536	2.5831	-0.0003	1.0000	ns
<i>S. habrochaites</i>	LA1753	15.8582	5.5225	0.0479	0.1275	ns
<i>S. habrochaites</i>	LA2864	23.7252	6.5906	0.0600	0.0107	*
<i>S. pennellii</i>	LA1809	-17.0236	1.6687	-0.1700	0.0000	***
<i>S. pennellii</i>	LA2657	-6.3068	1.3466	-0.0781	0.0001	***
<i>S. pennellii</i>	LA1941	-5.4652	1.7853	-0.0510	0.0713	.
<i>S. pennellii</i>	LA2963	-3.1692	3.2787	-0.0161	1.0000	ns
<i>S. pennellii</i>	LA2719	-0.3337	1.5238	-0.0036	1.0000	ns
<i>S. pennellii</i>	LA1282	1.5361	1.3216	0.0194	0.9998	ns
<i>S. pennellii</i>	LA0716	6.5780	1.8289	0.0599	0.0108	*
<i>S. pennellii</i>	LA1656	10.7843	1.8850	0.0954	0.0000	***
<i>S. pennellii</i>	LA1303	13.4000	1.9487	0.1146	0.0000	***
<i>S. lycopersicoides</i>	LA2772	-7.6031	1.5262	-0.0830	0.0000	***
<i>S. lycopersicoides</i>	LA2776	-5.5762	1.2054	-0.0771	0.0001	***
<i>S. lycopersicoides</i>	LA4130	-2.4261	1.5880	-0.0255	0.9847	ns
<i>S. lycopersicoides</i>	LA2777	1.4128	1.5828	0.0149	1.0000	ns
<i>S. lycopersicoides</i>	LA1964	4.4474	1.4488	0.0512	0.0693	.
<i>S. lycopersicoides</i>	LA4123	4.6261	1.4813	0.0520	0.0584	.
<i>S. lycopersicoides</i>	LA2951	5.1190	1.9937	0.0428	0.2865	ns
<i>S. pimpinellifolium</i>	LA1593	-7.8207	0.8582	-0.1519	0.0000	***
<i>S. pimpinellifolium</i>	LA2853	-6.1720	1.5283	-0.0673	0.0018	**
<i>S. pimpinellifolium</i>	LA1374	-6.0821	1.1340	-0.0894	0.0000	***
<i>S. pimpinellifolium</i>	LA1332	-5.4925	1.1039	-0.0829	0.0000	***
<i>S. pimpinellifolium</i>	LA1261	-3.5010	1.6940	-0.0344	0.7161	ns
<i>S. pimpinellifolium</i>	LA1659	-0.5469	0.8171	-0.0112	1.0000	ns
<i>S. pimpinellifolium</i>	LA4713	4.6669	4.1684	0.0187	0.9999	ns
<i>S. pimpinellifolium</i>	LA2347	5.5052	1.0240	0.0896	0.0000	***
<i>S. pimpinellifolium</i>	LA1348	9.0943	1.1659	0.1300	0.0000	***
<i>S. pimpinellifolium</i>	LA2983	10.3488	1.5771	0.1094	0.0000	***

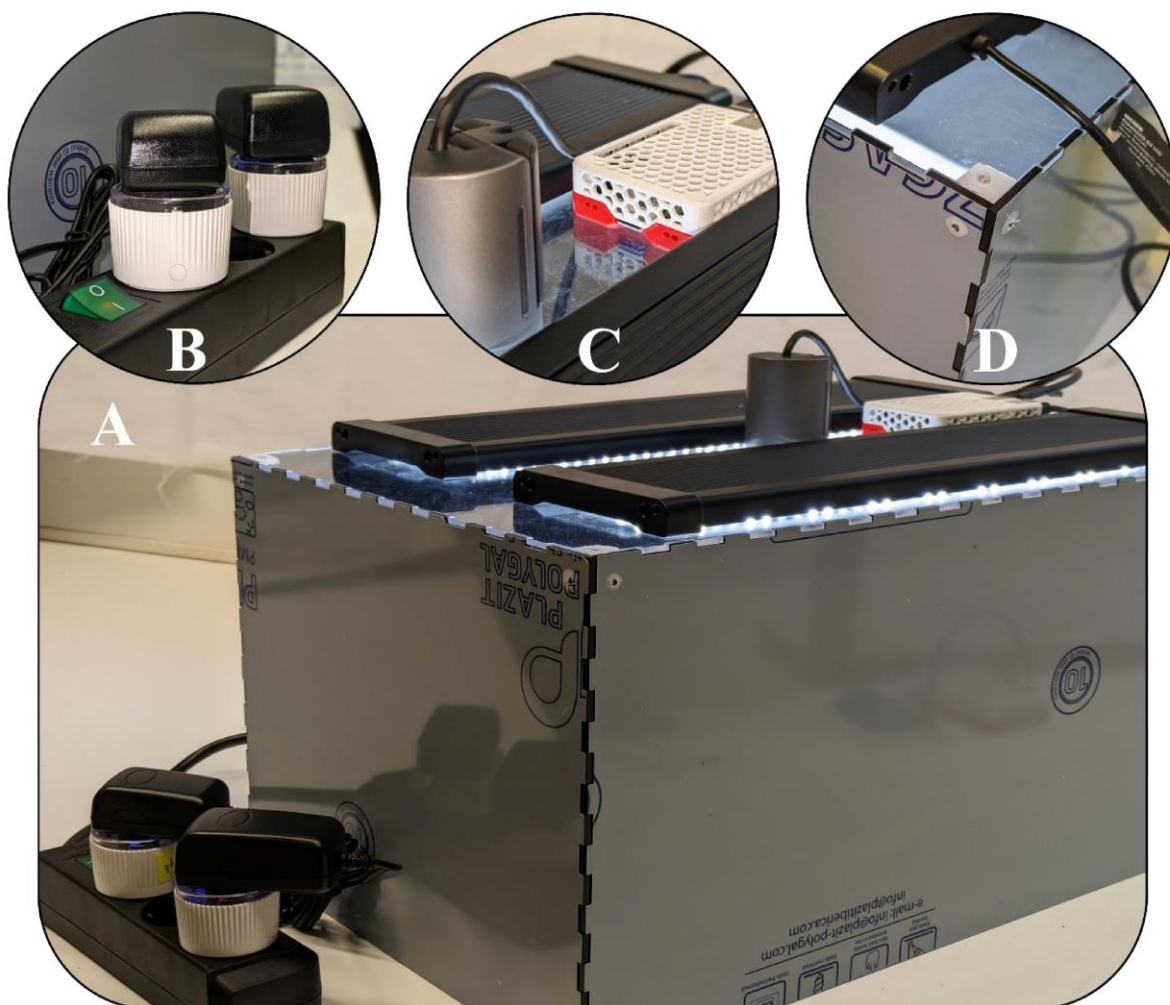
Suppl. Table 4: Grand Mean contrasts LDT

Species	Accession	Estimate	Std.Error	Statistic	Adj.p.value	signif.
<i>S. habrochaites</i>	LA2128	-0.3450	0.0984	-3.5052	0.0154	*
<i>S. habrochaites</i>	LA2167	-0.1418	0.0797	-1.7798	0.9157	ns
<i>S. habrochaites</i>	LA2409	-0.1036	0.0609	-1.7024	0.9466	ns
<i>S. habrochaites</i>	LA1731	-0.0322	0.0661	-0.4866	1.0000	ns
<i>S. habrochaites</i>	LA1753	0.0102	0.0890	0.1143	1.0000	ns
<i>S. habrochaites</i>	LA1559	0.0349	0.0619	0.5633	1.0000	ns
<i>S. habrochaites</i>	LA1721	0.1810	0.0837	2.1633	0.6332	ns
<i>S. habrochaites</i>	LA2864	0.3965	0.1654	2.3970	0.4207	ns
<i>S. lycopersicoides</i>	LA2777	-0.5631	0.0319	-17.6649	0.0000	***
<i>S. lycopersicoides</i>	LA4130	-0.3304	0.0469	-7.0464	0.0000	***
<i>S. lycopersicoides</i>	LA2776	-0.1336	0.0311	-4.2920	0.0006	***
<i>S. lycopersicoides</i>	LA4123	-0.1313	0.0450	-2.9176	0.1119	ns
<i>S. lycopersicoides</i>	LA2772	0.1880	0.0298	6.3131	0.0000	***
<i>S. lycopersicoides</i>	LA1964	0.4522	0.0423	10.6881	0.0000	***
<i>S. lycopersicoides</i>	LA2951	0.5182	0.0463	11.2031	0.0000	***
<i>S. pennellii</i>	LA1303	-0.2561	0.0324	-7.9098	0.0000	***
<i>S. pennellii</i>	LA2657	-0.1336	0.0229	-5.8337	0.0000	***
<i>S. pennellii</i>	LA1656	-0.1202	0.0396	-3.0352	0.0779	.
<i>S. pennellii</i>	LA1282	-0.0897	0.0230	-3.8936	0.0033	**
<i>S. pennellii</i>	LA1809	-0.0774	0.0267	-2.8946	0.1202	ns
<i>S. pennellii</i>	LA2719	-0.0714	0.0271	-2.6405	0.2405	ns
<i>S. pennellii</i>	LA0716	-0.0397	0.0288	-1.3792	0.9967	ns
<i>S. pennellii</i>	LA1941	0.2596	0.0501	5.1787	0.0000	***
<i>S. pennellii</i>	LA2963	0.5285	0.0445	11.8656	0.0000	***
<i>S. pimpinellifolium</i>	LA2983	-0.2359	0.0571	-4.1295	0.0013	**
<i>S. pimpinellifolium</i>	LA4713	-0.1162	0.0878	-1.3232	0.9983	ns
<i>S. pimpinellifolium</i>	LA1374	-0.0457	0.0302	-1.5143	0.9871	ns
<i>S. pimpinellifolium</i>	LA2853	-0.0209	0.0555	-0.3770	1.0000	ns
<i>S. pimpinellifolium</i>	LA2347	-0.0174	0.0356	-0.4882	1.0000	ns
<i>S. pimpinellifolium</i>	LA1659	-0.0172	0.0294	-0.5839	1.0000	ns
<i>S. pimpinellifolium</i>	LA1593	0.0622	0.0307	2.0227	0.7566	ns
<i>S. pimpinellifolium</i>	LA1332	0.0895	0.0302	2.9637	0.0972	.
<i>S. pimpinellifolium</i>	LA1348	0.1126	0.0319	3.5288	0.0142	*
<i>S. pimpinellifolium</i>	LA1261	0.1890	0.0741	2.5516	0.2996	ns

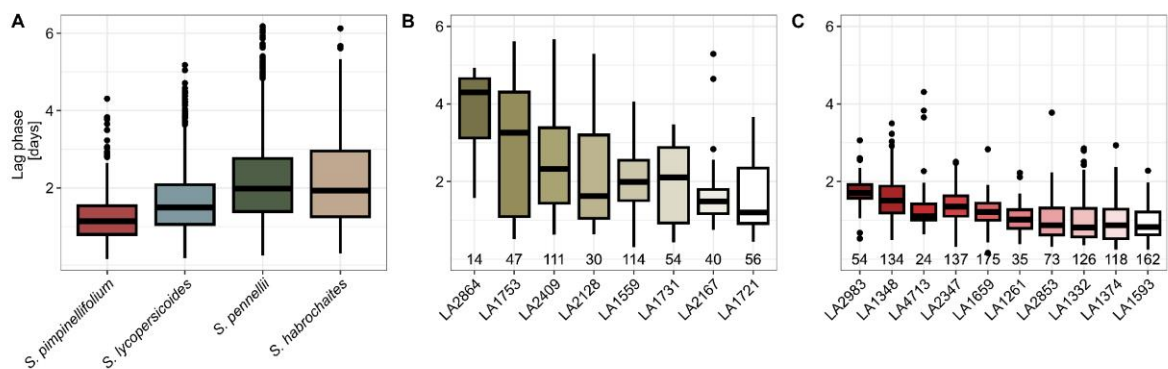
Suppl. Table 5 *Solanum* accessions used in this study

Accession	<i>Solanum</i> species
LA0716	<i>pennellii</i>
LA1261	<i>pimpinellifolium</i>
LA1282	<i>pennellii</i>
LA1303	<i>pennellii</i>
LA1332	<i>pimpinellifolium</i>
LA1348	<i>pimpinellifolium</i>
LA1374	<i>pimpinellifolium</i>
LA1559	<i>habrochaites</i>
LA1593	<i>pimpinellifolium</i>
LA1656	<i>pennellii</i>
LA1659	<i>pimpinellifolium</i>
LA1721	<i>habrochaites</i>
LA1731	<i>habrochaites</i>
LA1753	<i>habrochaites</i>
LA1809	<i>pennellii</i>
LA1941	<i>pennellii</i>
LA1964	<i>lycopersicoides</i>
LA2128	<i>habrochaites</i>
LA2167	<i>habrochaites</i>
LA2347	<i>pimpinellifolium</i>
LA2409	<i>habrochaites</i>
LA2657	<i>pennellii</i>
LA2719	<i>pennellii</i>
LA2772	<i>lycopersicoides</i>
LA2776	<i>lycopersicoides</i>
LA2777	<i>lycopersicoides</i>
LA2853	<i>pimpinellifolium</i>
LA2864	<i>habrochaites</i>
LA2951	<i>lycopersicoides</i>
LA2963	<i>pennellii</i>
LA2983	<i>pimpinellifolium</i>
LA4123	<i>lycopersicoides</i>
LA4130	<i>lycopersicoides</i>
LA4713	<i>pimpinellifolium</i>
C32	<i>lycopersicum</i>

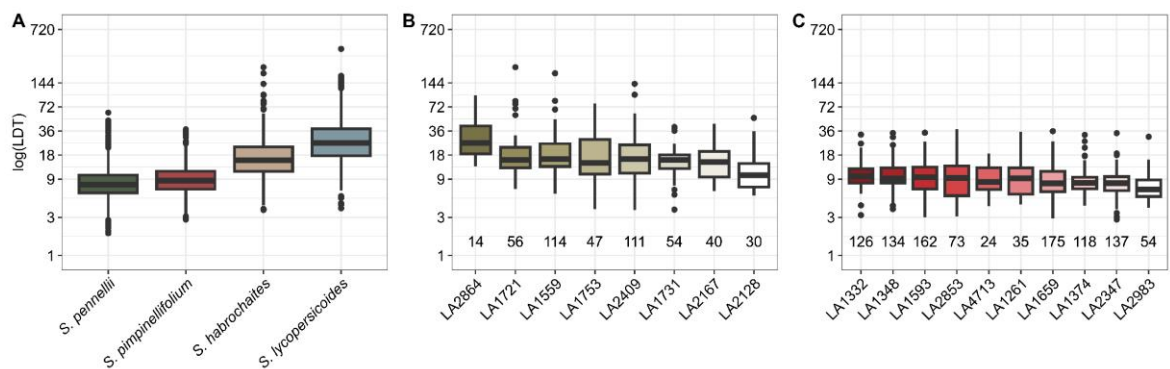
Figures



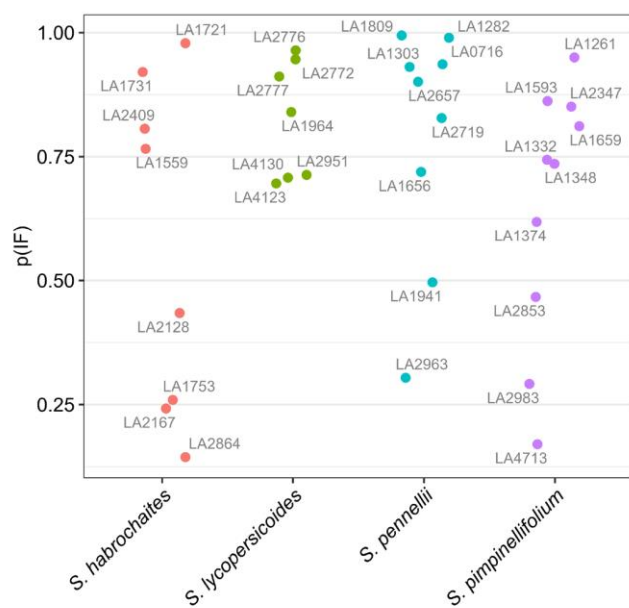
Suppl. figure 1: **Exemplary schematic of the “navatron” phenotyping platform.** The phenotyping system consists of a Poly(methyl methacrylate) box with custom fittings (D), LED growth lights, WiFi-smart plugs (B), and a 4k camera (C). A Raspberry Pi micro-computer controls the lights and the image acquisition (C). The raw images are stored on a separate file server. The PMMA-box can be customized to fit individual needs.



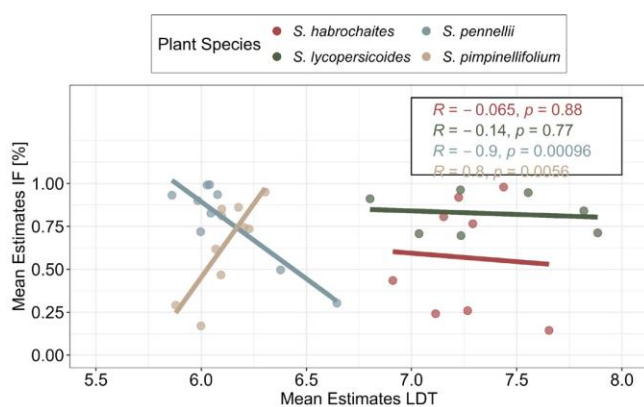
Suppl. Figure 2: **Lag-phase duration shows different levels of variation depending on the host species.** A) The lag phase duration (in days after infection) of *S. sclerotiorum* infection on *S. pennellii*, *S. lycopersicoides*, *S. pimpinellifolium* and *S. habrochaites* accessions. (B) Lag-phase duration of *S. habrochaites* accessions and C) *S. pimpinellifolium* accessions. The number on the x-axis indicates the count of individual leaves tested.



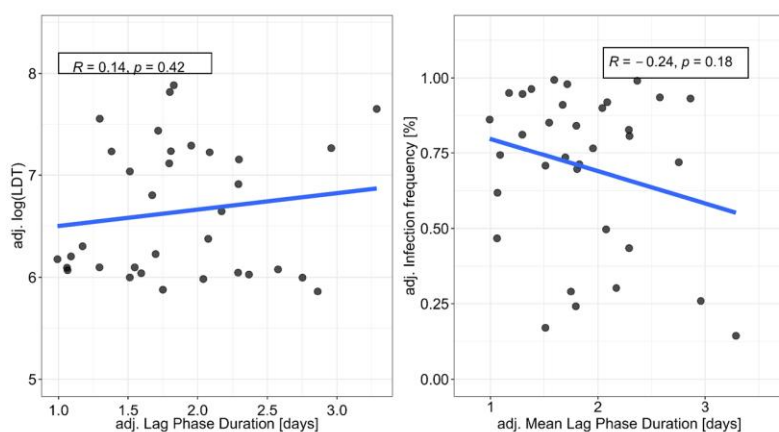
Suppl. Figure 3: **LDT shows different levels of variation depending on the host species.** A) The LDT (in hours) of *S. sclerotiorum* infection on *S. pennellii*, *S. lycopersicoides*, *S. pimpinellifolium* and *S. habrochaites* accessions. (B) LDT of *S. habrochaites* accessions and C) *S. pimpinellifolium* accessions. The number on the x-axis indicates the count of individual leaves tested.



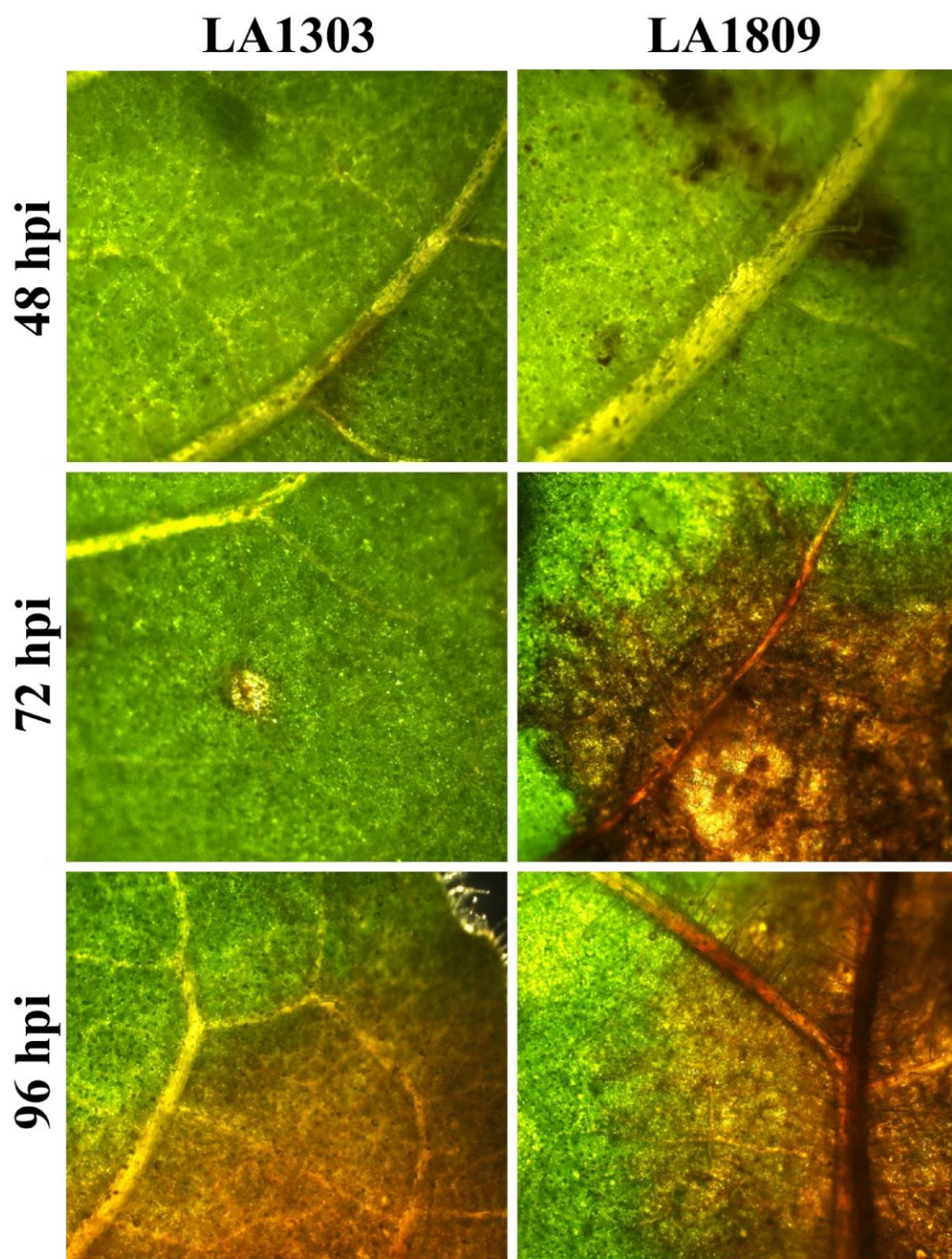
Suppl. Figure 4: Per-accession infection frequency estimates. Values derived from a glm on three independent repetitions.



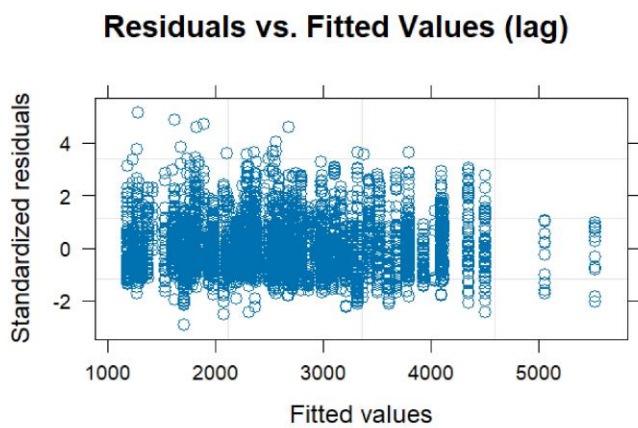
Suppl. Figure 5: Correlation analysis between Infection frequency estimates and LDT.



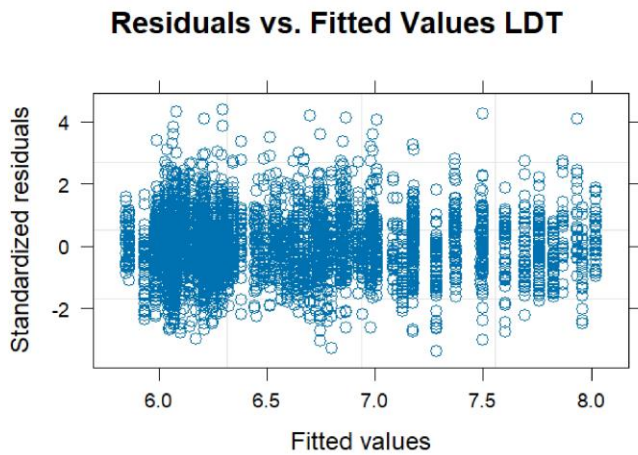
Suppl. Figure 6: Pooled correlation analysis of all accessions.



Suppl. Figure 7: **Bright light microscopy images of *S. sclerotiorum* infections on two *S. pennellii* accessions with different lag phase durations.**



Suppl. Figure 8: **Residual plot of lag-phase duration values.**



Suppl. Figure 9: **Residual plot of LDT values.**

Publication 2



Publication 2

Title: Co-optation of Transcription Factors Drives Evolution of Quantitative Disease Resistance Against a Necrotrophic Pathogen.

The manuscript is being peer-reviewed for publication and published as a preprint:

Severin Einspanier, Christopher Tominello-Ramirez, Florent Delplace, Remco Stam. Co-optation of Transcription Factors Drives Evolution of Quantitative Disease Resistance Against a Necrotrophic Pathogen. **bioRxiv** 2025.02.26.640262; doi: <https://doi.org/10.1101/2025.02.26.640262>

Contributions: I designed and conducted all experiments, led the data analysis and visualisation, and wrote the manuscript.

Please find detailed supplementary materials at doi.org/10.1101/2025.02.26.640262

**Co-optation of Transcription Factors Drives Evolution of Quantitative Disease
Resistance Against a Necrotrophic Pathogen.**

Einspanier, S.¹; Tominello-Ramirez, C^{2,1}.; Delplace, F.³; Stam, R.^{1*}

- 1 Department of Phytopathology and Crop Protection, Institute of Phytopathology,
Faculty of Agricultural and Nutritional Sciences, Christian Albrechts University,
Kiel, Germany
- 2 Department of Nutriinformatics, Institute of Human Nutrition and Food Sciences,
Faculty of Agricultural and Nutritional Sciences, Christian Albrechts University,
Kiel, Germany
- 3 Laboratoire des Interactions Plantes Microorganismes Environnement (LIPME),
INRAE, CNRS, Castanet Tolosan Cedex, France

* Address correspondence to: remco.stam@phytomed.uni-kiel.de

Short title: Co-optation Drives QDR Against Necrotrophic Pathogens.

Abstract

Wild relatives of crop species possess diverse levels of quantitative disease resistance (QDR) to biotic stresses, yet the genomic and regulatory mechanisms underlying these differences are poorly understood. In particular, how QDR against a generalist necrotrophic pathogen evolved and whether it is driven by conserved or species-specific regulatory networks remains unclear. Here, we examined the transcriptomic responses of five diverse wild tomato species that span a gradient of QDR. We initially hypothesised that conserved regulatory modules might control QDR. Instead, we use differential gene expression analysis and weighted gene co-expression network analysis (WGCNA) to find that species-specific regulatory features, encompassing both infection-induced and constitutively expressed genes, predominantly shape QDR levels. Although we identified an ethylene response factor among candidate genes for QDR-regulation, it did not fully account for the phenotypic variation. To further dissect the evolutionary basis of these regulatory patterns, we performed phylotranscriptomic analyses on gene regulatory networks. Notably, our findings reveal that the conserved NAC transcription factor 29 is pivotal in developing disease resistance only in *S. pennellii*. The differential regulation and altered downstream signalling pathways of NAC29 provide evidence for its co-option in the resistance mechanisms of *S. pennellii*. This finding highlights the species-specific rewiring of gene regulatory networks by repurposing a conserved regulatory element to enhance resistance against pathogens effectively. These results offer new insights into the evolutionary and regulatory complexity underlying QDR and emphasise the significance of species-specific gene regulation in shaping resistance against a cosmopolitan necrotrophic pathogen.

Introduction

Developing or engineering durable resistance against necrotrophic pathogens in crop plants displays a major bottleneck in modern plant breeding. Although the scientific community gained a comprehensive understanding of dominant R-gene-mediated resistance, especially against biotrophic pathogens, an R-gene-mediated resistance against necrotrophic generalist pathogens like *Sclerotinia sclerotiorum* or *Botrytis cinerea* has not yet been described (Mbengue et al. 2016; Wang et al. 2019). Accordingly, the primary goal of resistance breeding against necrotrophic pathogens is to enhance quantitative disease resistance (QDR), where many independent loci contribute marginally to a continuous pattern of resistance (Caseys et al. 2021). The current state of knowledge about mechanisms involved in QDR has been reviewed by (Corwin and Kliebenstein 2017; Poland et al. 2009; Roux et al. 2014; Gou et al. 2023).

Natural or wild plant pathosystems are a valuable tool for unravelling the complexity of the QDR mechanisms and their evolution, especially when looking into crop wild relatives (Kahlon and Stam 2021). Crop wild relatives harbour a wide diversity of morphological properties and represent a common source of novel traits in modern crops (Szymański et al. 2020; Albaladejo et al. 2017; Nosenko et al. 2016). Adapting to diverse habitats is accompanied by the evolution of resistance or tolerance against numerous stresses, including drought, temperature, and disease (Wei et al. 2024; Bolger et al. 2014). For instance, previous studies have demonstrated that accessions of the crop wild relative *Solanum chilense* exhibit a wide inter- and intrapopulation diversity in resistance response against pathogens like *Phytophthora infestans*, *Fusarium oxysporum* and *Alternaria* spp. (Kahlon et al. 2021; Stam et al. 2017; Schmey et al. 2023). Several wild tomato species also show distinct patterns of presence-absence variation, copy number variation, and specific patterns of selection on pathogen resistance genes within and between populations or species (Stam et al. 2019; Seong et al. 2020; Silva-Arias et al. 2025). We have previously shown that wild tomato species employ distinct mechanisms to achieve QDR against *S. sclerotiorum*, particularly by modulating the duration of the asymptomatic phase (lag phase) and the speed of lesion growth (lesion doubling time, LDT). These measures appear not correlated and exhibit significant host and population specificity. Thus, species or populations might have adapted specific strategies to regulate QDR. I.e. prolonging the lag phase in one case or increasing the pathogen's LDT in another (Einspanier et al. 2024). The possibility of such differentiation is supported by population genomic analyses, showing distinct genomic separation and differentiation among *S. chilense* populations, which

also exhibit diversifying elicitor responses and phytohormonal regulation (Kahlon et al. 2023; Stam et al. 2017; Böndel et al. 2015). Interestingly, a previous study investigating *S. pennellii* introgression lines described that genomic variation did not explain the phenotypic variability and ranked regulatory variability as the main determinant of *B. cinerea* resistance on fruits, highlighting how regulatory plasticity can enable new resistance traits (Szymański et al. 2020).

The underlying regulatory interplay governing QDR remains elusive. Although recent studies identified QDR-associated quantitative trait loci, the explained phenotypic variation remains relatively low (Thomas et al. 2024; Pink et al. 2022). While the genomic characterisation of QDR requires many resources (such as mapping populations, multiparent advanced generation intercross populations or introgression lines of sufficient size, (Corwin and Kliebenstein 2017; Thomas et al. 2024), RNA sequencing is suitable for determining QDR regulation, leveraging high throughput and decreasing costs to support large-scale sampling. This enables researchers to investigate complex regulatory networks, thereby identifying and characterising nuanced shifts in gene expression and their evolution (Gómez-Picos and Eames 2015; Delplace et al. 2020).

Gene networks are a powerful tool for characterising relationships or interactions among genes and help understand the underlying molecular mechanisms of various phenotypes (Delplace et al. 2022; Ovens et al. 2021). Typically, gene network analyses are separated into undirected coexpression networks (like weighted gene correlation network analysis, WGCNA) and directed gene regulatory networks (GRNs, (Li et al. 2015; Langfelder and Horvath 2008). Albeit fundamentally different in the underlying statistical concepts, both GRNs and WGCNAs can be used to characterise complex regulatory networks, as previously shown in cultivated tomatoes. Tominello-Ramirez et al. (2024) integrated WGCNA and GRN to characterise a specific class of ethylene response factors involved in defence against necrotrophic fungi of the genus *Alternaria*, illustrating how a system approach can be facilitated to describe QDR networks and their moderators. Although certain gene networks appear to be highly conserved (with some predating the existence of land plants), there is increasing evidence that gene regulation network evolution can be a relatively quick response to different stresses (Curci et al. 2022; Wu et al. 2021; Obertello et al. 2015; Crow et al. 2022; Wei et al. 2024). Accordingly, evolutionary flexibility was hypothesised to enhance QDR robustness (Derbyshire and Raffaele 2023). However, it remains unclear how network evolution drives QDR and how phylogenetic relationships determine the degree of QDR. This is mostly due to the high analytical

complexity, challenging construction of cross-species networks and multidimensional comparative analysis on non-model organisms exhibiting a wide range of complex phenotypes (Schoenrock et al. 2017).

This also involves the development of QDR against the generalist pathogen *S. sclerotiorum*, which infects a broad range of hosts, including agronomically relevant crops such as oilseed rape, sunflower, and tomatoes (Derbyshire et al. 2022; Derbyshire and Raffaele 2023). Although Sucher et al. (2020) showed signs of recent gene expression acquisition and exaptation in a group of ATP Binding Cassette type G transporters responding to *S. sclerotiorum* infection; the regulatory cues driving enhanced resistance through network reconfiguration against this pathogen remain unknown.

Here, we examine transcriptome dynamics and plasticity to identify both conserved and newly recruited regulators of QDR-level. We employ a novel approach integrating phylotranscriptomic analysis and network inference to elucidate gene network evolution and unravel the regulatory cues driving QDR. Specifically, we investigate the regulatory architecture underlying QDR against a generalist necrotrophic pathogen, comparing the rewiring of gene regulatory networks in resistant versus susceptible genotypes across five tomato species (*S. chilense*, *S. habrochaites*, *S. lycopersicoides*, *S. pennellii*, and *S. pimpinellifolium*). We test the hypothesis that shared regulatory networks drive QDR while downstream mechanisms fine-tune species-specific regulatory responses. By integrating phylogenetic insights with transcriptomic data, we uncover patterns of gene family expansion, functional divergence, and regulatory remodelling that collectively enhance QDR. This evolutionary approach helps pinpoint the “ancient core” of plant immune systems shared across species and novel, rapidly evolving genes that can contribute to the partial, durable form of resistance in wild tomato relatives. Our findings offer a valuable resource that contrasts regulatory responses among genotypes with varying QDR levels, laying the groundwork for further exploration of the functional mechanisms shaping QDR.

Materials and Methods

Plant growth conditions

We obtained germplasm from the C. M. Rick Tomato Genetics Resource Center at UC Davis (see suppl. tab. 1, TGRC UC-Davis, <https://tgrc.ucdavis.edu/>) and cultivated the plants in the greenhouse of the Phytopathology Department at Christian Albrechts University Kiel, Germany. We surface-sterilized the seeds with a 2.75% hypochlorite solution. We propagated mature plants through cuttings using Chryzotop Grün 0.25% in Stender C700 substrate. We maintained the growing environment at approximately 21 °C (± 10 °C), 65% relative humidity, and a 16-hour photoperiod. We fertilised the plants monthly using a drip irrigation system with a 1% Sagaphos Blue solution. For further methodological details, please refer to (Einspanier et al. 2024; Tominello-Ramirez et al. 2024).

Fungal growth conditions

We freshly grew the fungus *Sclerotinia sclerotiorum* (1980) on potato dextrose agar (Sigma-Aldrich) at 25 °C in the dark. We performed the inoculation using a liquid mycelium macerate, following the method described in Einspanier et al. (2024). Briefly, we incubated 100 mL of potato dextrose broth with four 1 cm pieces of fully overgrown PDA on a rotary shaker (120 rpm, 24 °C) for four days. After incubation, we mixed the culture using a dispenser and vacuum-filtered it through cheesecloth. We then concentrated the filtrate to an optical density at 600nm (OD₆₀₀) of 1 using the clear supernatant as dilution. We used fresh potato dextrose broth as a negative control and added Tween80 as a surfactant.

Experimental conditions

The experimental conditions of the sequencing experiment were identical to previous experiments conducted to measure LDT (Einspanier et al. 2024). In short, we placed detached leaflets on wet tissue papers in a tray with the adaxial side up. Then, the leaves were inoculated with 10 µL of fungal mycelial mixture (OD₆₀₀=1) or empty PDB. The hood was covered and incubated at 23 °C. LED lights were used to continue the 16-h photoperiod. We sampled relative to the lesion development in the middle of lesion spread, but always at the same daytime, minimising the influence of the circadian rhythm on gene expression. A sterile scalpel was used to sample a 2cm x 2cm big piece covering the lesion and the surrounding tissue. Two leaf segments were pooled into one sample. We sampled four biological replicates per condition

and genotype. The leaf segments were submerged in 750 µL DNA/RNA shield (Zymo Research) in ZR BashingBead Lysis Tubes (2 mm). We used the Zymo Research Quick-RNA Plant Kit for total RNA isolation following the manufacturer's protocol. We used a NanoDrop One (ThermoFisher) and agarose gels to determine RNA quality and integrity. For RNA yield quantification, we used a Fluorometer (Promega Quantus).

Sequencing and library preparation

We in-house prepped a Lexogen QuantSeq 3' mRNA-Seq V2 (Lexogen, Vienna, Austria) library, following the manufacturer's guidelines. Spike-RNA was added for quality assessment, as was the PCR Add-on Kit, to determine the correct number of PCR cycles required to amplify mRNA sequences. The library was sequenced at the Competence Centre for Genomic Analysis Kiel (CCGA) on an Illumina NovaSeq 600 (Illumina, San Diego, CA, USA) with 2 x 100 bp aiming for five mio. reads per sample.

Bioinformatic preprocessing

We performed a quality assessment on the raw reads using FastQC/MultiQC (Simon Andrews 2010; Ewels et al. 2016). Then, we used Cutadapt v4.8 for initial filtering and adapter trimming following recommendations from the library manufacturer (Martin 2011). This included the settings `-a "polyA=A{20}" -a "QUALITY=G{20}"` and custom options for adapter removal (see online resources). Subsequently, we depleted ribosomal RNA bioinformatically using a custom pipeline (see online resources). For this, we generated reference-rRNA sequences for all five species based on 45S rDNA-sequences of the 5.8S, 18S and 25S subunits from the *A. thaliana* quality reference genome (GeneBankIDs: 5.8S: AB373816.1, 25S: OK073662.1 18S: OK073663.1, (Rabanal et al. 2017) and the chloroplast/mitochondrial rRNA of *S. lycopersicum* (GeneIDs: 34678306, 3950431, 3950467, 3950435, 3950433, 34678288, 34678318, 34678306). We then extracted species-specific rRNA sequences using Blast v2.13 (Camacho et al. 2009). We inflated the flanking sequences by 100 bp and extracted the final sequences using bedtools v2.31.1 'getfasta' (Quinlan and Hall 2010). We used the following reference genomes: *S. lycopersicoides* (BioProject PRJNA727176, (Powell et al. 2022), *S. chilense* (BioProject: PRJNA1210999), *S. pennellii* (BioProject: PRJEB5809, (Bolger et al. 2014), *S. habrochaites* (BioProject: PRJCA008297, (Yu et al. 2022), and *S. pimpinellifolium* (BioProject: PRJNA607731, (Wang et al. 2020b). Trimmed reads of each species were mapped on the respective rRNA reference using the STAR-aligner v2.7.9 with custom settings retaining only

non-mapping reads (see online resources, (Dobin et al. 2013). Then, we mapped the rRNA-depleted reads against the respective reference genome using the STAR aligner with settings, following the library manufacturer's recommendations (see mapping statistics in suppl. tab. 2).

We used the RNAseq read-assisted tool GeneExt (<https://github.com/sebepedroslab/GeneExt>, last accessed Oct. 2024) to extend or predict missing UTR regions in our genome annotations. By using the options `--peak_perc 10 --orphan -j 16 -v 1 -m 5000`, we enhanced the annotation completeness significantly. (Zolotarov et al. 2023). Next, we quantified aligned sequencing reads with featureCounts v2.0.6 using custom options `-s 1 -T 16 -M -t exon -g gene_id` as this sequencing library allows only the quantification of expression on gene-level (Liao et al. 2014).

Annotation and Proteome

We developed a custom pipeline to improve the proteome of the five host plant species. First, we utilised per-species GeneExt-curated genome annotations to extract transcripts using gffread v0.12.7 and extracted protein sequences based on the longest open reading frames (ORF) with TransDecoder v5.7.1 (Pertea and Pertea 2020; Haas 2024a, 2024b). To retain proteins with functional significance, we employed **BLASTp** to identify homologous proteins in the UniProt database using the parameters `-max_target_seqs 1 -evalue 1e-5`. (Camacho et al. 2009; UniProt Consortium 2017). We kept only those proteins with significant UniProt matches for downstream analysis. For protein sequences that did not achieve a sufficient match in UniProt, we further assessed their homology to the ITAG4 proteome of *S. lycopersicum* (https://solgenomics.net/organism/Solanum_lycopersicum/genome/) using Orthofinder to retain tomato-specific proteins. Next, we evaluated sequences with low identity to the tomato proteome by assigning functional annotations using PANNZER2 (Törönen and Holm 2022). We retained all sequences with a PANNZER2 positive predictive value (PPV) score greater than 40%, ensuring that only confidently annotated proteins were included. Finally, we removed duplicated sequences from the proteome FASTA files using seqkit's v0.10.0.1 `rmdedub` command (Shen et al. 2024). For more information on the number of filtered proteins, please see suppl. table 3.

Differential gene expression analysis

We conducted a quality assessment of the expression data (see suppl. fig. 2) and performed differential gene expression analysis using DESeq2 v1.46.0, analysing each species separately (Love et al. 2014). Count tables were loaded, and a DESeqDataSet object was created with a design formula including genotype-treatment interaction. After setting the treatment reference level and prefiltering genes with low counts, we defined contrast matrices for comparisons such as infected vs. mock across all genotypes, within susceptible or resistant genotypes, and between resistant vs. susceptible genotypes under infected conditions. The `lfcShrink` function was applied to stabilise log fold changes, and DEGs were identified based on an absolute log2 fold change >1 and adjusted p-value ≤ 0.05 .

Phylogenomics and Orthology

We performed a BUSCO analysis v5.7.0 on the curated proteomes (custom options: `-m protein -l solanales_odb10`) for phylogenetic tree construction (Manni et al. 2021). Subsequently, we used the `busco_phylogenomics` pipeline to construct species phylogenies, which we visualised with Accurate Species Tree Estimator (ASTER*, v1.16). We used Orthofinder v2.5.5 to derive insight into orthologue genes among the different species. We built a central Orthofinder project incorporating the curated proteomes of the five core *Solanum* species and six more distantly related pentapetalae plant species using the same proteome versions as in Sucher et al. (2020). We then used the R package UpsetR v1.4.0 to visualise intersections of shared/unique orthogroups across different scales. In cases where multiple DEGs (e.g., isoforms) were detected per species and orthogroup, we selected those with the most significant and strongest differential expression.

Co-expression networks (WGCNA)

We constructed weighted gene correlation networks with the R-package WGCNA v1.73 (Langfelder and Horvath 2008). We generated multiple independent networks at the single-copy orthogroup and species levels. To generate the OG network, we first selected all genes of all five species, which were assigned to single-copy orthogroups and renamed them with the respective OG-ID. Then, we generated regularised log-transformed (`rlog`) expression values per sample and merged the per OG expression values of all species into one consensus file, which we used as a starting point for the WGCNA. We analysed both species- and OG-level networks as follows.

First, the data set was inspected for potential outliers by hierarchical clustering using the `hclust()` function v3.6.2 (see suppl. fig. 4A). To derive a soft threshold, we used the `pickSoftThreshold()` function. We evaluated the fit of the scale-free topology model and the mean connectivity (e.g., see suppl. fig. 4B). We then used a custom wrapper of the `blockwiseModules()` function to optimise the settings for each network separately (see suppl. tab. 4, and online resources). Additionally, we used the following custom options: `maxBlockSize=nrow(datExpr)`, `networkType="signed hybrid"`, `TOMType="signed"`, `minModuleSize=30`, `reassignThreshold=0`, `checkMissingData=F`, `replaceMissingAdjacencies=T`. We assessed the module assignment using `plotDendroAndColors()` and tested its robustness by preservation testing (see online resources, and suppl. fig. 4C and suppl. fig. 5).

We investigated per-species module-trait relationships for n modules using linear models accounting for the fixed binomial effects of *genotype* (hence, resistance phenotype) and infection. We excluded the random effect *repetition* to reduce the risk of overfitting the model, as the covariable *repetition* variance approached zero.

$$ME_n = Genotype + Infection + Genotype:Infection$$

We ranked the plant genotypes according to their LDT values to infer ordinal phenotypic data with the OG network and set the most resistant genotype as a contrast reference.

$$ME_n = Infection + Rank$$

We extracted the model estimates to visualise the OG-module-trait relationships for easier interpretation. Accordingly, we calculated partial- and non-partial η^2 -values for single-species networks and corrected the p-values with Benjamin-Hochberg correction (Yekutieli and Benjamini 1999).

$$\eta_{full}^2 = \frac{SS_{effect}}{SS_{total}}$$

$$\eta_{partial}^2 = \frac{SS_{effect}}{SS_{effect} + SS_{error}}$$

We used a custom script to define hub genes based on eigengene centrality and a dynamic thresholding method which identifies inflexion points of the weight distribution (Tominello-Ramirez et al. 2024). The hub-gene assignment was visually inspected and adjusted if needed (see online resources).

Gene Regulatory Network Analysis

We conducted a gene regulatory analysis to uncover causal regulatory relationships among the coregulatory genes identified by WGCNA. Accordingly, we discretely predicted transcription factors for all species using the Transcription Factor Prediction Tool of the Plant Transcription Factor Database (Jin et al. 2017). Then, we used the R-package GENIE3 v3.20 to construct the Gene Regulatory Network (GRN) using standard settings. We used the same custom script as before to filter low-weight edges and define GRN-hub genes based on eigenvector centrality.

GO-Term enrichment

To gain insights into the functional framework of the various sets of genes, we performed a gene ontology (GO) analysis on both species-level and cross-species levels. We derived GO terms using PANNZER2 for species-level analysis and converted the results into a BiNGO-compatible format with a custom R-script. We extracted the overlapping genes and GO terms from all species for cross-species analysis. Those were collected in a consensus orthogroup-based BiNGO file. Finally, we performed GO-term enrichment using the Cytoscape v3.10.3 application BiNGO v3.0.5 to interpret the functional implications of defined gene sets.

Phylostratum analysis

We employed a robust phylostratigraphic approach to classify all transcripts according to their phylogenetic origin, carefully addressing potential biases such as homology detection failure. We used the software GenEra v1.4.2, which uses the DIAMOND algorithm v2.0.14 to align the sequences of protein-coding genes of all five *Solanum* species against the NCBI non-redundant database (as of Sept. 2024). The most distant taxonomic node is considered as the age of this gene family (Barrera-Redondo et al. 2023; Buchfink et al. 2021; Lotharukpong et al. 2024; Schoch et al. 2020; Sayers et al. 2020).

Transcript Age Index

Following the association of genes with their putative age, we used the R-Package myTAI v0.9.3 to quantify shifts in the transcript age index (TAI) (Drost et al. 2018). TAI_s is defined by the number of treatments (s), the relative gene age of n genes i (ps_i) and the expression level of e_{is} , As:

$$TAI_s = \sum_{i=1}^n \left(\frac{ps_i \times e_{is}}{\sum_{i=1}^n e_{is}} \right)$$

We used normalised log2-transformed read counts (DESeq2 `rlog()`) as input-expression data.

Transcript Divergence Index

We employed a dN/dS-based approach to assess evolutionary divergence at the transcript level. After extracting the longest ORFs with TransDecoder v5.7.1, we applied `divergence_stratigraphy()` from orthologr v0.4.2 (Drost et al. 2015). This method identifies best reciprocal hits via BLASTp, aligns them pairwise with Needleman–Wunsch (Needleman and Wunsch 1970), and converts the protein alignments to codons in PAL2NAL for dN/dS calculations (Suyama et al. 2006; Comeron 1995), using *Solanum melongena* as an outgroup (Wei et al. 2020). The resulting dN/dS values were grouped into deciles (“divergence strata”) to facilitate comparisons with phylostratigraphic data. We used these strata to compute the Transcript Divergence Index (TDI) with myTAI, where TDI_s depends on each gene’s divergence stratum (ds_i) and the expression level (e_{is}) as:

$$TDI_s = \sum_{i=1}^n \left(\frac{ds_i \times e_{is}}{\sum_{i=1}^n e_{is}} \right)$$

Statistics and visualisation

We used the programming language R v4.4.0 in RStudio for statistical analysis. In particular, we used packages of the tidyverse v2.0.0, such as tidyr v1.3.1, stringr v1.5.1 and dplyr v1.1.4. All figures were prepared using ggplot2 v3.5.1 and curated for publishing in Inkscape.

Online resources

Detailed code, including all scripts, documentation and environment information, are available at the following GitHub repository: github.com/PHYTOPatCAU/SolanumPhylotranscriptomics

Data availability

Sequence data and processed read counts from this article are available in the NCBI GEO repository under accession number GSE288242 (see suppl. tab. 14).

Results

Wild tomatoes show signs of multiple transcriptome differentiation events.

We performed a phylogenomic analysis using curated proteome sequences to corroborate the understanding of the phylogenic relationships between the five tomato species (Solanum - sections Lycopersicon and Lycopersicoides): *S. chilense*, *S. lycopersicoides*, *S. habrochaites*, *S. pennellii*, and *S. pimpinellifolium* (fig. 1A). We found that most protein sequences (13,280 orthogroups of 26,249 total) were shared among all five species, highlighting a strong core proteomic foundation (fig. 1B). In contrast, species-specific unique protein sequences were relatively low, e.g., with *S. pennellii* carrying 2,028 unique proteins and *S. lycopersicoides* 1,795. This pattern underscores the evolutionary conservation within the sections while still allowing room for species-specific adaptations. To further characterise the proteomic landscape's evolutionary history, we employed phylostratigraphy to map the age of genes across all tested species.

By constructing phylostratigraphic maps, we can visualise the age of the genes and when key gene families emerged. This allows for assessing whether genes are conserved or have diversified across lineages. As anticipated, all five species exhibit a strongly conserved progression in the number of genes with a certain age (fig. 1C) and the number of associated gene family founder events (fig. 1D). Most genes trace their origins back to the emergence of cellular organisms (e.g., 18,056 *S. chilense* genes from 3,346 gene family founder events [GFFE]), with a marked decline in new gene origins over time. However, notable spikes occur during key evolutionary milestones: the development of land plants (Embryophyta, 290 GFFE, 1,362 new genes in *S. chilense*) and the rise of flowering plants (from Spermatophyta to Mesangiospermae, in sum 2,371 new genes and 637 GFFE in *S. chilense*). Following these periods, gene assignments gradually decrease until the clade Solanaceae, where there is a renewed burst of new gene families (*S. chilense*: 144 GFFEs). All species harbour a modest number of phylostratigraphically young genes (*S. chilense*: 210 GFFE), which may indicate ongoing species-specific differentiation or bursts of gene family innovation since the emergence of Solanaceae. However, these putatively young genes must be critically assessed, as they may partly reflect technical artefacts (such as reference genome annotation quality or analytical issues like homology detection failure).

The high number of shared orthogroups and remarkably similar age estimates for gene family founder events until the clade of *Solanum* illustrate the strongly conserved evolutionary history of the five wild tomato species. This conservation suggests that, despite species-specific innovations, their core genomic and evolutionary trajectories have remained remarkably stable.

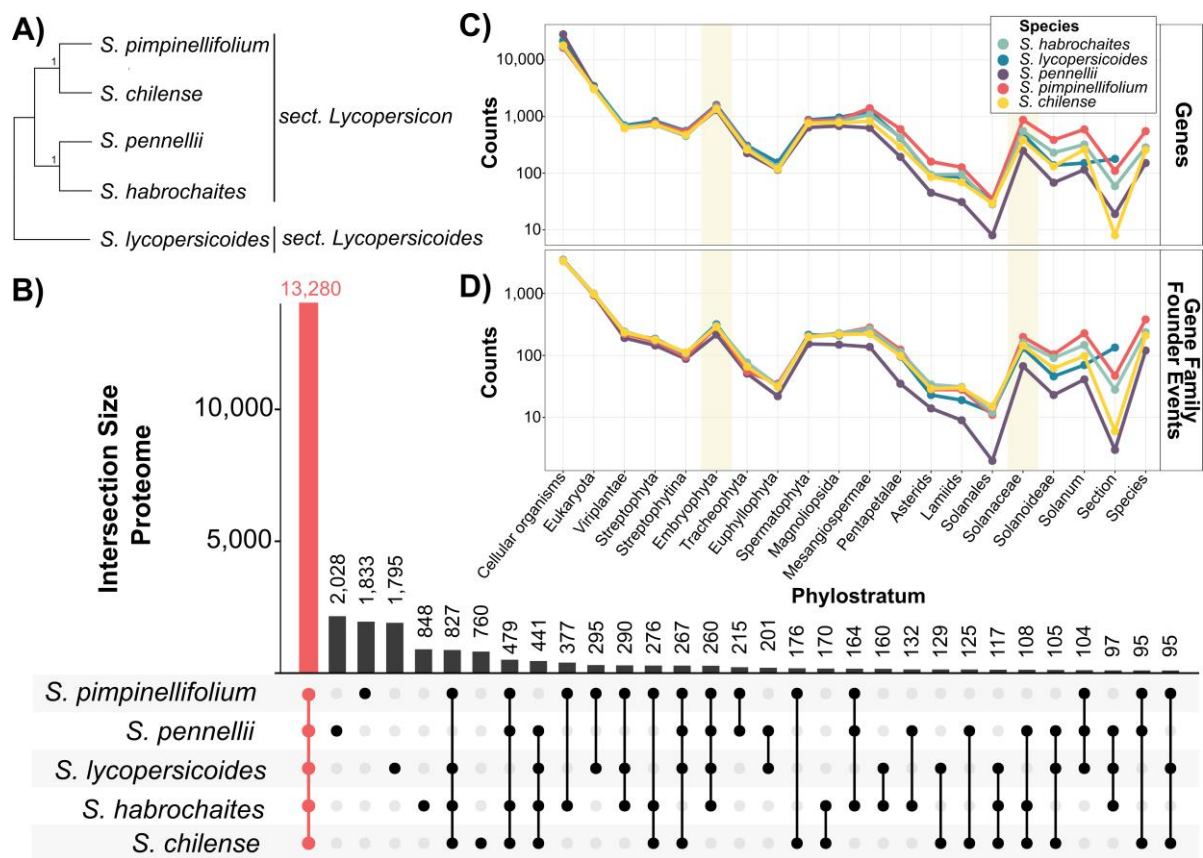


Figure 1: Phylogenomic Analysis Reveals a Highly Conserved Proteome and Recent Differentiation Among Five *Solanum* Species. **A)** Representative phylogenetic tree of the five tomato species based on BUSCO genes. Numbers represent branch support values based on quadripartition, considering the four clusters surrounding a branch. **B)** Orthofinder-based Upset plot of the proteomes, indicating that a large fraction of proteins is shared among species (in red), with only a small subset unique to individual species. Phylostratigraphic maps display the number of genes **(C)** and gene family founder events **(D)** across the tree of life. Shaded regions highlight phylostrata corresponding to the peaks of genetic innovation during the development of land plants and within the Solanaceae. Counts correspond to the number of genes or gene family founder events, respectively.

Sclerotinia sclerotiorum tolerance is highly diverse among and within wild tomato species.

We previously performed a study to identify genotypes differing in disease resistance against the fungal generalist-pathogen *S. sclerotiorum* (Einspanier et al. 2024). Generally, we observed a wide diversity in QDR phenotypes with strong species- and accession-specific patterns. Accordingly, we observed that the lesion growth rate (denominated Lesion Doubling Time, LDT) was generally shorter on *S. pennellii* and *S. pimpinellifolium* genotypes (i.e., pathogen growth is faster). At the same time, *S. lycopersicoides* accessions appeared relatively resistant (fig. 2A). We found the biggest quantitative differences between genotypes of the same species for *S. lycopersicoides* ($\text{lsmean}_{\text{susceptible}} = 6.80 \text{ h}$ vs. $\text{lsmean}_{\text{resistant}} = 7.88$) and *S. pennellii* ($\text{lsmean}_{\text{susceptible}} = 5.86 \text{ h}$ vs. $\text{lsmean}_{\text{resistant}} = 6.65 \text{ h}$, see suppl. tab. 1).

S. sclerotiorum infection-induced shift in gene expression underlies genotype specificity.

We then conducted gene expression profiling on detached leaves during the lesion growth phase, contrasting accessions with different LDT. An average of 4.3 mio. reads mapped to the respective reference genomes, with a mean mapping rate between 74% and 89% (mapping statistics in suppl. tab. 2). We performed differential gene expression analysis by genotype comparing infected versus control conditions. Interestingly, we observed strong variation in differential (infection-induced) gene expression levels between the species. We observed few weakly differentially expressed genes for both *S. chilense* (sus. genotype: 2,104 DEGs, res. genotype 194 DEGs, fig. 2B). and *S. habrochaites* genotypes (sus. genotype: 1,058 DEGs, res. genotype 65 DEGs) and a stronger regulatory response by the other host species (*S. pennellii*: sus. genotype: 4,808 DEGs, res. genotype 9,685 DEGs; *S. lycopersicoides*: sus. genotype: 3,627 DEGs, res. genotype 9,635 DEGs; and *S. pimpinellifolium*: sus. genotype: 9,007 DEGs, res. genotype 8,007 DEGs, see suppl. tab. 5). We performed a Pearson correlation analysis to test the relationship between the level of QDR and the absolute number of differentially expressed genes and observed a non-significant, negative association between the two parameters ($p=0.087$, $R^2=0.32$, fig. 2C). However, nested species effects with contrasting trends might not be reflected sufficiently by this analysis, as we measured a lower number of DEGs on the resistant *S. lycopersicoides* genotype vs. the susceptible genotype and the opposite trend for *S. pennellii*. These findings suggest that the absolute number of genes reprogrammed during

infection alone does not explain QDR variability at this level. We also found no relationship between sequencing/mapping depth and the number of DEGs (see suppl. fig. 1).

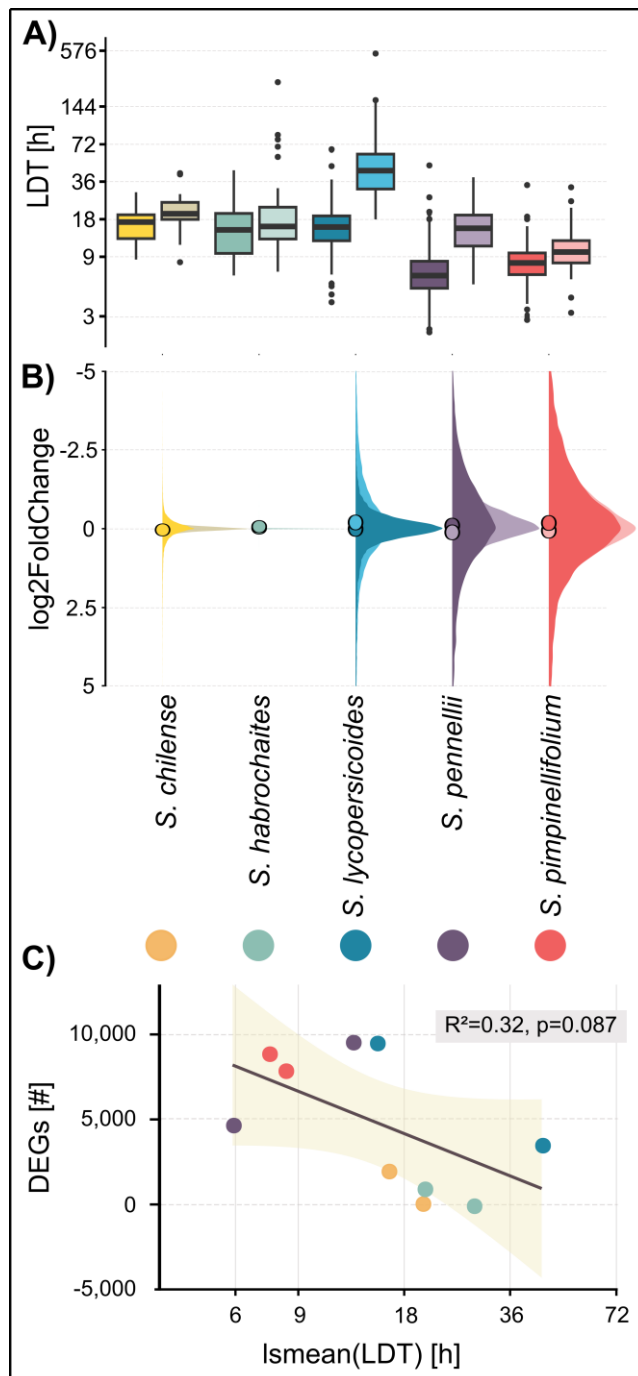


Figure 2: The inoculation with *S. sclerotiorum* leads to different levels of susceptibility and heterogeneous transcriptomic responses. **A)** Lesion Doubling Time (LDT) values in hours for five host species (two genotypes each) serve as a quantitative measure of the level of quantitative disease resistance (QDR). Data adapted from Einspanier et al. (2024). **B)** Density plot of $\log_2\text{FoldChange}$ in gene expression across all accessions following infection with *S. sclerotiorum* compared to mock treatment, illustrating the overall transcriptomic response to infection. Dots represent the mean $\log_2\text{FoldChange}$. **C)** Pearson correlation analysis testing the interaction between the number of differentially expressed genes by genotype (induced by infection) and levels of resistance (LDT). The shadow represents the SD.

Genotypes of the same species show strong regulatory plasticity.

Seeing the results above and knowing that constitutively expressed defence-associated genes might also govern QDR, we performed a differential gene expression analysis contrasting the resistant vs. the susceptible genotype by species in infected conditions. This allows the identification of infection-induced regulatory features and the expression of non-induced genes alike. Interestingly, the number of differentially expressed genes between the two genotypes varies strongly between the species (1,438 DEGs up and 1,644 DEGs down in *S. habrochaites* versus 5,855 DEGs up and 4,962 DEGs down in *S. lycopersicoides*). While we found strong alterations in the magnitude of differential gene expression between two *S. lycopersicoides* genotypes (5,855 sign. up-regulated genes in the resistant genotype, 4,962 downregulated, respectively), *S. pimpinellifolium* genotypes differed on a much smaller scale (1,483 up-regulated DEGs, 1,644 downregulated DEGs). Intermediate levels of differential expression between *S. pennellii* genotypes, in contrast to strong differences in *S. lycopersicoides*, clearly illustrate that the order of magnitude in gene expression does not explain the level of resistance or susceptibility (fig. 3A).

Next, we tested whether resistance- or susceptibility-DEGs are unique or shared among species. For this, we selected all DEGs between resistant and susceptible accessions within a species and conducted a membership analysis based on gene orthologs to classify differentially expressed orthologs (DEOGs). We observed that most DEOGs were unique to the respective species. Accordingly, we measured 2,607 specific DEOGs (sDEOGs) for *S. lycopersicoides*, 1,194 sDEOGs for *S. chilense* and 903 sDEOGs from *S. pennellii*. However, we also identified 239 core DEOGs (cDEOGs) shared among all five tomato species, indicating that those genes are differentially expressed between the two genotypes of all species. Interestingly, we could show that the majority of those cDEOGs is differentially expressed upon *S. sclerotiorum* inoculation in six further related pentapetalae plants: 62 of the cDEOGs are induced in all tested plant species (*Ricinus communis*, *Arabidopsis thaliana*, *Beta vulgaris*, *Phaseolus vulgaris*, *Helianthus annuus* and *S. lycopersicum*), and 94 cDEOGs are infection-induced in all plants of this set excluding *R. communis*. We further identified 19 cDEOGs, which might be specific to the genus *Solanum* (fig. 3C). These findings illustrate that only a small proportion of all DEOGs show a conserved expression pattern over pentapetalae plants. At the same time, regulatory differentiation between genotypes with contrasting QDR appears to be mostly specific to the nested species.

In the pentapetalae plant set, most conserved differentially expressed orthologous genes (cDEOGs) are significantly induced by infection. However, within our wild tomato dataset, only a small fraction of these genes (n=16) is both infection-induced and vary significantly between genotypes of differing QDR. Notably, most cDEOGs exhibited pronounced presence-absence patterns in their infection response (see suppl. fig. 3), suggesting that their regulation is highly variable across species. Species-specific DEOGs also display differing regulatory profiles: While ~60% of *S. pimpinellifolium*, *S. pennellii*, and *S. lycopersicoides* sDEOGs are induced by infection, only a marginal fraction of sDEOGs in *S. chilense* or *S. habrochaites* is induced (suppl. fig. 3). This pattern underscores the regulatory flexibility and diversity among wild tomato species in their response to pathogenic infection, likely reflecting a wide range of adaptive strategies in their defence mechanisms.

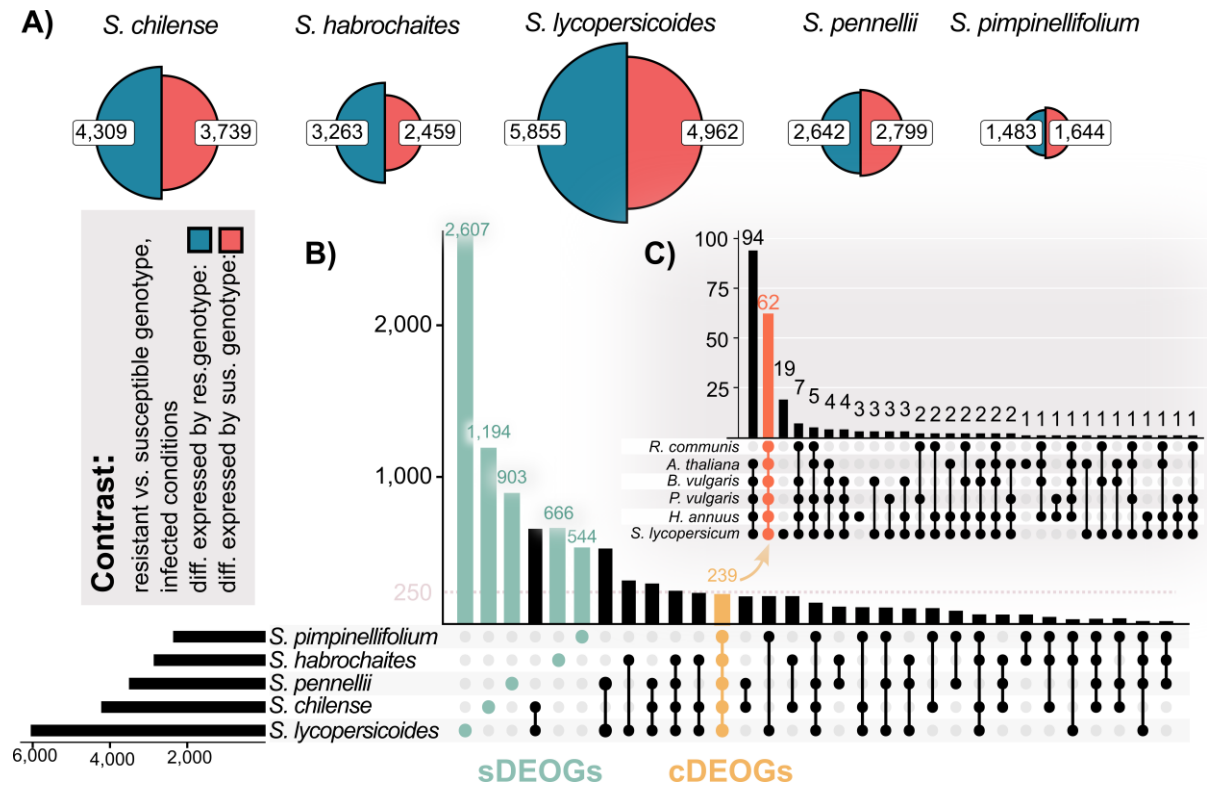


Figure 3: Species-Specific Differential Gene Expression Related to Varying QDR Levels. A) Pie charts showing the number of genes differentially regulated between genotypes with varying levels of quantitative disease resistance (QDR) within each species. DEGs were defined between genotypes with differing levels of QDR in infected conditions. B) Upset plot illustrating the overlap of between-genotype differentially expressed orthogroups across the five tomato species. This intersection distinguishes species-specific differentially expressed orthogroups (sDEOGs) from a set of shared core differentially expressed orthogroups (cDEOGs). C) Upset plot presenting the number of differentially expressed core DEOGs (cDEOGs) observed in other Pentapetalae species upon *S. sclerotiorum* infection, highlighting the conservation and variability of these core genes across a broader phylogenetic context. Data adapted from Sucher et al. (2020).

The regulation of induced cDEOGs is diversifying among *Solanum* species.

We characterised the function of the 16 infection-induced cDEOGs (see suppl. tab. 6). Interestingly, we identified two genes (OG0006904 and OG0018399) matching transcription factors of the AP2/ERF family. One of them, OG0018399, was previously characterised as an *S. lycopersicum* ERF-D6 transcription factor (Tominello-Ramirez et al. 2024). Furthermore, we found a putative chitinase/cell-wall degrading enzyme (OG0005084) and a putative UDP-glycosyltransferase (OG0000514) among oxidative stress regulation (fig. 4).

We hypothesised that the expression pattern of those infection-induced cDEOGs might be mostly uniform, as they are induced by infection and differentially regulated between susceptible and resistant genotypes. However, we observed a diversified regulatory pattern among all induced cDEOGs with contradictory regulation. Most interesting, the putative ERF D6 (OG0018399) is significantly upregulated in the resistant genotypes of *S. habrochaites*, *S. pennellii* and *S. chilense*. Yet, it is downregulated in the resistant genotypes of *S. pimpinellifolium* and *S. lycopersicoides* (indicating a higher induction in the susceptible genotypes, fig. 4). Interestingly, except for OG0004836, all induced cDEOGs share an evolutionary origin predating the emergence of flowering plants, suggesting that these highly conserved genes remain subject to differential regulation (suppl. tab. 6). Concluding, our differential gene expression (DEG) analysis gained initial insights into the regulatory dynamics driven by contrasting infection conditions and/or genotypes and shows that rewiring of expression pattern of shared infection-induced DEOGs may be source of QDR adaptation at the species level.

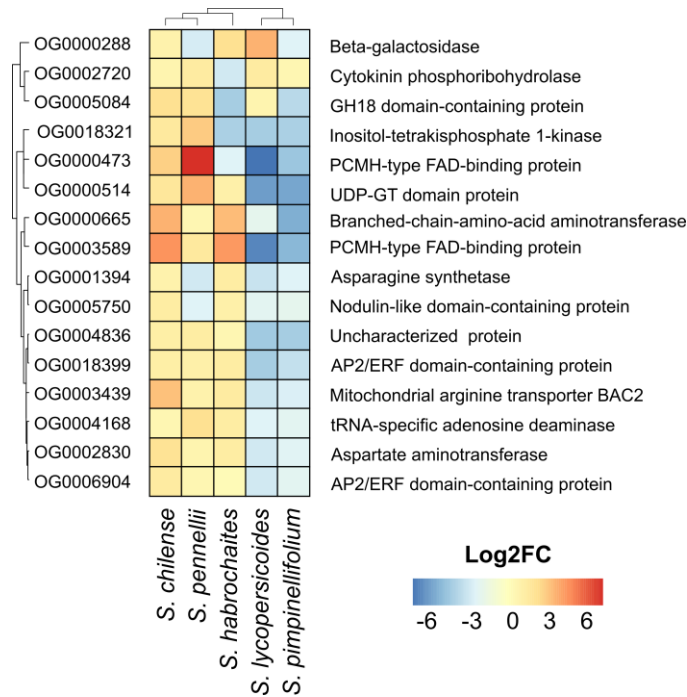


Figure 4: Differential Expression of 16 core infection-induced DEOGs. The heatmap illustrates the differential expression levels of 16 core infection-induced differentially expressed orthologous genes (DEOGs) across the five tomato species. Each row represents a gene, and columns correspond to comparisons between resistant and susceptible genotypes within each species. The colors indicate the magnitude and direction of expression differences in infected conditions, showing inconsistent gene regulation patterns associated with resistance and susceptibility to infection.

Weighted Gene Correlation Network Analysis reveals evidence of transcriptome specification.

While informative, DEG analysis alone cannot fully capture the complexity of the underlying regulatory pathways and networks. Thus, to further investigate global transcriptional rewiring of QDR responses in our five species and to achieve a more comprehensive understanding of QDR across species, we employed multiple Weighted Gene Correlation Network Analyses (WGCNA).

First, we constructed an orthology-based pan-species network. We hypothesised that the overarching gain of QDR might be correlated with the module eigengenes. To test this, we constructed a gene-correlation network based on 7,419 single-copy orthogroups, which were grouped into eleven distinct coregulatory modules, with a total of 462 hub genes (fig. 5A&B, suppl. fig. 4). Following network construction, we examined both inter- and intramodular edges. We validated the biological relevance of module assignments through functional assignments using Gene Ontology terms. We used a linear model to infer QDR-phenotypes as ranks with the module eigengenes (MEs).

Interestingly, we found no significant and biologically meaningful association of module eigengene expression with the LDT. While certain modules (e.g., blue, yellow, turquoise) showed a strong association with the infection as such, there was no clear gradient in module eigengene estimates from the most susceptible to the most resistant genotype. Moreover, despite having similar LDT (Rank7/Rank8, suppl. tab 1), these two genotypes show notably contrasting module eigengenes in infection-associated modules (for instance, Rank7 blue = -1.86 versus Rank8 blue = 0.41). At the same time, the strongest associations in the module-trait relationships emerge between genotypes within the same species (such as Rank2 and Rank3 or Rank1 and Rank4), suggesting that QDR regulation could be tightly integrated into genotype- or species-specific regulatory frameworks.

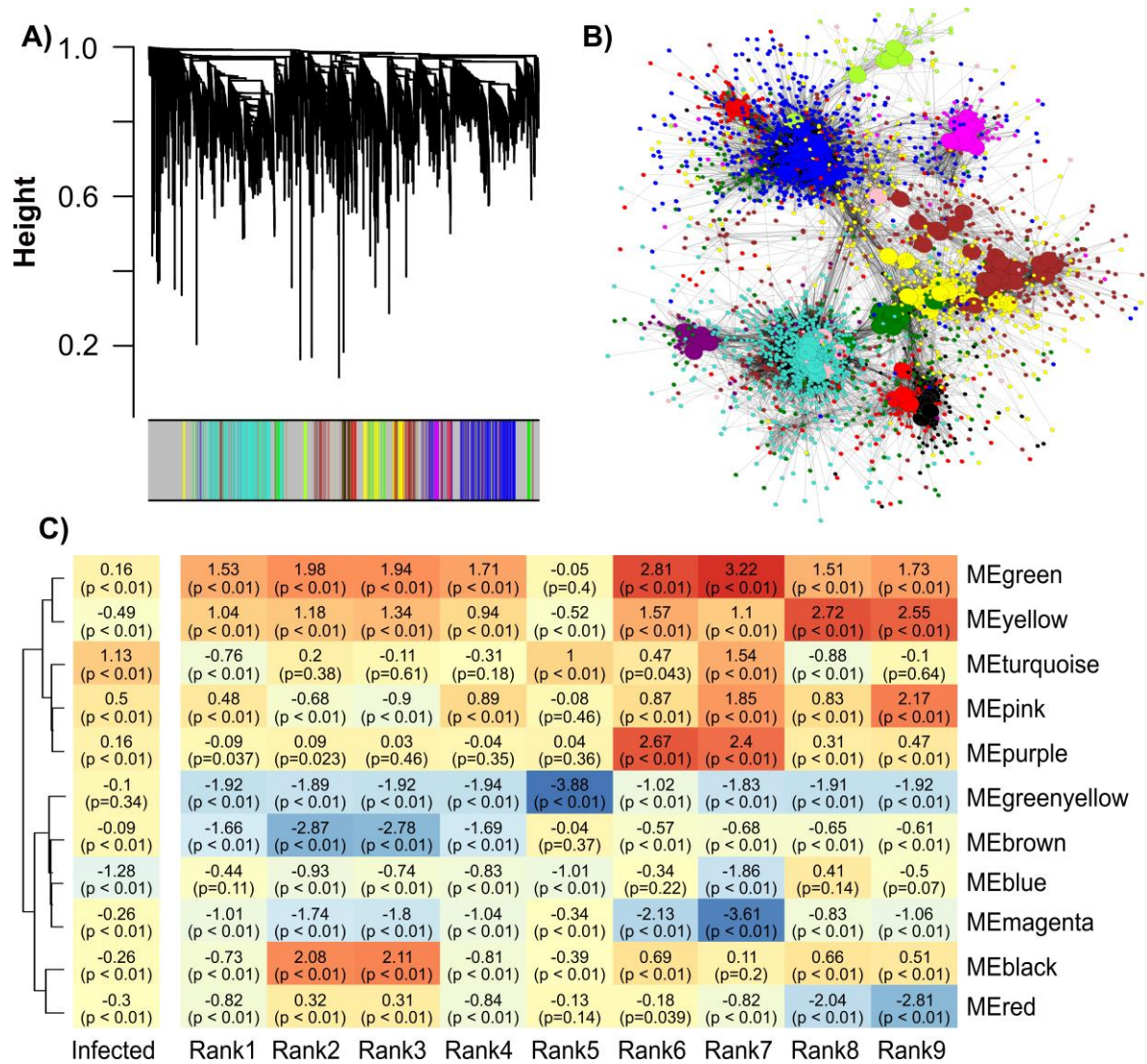


Figure 5: Weighted Gene Correlation Analysis of a single-copy orthogroup across five tomato species. **A)** Dendrogram illustrating the clustering of single-copy orthogroups into modules, with each module assigned a unique color. **B)** Network visualization of the orthogroup-based modules, where large nodes represent highly connected hub genes. **C)** Module-trait relationships derived from a linear model using module eigengenes as the response and infection state plus resistance rank as predictors. Resistance rank is relative to the most resistant genotype (*S. lycopersicoides*, LA2951), and infection status is compared to mock conditions (see suppl. tab. 1). The coefficients shown represent effect size estimates from ANOVA, while the accompanying p-values indicate significance after FDR correction.

Accordingly, we hypothesise that the OG-based network (based on two genotypes per species) may lack the statistical power to link regulatory patterns to cross-species phenotypes confidently or that phenotypic resistance is achieved through interlinked, species-specific pathways (fig. 5C, suppl. tab. 7).

Species-specific network topology is linked to QDR variation.

We, therefore, performed per-species regulatory network analyses to gain higher-resolution insights into QDR regulation. Specifically, we compared *S. lycopersicoides* and *S. pennellii* - the two species that displayed the most pronounced differences in resistance phenotypes across the tested genotypes. In *S. pennellii*, 16,577 genes were clustered into eight co-expression modules, while 18,558 *S. lycopersicoides* genes were grouped into nine modules (fig. 6A&B). For both species, we identified modules with predominant genotype association (exhibiting no significant interaction with infection), thus reflecting basal, genotype-specific alteration of gene expression (e.g., black and green modules in *S. pennellii* and the brown and yellow modules in *S. lycopersicoides*, fig. 6C&D). Conversely, we detected six *S. pennellii* and seven *S. lycopersicoides* modules significantly associated with infection (estimate > 0.2). The modules showing a significant association with the infection:genotype interaction are particularly interesting, as these are likely the strongest candidates for explaining the differential QDR phenotypes. Complementary to the statistical analysis, we evaluated the module eigengenes (MEs) visually and used functional annotation to identify modules with a putative role in resistance (suppl. fig. 6&7, suppl. tab. 8&9). Accordingly, we identified three modules in *S. pennellii* ('red,' 'pink,' and 'blue') and three *S. lycopersicoides* modules ('pink,' 'green,' and 'turquoise') with a putative role in resistance. Next, we combined both datasets using orthogroups to quantify the extent of overlap between resistance modules of the respective species. We assessed the robustness of this overlap using Fisher's exact test with FDR-corrected p-values. 2,264 of 3,683 orthologous *S. pennellii* resistance genes were significantly enriched in the *S. lycopersicoides* resistance modules (suppl. tab. 10&11, fig. 6E&F). However, a significant number of *S. pennellii* genes did not cluster in *S. lycopersicoides* resistance modules: 386 genes were assigned to the yellow module and 240 to the green module. Interestingly, 1,277 genes from the *S. pennellii* resistance modules could not be assigned to a specific *S. lycopersicoides* module and were assigned to the grey module. We observed a similar pattern when projecting genes from the *S. lycopersicoides* resistance modules onto the *S. pennellii* gene regulatory network. In this case, 1,918 of the 3,702 orthologous genes were located in the *S. pennellii* resistance-associated blue module.

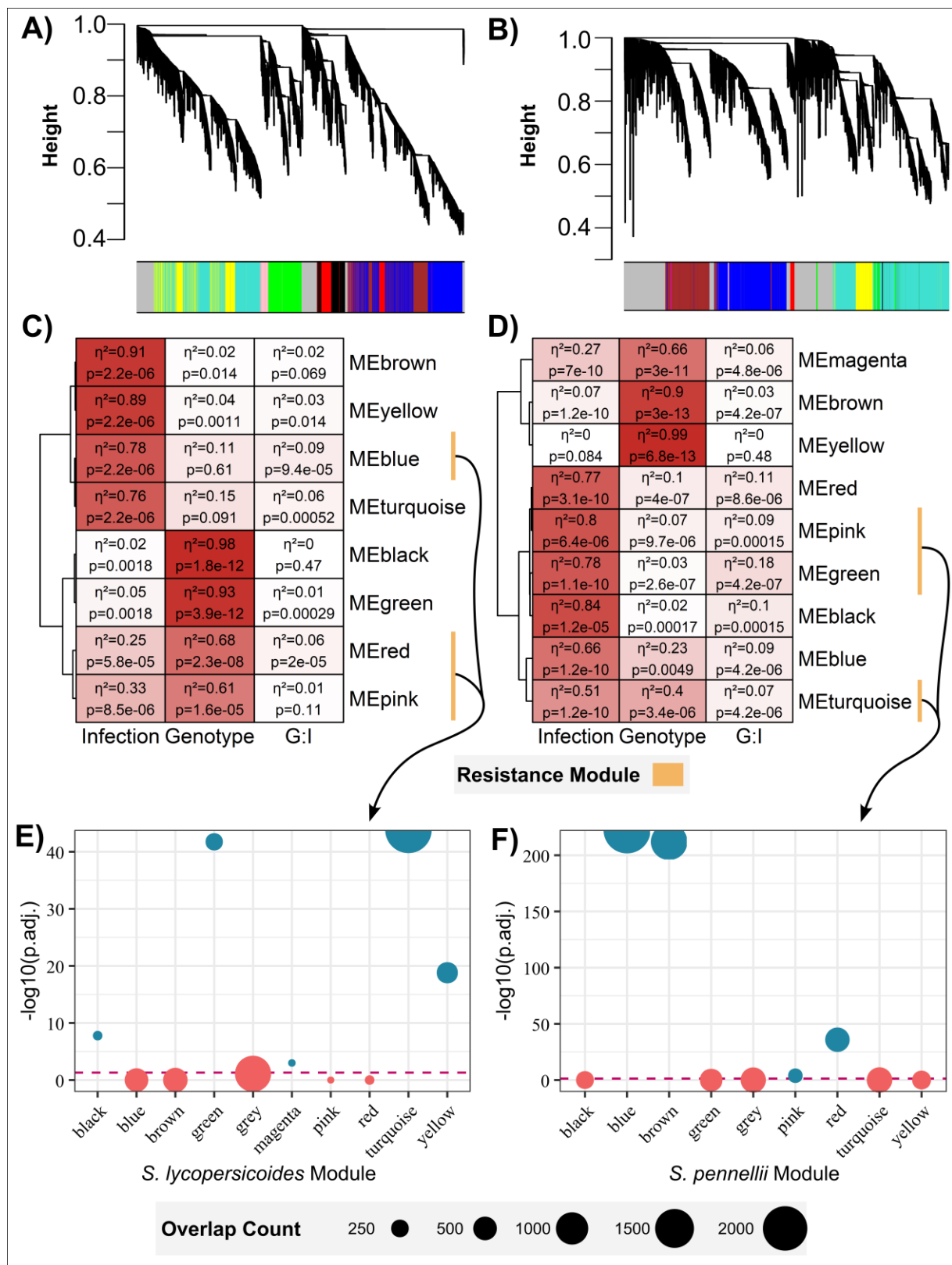


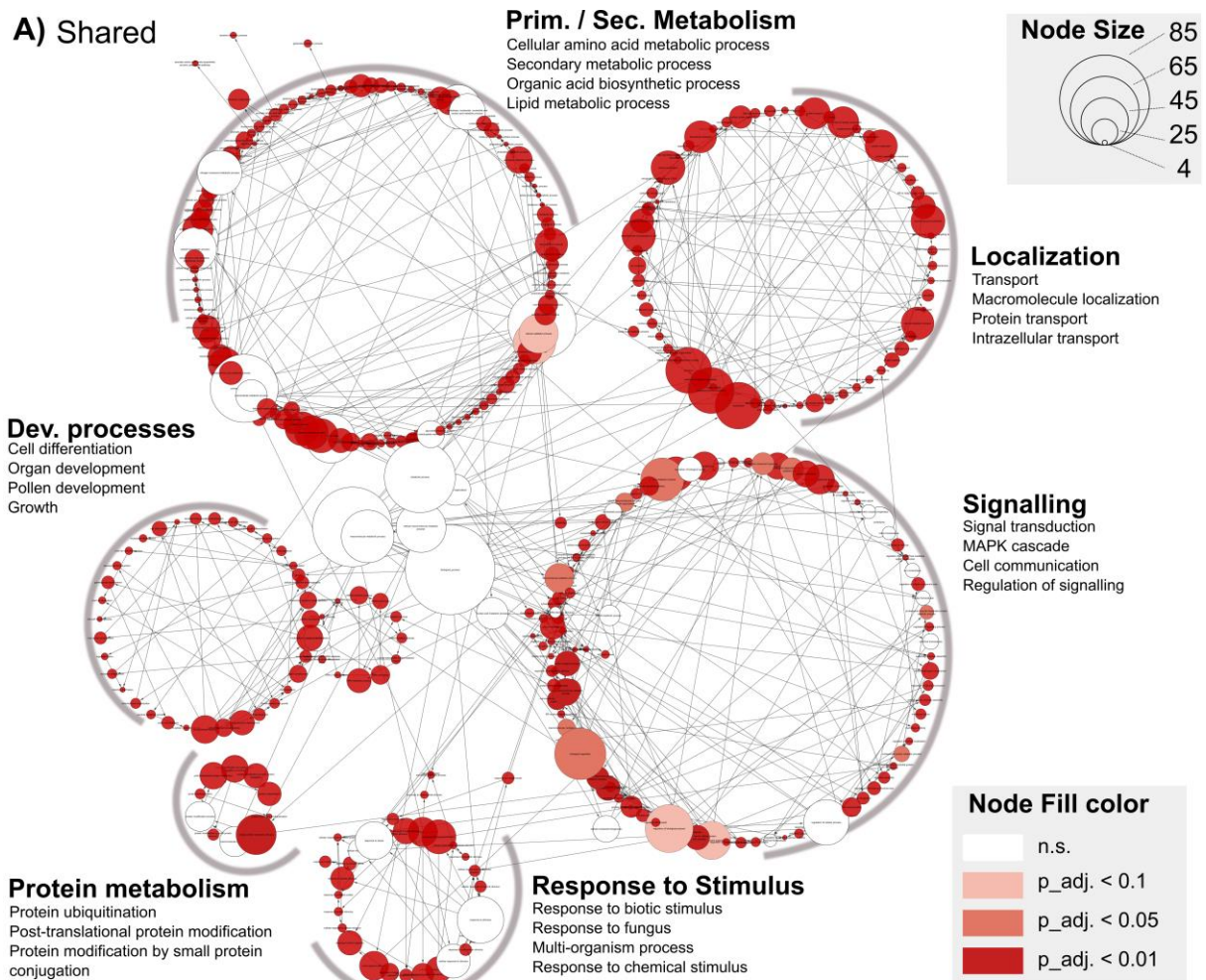
Figure 6: Weighted Gene Correlation Network Analysis of A) *S. pennellii* and B) *S. lycopersicoides* RNAseq data. Module eigengenes were correlated with the traits "Infection", "Genotype", and the interaction "Genotype x Infection" using a linear model. The effect size is provided as η^2 , and FDR-corrected p-values are provided for C) *S. pennellii* and D) *S. lycopersicoides*. Resistance-associated modules were marked. The module preservation of E) *S. pennellii* resistance genes in *S. lycopersicoides* modules and F) *S. lycopersicoides* resistance genes in *S. pennellii* modules were tested using orthogroup-based inference and a Fisher's exact test. The dot size indicates the number of overlapping genes, while the blue colour indicates a significant enrichment.

In comparison, a significant number of genes (1,101 genes) was assigned to the brown module, which is specific to infection response rather than resistance. These findings indicate that although several QDR-related genes might be shared across species, a significant subset of QDR genes remains associated with distinct non-resistance modules reflecting species-specific regulatory fine-tuning.

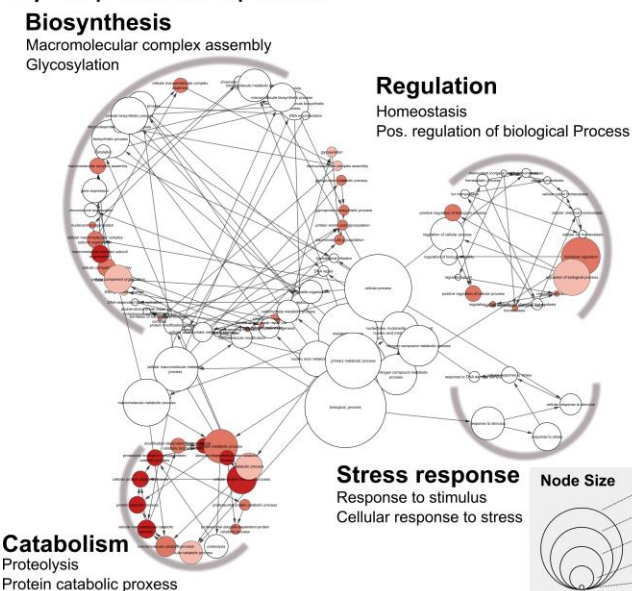
Functional enrichment reveals a broad core functional set and specific species functions.

We then performed a GO-term enrichment analysis on both species' shared and unique QDR-module gene sets to assess whether those harboured specific functional traits. Among the 2,264 overlapping genes, we identified a diverse array of significantly enriched GO-terms clustered into six groups: primary/secondary metabolism, localisation, developmental processes, protein metabolism, signalling, and response to stimulus. Within these clusters, we found enrichment of protein transport and localisation, lipid and carbohydrate metabolism, and cinnamic acid synthesis involving processes. Notably, we did not observe a clear enrichment for hormone homeostasis (fig. 7A). In contrast, the *S. pennellii*-specific genes were clustered into four functional groups: biosynthesis (including macromolecule/protein glycosylation), positive regulation of cellular/biological processes, stress response, and catabolism, with modest enrichment for signalling functions (fig. 7B).

A) Shared



B) *S. pennellii* specific



C) *S. lycopersicoides* specific

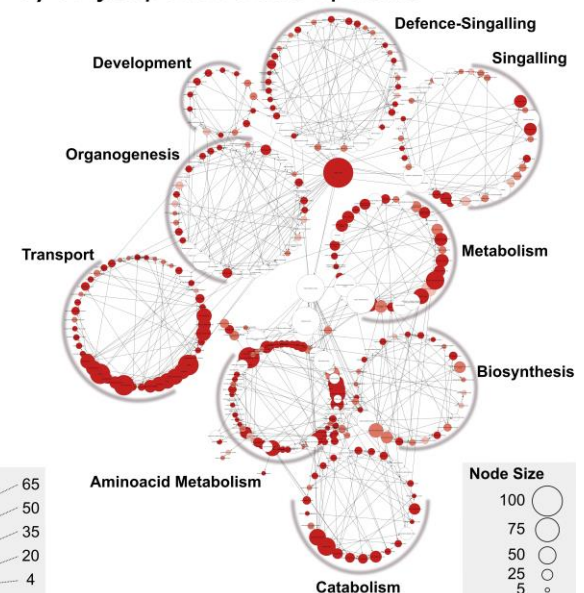


Figure 7: Gene Ontology (GO) Enrichment Analysis of Resistance Coexpression Modules. A) Core genes shared across the resistance modules of *S. pennellii* and *S. lycopersicoides*. B) *S. pennellii*-specific genes, C) *S. lycopersicoides*-specific genes. In each panel, the size of a dot corresponds to the number of genes associated with a GO term, while the fill colour indicates the FDR-corrected significance level of the enrichment. This visualisation highlights key functional categories enriched in core and species-specific resistance responses.

For *S. lycopersicoides*, we identified nine differentially regulated functional clusters, with a particular emphasis on transport, amino acid metabolism, general metabolism, and defence signalling (fig. 7C). These findings support a two-tier model of QDR regulation between species: a broad, shared set of genes provides general disease resistance, while host-specific mechanisms offer more targeted functions. For example, *S. pennellii* may rely on detoxification via glycosylation, whereas *S. lycopersicoides* could depend more on specialised transport processes. This model underscores how an equilibrium of shared and species-specific strategies may shape effective defence responses across different *Solanum* species.

Shared QDR regulation comprises evolutionarily conserved genes.

To test the hypothesis that the specification of QDR signalling may be subject to diversifying selection, we calculated the Transcript Age Index (TAI) and Transcript Divergence Index (TDI) for both shared and species-specific gene sets. Our analysis revealed that species-specific genes are evolutionarily younger, as suggested by increased TAI (e.g., *S. pennellii*: overlap TAI = 1.69 vs. unique TAI = 1.92; *S. lycopersicoides*: overlap TAI = 1.73 vs. unique TAI = 2.4, see table 1). Additionally, shared genes from resistance modules showed lower TDI values, indicating signs of stronger purifying selection than observed on the unique sub-modules (*S. pennellii*: 4.3 vs 4.7; *S. lycopersicoides*: 4.3 vs 4.9, see suppl. tab. 12). This is further supported by significantly elevated ratio of nonsynonymous mutations to synonymous mutations (dNdS) in each species' uniquely regulated gene set compared to the whole resistance modules (suppl. fig. 8). Accordingly, we hypothesise that both species share a conserved, ancestral suite of genes that presumably form the “backbone” of the quantitative defence network regulation, while younger, less strongly conserved genes underlie specification. This balance between conservation and innovation might be critical for the dynamic fine-tuning of defence responses against generalist pathogens over evolutionary timescales.

Table 1: Per-Species Transcript Age Index (TAI) of Resistance-Modules covering shared and unique gene sets. Mean TAI values are provided with +/- SD.

Species	Whole Resistance Modules	Overlap	Unique
<i>S. pennellii</i>	1.77319975 ± 0.006335785	1.6909445 ± 0.00817666	1.922385 ± 0.007211685
<i>S. lycopersicoides</i>	1.981305 ± 0.019387067	1.7368255 ± 0.009673017	2.4065145 ± 0.035387022

QDR in *S. pennellii* genotype LA2963 may have evolved by co-optation of a transcription factor.

To test the above hypothesis whether regulatory hubs or the periphery drive the evolutionary signature of the network, we integrated gene-regulatory network analysis with dN/dS analysis across multiple species. We extracted potentially interesting transcription factors according to the following criteria: a) hub in the WGCNA network (high connectivity), b) gene in the resistance module, c) hub in the gene regulatory network and identified highly connected transcription factors for both focal species (18 in *S. lycopersicoides* and 10 in *S. pennellii*). We then focussed on TFs exhibiting differential expression patterns in response to infection and between genotypes with varying resistance levels and compared their subnetworks across multiple species.

In *S. pennellii*, this subset includes a putative Trihelix transcription factor GT-3b (Sopen09g001470, OG0007365), a MADS-box domain containing-protein (Sopen10g006210, OG0015518) and NAC transcription factor 29 (Sopen05g003630, OG0005445, fig. 8A). In *S. lycopersicoides*, we observed an ethylene-response transcription factor 14 (Solyd03g050610, OG0003738), and two HSF-type DNA-binding domain-containing proteins (Solyd02g064330, OG0000116, Solyd09g071070, OG0009560) with a strong association with the resistant genotype (fig. 8C). Generally, these TFs were more strongly induced in the resistant genotype and are part of a resistance-associated coregulatory module.

We then examined whether the orthologues of these putative resistance-related transcription factors (TFs) showed similar patterns in the other species. We discovered a wide diversity in TF expression among all members of the same orthogroup. For example, the TF Sopen05g003630 (OG0005445) was strongly induced only in the resistant genotype of *S. pennellii*, although this gene is present and expressed in other species. Moreover, OG0005445

is not specifically induced in resistant genotypes nor assigned to a resistance module of the other species. This suggests that the regulation of Sopen05g003630 (OG0005445) might represent a resistance mechanism unique to the *S. pennellii* – *S. sclerotiorum* interaction. So, the regulation and the downstream processes of this TF might have shifted in *S. pennellii* compared to the other species (fig. 8A&B). The genes Sopen10g006210 (OG0015518) and Sopen09g001470 (OG0007365) show an elevated expression pattern specific to the resistant *S. pennellii* genotype. While we could not detect a strong expression of Sopen10g006210 in the other species, the expression pattern of Sopen09g001470 is not linked to the QDR phenotypes (suppl. fig. 9). We observed a similar pattern of diversifying regulation on the *S. lycopersicoides* genes Solyd03g05610 (OG0003738) and Solyd09g071070 (OG0009560), with no clear interspecific QDR-regulation (suppl. fig. 9).

In contrast, the *S. lycopersicoides* gene Solyd02g064330 (OG0000116) appeared highly conserved across species with high similarity in expression pattern among the other species (orthologues also belong to resistance modules and are more highly expressed in resistant genotypes). Even so, we found strong differential regulation depending on the individual paralog (fig. 8D). Interestingly, low dN/dS ratios suggest that both, Sopen05g003630 and Solyd02g064330, transcription factors are under purifying selection (Solyd02g064330 dN/dS = 0.4539 and Sopen05g003630 dN/dS = 0.1884) (suppl. tab. 13). Additionally, the GRNs of all resistance TFs are enriched for younger genes that emerged with the flowering plants and show a significant under-representation of older genes compared to the entire transcriptome (suppl. fig. 10). These younger genes and the low dN/dS ratios do not fully explain the novel regulatory functions. Therefore, we propose that regulatory evolution, rather than changes in nucleotide sequences, drives the evolution and short-term adaptation of these TFs.

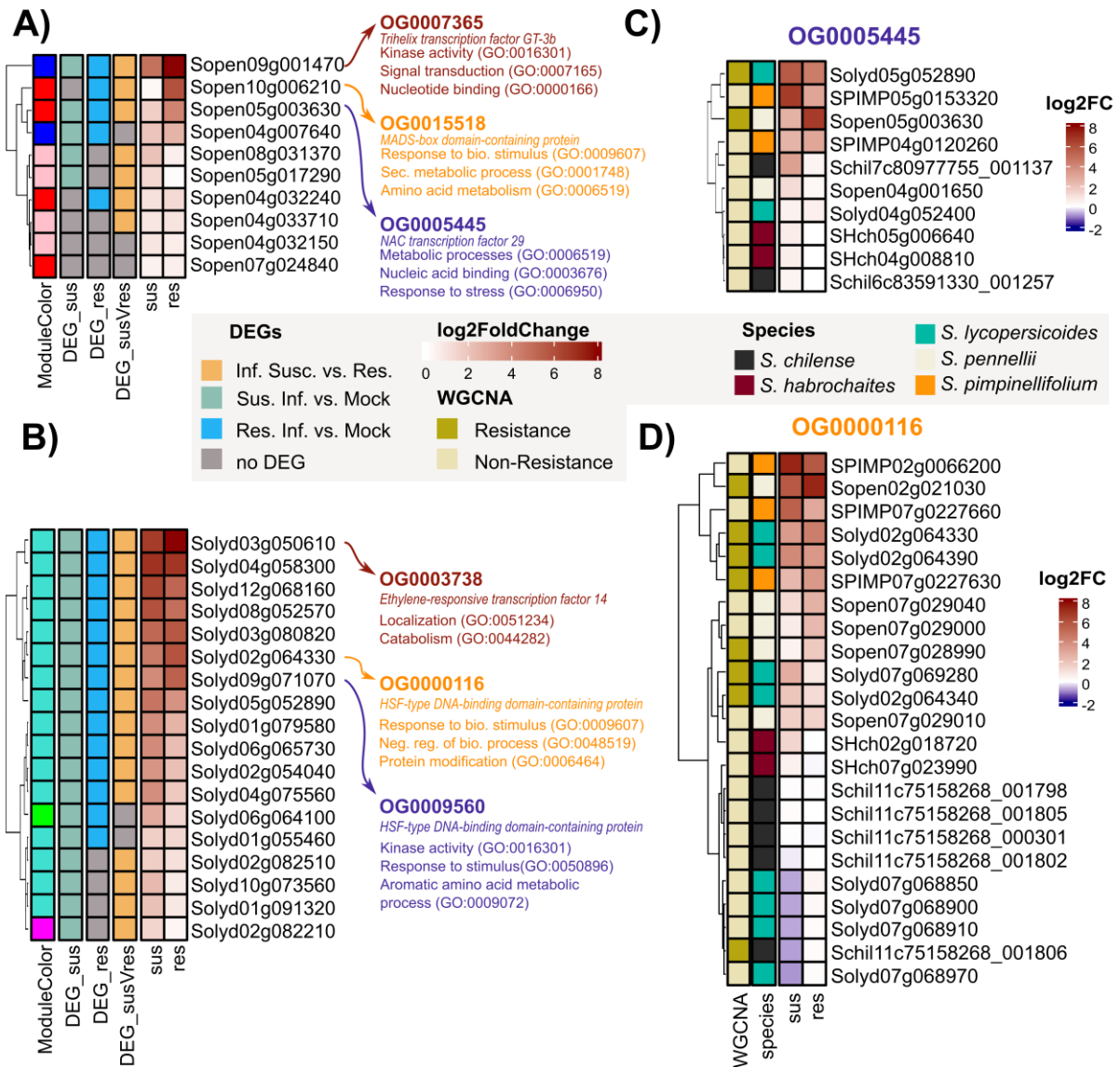


Figure 8: Gene Regulatory Network Analysis Reveals a Shared Transcription Factor Co-opted for Divergent Regulation and Coexpression. The heatmaps in panels A) and B) illustrate transcription factor (TF) regulation in susceptible and resistant genotypes of *S. pennellii* and *S. lycopersicoides*, respectively. Each TF is a hub gene in the GRN and WGCNA and is located in a resistance module. Each heatmap row corresponds to a TF, with the 'ModuleColor' column indicating its assignment to a specific WGCNA resistance module. Differential expression analysis of relevant contrasts is also displayed, with the three most strongly regulated TFs highlighted along with their corresponding orthogroups. For these key TFs, summarized GO terms for their downstream coexpressed genes are provided, offering insights into their functional roles in resistance pathways. The regulation of these resistance-associated TFs ((C) *S. pennellii*: Sopen05g003630-OG0005445, (D) *S. lycopersicoides*: Solyd02g064330-OG0000116) was then compared across species using orthogroups. The expression of each gene within the respective orthogroup was visualised across varying levels of QDR (susceptible | resistant), with colour coding indicating the respective species and the assignment of each TF to its species-specific resistance module.

Discussion

In this study, we asked whether variance in observed quantitative disease resistance phenotypes against generalist pathogens in closely related yet diverse species is governed by one or multiple mechanisms and how such variance can evolve. Singular studies on gene or gene family evolution alone cannot fully capture this complexity (Kahlon and Stam 2021). Therefore, we performed integrated transcriptomics across five wild tomato species infected with *S. sclerotiorum*. By combining differential expression, WGCNA, GRN, and deeper evolutionary analysis, we uncover both conserved and species-specific QDR strategies, highlighting a complex interplay between core and adaptive regulatory mechanisms.

Resistance against *S. sclerotiorum* underlies a complex regulatory interplay.

Studies on diverse crops and model plants (e.g., soybean, rapeseed, sunflower, bean, pepper, tomato, *A. thaliana*) reveal broad variation in QDR against *S. sclerotiorum* (Boland and Hall 1994; Boudhrioua et al. 2020; Chauhan et al. 2020; Ding et al. 2021; Fusari et al. 2012; Mazumdar 2021; Mei et al. 2012; Musa-Khalifani et al. 2021; Sucher et al. 2020; Uloth et al. 2013; Yanar and Miller 2003; Einspanier et al. 2024). Accordingly, QDR may be governed by a complex array of regulatory and genomic features, as suggested by the large variation in differentially expressed genes (DEGs), ranging from a few dozen to over 20,000, observed under diverse experimental conditions (Fass et al. 2020; Joshi et al. 2016; Tang et al. 2023; Wu et al. 2016; Sucher et al. 2020; Chen et al. 2022). However, our findings highlight that the number of DEGs following *S. sclerotiorum* infection is not directly linked to QDR levels within or between species. In a broad-scale study, Sucher et al. (2020) proposed that regulatory flexibility and specificity of gene expression changes are essential for QDR. We show that the differential expression of resistance-associated genes is highly diverging between the species, and shared genes show contrasting regulatory patterns among the species. The wide variability of DEG counts and -regulation, as well as the dominance of species-specific patterns, underscores the complexity of plant-pathogen interactions and suggests the role of distinct molecular strategies.

QDR-Regulation is based on both host-specific and conserved genes.

We examined both interspecific and intraspecific regulatory responses to infection. Comparing gene regulatory and co-expression networks across species remains challenging, and cross-

species mapping doesn't allow the identification of species-specific genes. Therefore, we directly compared differentially expressed genes (DEGs) and network topologies by focusing on orthologous genes (Külahoglu et al. 2014; Langfelder et al. 2011; Ovens et al. 2021; Hu et al. 2016). This approach preserves a larger number of species-specific transcripts and facilitates the projection of findings onto more distantly related plant species. Furthermore, leveraging orthologs maintains the integrity of each species' unique transcriptome and enhances our ability to uncover both conserved and unique regulatory mechanisms that underpin similar phenotypic outcomes.

Although the tested genotypes share notable genome/proteome similarity, the regulatory networks remain highly species-specific, suggesting that fine-scale shifts in gene regulation may drive the emergence of unique traits (Halfon 2017; Smith et al. 2014). In some cases, genotype effects surpass those induced by infection, suggesting genotype-specific signalling dominates in certain backgrounds. This aligns with our WGCNA-based observation that regulatory patterns correlate more strongly with species identity than any uniform resistance gradient. Nevertheless, each species possesses co-regulatory modules linked to resistance. Focusing on the overlap between *S. pennellii* and *S. lycopersicoides*, we found that shared modules appear involved in common defence responses. In contrast, unique sub-modules focus on specialised traits (e.g., signalling or detoxification). This suggests that GRNs are finetuned on a species level, also when it comes to defence against broad-host-range necrotrophic pathogens (Smith et al. 2014). Other indications of GRN specialisation for supposedly generic tasks exist: only a minority of *S. lycopersicum* cis-regulatory elements controlling wound response overlap with *S. pennellii* (Liu et al. 2018; Jones and Vandepoele 2020).

Rewiring Gene Networks as an Adaptive Strategy.

The pattern of gene expression can change faster than the divergence of nucleotides. This may be due to the modification of transcription factor binding sites or the emergence of cis-regulatory elements leading to new TF expression profiles (Winkelmüller et al. 2021). Accordingly, shifts in gene regulation provide a more flexible means of adapting to changing environmental conditions and finetuning genomic predisposition (Koenig et al. 2013). The evolution of gene regulatory networks has been subject to intensive debates, with two main hypotheses proposed to explain regulatory diversity: hub conservation, where downstream differentiation occurs, versus hub divergence, where central regulatory genes shift in function. Some studies suggest that regulatory hub genes might remain conserved (Masalia et al. 2017).

However, Wei et al. (2024) emphasised the importance of hub gene divergence and subsequent network topology shifts as the key driver of *S. chilense* adaptation to drought stress. Indeed, network re-wiring, potentially via modifying a single core gene, can significantly affect phenotypic plasticity (Koubkova-Yu et al. 2018). This may lead to highly specific responses, such as detoxification or enhanced protein localisation processes, as observed in this study. A recent study by Dong et al. (2024) found evidence for GRN-rewiring by reimplementing an ancient transcription factor, which altered the response to nutrient status in *Marchantia polymorpha*. Here, we present the first evidence of gene regulatory network rewiring leading to increased levels of QDR against a necrotrophic pathogen. Interestingly, both conserved and shared QDR-GRNs significantly enrich evolutionary younger genes dating back to Mesangiospermae-Solanales and discriminate older genes. Accordingly, we speculate that the adaptation to biotic stresses is modulated via shifts in the regulation and not adaptation via gene family founder events. Following this, core genes might be subject to negative selection, but regulating core TFs and the periphery might facilitate nuanced adaptation (Fagny and Austerlitz 2021).

Co-optation of a TF might govern QDR in *S. pennellii* LA2963.

Co-optation/exaptation or gene duplication followed by divergence are two potential mechanisms driving neofunctionalisation in plant-parasite interactions (Macquet et al. 2022; Plachetzki and Oakley 2007). Especially, the co-optation of transcription factors might display a major source of new regulatory patterns in GRNs (Artur and Kajala 2021). We identified a NAC29 transcription factor as a key modulator of QDR in *S. pennellii*. NAC transcription factors govern a wide array of developmental processes (e.g. flowering, cell cycle progression, and cell division) and may play a role in abiotic stress resistance (Zhang et al. 2018b; Nakashima et al. 2012; Kim et al. 2006; Ueda et al. 2020; Gonzalez-Bayon et al. 2019). Although some members of the NAP subgroup of NAC TFs might be involved in biotic stress response, only a few studies have linked them to resistance against necrotrophic pathogens (Lu et al. 2024; Tominello-Ramirez et al. 2024; Ma et al. 2021; Zhang et al. 2018a; Wang et al. 2020a; Masri and Kiss 2023). However, their role in promoting ROS tolerance could bolster disease resistance against *S. sclerotiorum* (Liu et al. 2014; Kabbage et al. 2015). The potential of NAC TFs in regulating diverse, species-specific processes highlights their evolutionary plasticity and adaptability. Interestingly, we observed differential regulation of NAC29 and changes in the downstream targets. However, the identification of co-optation events can be challenging.

By studying the phylotranscriptomics signature of resistance-associated GRNs, we can significantly enrich our understanding of QDR by integrating gene expression data with gene age (phylostratigraphy). By classifying genes into evolutionary “strata” and evaluating their expression profiles during pathogen challenge, we can assess whether older, highly conserved defence mechanisms or younger, lineage-specific expansions (perhaps newly co-opted for defence) drive quantitative resistance. We identified peaks in gene-family founder events that we can link to predicted genome expansions, such as a putative whole-genome triplication before solanales divergence. (Clark and Donoghue 2018; Huang et al. 2023; Maheepala et al. 2019). Subsequent expansions in angiosperms (Magnoliopsida) correlate with the reported emergence of flowering-specific genes, phytohormone signalling, pathogen defence, and secondary metabolism, underscoring genome duplication’s role in trait diversification (Huang et al. 2023; Maheepala et al. 2019; Clark and Donoghue 2018; Chanderbali et al. 2016; Bowles et al. 2020). Furthermore, the subsequent rise in taxonomically restricted genes within the Solanaceae may be attributed to the same genome triplication event, suggesting that such duplications drive species-specific adaptations and innovations (Clark and Donoghue 2018). Although we found evidence for species-specific gene-family expansion, we did not observe a link between taxonomically restricted genes on species level with QDR.

Conclusion

Based on the phylotranscriptomic signature (i.e., shared copy numbers across *Solanum* species, broad basal expression patterns, and an ancient origin dating back to cellular organisms) and its unique functional role in *S. pennellii* LA2963, we propose that NAC29 has been co-opted for resistance-related functions against a necrotrophic pathogen. The parallel shifts in TF expression and downstream genes suggest that different mechanisms determine NAC29 co-optation. Possibly, altered TF regulation and differentiation of TF targets might underlie strong species-specific variability (e.g., cis-/trans-regulation and/or chromatin modifications, Jones and Vandepoele 2020). Possibly, the combination of trans- and cis-regulation might influence the equilibrium between conserved and specified QDR responses, as cis-regulation might underlie stronger differentiation (Wu et al. 2021). However, further research is needed to clarify the mechanisms underlying the co-optation of transcription factors driving resistance (Yuan et al. 2019). Additionally, it remains unclear how many ‘silent’ regulatory changes without a phenotypic effect (so-called developmental system drift) might influence the capacity to respond to environmental stress (Halfon 2017). Overall, NAC29 may serve as a prime example

of how transcription factors can be repurposed for QDR, illustrating the broader role of TF co-optation in plant adaptation.

Acknowledgements

We warmly thank Bettina Bastian for maintaining the plant material, Susanne Kleingarn for her wet lab support and Janina Fuß (CCGA) for her support during the sequencing. We also thank the TGRC at UC Davis (USA) for curating the germplasm used in this study. This work was partly funded by the DFG (STA1547/6) and the Agence Nationale pour la Recherche (ANR-21-813 CE20-30).

Author Contributions

RS & SE designed the research, SE performed the experiments and conducted bioinformatic analysis, and SE & CTR & FD performed the data analysis. SE & RS wrote the manuscript. All authors read and approved the manuscript.

Publication bibliography

- Albaladejo, Irene; Meco, Victoriano; Plasencia, Felix; Flores, Francisco B.; Bolarin, Maria C.; Egea, Isabel (2017): Unravelling the strategies used by the wild tomato species *Solanum pennellii* to confront salt stress: From leaf anatomical adaptations to molecular responses. In *Environmental and Experimental Botany* 135, pp. 1–12. DOI: 10.1016/j.envexpbot.2016.12.003.
- Artur, Mariana A. S.; Kajala, Kaisa (2021): Convergent evolution of gene regulatory networks underlying plant adaptations to dry environments. In *Plant, Cell & Environment* 44 (10), pp. 3211–3222. DOI: 10.1111/pce.14143.
- Barrera-Redondo, Josué; Lotharukpong, Jaruwatana Sodai; Drost, Hajk-Georg; Coelho, Susana M. (2023): Uncovering gene-family founder events during major evolutionary transitions in animals, plants and fungi using GenEra. In *Genome Biology* 24 (1), p. 54. DOI: 10.1186/s13059-023-02895-z.
- Boland, G. J.; Hall, R. (1994): Index of plant hosts of *Sclerotinia sclerotiorum*. In *Canadian Journal of Plant Pathology* 16 (2), pp. 93–108. DOI: 10.1080/07060669409500766.
- Bolger, Anthony; Scossa, Federico; Bolger, Marie E.; Lanz, Christa; Maumus, Florian; Tohge, Takayuki et al. (2014): The genome of the stress-tolerant wild tomato species *Solanum pennellii*. In *Nature Genetics* 46 (9), pp. 1034–1038. DOI: 10.1038/ng.3046.
- Böndel, Katharina B.; Lainer, Hilde; Nosenko, Tetyana; Mboup, Mamadou; Tellier, Aurélien; Stephan, Wolfgang (2015): North–South Colonization Associated with Local Adaptation of the Wild Tomato Species *Solanum chilense*. In *Molecular Biology and Evolution* 32 (11), pp. 2932–2943. DOI: 10.1093/molbev/msv166.
- Boudhrioua, Chiheb; Bastien, Maxime; Torkamaneh, Davoud; Belzile, François (2020): Genome-wide association mapping of *Sclerotinia sclerotiorum* resistance in soybean using whole-genome resequencing data. In *BMC Plant Biology* 20 (1), p. 195. DOI: 10.1186/s12870-020-02401-8.
- Bowles, Alexander M. C.; Bechtold, Ulrike; Paps, Jordi (2020): The Origin of Land Plants Is Rooted in Two Bursts of Genomic Novelty. In *Current biology : CB* 30 (3), 530–536.e2. DOI: 10.1016/j.cub.2019.11.090.
- Buchfink, Benjamin; Reuter, Klaus; Drost, Hajk-Georg (2021): Sensitive protein alignments at tree-of-life scale using DIAMOND. In *Nature methods* 18 (4), pp. 366–368. DOI: 10.1038/s41592-021-01101-x.
- Camacho, Christiam; Coulouris, George; Avagyan, Vahram; Ma, Ning; Papadopoulos, Jason; Bealer, Kevin; Madden, Thomas L. (2009): BLAST+: architecture and applications. In *BMC bioinformatics* 10, p. 421. DOI: 10.1186/1471-2105-10-421.
- Caseys, Celine; Shi, Gongjun; Soltis, Nicole; Gwinner, Raoni; Corwin, Jason; Atwell, Susanna; Kliebenstein, Daniel J. (2021): Quantitative interactions: the disease outcome of *Botrytis cinerea* across the plant kingdom. In *G3 Genes\textbarGenetics* 11 (8), jkab175. DOI: 10.1093/g3journal/jkab175.
- Chanderbali, Andre S.; Berger, Brent A.; Howarth, Dianella G.; Soltis, Pamela S.; Soltis, Douglas E. (2016): Evolving Ideas on the Origin and Evolution of Flowers: New Perspectives in the Genomic Era. In *Genetics* 202 (4), pp. 1255–1265. DOI: 10.1534/genetics.115.182964.
- Chauhan, Sonali; Katoch, Shabnam; Sharma, S. K.; Sharma, P. N.; Rana, J. C.; Singh, Kuldeep; Singh, Mohar (2020): Screening and identification of resistant sources against *Sclerotinia sclerotiorum* causing white mold disease in common bean. In *Crop Science* 60 (4), pp. 1986–1996. DOI: 10.1002/csc2.20160.
- Chen, Na; Shao, Qin; Lu, Qineng; Li, Xiaopeng; Gao, Yang (2022): Transcriptome analysis reveals differential transcription in tomato (*Solanum lycopersicum*) following inoculation with *Ralstonia solanacearum*. In *Scientific Reports* 12 (1), p. 22137. DOI: 10.1038/s41598-022-26693-y.
- Clark, James W.; Donoghue, Philip C. J. (2018): Whole-Genome Duplication and Plant Macroevolution. In *Trends in Plant Science* 23 (10), pp. 933–945. DOI: 10.1016/j.tplants.2018.07.006.
- Comeron, Josep M. (1995): A method for estimating the numbers of synonymous and nonsynonymous substitutions per site. In *Journal of Molecular Evolution* 41, pp. 1152–1159.

- Corwin, Jason A.; Kliebenstein, Daniel J. (2017): Quantitative Resistance: More Than Just Perception of a Pathogen. In *The Plant Cell* 29 (4), pp. 655–665. DOI: 10.1105/tpc.16.00915.
- Crow, Megan; Suresh, Hamsini; Lee, John; Gillis, Jesse (2022): Coexpression reveals conserved gene programs that co-vary with cell type across kingdoms. In *Nucleic acids research* 50 (8), pp. 4302–4314. DOI: 10.1093/nar/gkac276.
- Curci, Pasquale Luca; Zhang, Jie; Mähler, Niklas; Seyffert, Carolin; Mannapperuma, Chanaka; Diels, Tim et al. (2022): Identification of growth regulators using cross-species network analysis in plants. In *Plant Physiology* 190 (4), pp. 2350–2365. DOI: 10.1093/plphys/kiac374.
- Delplace, Florent; Huard-Chauveau, Carine; Berthomé, Richard; Roby, Dominique (2022): Network organization of the plant immune system: from pathogen perception to robust defense induction. In *The Plant journal : for cell and molecular biology* 109 (2), pp. 447–470. DOI: 10.1111/tj.15462.
- Delplace, Florent; Huard-Chauveau, Carine; Dubiella, Ullrich; Khafif, Mehdi; Alvarez, Eva; Langin, Gautier et al. (2020): Robustness of plant quantitative disease resistance is provided by a decentralized immune network. In *Proceedings of the National Academy of Sciences* 117 (30), pp. 18099–18109. DOI: 10.1073/pnas.2000078117.
- Derbyshire, Mark C.; Newman, Toby E.; Khentry, Yuphin; Owolabi Taiwo, Akeem (2022): The evolutionary and molecular features of the broad-host-range plant pathogen *Sclerotinia sclerotiorum*. In *Molecular Plant Pathology* 23 (8), pp. 1075–1090. DOI: 10.1111/mpp.13221.
- Derbyshire, Mark C.; Raffaele, Sylvain (2023): Till death do us pair: Co-evolution of plant–necrotroph interactions. In *Current Opinion in Plant Biology* 76, p. 102457. DOI: 10.1016/j.pbi.2023.102457.
- Ding, Li-Na; Li, Teng; Guo, Xiao-Juan; Li, Ming; Liu, Xiao-Yan; Cao, Jun; Tan, Xiao-Li (2021): *Sclerotinia* Stem Rot Resistance in Rapeseed: Recent Progress and Future Prospects. In *Journal of Agricultural and Food Chemistry* 69 (10), pp. 2965–2978. DOI: 10.1021/acs.jafc.0c07351.
- Dobin, Alexander; Davis, Carrie A.; Schlesinger, Felix; Drenkow, Jorg; Zaleski, Chris; Jha, Sonali et al. (2013): STAR: ultrafast universal RNA-seq aligner. In *Bioinformatics (Oxford, England)* 29 (1), pp. 15–21. DOI: 10.1093/bioinformatics/bts635.
- Dong, Yating; Krishnamoorthi, Shalini; Tan, Grace Zi Hao; Poh, Zheng Yong; Urano, Daisuke (2024): Co-option of plant gene regulatory network in nutrient responses during terrestrialization. In *Nature plants* 10 (12), pp. 1955–1968. DOI: 10.1038/s41477-024-01851-4.
- Drost, Hajk-Georg; Gabel, Alexander; Grosse, Ivo; Quint, Marcel (2015): Evidence for active maintenance of phylotranscriptomic hourglass patterns in animal and plant embryogenesis. In *Molecular Biology and Evolution* 32 (5), pp. 1221–1231. DOI: 10.1093/molbev/msv012.
- Drost, Hajk-Georg; Gabel, Alexander; Liu, Jialin; Quint, Marcel; Grosse, Ivo (2018): myTAI: evolutionary transcriptomics with R. In *Bioinformatics (Oxford, England)* 34 (9), pp. 1589–1590. DOI: 10.1093/bioinformatics/btx835.
- Einspanier, Severin; Tominello-Ramirez, Christopher; Hasler, Mario; Barbacci, Adelin; Raffaele, Sylvain; Stam, Remco (2024): High-Resolution Disease Phenotyping Reveals Distinct Resistance Mechanisms of Tomato Crop Wild Relatives against *Sclerotinia sclerotiorum*. In *Plant Phenomics* 6, Article 0214. DOI: 10.34133/plantphenomics.0214.
- Ewels, Philip; Magnusson, Måns; Lundin, Sverker; Käller, Max (2016): MultiQC: summarize analysis results for multiple tools and samples in a single report. In *Bioinformatics (Oxford, England)* 32 (19), pp. 3047–3048. DOI: 10.1093/bioinformatics/btw354.
- Fagny, Maud; Austerlitz, Frédéric (2021): Polygenic Adaptation: Integrating Population Genetics and Gene Regulatory Networks. In *Trends in genetics : TIG* 37 (7), pp. 631–638. DOI: 10.1016/j.tig.2021.03.005.
- Fass, Mónica I.; Rivarola, Máximo; Ehrenbolger, Guillermo F.; Maringolo, Carla A.; Montecchia, Juan F.; Quiroz, Facundo et al. (2020): Exploring sunflower responses to *Sclerotinia* head rot at early stages of infection using RNA-seq analysis. In *Scientific Reports* 10 (1), p. 13347. DOI: 10.1038/s41598-020-70315-4.

- Fusari, Corina M.; Di Rienzo, Julio A.; Troglia, Carolina; Nishinakamasu, Verónica; Moreno, María Valeria; Maringolo, Carla et al. (2012): Association mapping in sunflower for sclerotinia head rot resistance. In *BMC Plant Biology* 12 (1), p. 93. DOI: 10.1186/1471-2229-12-93.
- Gómez-Picos, Patsy; Eames, B. Frank (2015): On the evolutionary relationship between chondrocytes and osteoblasts. In *Frontiers in genetics* 6, p. 297. DOI: 10.3389/fgene.2015.00297.
- Gonzalez-Bayon, Rebeca; Shen, Yifei; Groszmann, Michael; Zhu, Anyu; Wang, Aihua; Allu, Annapurna D. et al. (2019): Senescence and Defense Pathways Contribute to Heterosis. In *Plant Physiology* 180 (1), pp. 240–252. DOI: 10.1104/pp.18.01205.
- Gou, Mingyue; Balint-Kurti, Peter; Xu, Mingliang; Yang, Qin (2023): Quantitative disease resistance: Multifaceted players in plant defense. In *Journal of Integrative Plant Biology* 65 (2), pp. 594–610. DOI: 10.1111/jipb.13419.
- Haas, Brian John (2024a): TransDecoder. <https://github.com/TransDecoder/TransDecoder>: GitHub. Available online at <https://github.com/TransDecoder/TransDecoder>, checked on 9/16/2024.
- Halfon, Marc S. (2017): Perspectives on Gene Regulatory Network Evolution. In *Trends in genetics : TIG* 33 (7), pp. 436–447. DOI: 10.1016/j.tig.2017.04.005.
- Hu, Guanjing; Hovav, Ran; Grover, Corrinne E.; Faigenboim-Doron, Adi; Kadmon, Noa; Page, Justin T. et al. (2016): Evolutionary Conservation and Divergence of Gene Coexpression Networks in *Gossypium* (Cotton) Seeds. In *Genome Biology and Evolution* 8 (12), pp. 3765–3783. DOI: 10.1093/gbe/evw280.
- Huang, Jie; Xu, Weibin; Zhai, Junwen; Hu, Yi; Guo, Jing; Zhang, Caifei et al. (2023): Nuclear phylogeny and insights into whole-genome duplications and reproductive development of Solanaceae plants. In *Plant communications* 4 (4), p. 100595. DOI: 10.1016/j.xplc.2023.100595.
- Jin, Jinpu; Tian, Feng; Yang, De-Chang; Meng, Yu-Qi; Kong, Lei; Luo, Jingchu; Gao, Ge (2017): PlantTFDB 4.0: toward a central hub for transcription factors and regulatory interactions in plants. In *Nucleic acids research* 45 (D1), D1040–D1045. DOI: 10.1093/nar/gkw982.
- Jones, D. Marc; Vandepoele, Klaas (2020): Identification and evolution of gene regulatory networks: insights from comparative studies in plants. In *Current Opinion in Plant Biology* 54, pp. 42–48. DOI: 10.1016/j.pbi.2019.12.008.
- Joshi, Raj Kumar; Megha, Swati; Rahman, Muhammad Hafizur; Basu, Urmila; Kav, Nat N. V. (2016): A global study of transcriptome dynamics in canola (*Brassica napus* L.) responsive to *Sclerotinia sclerotiorum* infection using RNA-Seq. In *Gene* 590 (1), pp. 57–67. DOI: 10.1016/j.gene.2016.06.003.
- Kabbage, Mehdi; Yarden, Oded; Dickman, Martin B. (2015): Pathogenic attributes of *Sclerotinia sclerotiorum* : Switching from a biotrophic to necrotrophic lifestyle. In *Plant Science* 233, pp. 53–60. DOI: 10.1016/j.plantsci.2014.12.018.
- Kahlon, Parvinderdeep S.; Förner, Andrea; Muser, Michael; Oubounyt, Mhaned; Gigl, Michael; Hammerl, Richard et al. (2023): Laminarin-triggered defence responses are geographically dependent in natural populations of *Solanum chilense*. In *Journal of Experimental Botany*, erad087. DOI: 10.1093/jxb/erad087.
- Kahlon, Parvinderdeep S.; Stam, Remco (2021): Polymorphisms in plants to restrict losses to pathogens: From gene family expansions to complex network evolution. In *Current Opinion in Plant Biology* 62, p. 102040. DOI: 10.1016/j.pbi.2021.102040.
- Kahlon, Parvinderdeep S.; Verin, Melissa; Hückelhoven, Ralph; Stam, Remco (2021): Quantitative resistance differences between and within natural populations of *Solanum chilense* against the oomycete pathogen *Phytophthora infestans*. In *Ecology and Evolution* 11 (12), pp. 7768–7778. DOI: 10.1002/ece3.7610.
- Kim, Youn-Sung; Kim, Sang-Gyu; Park, Jung-Eun; Park, Hye-Young; Lim, Mi-Hye; Chua, Nam-Hai; Park, Chung-Mo (2006): A membrane-bound NAC transcription factor regulates cell division in *Arabidopsis*. In *The Plant Cell* 18 (11), pp. 3132–3144. DOI: 10.1105/tpc.106.043018.

- Koenig, Daniel; Jiménez-Gómez, José M.; Kimura, Seisuke; Fulop, Daniel; Chitwood, Daniel H.; Headland, Lauren R. et al. (2013): Comparative transcriptomics reveals patterns of selection in domesticated and wild tomato. In *Proceedings of the National Academy of Sciences of the United States of America* 110 (28), E2655–62. DOI: 10.1073/pnas.1309606110.
- Koubkova-Yu, Tracy Chih-Ting; Chao, Jung-Chi; Leu, Jun-Yi (2018): Heterologous Hsp90 promotes phenotypic diversity through network evolution. In *PLOS Biology* 16 (11), e2006450. DOI: 10.1371/journal.pbio.2006450.
- Kulahoglu, Canan; Denton, Alisandra K.; Sommer, Manuel; Maß, Janina; Schliesky, Simon; Wrobel, Thomas J. et al. (2014): Comparative transcriptome atlases reveal altered gene expression modules between two Cleomaceae C3 and C4 plant species. In *The Plant Cell* 26 (8), pp. 3243–3260. DOI: 10.1105/tpc.114.123752.
- Langfelder, Peter; Horvath, Steve (2008): WGCNA: an R package for weighted correlation network analysis. In *BMC bioinformatics* 9 (1). DOI: 10.1186/1471-2105-9-559.
- Langfelder, Peter; Luo, Rui; Oldham, Michael C.; Horvath, Steve (2011): Is my network module preserved and reproducible? (7).
- Li, Yupeng; Pearl, Stephanie A.; Jackson, Scott A. (2015): Gene Networks in Plant Biology: Approaches in Reconstruction and Analysis. In *Trends in Plant Science* 20 (10), pp. 664–675. DOI: 10.1016/j.tplants.2015.06.013.
- Liao, Yang; Smyth, Gordon K.; Shi, Wei (2014): featureCounts: an efficient general purpose program for assigning sequence reads to genomic features. In *Bioinformatics (Oxford, England)* 30 (7), pp. 923–930. DOI: 10.1093/bioinformatics/btt656.
- Liu, Bo; Ouyang, Zhigang; Zhang, Yafen; Li, Xiaohui; Hong, Yongbo; Huang, Lei et al. (2014): Tomato NAC transcription factor SISR1 positively regulates defense response against biotic stress but negatively regulates abiotic stress response. In *PLoS ONE* 9 (7), e102067.
- Liu, Ming-Jung; Sugimoto, Koichi; Uygun, Sahra; Panchy, Nicholas; Campbell, Michael S.; Yandell, Mark et al. (2018): Regulatory Divergence in Wound-Responsive Gene Expression between Domesticated and Wild Tomato. In *The Plant Cell* 30 (7), pp. 1445–1460. DOI: 10.1105/tpc.18.00194.
- Lotharukpong, Jaruwatana S.; Zheng, Min; Luthringer, Remy; Drost, Hajk-Georg; Coelho, Susana M. (2024): A Transcriptomic Hourglass In Brown Algae.
- Love, Michael I.; Huber, Wolfgang; Anders, Simon (2014): Moderated estimation of fold change and dispersion for RNA-seq data with DESeq2. In *Genome Biology* 15 (12), p. 550. DOI: 10.1186/s13059-014-0550-8.
- Lu, Yan; Liu, Dongqi; Kong, Xiangjiu; Song, Yang; Jing, Lan (2024): Pangenome characterization and analysis of the NAC gene family reveals genes for Sclerotinia sclerotiorum resistance in sunflower (*Helianthus annuus*). In *BMC genomic data* 25 (1), p. 39. DOI: 10.1186/s12863-024-01227-9.
- Ma, Lan; Li, Rongping; Ma, Luoyan; Song, Na; Xu, Zhen; Wu, Jinsong (2021): Involvement of NAC transcription factor NaNAC29 in *Alternaria alternata* resistance and leaf senescence in *Nicotiana attenuata*. In *Plant diversity* 43 (6), pp. 502–509. DOI: 10.1016/j.pld.2020.11.003.
- Macquet, Joris; Mounichetty, Shantala; Raffaele, Sylvain (2022): Genetic co-option into plant-filamentous pathogen interactions. In *Trends in Plant Science* 27 (11), pp. 1144–1158. DOI: 10.1016/j.tplants.2022.06.011.
- Maheepala, Dinusha C.; Emerling, Christopher A.; Rajewski, Alex; Macon, Jenna; Strahl, Maya; Pabón-Mora, Natalia; Litt, Amy (2019): Evolution and Diversification of FRUITFULL Genes in Solanaceae. In *Frontiers in Plant Science* 10, p. 43. DOI: 10.3389/fpls.2019.00043.
- Manni, Mosè; Berkeley, Matthew R.; Seppely, Mathieu; Simão, Felipe A.; Zdobnov, Evgeny M. (2021): BUSCO Update: Novel and Streamlined Workflows along with Broader and Deeper Phylogenetic Coverage for Scoring of Eukaryotic, Prokaryotic, and Viral Genomes. In *Molecular Biology and Evolution* 38 (10), pp. 4647–4654. DOI: 10.1093/molbev/msab199.

- Martin, Marcel (2011): Cutadapt removes adapter sequences from high-throughput sequencing reads. In *EMBnet.journal* 17.1, pp. 10–12. Available online at <http://dx.doi.org/10.14806/ej.17.1.200>.
- Masalia, Rishi R.; Bewick, Adam J.; Burke, John M. (2017): Connectivity in gene coexpression networks negatively correlates with rates of molecular evolution in flowering plants. In *PLoS ONE* 12 (7), e0182289. DOI: 10.1371/journal.pone.0182289.
- Masri, Ribal; Kiss, Erzsébet (2023): The role of NAC genes in response to biotic stresses in plants. In *Physiological and Molecular Plant Pathology* 126, p. 102034. DOI: 10.1016/j.pmpp.2023.102034.
- Mazumdar, Purabi (2021): Sclerotinia stem rot in tomato: a review on biology, pathogenicity, disease management and future research priorities. In *Journal of Plant Diseases and Protection* 128 (6), pp. 1403–1431. DOI: 10.1007/s41348-021-00509-z.
- Mbengue, Malick; Navaud, Olivier; Peyraud, Rémi; Barascud, Marielle; Badet, Thomas; Vincent, Rémy et al. (2016): Emerging Trends in Molecular Interactions between Plants and the Broad Host Range Fungal Pathogens *Botrytis cinerea* and *Sclerotinia sclerotiorum*. In *Frontiers in Plant Science* 7. DOI: 10.3389/fpls.2016.00422.
- Mei, Jiaqin; Wei, Dayong; Disi, Joseph Onwusemu; Ding, Yijuan; Liu, Yao; Qian, Wei (2012): Screening resistance against *Sclerotinia sclerotiorum* in Brassica crops with use of detached stem assay under controlled environment. In *European Journal of Plant Pathology* 134 (3), pp. 599–604. DOI: 10.1007/s10658-012-0040-3.
- Musa-Khalifani, Khadijeh; Darvishzadeh, Reza; Abrinbana, Masoud (2021): Resistance against *Sclerotinia* basal stem rot pathogens in sunflower. In *Tropical Plant Pathology* 46 (6), pp. 651–663. DOI: 10.1007/s40858-021-00463-z.
- Nakashima, Kazuo; Takasaki, Hironori; Mizoi, Junya; Shinozaki, Kazuo; Yamaguchi-Shinozaki, Kazuko (2012): NAC transcription factors in plant abiotic stress responses. In *Biochimica et biophysica acta* 1819 (2), pp. 97–103. DOI: 10.1016/j.bbagr.2011.10.005.
- Needleman, Saul B.; Wunsch, Christian D. (1970): A general method applicable to the search for similarities in the amino acid sequence of two proteins. In *Journal of Molecular Biology* 48 (3), pp. 443–453. DOI: 10.1016/0022-2836(70)90057-4.
- Nosenko, Tetyana; Böndel, Katharina B.; Kumpfmüller, Gabriele; Stephan, Wolfgang (2016): Adaptation to low temperatures in the wild tomato species *Solanum chilense*. In *Molecular Ecology* 25 (12), pp. 2853–2869. DOI: 10.1111/mec.13637.
- Obertello, Mariana; Shrivastava, Stuti; Katari, Manpreet S.; Coruzzi, Gloria M. (2015): Cross-Species Network Analysis Uncovers Conserved Nitrogen-Regulated Network Modules in Rice. In *Plant Physiology* 168 (4), pp. 1830–1843. DOI: 10.1104/pp.114.255877.
- Ovens, Katie; Eames, B. Frank; McQuillan, Ian (2021): Comparative Analyses of Gene Co-expression Networks: Implementations and Applications in the Study of Evolution. In *Frontiers in genetics* 12, p. 695399. DOI: 10.3389/fgene.2021.695399.
- Pertea, Geo; Pertea, Mihaela (2020): GFF Utilities: GffRead and GffCompare. In *F1000Res* 9, p. 304. DOI: 10.12688/f1000research.23297.1.
- Pink, Harry; Talbot, Adam; Graceson, Abi; Graham, Julian; Higgins, Gill; Taylor, Andrew et al. (2022): Identification of genetic loci in lettuce mediating quantitative resistance to fungal pathogens. In *Theoretical and Applied Genetics* 135 (7), pp. 2481–2500. DOI: 10.1007/s00122-022-04129-5.
- Plachetzki, David C.; Oakley, Todd H. (2007): Key transitions during the evolution of animal phototransduction: novelty, “tree-thinking,” co-option, and co-duplication. In *Integrative and comparative biology* 47 (5), pp. 759–769. DOI: 10.1093/icb/icm050.
- Poland, Jesse A.; Balint-Kurti, Peter J.; Wissner, Randall J.; Pratt, Richard C.; Nelson, Rebecca J. (2009): Shades of gray: the world of quantitative disease resistance. In *Trends in Plant Science* 14 (1), pp. 21–29. DOI: 10.1016/j.tplants.2008.10.006.

- Powell, Adrian F.; Feder, Ari; Li, Jie; Schmidt, Maximilian H.-W.; Courtney, Lance; Alseekh, Saleh et al. (2022): A *Solanum lycopersicoides* reference genome facilitates insights into tomato specialized metabolism and immunity. In *The Plant Journal* 110 (6), pp. 1791–1810. DOI: 10.1111/tpj.15770.
- Quinlan, Aaron R.; Hall, Ira M. (2010): BEDTools: a flexible suite of utilities for comparing genomic features. In *Bioinformatics (Oxford, England)* 26 (6), pp. 841–842. DOI: 10.1093/bioinformatics/btq033.
- Rabanal, Fernando A.; Nizhynska, Viktoria; Mandáková, Terezie; Novikova, Polina Yu; Lysak, Martin A.; Mott, Richard; Nordborg, Magnus (2017): Unstable Inheritance of 45S rRNA Genes in *Arabidopsis thaliana*. In *G3 Genes\textbarGenetics* 7 (4), pp. 1201–1209. DOI: 10.1534/g3.117.040204.
- Roux, Fabrice; Voisin, Derry; Badet, Thomas; Balagué, Claudine; Barlet, Xavier; Huard-Chauveau, Carine et al. (2014): Resistance to phytopathogens e tutti quanti : placing plant quantitative disease resistance on the map: Quantitative disease resistance in plants. In *Molecular Plant Pathology* 15 (5), pp. 427–432. DOI: 10.1111/mpp.12138.
- Sayers, Eric W.; Cavanaugh, Mark; Clark, Karen; Ostell, James; Pruitt, Kim D.; Karsch-Mizrachi, Ilene (2020): GenBank. In *Nucleic acids research* 48 (D1), D84–D86. DOI: 10.1093/nar/gkz956.
- Schmey, Tamara; Small, Corinn; Einspanier, Severin; Hoyoz, Lina Muñoz; Ali, Tahir; Gamboa, Soledad et al. (2023): Small-spored *Alternaria* spp. (section *Alternaria*) are common pathogens on wild tomato species. In *Environmental Microbiology*, 1462–2920.16394. DOI: 10.1111/1462-2920.16394.
- Schoch, Conrad L.; Ciufo, Stacy; Domrachev, Mikhail; Hotton, Carol L.; Kannan, Sivakumar; Khovanskaya, Rogneda et al. (2020): NCBI Taxonomy: a comprehensive update on curation, resources and tools. In *Database : the journal of biological databases and curation* 2020. DOI: 10.1093/database/baaa062.
- Schoenrock, Andrew; Burnside, Daniel; Moteshareie, Houman; Pitre, Sylvain; Hooshyar, Mohsen; Green, James R. et al. (2017): Evolution of protein-protein interaction networks in yeast. In *PLoS ONE* 12 (3), e0171920. DOI: 10.1371/journal.pone.0171920.
- Seong, Kyungyong; Seo, Eunyoung; Witek, Kamil; Li, Meng; Staskawicz, Brian (2020): Evolution of NLR resistance genes with noncanonical N-terminal domains in wild tomato species. In *The New phytologist* 227 (5), pp. 1530–1543. DOI: 10.1111/nph.16628.
- Shen, Wei; Sipos, Botond; Zhao, Liuyang (2024): SeqKit2: A Swiss army knife for sequence and alignment processing. In *iMeta* 3 (3), e191. DOI: 10.1002/imt2.191.
- Silva-Arias, Gustavo A.; Gagnon, Edeline; Hembrom, Surya; Fastner, Alexander; Khan, Muhammad Ramzan; Stam, Remco; Tellier, Aurélien (2025): Patterns of presence-absence variation of NLRs across populations of *Solanum chilense* are clade-dependent and mainly shaped by past demographic history. In *The New phytologist* 245 (4), pp. 1718–1732. DOI: 10.1111/nph.20293.
- Simon Andrews (2010): FastQC. A quality control tool for high throughput sequence data. Available online at <https://www.bioinformatics.babraham.ac.uk/projects/fastqc/>, checked on 8/27/2024.
- Smith, Jonathon E.; Mengesha, Bemnet; Tang, Hua; Mengiste, Tesfaye; Bluhm, Burton H. (2014): Resistance to *Botrytis cinerea* in *Solanum lycopersicoides* involves widespread transcriptional reprogramming. In *BMC Genomics* 15, p. 334. DOI: 10.1186/1471-2164-15-334.
- Stam, Remco; Scheikl, Daniela; Tellier, Aurélien (2017): The wild tomato species *Solanum chilense* shows variation in pathogen resistance between geographically distinct populations. In *PeerJ* 5, e2910. DOI: 10.7717/peerj.2910.
- Stam, Remco; Silva-Arias, Gustavo A.; Tellier, Aurelien (2019): Subsets of NLR genes show differential signatures of adaptation during colonization of new habitats. In *The New phytologist* 224 (1), pp. 367–379. DOI: 10.1111/nph.16017.
- Sucher, Justine; Mbengue, Malick; Dresen, Axel; Barascud, Marielle; Didelon, Marie; Barbacci, Adelin; Raffaele, Sylvain (2020): Phylotranscriptomics of the Pentapetalae Reveals Frequent Regulatory Variation in Plant Local

Responses to the Fungal Pathogen *Sclerotinia sclerotiorum*. In *The Plant Cell* 32 (6), pp. 1820–1844. DOI: 10.1105/tpc.19.00806.

Suyama, Mikita; Torrents, David; Bork, Peer (2006): PAL2NAL: robust conversion of protein sequence alignments into the corresponding codon alignments. In *Nucleic acids research* 34 (Web Server issue), W609–12. DOI: 10.1093/nar/gkl315.

Szymański, Jędrzej; Bocobza, Samuel; Panda, Sayantan; Sonawane, Prashant; Cárdenas, Pablo D.; Lashbrooke, Justin et al. (2020): Analysis of wild tomato introgression lines elucidates the genetic basis of transcriptome and metabolome variation underlying fruit traits and pathogen response. In *Nature Genetics* 52 (10), pp. 1111–1121. DOI: 10.1038/s41588-020-0690-6.

Tang, Liguang; Wang, Bincai; Song, Liping; Yu, Chuying; Lin, Chufa; Gao, Changbin et al. (2023): RNAseq-based transcriptome analysis of lettuce infected by the necrotrophic fungus *Sclerotinia Sclerotiorum*. In *Eur J Plant Pathol* 165 (1), pp. 85–96. DOI: 10.1007/s10658-022-02590-y.

Thomas, William J. W.; Amas, Junrey C.; Dolatabadian, Aria; Huang, Shuanglong; Zhang, Fangning; Zandberg, Jacob D. et al. (2024): Recent advances in the improvement of genetic resistance against disease in vegetable crops. In *Plant Physiology* 196 (1), pp. 32–46. DOI: 10.1093/plphys/kiae302.

Tominello-Ramirez, Christopher S.; Muñoz Hoyos, Lina; Oubounyt, Mhaned; Stam, Remco (2024): Network analyses predict major regulators of resistance to early blight disease complex in tomato. In *BMC Plant Biology* 24 (1), p. 641. DOI: 10.1186/s12870-024-05366-0.

Törönen, Petri; Holm, Liisa (2022): PANNZER-A practical tool for protein function prediction. In *Protein science : a publication of the Protein Society* 31 (1), pp. 118–128. DOI: 10.1002/pro.4193.

Ueda, Hiroaki; Ito, Takeshi; Inoue, Ryouhei; Masuda, Yu; Nagashima, Yumi; Kozuka, Toshiaki; Kusaba, Makoto (2020): Genetic Interaction Among Phytochrome, Ethylene and Absciscic Acid Signaling During Dark-Induced Senescence in *Arabidopsis thaliana*. In *Frontiers in Plant Science* 11, p. 564. DOI: 10.3389/fpls.2020.00564.

Uloth, Margaret B.; You, Ming Pei; Finnegan, Patrick M.; Banga, Surinder S.; Banga, Shashi K.; Sandhu, Prabhjot S. et al. (2013): New sources of resistance to *Sclerotinia sclerotiorum* for crucifer crops. In *Field Crops Research* 154, pp. 40–52. DOI: 10.1016/j.fcr.2013.07.013.

UniProt Consortium, The (2017): UniProt: the universal protein knowledgebase. In *Nucleic acids research* 45 (D1), D158–D169. DOI: 10.1093/nar/gkw1099.

Wang, Jiao; Zheng, Chenfei; Shao, Xiangqi; Hu, Zhangjian; Li, Jianxin; Wang, Ping et al. (2020a): Transcriptomic and genetic approaches reveal an essential role of the NAC transcription factor SINAP1 in the growth and defense response of tomato. In *Horticulture Research* 7 (1), p. 209. DOI: 10.1038/s41438-020-00442-6.

Wang, Xin; Gao, Lei; Jiao, Chen; Stravoravdis, Stefanos; Hosmani, Prashant S.; Saha, Surya et al. (2020b): Genome of *Solanum pimpinellifolium* provides insights into structural variants during tomato breeding. In *Nature communications* 11 (1), p. 5817. DOI: 10.1038/s41467-020-19682-0.

Wang, Zheng; Ma, Lu-Yue; Cao, Jun; Li, Yu-Long; Ding, Li-Na; Zhu, Ke-Ming et al. (2019): Recent Advances in Mechanisms of Plant Defense to *Sclerotinia sclerotiorum*. In *Frontiers in Plant Science* 10, p. 1314. DOI: 10.3389/fpls.2019.01314.

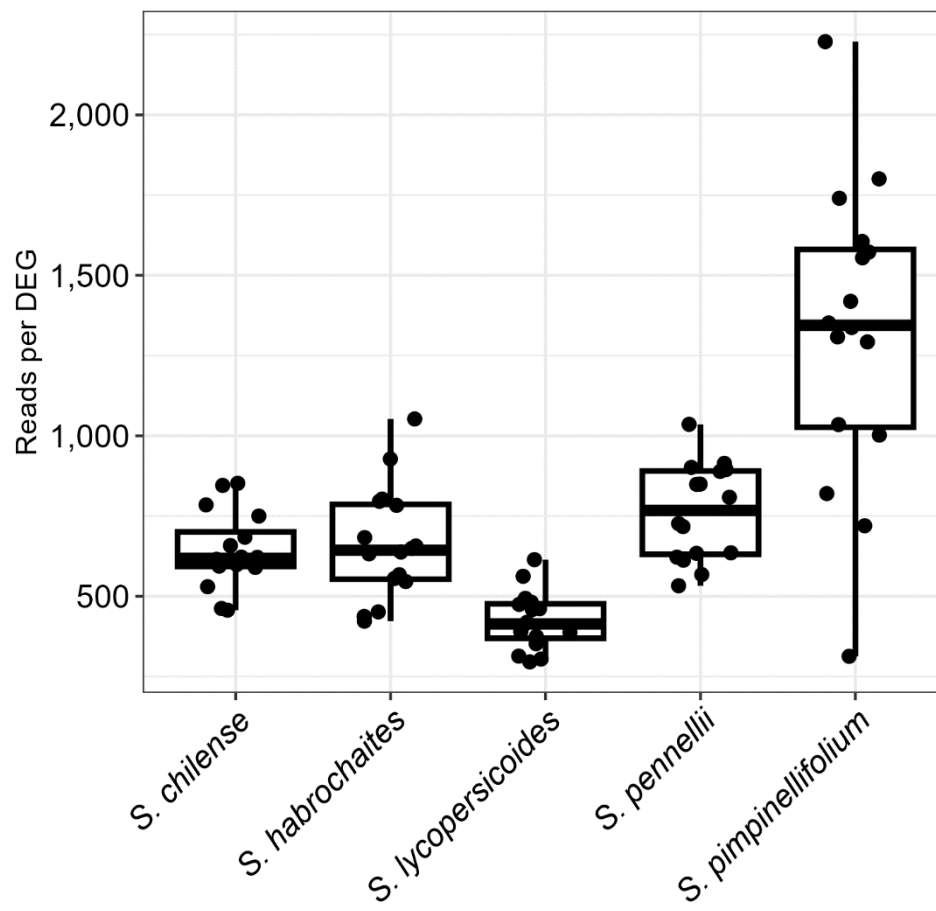
Wei, Kai; Sharifova, Saida; Zhao, Xiaoyun; Sinha, Neelima; Nakayama, Hokuto; Tellier, Aurélien; Silva-Arias, Gustavo A. (2024): Evolution of gene networks underlying adaptation to drought stress in the wild tomato *Solanum chilense*. In *Molecular Ecology*, Article e17536. DOI: 10.1111/mec.17536.

Wei, Qingzhen; Wang, Jinglei; Wang, Wuhong; Hu, Tianhua; Hu, Haijiao; Bao, Chonglai (2020): A high-quality chromosome-level genome assembly reveals genetics for important traits in eggplant. In *Horticulture Research* 7 (1), p. 153. DOI: 10.1038/s41438-020-00391-0.

Winkelmüller, Thomas M.; Entila, Frederickson; Anver, Shajahan; Piasecka, Anna; Song, Baoxing; Dahms, Eik et al. (2021): Gene expression evolution in pattern-triggered immunity within *Arabidopsis thaliana* and across Brassicaceae species. In *The Plant Cell* 33 (6), pp. 1863–1887. DOI: 10.1093/plcell/koab073.

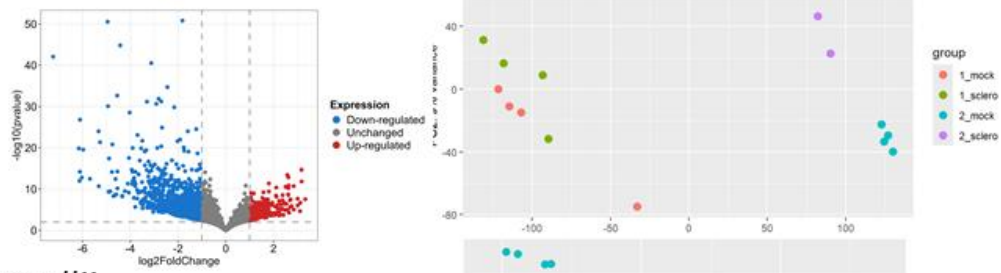
- Wu, Jian; Zhao, Qing; Yang, Qingyong; Liu, Han; Li, Qingyuan; Yi, Xinqi et al. (2016): Comparative transcriptomic analysis uncovers the complex genetic network for resistance to *Sclerotinia sclerotiorum* in *Brassica napus*. In *Scientific Reports* 6, p. 19007. DOI: 10.1038/srep19007.
- Wu, Ting-Ying; Goh, HonZhen; Azodi, Christina B.; Krishnamoorthi, Shalini; Liu, Ming-Jung; Urano, Daisuke (2021): Evolutionarily conserved hierarchical gene regulatory networks for plant salt stress response. In *Nature plants* 7 (6), pp. 787–799. DOI: 10.1038/s41477-021-00929-7.
- Yanar, Y.; Miller, S. A. (2003): Resistance of Pepper Cultivars and Accessions of *Capsicum* spp. to *Sclerotinia sclerotiorum*. In *Plant Disease* 87 (3), pp. 303–307. DOI: 10.1094/PDIS.2003.87.3.303.
- Yekutieli, Daniel; Benjamini, Yoav (1999): Resampling-based false discovery rate controlling multiple test procedures for correlated test statistics. In *Journal of Statistical Planning and Inference* 82 (1-2), pp. 171–196. DOI: 10.1016/S0378-3758(99)00041-5.
- Yu, Xiaofen; Qu, Minghao; Shi, Yanna; Hao, Chenlu; Guo, Sumin; Fei, Zhangjun; Gao, Lei (2022): Chromosome-scale genome assemblies of wild tomato relatives *Solanum habrochaites* and *Solanum galapagense* reveal structural variants associated with stress tolerance and terpene biosynthesis. In *Horticulture Research* 9, uhac139. DOI: 10.1093/hr/uhac139.
- Yuan, Xi; Wang, Hui; Cai, Jiating; Li, Dayong; Song, Fengming (2019): NAC transcription factors in plant immunity. In *Phytopathol Res* 1 (1). DOI: 10.1186/s42483-018-0008-0.
- Zhang, He; Kang, Hao; Su, Chulian; Qi, Yanxiang; Liu, Xiaomei; Pu, Jinji (2018a): Genome-wide identification and expression profile analysis of the NAC transcription factor family during abiotic and biotic stress in woodland strawberry. In *PLoS ONE* 13 (6), e0197892. DOI: 10.1371/journal.pone.0197892.
- Zhang, Hehua; Cui, Xiaoyue; Guo, Yuxiao; Luo, Chaobing; Zhang, Lingyun (2018b): *Picea wilsonii* transcription factor NAC2 enhanced plant tolerance to abiotic stress and participated in RFCP1-regulated flowering time. In *Plant molecular biology* 98 (6), pp. 471–493. DOI: 10.1007/s11103-018-0792-z.
- Zolotarov, Grygoriy; Grau-Bové, Xavier; Sebé-Pedrós, Arnau (2023): GeneExt: a gene model extension tool for enhanced single-cell RNA-seq analysis. In *BioRxiv*. DOI: 10.1101/2023.12.05.570120.

Supplementary Figures

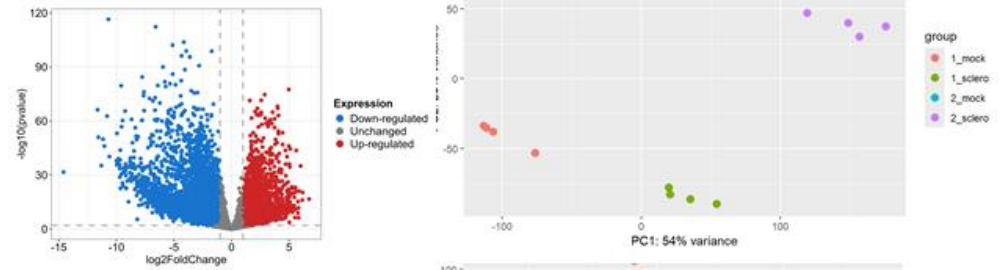


Suppl. Figure 1: Relationship of read count and number of assigned DEGs. We calculated the ratio based on the number of DEGs (contrast: infection vs. mock) per genotype and normalised it against the individual reads per sample (as represented by the dots).

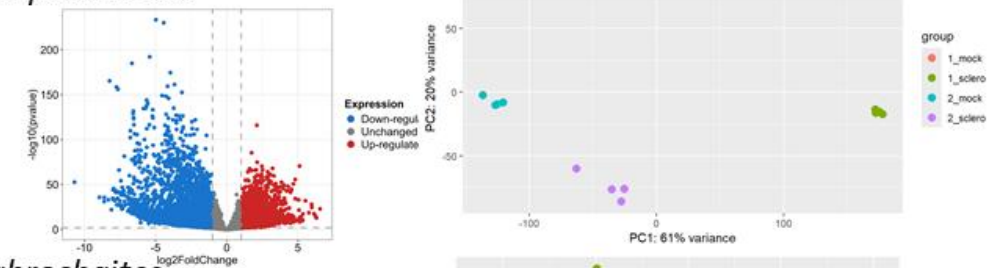
S. chilense



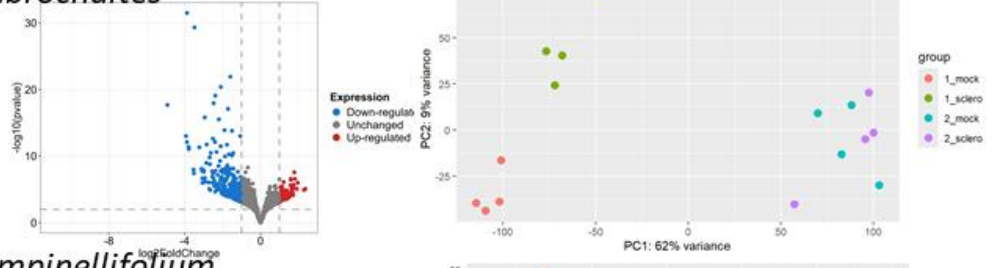
S. pennellii



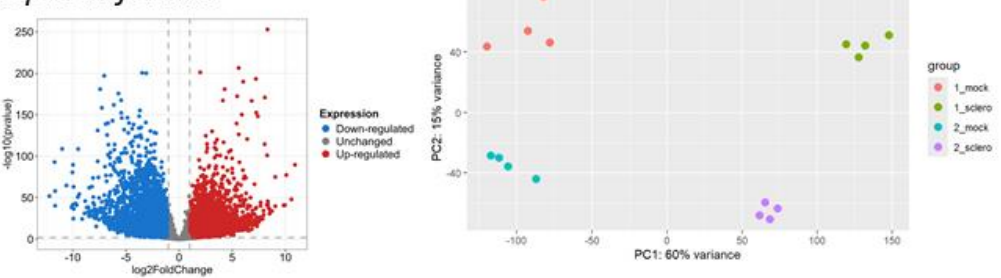
S. lycopersoides



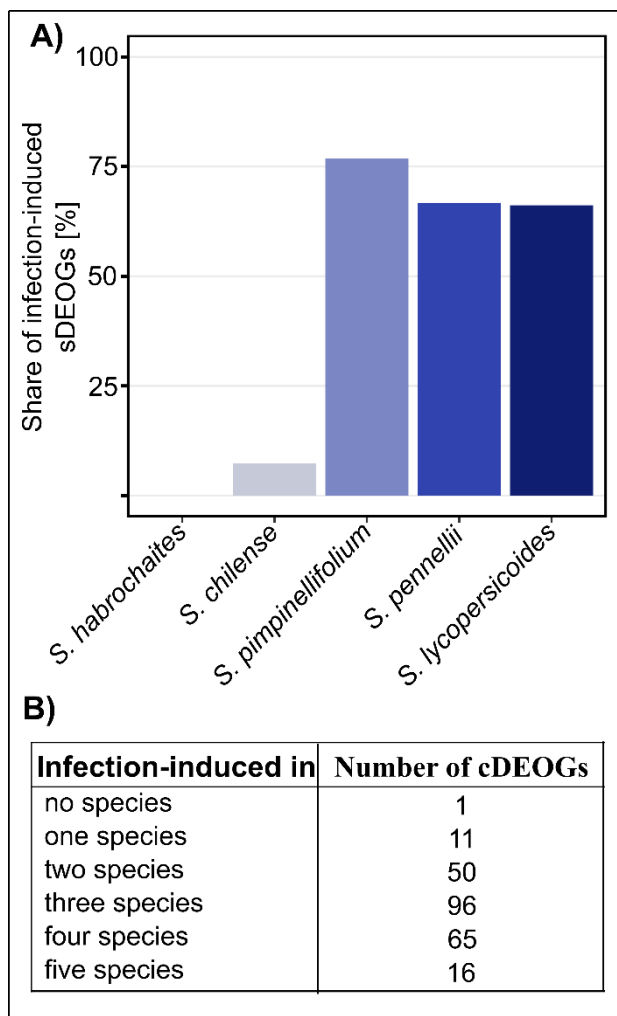
S. habrochaites



S. pimpinellifolium



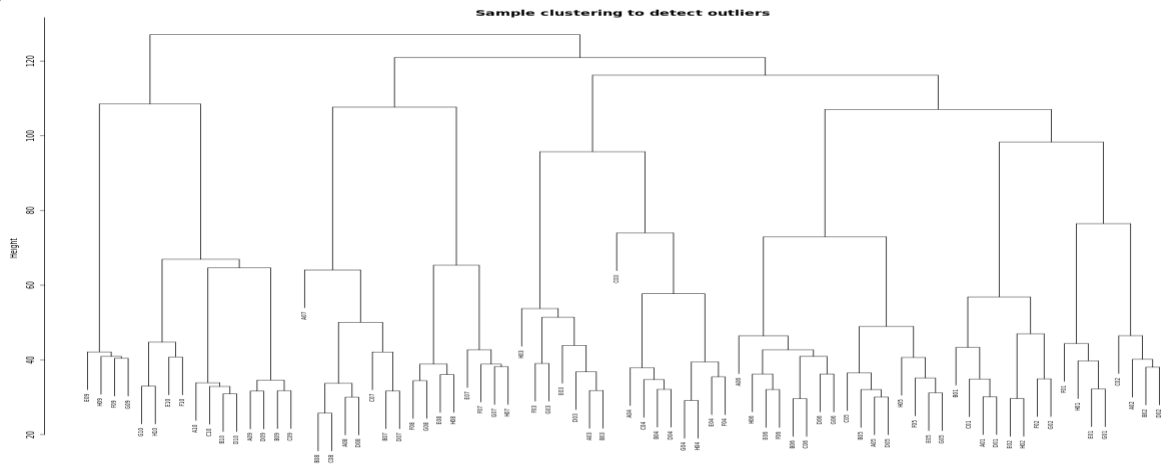
Suppl. Figure 2: Basic Differential Gene Expression Analysis of all five tomato species. The volcano plots show log2 foldchange against the pvalue of all five tomato species (contrast: Infected conditions res.-sus. genotype). Upregulated genes (red) are compared with downregulated genes (blue). The principal component analysis shows a clear separation of genotypes and treatments. Dots represent individual samples, with the colour defining the experimental treatment (1-susceptible, 2-resistant, mock and infected).



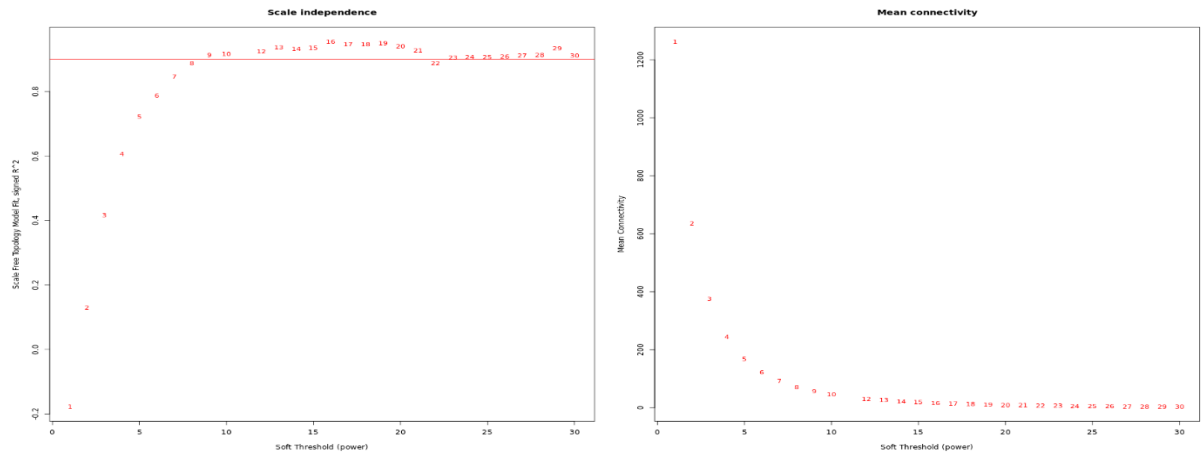
Suppl. Figure 3: Amount of infection-induced differentially expressed orthogroups.

A) species-specific sDEOGs and **B)** cDEOGs.

A)

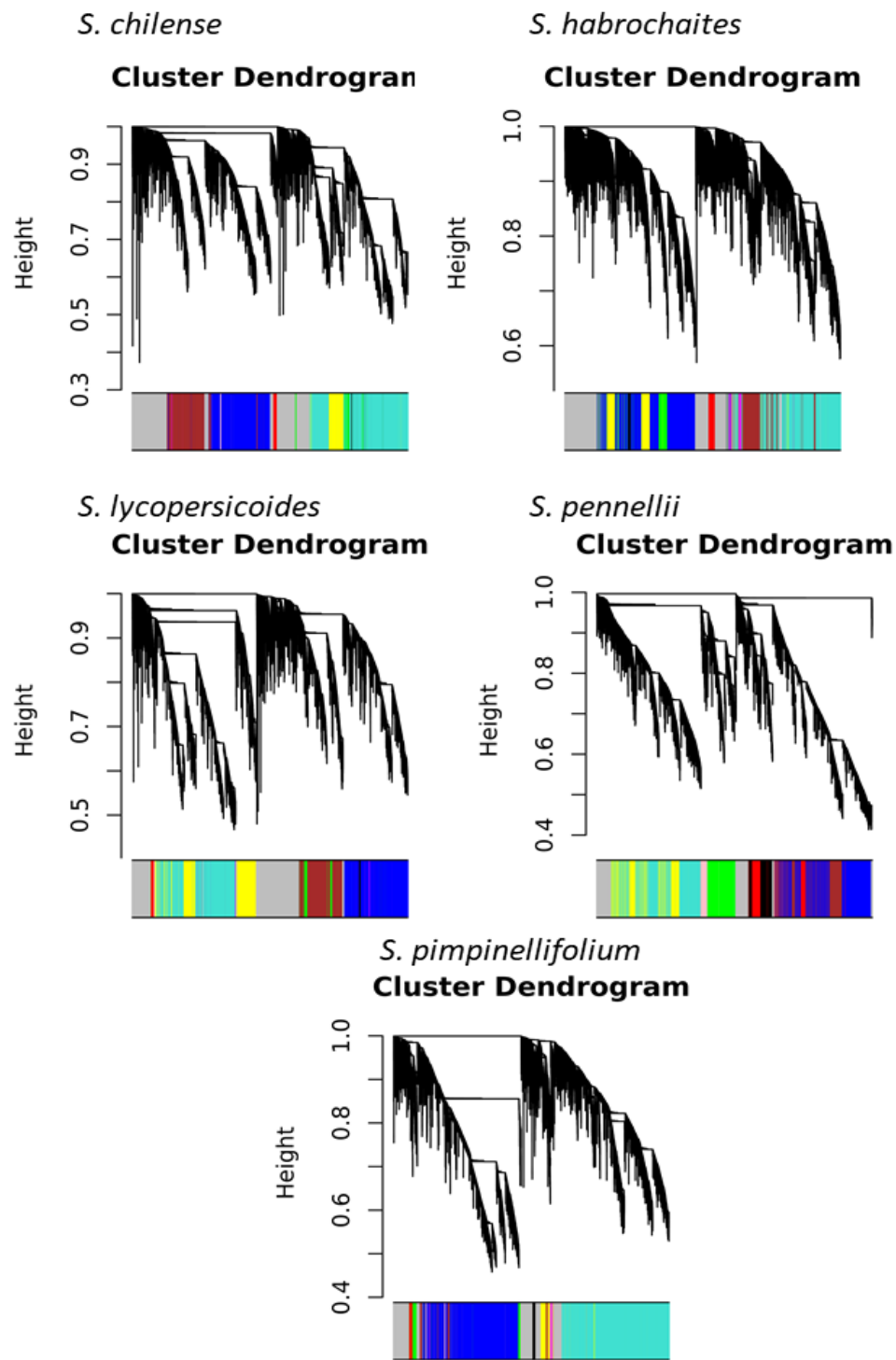


B)

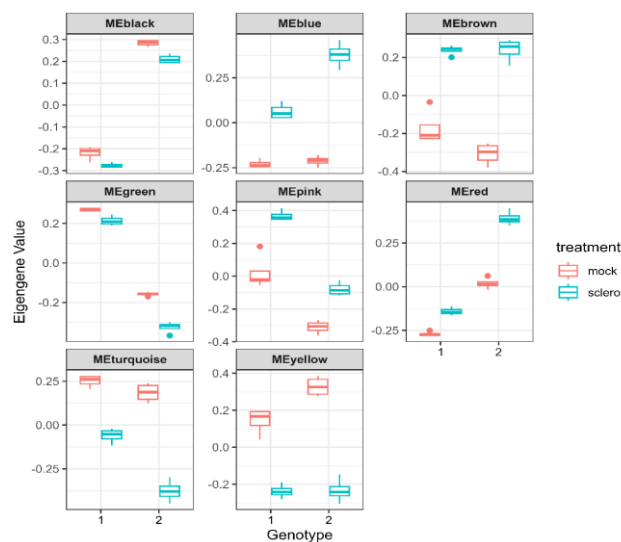


Suppl. Figure 4: Sample evaluation for the OG-based WGCNA.

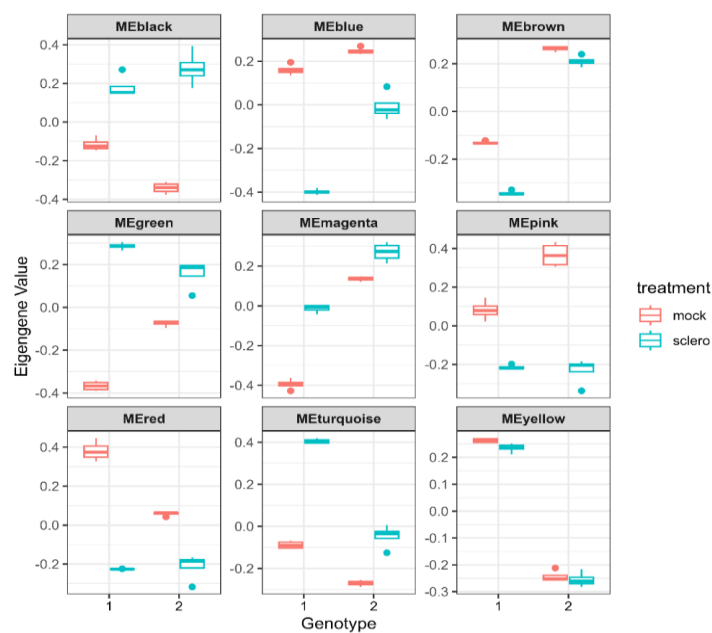
A) Hierarchical clustering of all samples used in the study. **B)** Selection of the Soft power threshold for WGCNA network construction on the OG-data set. The red line indicates the signed R^2 threshold of 0.85. The SFT threshold was selected based on the scale-free topology model's plateau and mean connectivity.



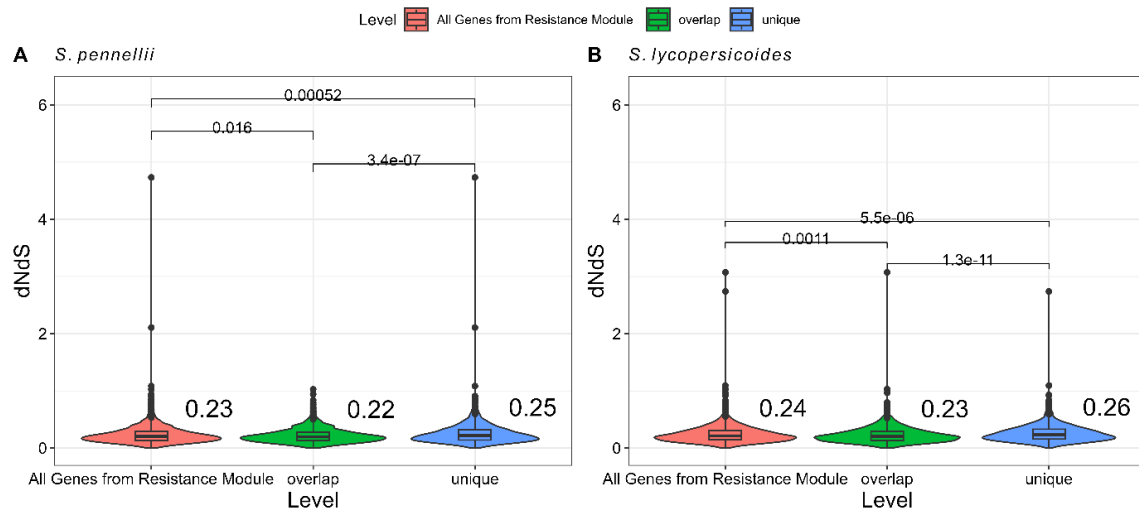
Suppl. Figure 5: WGCNA dendrogram showing network topology and module assignment of each species.



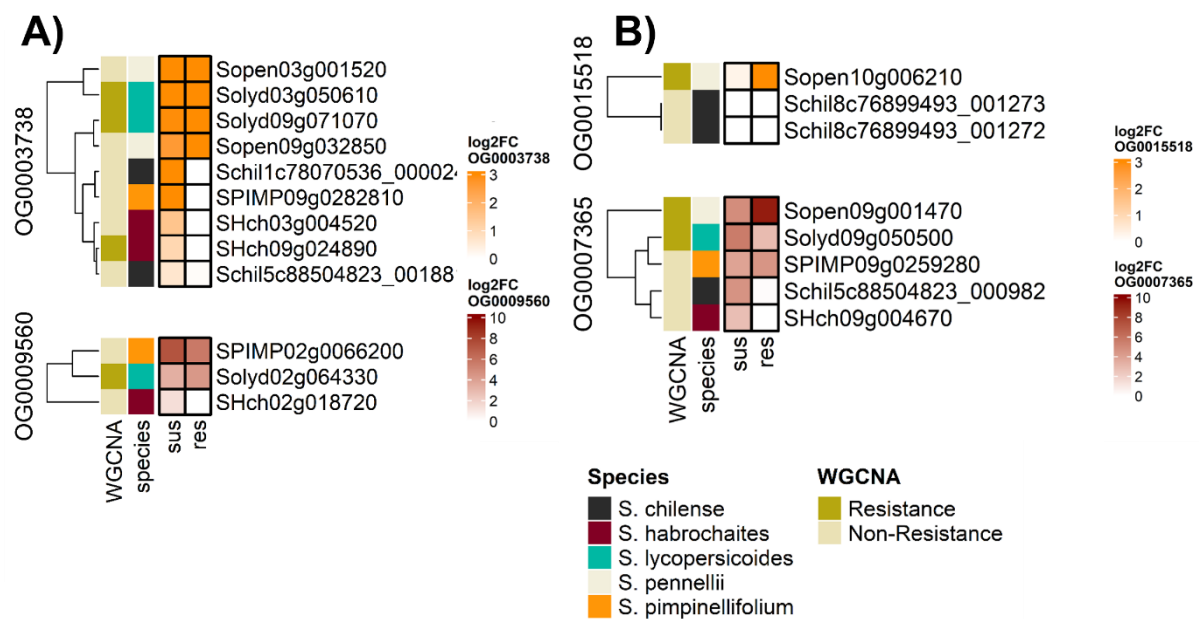
Suppl. Figure 6: Module Eigengenes of the *S. pennellii* network. The individual facets define coexpression modules assigned by the WGCNA. The Y-axis denominates the module eigengenes (MEs) of the two genotypes (1 susceptible, 2 resistant). The colour indicates experimental treatment. Boxplots summarise four independent samples.



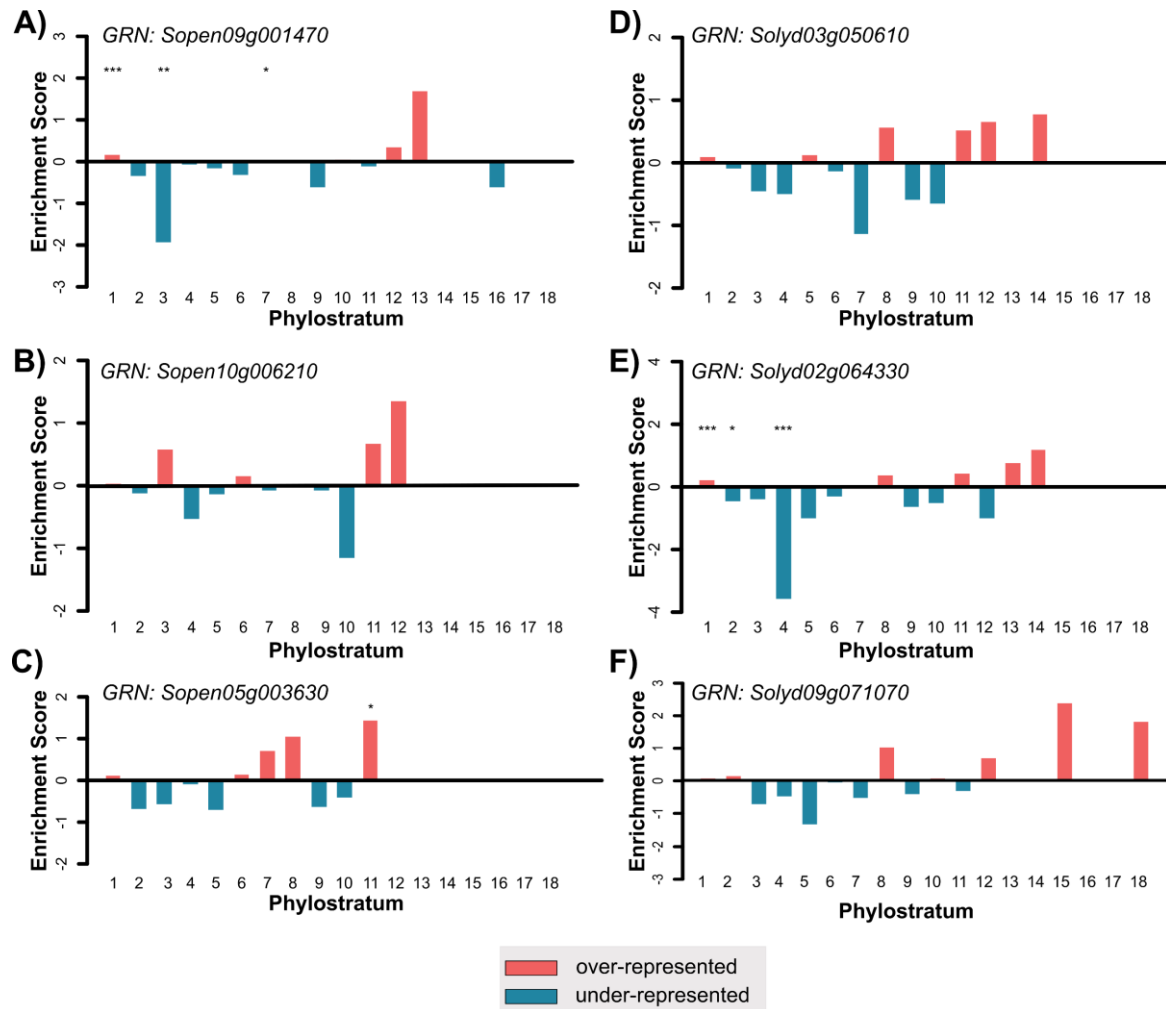
Suppl. Figure 7: Module Eigengenes of the *S. lycopersicoides* Network. The individual facets define coexpression modules assigned by the WGCNA. The Y-axis denominates the module eigengenes (MEs) of the two genotypes (1 susceptible, 2 resistant). The colour indicates experimental treatment. The boxplots summarise four independent samples.



Suppl. Figure 8: dNds ratios contrasting overlapping vs. unique vs. all genes from the resistance modules on A) *S. pennellii* and B) *S. lycopersicoides*. Statistical significance was determined using the Wilcoxon test. Numbers next to the violin charts represent the mean.



Suppl. Figure 9: Regulatory pattern of resistance-associated TFs of A) *S. lycopersicoides* and B) *S. pennellii* compared across the other species using orthogroups. The expression of each gene within the respective orthogroup was visualised across varying levels of QDR (susceptible | resistant), with colour coding indicating the respective species and the assignment of each TF to its species-specific resistance module



Suppl. Figure 10: Phylostratum enrichment analysis per species of the three focal transcription factors. We performed phylostratum enrichment analysis on the gene-regulatory networks downstream of three TFs on *S. pennellii* (A-C) and *S. lycopersicoides* (C-E). The enrichment score is indicated by the y-axis, and the respective phylostrata (cellular organisms till solanum) are located on the x-axis. Stars indicate the significance level of the respective enrichment after Fisher's exact test and BH FDR correction.

Publication 3



Publication 3

Title: Temporal Shifts in Gene Expression Drive Quantitative Resistance to *Sclerotinia sclerotiorum* in *Solanum pennellii*

Unpublished preprint.

Contributions: I designed and conducted all experiments, analysed and visualised data, and wrote the manuscript.

**Temporal Shifts in Gene Expression Drive Quantitative Resistance to *Sclerotinia*
sclerotiorum in *Solanum pennellii***

Einspanier, S.^{1*}; Stam, R.^{1*}

1 Department of Phytopathology and Crop Protection, Institute of Phytopathology,
Faculty of Agricultural and Nutritional Sciences, Christian Albrechts University, Kiel,
Germany

* Address correspondence to: s.einspanier@phytomed.uni-kiel.de or
remco.stam@phytomed.uni-kiel.de

Abstract

Resistance breeding against generalist necrotrophic pathogens heavily relies on quantitative disease resistance (QDR). Lesion growth dynamics involve distinct phases (e.g., lag phase duration or lesion doubling time), each independently affecting the overall symptom severity. While the genetic and regulatory basis of lesion growth rate has been studied, the host-derived regulation of the lag-phase duration remains largely uncharacterised.

In this study, we tested the regulatory response of *Solanum pennellii* genotypes exhibiting different lag-phase durations. We conducted a time-series gene expression profiling experiment dissecting genotype-specific regulatory responses to *Sclerotinia sclerotiorum* inoculation. We observed genotype-specific regulatory trajectories, with resistant plants displaying early activation of defence-related genes during the asymptomatic phase. These genes, regulated by a WRKY6-centered gene regulatory network, exhibited elevated basal expression in resistant genotypes and a fine-tuned longitudinal expression with induction before lesion onset. In contrast, susceptible genotypes lacked this early response, showing gene induction only post-infection.

This study is the first to link host regulatory dynamics to lag-phase duration, suggesting that elevated basal expression of receptor genes and a WRKY6-mediated gene regulatory network may enhance QDR. These findings provide insights into the regulatory foundation of QDR and establish a functional basis for more focused breeding of QDR traits.

Introduction

Inoculating plant leaves with a necrotrophic pathogen, like *Sclerotinia sclerotiorum*, does not always cause instant lesion onset. This phase, marked by the absence of symptoms and fungal growth, is commonly referred to as the lag phase. Originally, the lag phase was mostly studied in human medicine, focussing on bacterial infectious diseases such as *Streptococcus pneumoniae* or *Escherichia coli*. This research led to the identification of microbial mechanisms determining the lag phase duration, such as microbial promotor activity or the structure of the polysaccharide capsule protecting bacteria (Madar et al. 2013; Hathaway et al. 2012). Although well understood in microbiology, modern plant pathology lacks a fundamental understanding of the processes determining this complex phenotype. Yet, the lag phase has recently gained some attention in the light of quantitative disease resistance (QDR).

During the last decades, the research on resistance breeding has mostly focused on investigating R-gene-mediated qualitative disease resistance (Chen et al. 2024; Kaur et al. 2021). Prominent examples like the tomato R gene *Pto*, which confers complete race-specific resistance against the bacterial pathogen *Pseudomonas syringae* pv tomato, show the powerful capabilities of R-genes and led to wide use in crops (Tang et al. 1999). However, R-genes against major necrotrophic pathogens like the cosmopolitan ascomycetes *Botrytis cinerea* and *S. sclerotiorum* are yet to be found (Bi et al. 2023; Derbyshire et al. 2022). Additionally, R-genes (even as pyramids) display a major bottleneck on the pathogen populations, leading to rapid pathogen adaptation and the loss of efficacy (Stam and McDonald 2018). Thus, the polygenic QDR serves as an essential source of resistance traits (Roux et al. 2014; Poland et al. 2009; Corwin and Kliebenstein 2017).

QDR is a non-complete form of resistance (sometimes called disease tolerance) underlying complex polymorphic control (regulatorily and genomically). Targeted breeding for QDR presents major challenges because of the complexity of linking nuanced phenotypes with interconnected regulatory and genomic determinants (Roux et al. 2014; Derbyshire et al. 2022). Most QDR studies rely on single-timepoint measurements of severity, which is often estimated by lesion size or AUDPC as the primary resistance phenotype. However, focusing solely on lesion severity might undervalue temporal components of disease progression, such as lag phase duration and lesion doubling time (LDT), which can be crucial elements of a plant's successful QDR, as delayed infection of reduced growth speed might allow the host plant to complete its life cycle without large fitness costs.

We recently hypothesised that distinct parameters of the lesion growth dynamics, including the lag phase duration and LDT, are host-dependent QDR phenotypes, each contributing independently to symptom severity in a genotype-specific manner (Einspanier et al. 2024). Defining these two metrics as separate drivers of QDR allows for the functional characterisation of independent resistance mechanisms. Here, we focus on lag phase duration, investigating its role in shaping quantitative resistance and its potential as a tool in breeding for QDR.

Most research in both humans and plants indicates that the duration of the lag phase is primarily influenced by the pathogen's genotype (Barbacci et al. 2020; Hamill et al. 2020). Accordingly, several reports indicated that infection delays caused by necrotrophic pathogens are primarily associated with fungal characteristics like secreted proteins (effectors) and phytotoxins (Leisen et al. 2022; Denton-Giles et al. 2020). However, Hamill et al. (2020) demonstrated that cellular stress in microbial model organisms can significantly alter lag phase duration, which, in turn, may be influenced by the host genotype. Similarly, in a previous study on tomato crop wild relatives, we found that lag-phase duration varies significantly across different host genotypes (Einspanier et al. 2024). This observation aligns with recent reports by Sperfeld et al. (2024), who showed that methylated compounds secreted by photosynthetic organisms can alter the lag phase duration of the bacteria *Phaeobacter inhibens*. It is crucial to emphasise that we have shown a strong connection between delayed lesion onset of *S. sclerotiorum* infection and fungal development, distinguishing it from an asymptomatic growth phase, often referred to as the latency phase (Einspanier et al. 2024).

Building on recent insights, we hypothesise that host-specific regulatory mechanisms, besides pre-formed morphological properties, influence the lag-phase-mediated level of QDR against *S. sclerotiorum*. We speculate that early host-parasite interactions play a critical role in disease progression, possibly involving a complex network of genes responsible for detoxification, phytoalexin transport, and stress response. To assess early stress responses, we use the maximum quantum efficiency of PSII (Fv/Fm) as a key physiological marker.

We further hypothesise that the lag phase duration is controlled by a host-specific regulatory pattern, where gene expression composition, orchestration, and magnitude ultimately determine the disease outcome. To test this, we conducted RNA sequencing on a time-series experiment integrated with high-resolution phenotyping. By linking RGB-imagery and Fv/Fm

measurements to longitudinal gene regulatory clusters and gene regulatory networks, we provide new insights into the determinants of lag-phase duration as key factor of QDR.

The findings of this study leverage our understanding of QDR and its pleiotropic regulation, with clear applications in crop improvement for durable disease resistance.

Materials and Methods

Plant growth conditions

To characterise the regulation of lag phase duration, we selected three *S. pennellii* accessions (LA1282, LA1809, LA1941) with contrasting lag-phase duration based on findings of an earlier study (Einspanier et al. 2024). We initially acquired seed material from the C. M. Rick tomato Genetics Resource Center of the University of California, Davis (TGRC UC-Davis, <https://tgrc.ucdavis.edu/>). After the germination, each plant was routinely grown in the greenhouse facility of the Department of Phytopathology and Crop Protection, Faculty of Agricultural and Nutritional Sciences of the Christian Albrechts University Kiel, Germany. We maintained adult plants via cuttings (Chryzotop Grün 0.25 %) on Stender C700 substrate. Plants were cultivated in a controlled environment with a temperature of $21^{\circ}\text{C} \pm 10^{\circ}\text{C}$, 65% relative humidity, and a 16-hour light cycle. We applied 1% Sagaphos Blue to fertilise the plants monthly using the drip irrigation system. For the experiment, we grew 20 plants per accession from cuttings and harvested the first fully matured leaves.

Fungal growth conditions

For our infection experiments, we utilised the generalist plant pathogen *Sclerotinia sclerotiorum* isolate 1980. We freshly cultivated the fungus from sclerotia on potato dextrose agar (PDA) at 25°C in dark conditions. To create the inoculum, we incubated four 1 cm diameter agar plugs in 100 mL of potato dextrose broth (PDB). After incubating for four days on a rotating shaker at 24°C , we mixed the suspension and vacuum-filtered it through cheesecloth. We then concentrated the resulting filtrate with empty PDB to achieve an optical density (OD) at 600 nm of $\text{OD}_{600}=1$, using empty PDB as a mock treatment. Lastly, Tween80 was added as a surfactant to enhance the dispersion of the fungal material.

Lag-phase duration measurement

The lag-phase duration estimates for the respective *S. pennellii* accessions were reported earlier. In short, camera-monitored detached-leaf assays were carried out in a custom-built phenotyping system called navatron (Einspanier et al. 2024; Barbacci et al. 2020). Following thresholding-based image analysis, the per-leaf lesion progression was subjected to segmented regression analysis to determine the inflexion point that marks the start of lesion growth. The time until this point defines the lag-phase duration. We repeated the experiment using multispectral

imaging with the PlantExplorer Pro phenotyping platform (PhenoVation, The Netherlands) to further validate our findings. The experimental setup mirrored previous studies, except that leaves were placed on custom 3D-printed trays to facilitate transfer from Navautron conditions to the PE chamber. A 12-hour time series was conducted, and the experiment was repeated twice independently, using 18 leaves per genotype and condition. Each repetition was based on an independent plant stock.

Measurement of Fv/Fm

We used the PlantExplorer platform to measure the maximum photochemical quantum yield of photosystem II. The measure is calculated as the ratio of the variable to the maximum chlorophyll *a* fluorescence (Murchie and Lawson 2013; Xia et al. 2023). This was facilitated following a 20 min dark-adaptation of the leaves. Categorical per-leaf Fv/Fm was later determined using the PhenoVation DataAnalysis software v5.8.4-64b.

Sequencing experiment

To capture the transcriptomic profile over the gradient of lag-phase duration, we conducted an independent navautron-like infection experiment on detached leaves. Samples were collected at 24-hour intervals (24–96 hours post-inoculation), pooling two leaves per biological replicate. We obtained four independent replicates for each time point and genotype, which were then sequenced.

We transferred the leaf samples directly into a lysis-tube containing 750 μ L RNA/DNA-shield (ZymoResearch, Germany). Then, full RNA isolation was performed using the Quick-RNA Plant Miniprep kit (ZymoResearch). We measured RNA integrity and quality using gel-electrophoresis and a nanodrop one (ThermoFisher); RNA quantity was measured using a fluorometer (Promega Quantus) and a 5300 Fragment Analyzer System (Agilent). Lexogen NGS Services (Vienna, Austria) performed the library preparation and sequencing using the QuantSeq Fwd V2 UID library kit with additional unique molecular identifiers (UMIs).

Bioinformatic processing

We assessed raw-read quality using MultiQC/FastQC, then processed the reads using the RNAseq-pipeline v3.17.0 from the Nextflow-based nf-core v24.04.2 framework. In short, reads

are checked for sequencing quality and unique molecular identifiers (UMIs) extracted using UMI-tools v1.1.5. Then, adapter sequences and low-quality reads were removed with cutadapt v4.9 and trimgalore v0.6.10. rRNA depletion was skipped as no overrepresented sequences were detected. Next, the trimmed reads were aligned against the reference genome using STAR v2.7.11b followed by SALMON v1.10.3 quantification. Reads were then deduplicated using UMI-tools. We did not assemble isoforms; only gene-level expression was quantified. To accommodate 3'UTR sequencings, we executed the pipeline with custom settings:

```
--with_umi      --umitools_extract_method    "regex"      --umitools_bc_pattern
"^(?P<umi_1>.{6})(?P<discard_1>.{4}).*",      --extra_star_align_args      "--
alignIntronMax 1000000 --alignIntronMin 20 --alignMatesGapMax 1000000 --
alignSJoverhangMin 8 --outFilterMismatchNmax 999 --outFilterMultimapNmax 20
--outFilterType BySJout --outFilterMismatchNoverLmax 0.1 --clip3pAdapterSeq
AAAAAAAAA"
```

We mapped the reads against the *S. pennellii* reference genome (GenBank assembly GCA_001406875.2, updated Version of (Bolger et al. 2014) and used a curated genome annotation (Einspanier et al. 2025, in preparation). During the same pipeline, we concatenated the *S. sclerotiorum* 1980 reference genome to the *S. pennellii* reference, allowing us to measure fungal gene expression (GenBank assembly GCA_001857865.1, (Derbyshire et al. 2017)).

We listed detailed execution reports, QC metrics and software versions in the digital resources.

Differential Gene Expression Analysis

We used the R-package DESeq2 v1.46.0 to identify differential gene expression between the treatments or genotypes (Love et al. 2014). For the treatment effects, we converted each genotype's count matrix into a DESeqDataSet using the `DESeqDataSetFromMatrix()` function, applying the following model:

$$design = \sim inoculum + timepoint$$

To test genotype effects, we converted the consensus count matrix into the DESeqDataSet while accounting for the genotype effect:

$$design = \sim accession + inoculum + timepoint$$

We filtered out low-variance and low-expression genes before performing posthoc tests, which were based on manually defined contrast matrixes (e.g., infected vs mock at each time point). We stabilised the variance using the DESeq2-function `lfcShrink(type="ashr")` to account for noise and outlier effects. Genes with an absolute log2 fold-change greater than one and an adjusted p-value below 0.05 were designated as differentially expressed.

Time course analysis

We performed time course clustering on focal DEGs for each genotype separately, using a Dirichlet process Gaussian process model (McDowell et al. 2018). This approach addresses three major challenges in RNAseq time-series analysis: selection of the optimal number of clusters, accurate modelling of temporal trajectories and handling uncertainty. Accordingly, a Dirichlet Process is facilitated to dynamically determine the number of clusters based on the input data. Following this, a Gaussian process is used to model non-random changes in gene expression over time by fitting smooth trajectories for each cluster. Bayesian inference is then used to quantify uncertainty and estimates probabilities of cluster membership. We selected clusters using a Maximum a Posteriori (MAP) approach, which accounts for missing or noisy data. This model is implemented in the **DP_GP** software (https://github.com/PrincetonUniversity/DP_GP_cluster?tab=readme-ov-file, last accessed Feb. 2025).

Gene Ontology Analysis

To characterise the putative function of gene sets, we extracted gene ontology-terms (GO-terms) using the tool PANNZER2 and filtered for a reliability estimate (positive predictive value, PPV) greater 0.4 (Törönen and Holm 2022). Redundant or outdated GO-terms were filtered using REVIGO v1.8.1 implemented in a custom script (Supek et al. 2011). We then performed Gene Set Enrichment Analysis (GSEA) for each genotype at defined timepoints using the clusterprofiler v4.14.4 package with the options `pvalueCutoff=0.05`, `exponent=0.5`, `pAdjustMethod="BH"`, `by="fgsea"` (Xu et al. 2024). We conducted the analysis of the REVIGO annotations discretely for molecular functions and biological processes. Putative protein IDs of candidate genes were identified using the blastp function of the UniProt database (The UniProt Consortium 2025).

Functional Characterization

We performed an OrthoFinder v2.5.5 analysis comparing the *S. pennellii* proteome with *A. thaliana* and *S. lycopersicum* to infer putative gene functions based on sequence homology. Protein names were assigned according to their homology with *A. thaliana* for broadly conserved genes and with *S. lycopersicum* for Solanum-specific genes. Additionally, using a custom pipeline, we previously identified putative receptor-like proteins and receptor-like kinases specifically for *S. pennellii* (Range Gowda, unpublished).

Gene-Regulatory-Network

We used the Plant Transcription Factor Database to predict *S. pennellii* transcription factors based on the proteome sequences (Jin et al. 2017). We then generated a directed gene regulatory network based on variance-stabilized read counts of all inoculated samples using the R-package GENIE3 v1.28.0. For this, we used the `GENIE3()` function. We edge-weight-filtered the network using a ranked inflexion point thresholding approach developed by previous studies (Tominello-Ramirez et al. 2024). We used the same thresholding method to determine hub genes based on eigencentality (see digital resources.).

Statistical analysis, Visualization and basic programming

Most analyses were conducted in the R programming environment v4.4.1 within RStudio v2024.12.0. The tidyverse package v2.0.0 was used for data manipulation *dplyr* v1.1.4, visualisation *ggplot2* v3.5.1, and string processing *stringr* v1.5.1. Principal component analysis was performed using the pcatools v2.18.0 package, while ComplexHeatmap v2.22.0 was used for heatmap visualisation. All other plots were generated with *ggplot2*. Vectorised graphics were refined in Inkscape to create multi-panel figures and ensure consistent aesthetics, while GIMP was used for exemplary overlays. For more details about the software versions, please refer to the session info in the digital appendix.

Data availability

All raw files and the final count matrices are publicly available at the NCBI Gene Expression Omnibus (GEO) under the accession GSE292483.

Online resources

The scripts and pipelines used in this study are publicly available at github.com/PHYTOPatCAU/Spen_lag_phase_RNAseq.

Results

S. pennellii genotypes harbour significant QDR diversity.

In a previous study, we performed a high-resolution phenotyping experiment to characterise the lag phase duration on different *Solanum* species using commonly available RGB cameras (Einspanier et al. 2024). We observed significant differences in the lag phase duration between the *S. pennellii* accessions LA1809, LA1941 and LA1282. We measured the shortest lag phase duration on the genotype LA1809 (lsmean 1.59d, 38.16 h), an intermediary lag phase duration of 2.08d (49.92 h) on LA1941, and a significantly increased lag phase duration on LA1282 (lsmean 2.37 d, 56.88h, fig. 1A).

To validate these findings and deepen their biological significance, we assessed photosynthetic stress by measuring the ratio of variable to maximum chlorophyll *a* fluorescence (Fv/Fm). We hypothesised that early photosynthetic stress could indicate the plant's defence capacity and, in turn, affect the duration of the lag phase. To test this, we conducted a phenotyping experiment using detached leaves, monitoring Fv/Fm at 12-hour intervals to capture dynamic changes in photosynthetic efficiency over time. The most pronounced differences in photosynthetic stress among the genotypes emerged 48 hours post-inoculation (hpi). In LA1282, Fv/Fm remained largely unaffected, whereas LA1809 and LA1941 exhibited distinct regions of reduced fluorescence (fig. 1B). Interestingly, we observed a halo with intermediate Fv/Fm values (0.48 - 0.64) surrounding areas of high photosynthetic stress (Fv/Fm < 0.48). This suggests a narrow intersection of intermediate photosynthetic stress between healthy and diseased tissues, marked by slightly reduced photosynthetic stress levels. We further assessed the proportions of Fv/Fm categories per genotype to quantify the extent of photosynthetic stress, independent of leaf size effects. While we observed genotype-dependent temporal dynamics of the Fv/Fm classes, we found the first changes in the Fv/Fm approximately at the same time as the lesion appeared. In LA1809 first stress was measured at 36 hpi (lsmean lag phase: 38.16 h). We observed the first drops in Fv/Fm on LA1941 at 40hpi (lag phase duration 49 h), while photosynthetic stress appeared the latest in LA1282 at 60 hpi (lag phase duration 56.88h). Accordingly, we conclude that *S. sclerotiorum* inoculation leads to photosynthetic stress, which is mostly associated with lesion formation. Consequently, Fv/Fm reflects the visual phenotypes if measured on 12 h rhythms (see fig. 1C).

We observed that the proportion of transient Fv/Fm categories (i.e., categories II, III, or IV) remains stable throughout the infection process across all genotypes. Notably, the intermediate stress zone (class IV) was relatively narrow, with a transition to severe stress and eventual total loss of chlorophyll fluorescence. Over time, the ‘dead’ class (class I, Fv/Fm < 0.160) progressively expanded, while transient classes remained localized at the advancing lesion edge. Contrary to our expectations, we did not measure photosynthetic stress on infected yet asymptomatic areas of the leaf. This observation is persistent even during the lesion growth phase, suggesting that the photosynthetic stress response to *S. sclerotiorum* inoculation is spatially restricted to regions of direct pathogen interaction.

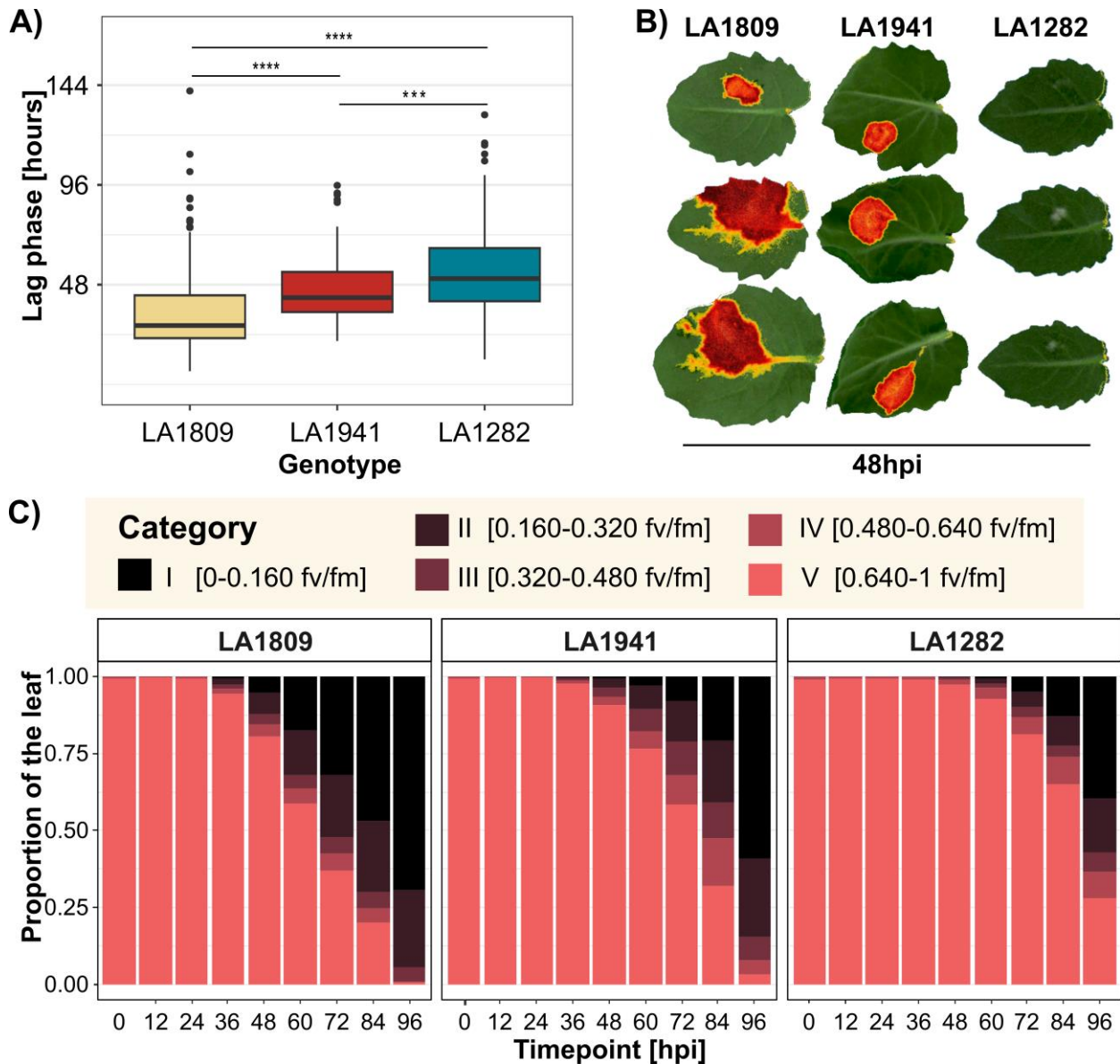


Figure 1: Genotypic Variation in Lag-Phase Duration and Photosynthetic Stress Response. The time until lesion onset varies significantly among the three *S. pennellii* genotypes: LA1282 (n = 205), LA1809 (n = 148), and LA1941 (n = 98). We previously assessed lag-phase duration in a screening study of *Solanum* accessions and now present the duration for these three focal genotypes. The y-axis indicates the asymptomatic phase (in hours after infection). Stars denote statistical significance from pairwise Wilcoxon tests: *** $p \leq 0.001$, ** $p \leq 0.0001$ (A, data adapted from Einspanier et al. 2024). We reproduced the lag-phase phenotype using the “PlantExplorer Pro” phenotyping platform, measuring dark-adapted chlorophyll fluorescence (Fv/Fm) every 12 hours. (B) A representative 48 hpi overlay visualises photosynthetic stress areas, where non-stressed regions appear in standard RGB, while regions with reduced Fv/Fm are highlighted in yellow-to-red overlay according to stress severity. (C) Stacked bar plots show the mean categorical distribution of Fv/Fm values in a time series experiment across the three genotypes. We performed two independent experiments, each with 18 leaflets per genotype and treatment.

Transcriptomic response to infection underlies genotype-dependent longitudinal dynamics.

We then performed an RNA sequencing experiment to investigate how longitudinal infection-induced gene expression dynamics influence the lag phase duration. First, we mapped 3'UTR sequencing reads to the *S. pennellii* reference genome, resulting in consistently high mapping rates in mock samples (85% - 97.81%, fig. 2A). The mapping rates in infected conditions gradually declined over time (70% - 97% fig. 2A), likely due to the increasing number of fungal reads reflecting the pathogen proliferation during pathogenesis (see suppl. fig 1). We conducted a principal components analysis (PCA) on the mapped reads to assess the overall data structure concerning plant genotype and inoculum (suppl. fig. 2). In the PC1 vs PC2 projection, we observed a clear separation between later-stage infected samples and the other samples, indicating a strong infection-driven effect. Moreover, LA1282 and LA1809 clustered more closely together, suggesting a higher degree of transcriptome similarity between these genotypes. In the PC2 vs PC3 space, the three genotypes were more distinctly differentiated, appearing approximately equidistant. These patterns indicate that the dataset captures biologically meaningful variation, with PC1 distinguishing time-dependent inoculation effects and PC2&3 genotype-specific transcriptomic differences.

We then performed a differential gene expression analysis, extracting the number of differentially expressed genes upon fungal infection (DEGs, defined as $\text{padj.} < 0.05$, $|\log_2\text{FoldChange}| > 1$) on each time point for all genotypes. Overall, we observed that the number of DEGs (contrast infection vs mock) increased for all genotypes over time. At 24 hpi, LA1941 showed 29 upregulated and 48 downregulated genes, while LA1809 exhibited only 8 downregulated DEGs. Interestingly, we found no DEGs at 24 hpi on the most resistant genotype LA1282. By 48hpi we measured 71 upregulated DEGs on the genotype LA1282, while we found 11 DEGs on LA1941 (9 up-, 2 downregulated). Interestingly, at this time point, we did not detect any DEGs on the most susceptible genotype LA1809.

We observed a stronger regulatory response once the lag phase passed, during progressing lesion formation. Accordingly, all genotypes displayed a considerable number of DEGs at 72 hpi (LA1282 1,191 up- and 627 downregulated, LA1809 2,177 up- and 1,803 downregulated, and LA1941 1,785 up- and 498 downregulated) and 96 hpi (LA1282 2,290 up- and 1,652

downregulated, LA1809 2,122 up- and 1,834 downregulated, and LA1941 1,536 up- and 1,209 downregulated). However, we could not establish a connection between the late regulatory response (72 hpi and later) and the level of lag-phase-mediated QDR. Therefore, we hypothesise that late regulatory adjustments triggered by infection may impact other QDR phenotypes, such as the lesion growth rate or result from plant tissue degradation. Still, we observed a weak yet genotype-dependent differential response in early time points after *S. sclerotiorum* inoculation, with the most pronounced regulatory shift in LA1282 shortly before the lag phase ends.

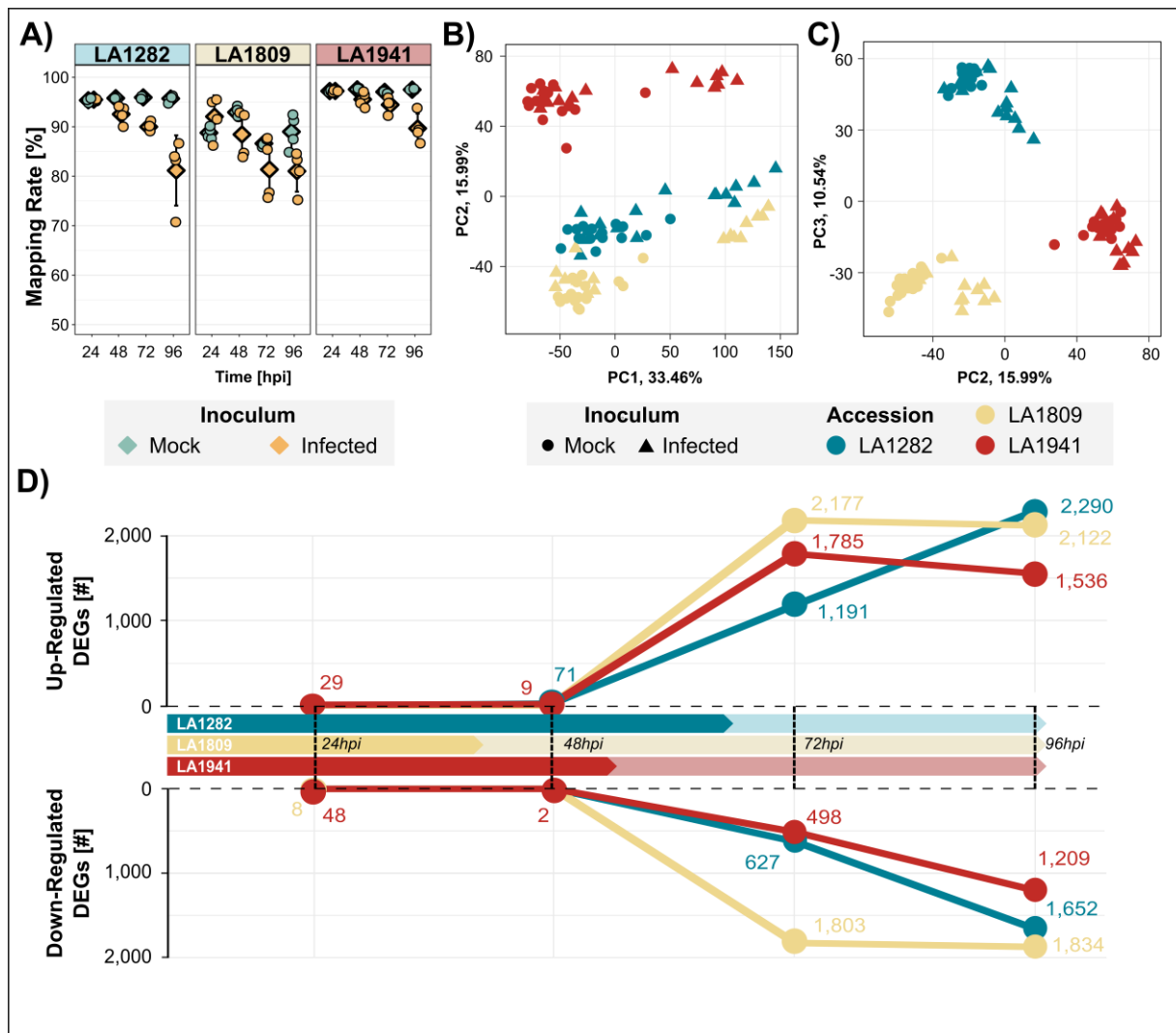


Figure 2: *S. sclerotiorum* infection induces gene expression shifts in all *S. pennellii* genotypes. (A) Mapping rates of all samples to the *S. pennellii* reference genome. The gradual decline in inoculated samples over time reflects the increasing number of fungal reads during infection. The whiskers represent the standard deviation, while diamonds indicate the mean. (B, C) Principal Component Analyses (PC1 vs. PC2 and PC2 vs. PC3) show clear treatment-dependent expression shifts over time (B), and genotype separation (C). (D) Differential gene expression analysis (infection vs. mock, at each time point) reveals distinct longitudinal regulation patterns. The x-axis corresponds to the respective time points (24-, 48-, 72-, and 96-hours past inoculation), and the colour indicates the genotype. The y-axis defines the number of differentially expressed genes ($|\log_2FC| > 1$ and $p. adj < 0.05$) of up- (top panel) and downregulated genes (bottom panel). The solid arrow indicates the approx. mean lag phase duration of each genotype. If no dot/number is shown, no DEGs were found for that genotype at that particular time point.

LA1282 shows significant transcriptomic reprogramming before lesion onset.

Next, we focused on the 48 hpi time point, hypothesising that regulatory shifts during the lag phase could determine its duration. Notably, inoculated LA1282 leaves remain asymptomatic at this stage, whereas LA1809 leaves already show visible symptoms (fig. 1).

In total, we found 71 differentially expressed genes in LA1282 (fig. 2D). Among these DEGs we found mostly defence-associated genes, including several pathogenesis-related (PR) genes such as PR-4 (two paralogs: Sopen01g040940, $\log_2FC=1.5$, and Sopen01g040950, $\log_2FC=1.17$), PR-1 protein 38 (two paralogs: Sopen01g026170, $\log_2FC=1.43$, and Sopen01g048970, $\log_2FC=1.21$) and the strongly infection-induced protein LOX1 ($\log_2FC=4.3$). We also identified proteins involved in the protection against oxidative stress (DOX1, $\log_2FC=3.95$), interaction with fungal pathogens (e.g., chitinases, and β -1,3-endoglucanases), and detoxification (glycosyltransferases, cytochrome p450). Among those DEGs were several transcription factors, such as WRKY45 and WRKY51, as well as ethylene-response factors, illustrating a broad regulatory response to the inoculum. In addition to those well-characterized defence genes, we found several proteins of unknown function, including Sopen08g008720, Sopen12g023430, and Sopen03g007540. Interestingly, we did not detect any genes with negative (i.e., down-) regulated at this genotype 48 hpi (suppl. tab. 1, fig. 3A).

Although the average lag phase duration of LA1809 ends prior to 48hpi, we did not detect any statistically significant regulatory reprogramming. This finding suggests an incomplete, or delayed response that lags behind the infection process (fig. 2D, fig. 3B).

In contrast, we identified two downregulated and nine upregulated DEGs at 48 hpi in the intermediate-resistant genotype LA1941. Among these, we detected MYB ($\log_2FC=1.8$), and ERF ($\log_2FC=1.05$) transcription factors as well as genes directly linked to pathogenesis. These include a putative lipoxygenase (PLAT3, $\log_2FC=1.15$) and a putative PR-5 family protein (thaumatin-like protein 1, $\log_2FC=1.8$). Interestingly, we found that OXIDATIVE STRESS 3, a key regulator of ROS homeostasis and stress resilience, was significantly downregulated ($\log_2FC = -1.5$) at this time point (suppl. tab. 2, Fig. 3C).

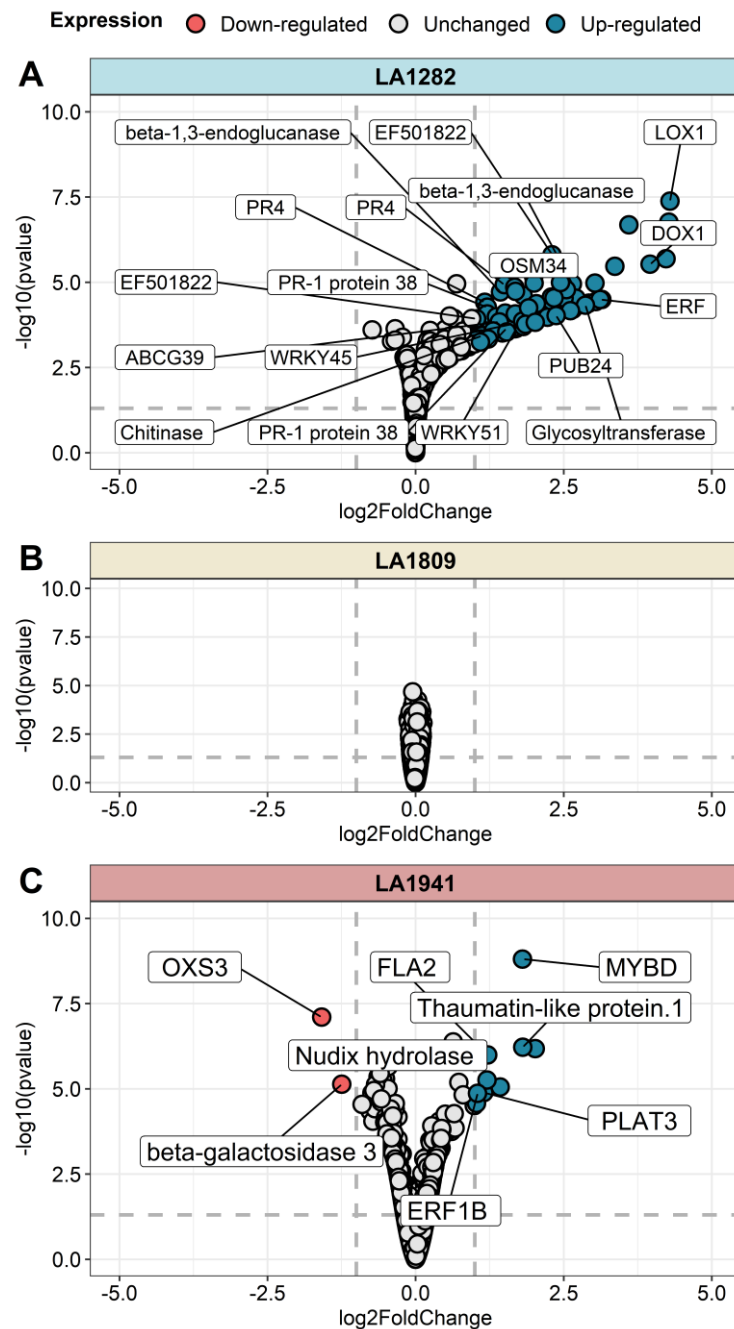


Figure 3: LA1282 exhibits distinct regulatory reprogramming at 48 hpi. The volcano plots display differential gene expression analysis results comparing infected vs mock conditions at 48 hpi. We tested the genotypes LA1282 (A), LA1809 (B), and LA1941 (C). Each dot represents a single gene. The y-axis shows the $-\log_{10}$ of the FDR-corrected p-value, while the x-axis represents the \log_2 fold-change. The dotted lines mark the thresholds for DEG assignment ($|\log_2 \text{ fold-change}| > 1$ and $p.\text{adj.} < 0.05$). Genes meeting these criteria are considered differentially expressed. Red dots indicate downregulated DEGs, while blue dots highlight genes with increased expression in infected conditions. Labelled genes indicated transcripts of interest.

Gene Set Enrichment Analysis on LA1282 at 48hpi reveals clear defence responses.

To further validate the early transcriptomic reprogramming in the resistant genotypes, we performed a gene set enrichment analysis (GSEA). This approach allows for a functional interpretation of subtle regulatory changes by analysing ranked gene expression patterns across the entire transcriptome rather than focusing solely on DEGs.

We observed that the LA1809 transcriptome is largely dominated by basal homeostasis processes at 48hpi. This includes the processes “translation” (GO:0006412, NES=4.05), “ribosomal small subunit assembly” (GO:0000028, NES=3.79), and “energy reserve metabolic processes” (GO:0006112, NES=2.88, suppl. tab. 3). This pattern is further reinforced by the absence of defence-related processes in the LA1809 GSEA analysis 24hpi. These insights further highlight how LA1809 cannot mount a robust defence response both before and after lesion onset.

In accordance with our previous findings, we observed a significant enrichment of defence-related processes in LA1282 48hpi. This set includes “response to fungus” (GO:0009620, NES=2.9), “ethylene metabolic process” (GO:0009692, NES=2.79), and the jasmonic acid-associated “oxylipin biosynthetic process” (GO:0031408, NES=2.83). We also identified a more general “defence response” (GO:0006952, NES=2.09, set size=151). We found evidence for secondary defence-related processes, such as “lipid biosynthetic processes” (GO:0008610, NES=2.85) and “carbohydrate metabolic processes” (GO:0005975, NES=2.38), which might reflect the plant's ability to recognise and metabolise fungal structures such as chitin or glucans. Interestingly, we detected no defence-related enriched gene sets at 24 hpi. Although these enrichments largely mirror the DEGs observed in this genotype, we argue that the significantly expanded defence-associated gene set indicates a broad transcriptomic reprogramming, involving a larger number of genes under nuanced regulatory control (tab.1).

Table 1: Gene Set Enrichment Analysis (GSEA) of ranked log2FC gene expression data in LA1282 at 48hpi. All genes were ranked according to their differential expression, and significant enrichments (padj. < 0.05) GO terms (biological process) were identified. The normalised enrichment score (NES) measures the magnitude of enrichment of a given gene set relative to its size and compares enrichment across different gene sets. P-values were FDR-corrected using the Benjamini-Hochberg procedure.

ID	Description	NES	p.adjust	setSize
GO:0009620	response to fungus	2.906	0.0048	15
GO:0008610	lipid biosynthetic process	2.851	0.0015	24
GO:0031408	oxylipin biosynthetic process	2.838	0.0079	12
GO:0009692	ethylene metabolic process	2.795	0.0137	10
GO:0006044	N-acetylglucosamine metabolic process	2.749	0.0048	18
GO:0032787	monocarboxylic acid metabolic process	2.710	0.0079	24
GO:0009806	lignan metabolic process	2.659	0.0140	20
GO:0048544	recognition of pollen	2.659	0.0426	14
GO:0006629	lipid metabolic process	2.641	0.0014	46
GO:0034440	lipid oxidation	2.481	0.0140	32
GO:0005975	carbohydrate metabolic process	2.388	0.0014	95
GO:0009395	phospholipid catabolic process	2.238	0.0079	71
GO:0006952	defence response	2.090	0.0015	151

At 24 hpi, we observed a significant enrichment of “response to fungus” (GO:0009620, NES = 3.05, set size = 11) and “cellular detoxification of aldehyde” (GO:0110095, NES = 2.87) in the LA1941 transcriptome (tab. 2). However, by 48 hpi, only three processes remained significantly enriched: “defence response” (GO:0006952, NES = 2.92), “cytoplasmic translation” (GO:0002181, NES = 3.24), and “microtubule-based movement” (GO:0007018, NES = 3.1; suppl. tab. 4). These findings suggest an early activation of pathogen recognition and detoxification mechanisms, followed by a later shift toward defence activation, protein synthesis, and cytoskeletal rearrangements.

These findings suggest that the high-QDR genotypes LA1282 and LA1941 mount infection-induced regulatory changes towards defence processes. Notably, there is little overlap between the two genotypes: LA1941 initiates a subtle yet earlier characterised by a small set size and weakly differentially expressed genes. In contrast, LA1282 initiates a later but more robust defence response, with a larger set size and a greater number of strongly regulated DEGs, particularly at 48 hpi. The lack of overlap between these responses suggests that each genotype employs independent regulatory mechanisms to achieve quantitative disease resistance (QDR).

Meanwhile, LA1809 fails to mount any detectable response during early pathogenesis, further underscoring its susceptibility.

Table 2: Gene Set Enrichment Analysis (GSEA) of ranked log2FC gene expression data in LA1941 at 24hpi.

All genes were ranked according to their differential expression, and significant enrichments (padj. < 0.05) GO terms (biological process) were identified. The normalised enrichment score (NES) measures the magnitude of enrichment of a given gene set relative to its size and compares enrichment across different gene sets. P-values were FDR-corrected using the Benjamini-Hochberg procedure.

ID	Description	NES	p.adjust	setSize
GO:0006457	protein folding	3.388	0.00014	82
GO:0006412	translation	3.095	0.00014	98
GO:0009620	response to fungus	3.055	0.02500	11
GO:0006730	one-carbon metabolic process	3.005	0.03705	10
GO:0009813	flavonoid biosynthetic process	2.900	0.02500	23
GO:0110095	cellular detoxification of aldehyde	2.879	0.00563	54
GO:0006516	glycoprotein catabolic process	2.579	0.03705	51
GO:0000028	ribosomal small subunit assembly	2.311	0.01930	121

The resistant accession LA1282 shows distinct regulation of putative resistance-associated genes

We hypothesised that the early induction of pathogenesis-related genes might confer a QDR advantage to LA1282. Based on our previous findings, we selected the 71 DEGs identified in LA1282 at 48 hpi for further analysis, hereafter referred to as “focal DEGs” (see fig. 3A). Following this, we expect increased susceptibility associated with altered temporal orchestration, such as delayed or absent expression of the focal DEGs. To test this hypothesis, we examined the longitudinal (temporal) trajectories of the focal genes across the three genotypes.

Firstly, we performed a PCA on the per-genotype log₂ fold-change (infected vs mock) across all time points for each focal DEG, revealing a clear separation among the genotypes. Each dot in the PCA represents a single focal DEG in a specific genotype, covering its regulation across all four time points. Notably, LA1809 and LA1941 cluster more closely, with some trajectories overlapping, whereas LA1282 trajectories were more separated (fig. 4A).

We performed a temporal clustering analysis to describe the regulatory dynamics among the three genotypes. For this, we analysed the longitudinal expression pattern of the 71 focal DEGs per genotype (3 x 71 focal DEGs). All focal DEGs show clear evidence of expression in each genotype at least once during our timeseries experiment. Using a Dirichlet Process Gaussian Process Model (DP_GP), we grouped trajectories into clusters based on their shared temporal expression profiles, allowing us to determine whether the same genes followed similar or divergent regulatory patterns across genotypes.

Through this analysis, we identified five distinct expression patterns. Cluster 1 includes 56 genes with a continuous increase in expression from 24hpi to 96hpi. In contrast, the 12 trajectories in cluster 2 followed a zigzag pattern with expression peaks at 48hpi and 96hpi. Cluster 3, containing only six genes, shows a modest rise at 48hpi followed by a stronger increase till 96hpi. The remaining gene trajectories fell into Cluster 4 (n=67) and Cluster 5 (n=70). Both clusters show increased expression after 48 hpi, but Cluster 5 peaks sharply at 72hpi, while Cluster 4 plateaus at its maximum.

Consequently, we grouped the gene trajectories of the focal genes into three major regulatory categories:

1. Early-response genes (clusters 1–3)
2. Late-expression trajectories with sustained expression (cluster 4)
3. Late-expression gene trajectories with transient expression peaking at 72hpi before declining (cluster 5).

We performed a membership analysis of cluster assignment to test whether LA1282 trajectories exhibit an early increase while those of LA1941 and LA1809 are expressed late. Strikingly, all but one of the LA1282 trajectories clustered within the early response group (Clusters 1-3). In contrast, most focal DEG trajectories of LA1809 and LA1941 fell into the late-responding Clusters 4 and 5.

Interestingly, most LA1941 trajectories showed clear downregulation at 96 hpi, whereas those genes remained highly upregulated in LA1809. We observed very little overlap between the genotypes, strengthening the hypothesis that the longitudinal expression dynamics are highly genotype-specific. Although LA1282 trajectories were distributed across multiple clusters, LA1809 genes predominantly grouped in Cluster 4, while LA1941 genes primarily fell into Cluster 5, suggesting distinct regulatory strategies.

In conclusion, all focal DEGs show infection-induced regulation in all genotypes, highlighting that LA1809 susceptibility is not due to the absence of the focal DEGs from its regulatory repertoire. Moreover, we observed that the focal DEGs underlie clear genotype-dependent and infection-induced temporal dynamics in the tested genotypes. Building on these results, we hypothesise that the resistance of LA1282 is determined by the distinct regulatory trajectory of focal DEGs (zig-zag pattern), characterised by subtle early induction followed by deregulation.

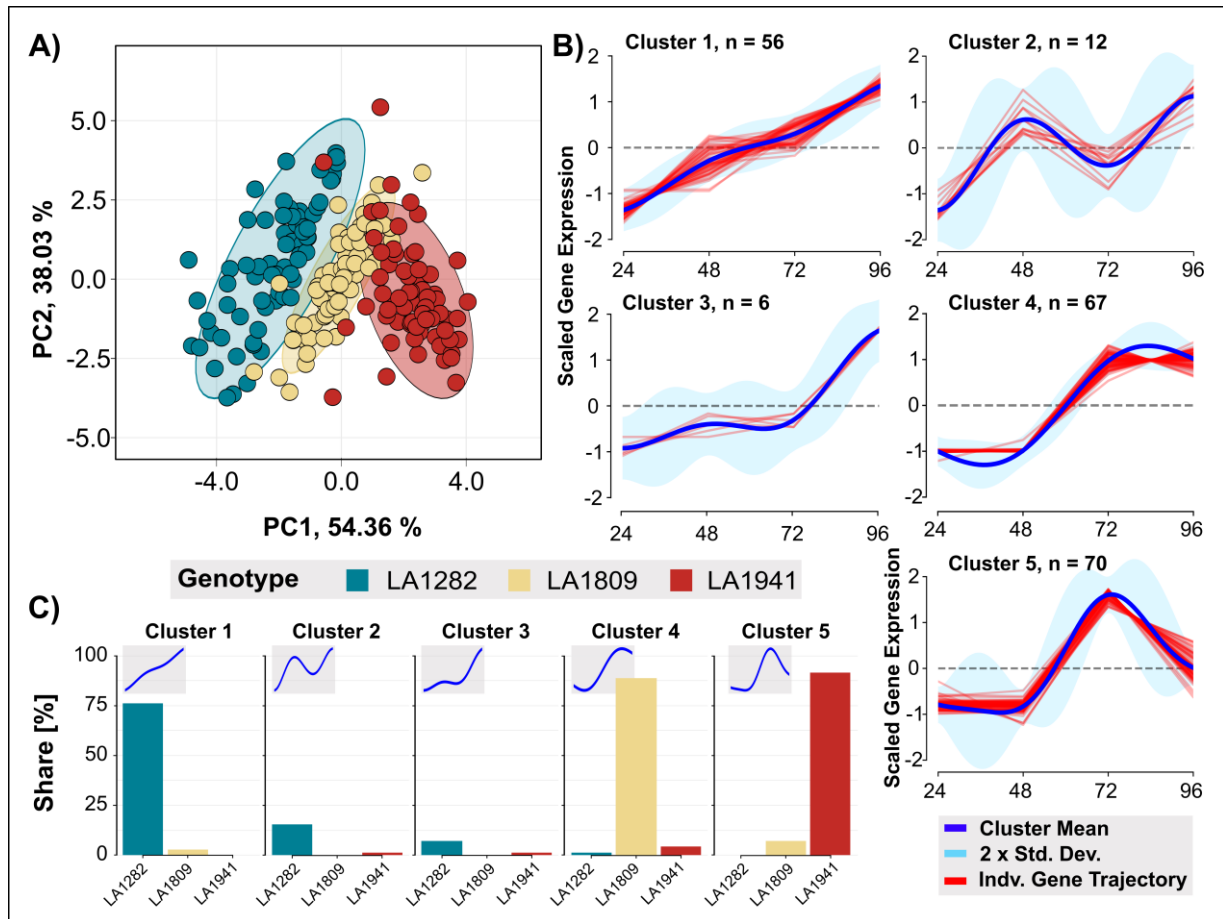


Figure 4: LA1282-specific early response DEGs underlie divergent temporal trajectories in more susceptible genotypes. **A)** Principal component analysis (PCA) of the 71 focal gene trajectories across the three genotypes. Each dot represents the temporal trajectory of a single focal DEG (incorporating the four time points). Colours represent the genotype identity, while the ellipses denote each genotype's 95 % confidence interval. **B)** Clustering analysis of the genotype-dependent trajectories of the 71 focal genes. A Dirichlet Process Gaussian model was used to determine the ideal number of clusters and model the individual gene trajectories over time. The algorithm identified five clusters. The y-axis defines the scaled gene expression, while the x-axis denotes the time. The blue line represents the mean trajectory of each cluster, while the red lines show individual gene trajectories. The shaded regions represent two standard deviations (2x SD). deviation. The number of genes assigned to each cluster is indicated by n. **C)** Cluster membership analysis of the focal gene trajectories per genotype. The y-axis represents the per-genotype proportion of focal DEGs assigned to each cluster. The colour and x-axis define the different genotypes Clusters correspond to those defined in (B).

Basal expression of a WRKY transcription factor might determine the level of QDR.

Building on the high genotypic specificity of focal DEG trajectories, we hypothesised that these genes might be regulated by a shared transcription factor (TF). We performed a directed gene regulatory network analysis to test this, identifying 28 potential regulatory hub genes. We identified one transcription factor (Sopen02g011350) with regulatory connections to all 71 focal genes. Notably, this TF is not part of the focal DEGs.

Interestingly, Sopen02g011350 is an ortholog of the *A. thaliana* WRKY6, a TF with a documented role in resistance, primarily against abiotic stresses (Chen et al. 2009; Huang et al. 2016; Niu et al. 2024). We found that Sopen02g011350 had a significantly elevated eigencentality in the GRN, indicating a key role in network regulation. Additionally, this TF displayed a high edge weight to all focal DEGs, supporting a potential function as a central regulator of the focal DEGs.

Next, we analysed the expression pattern of this TF in both mock and infected conditions across three genotypes to verify its role in genotype-dependent longitudinal regulation. Compared to LA1809 and LA1941, LA1282 exhibited consistently higher expression of Sopen02g011350, a trend observed in both infected and non-infected conditions, independent of time. Notably, under mock conditions at 24 hpi, LA1282 expressed Sopen02g011350 significantly higher than the other genotypes. Upon infection, Sopen02g011350 expression increased in all genotypes, though its basal expression level in LA1282 remained consistently elevated (fig. 5, suppl. table 10).

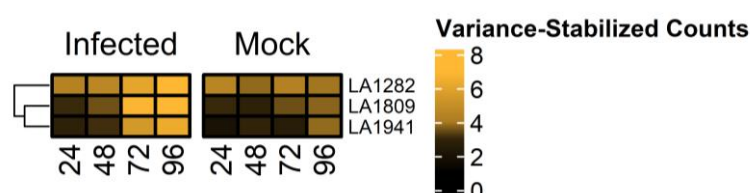


Figure 5: The gene regulatory network hub Sopen02g011350 (WRKY6 ortholog), exhibits high basal and induced expression in the resistant genotype LA1282. We identified Sopen02g011350, a putative WRKY6 ortholog, as a gene regulatory network (GRN) hub based on high eigencentality and connectivity to all focal DEGs. We analysed its expression using mean variance-stabilized of absolute (deduplicated) read counts. The heatmap displays Sopen02g011350 expression levels, where red indicates high expression and blue represents low expression. We compared four time points (24–96 hpi) under infected and mock conditions across the three genotypes: LA1282, LA1809, and LA1941.

Basal expression of focal DEGs is significantly elevated in LA1282.

Following the observation that the putative core regulator of the focal DEGs (Sopen02g011350) exhibited significantly higher basal expression in LA1282, we next investigated whether the focal DEGs also show constitutively elevated expression in this genotype.

Strikingly, most focal DEGs (56 out of 71, suppl. tab. 9) are significantly more expressed in LA1282 mock conditions than the susceptible genotype LA1809. In particular, pathogenesis-related genes PR-1, PR-4, and β -1,3-endoglucanases displayed stronger basal expression (fig. 6, suppl. tab. 9). This further provides evidence that basal or preformed defence mechanisms contribute to QDR in LA1282. Since LA1282 exhibits elevated basal expression of both the core regulator Sopen02g011350 and its downstream focal DEGs, we next asked whether pathogen perception might contribute to QDR in this genotype. To explore this, we analysed the basal expression of key pathogen recognition proteins, including BAK1, SOBIR1, CERK1, receptor-like proteins (RLPs), and receptor-like kinases (RLKs).

Interestingly, we found eight RLKs with significantly elevated basal expression in LA1282 compared to LA1809. Moreover, we identified seven differentially expressed RLPs, including three upregulated in LA1282 and one allele each of CERK1 and BAK1 (see suppl. tables 5-8). These findings illustrate first evidence of how the basal expression of key defence genes and the pre-activation of immune receptors might facilitate an earlier and more rapid defence response in LA1282, resulting in enhanced QDR.

However, a more detailed pathway analysis, along with molecular characterisation assays (such as ROS burst measurements, MAPK-phosphorylation or phytohormone measurements), is required to determine the functional link between basal RLK/RLP expression and the regulation of focal DEGs.

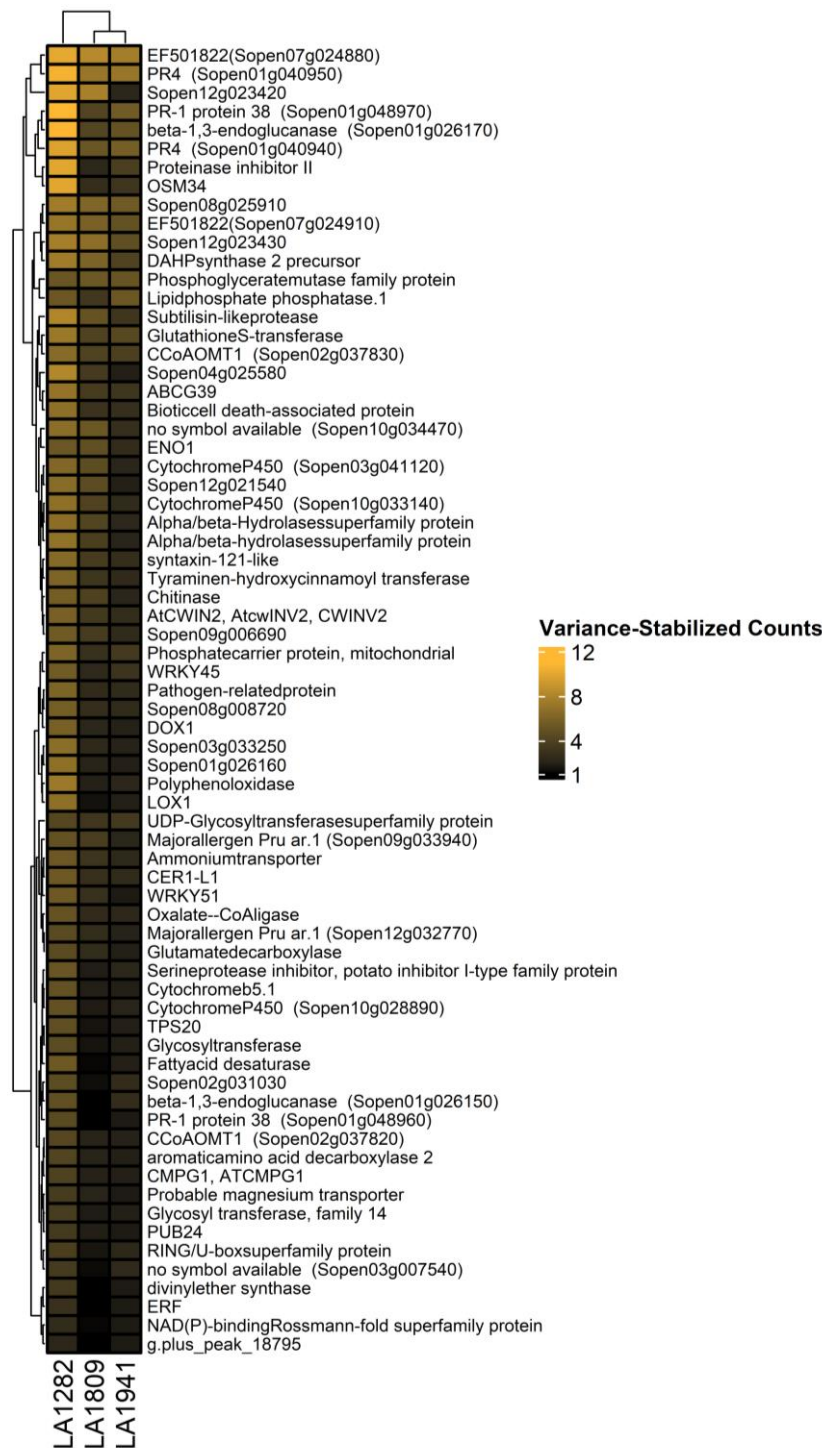


Figure 6: LA1282 Exhibits Higher Basal Expression of Focal DEGs. We analysed the basal expression of the 71 focal genes (identified in LA1282 at 48 hpi) by comparing their expression under mock conditions across the three genotypes. We used variance-stabilized mean expression values, which were min-max normalised to the highest and lowest observed values. The heatmap visualises gene expression levels, where red indicates the highest expression and dark blue denotes the lowest. The expression values represent measurements at 24 hpi under mock conditions across four independent biological replicates. Rows and columns were clustered using Euclidean distance.

Discussion

We performed a longitudinal transcriptome analysis to identify regulatory factors driving the lag phase duration on *S. pennellii* upon *S. sclerotiorum* inoculation. Our goal was to characterise the composition and temporal dynamics of the regulatory response in high-QDR genotypes. Specifically, we tested whether QDR is driven by induced or basal expression.

The lag phase duration is determined by common defence genes.

In the high-QDR genotype LA1282, we identified a set of focal DEGs which we associated with resistance. These genes show evidence for late infection-induced expression (72 – 96hpi) in more susceptible genotypes yet lack the longitudinal pattern found in LA1282. In particular, the genotype LA1282 facilitates early defence gene expression at 48hpi, before lesion onset. Many of these focal DEGs, including glutathione S-transferases, ABC-transporters, p450 cytochromes, receptor-like kinases/proteins and PR-genes, have been previously linked to *S. sclerotiorum*-induced defence responses across multiple hosts (Xue et al. 2024; Seifbarghi et al. 2017; Sucher et al. 2020; Wei et al. 2016; Gullner et al. 2018). These genes contribute to necrotrophic pathogen defence by regulating detoxification, reactive oxygen species homeostasis, transport and cell death (Xue et al. 2024).

While general defence responses to *S. sclerotiorum* inoculation are well understood, comparative studies examining multiple genotypes with varying levels of QDR remain scarce. Little is known about how temporal regulation influences QDR phenotypes. However, some reports have linked early gene expression patterns to QDR against *S. sclerotiorum* on *Brassica juncea* or soybean (Que et al. 2014; Ranjan et al. 2019; Yang et al. 2025). Ranjan et al. (2019) observed that early jasmonate (JA) accumulation enhances ROS scavenging capacity in a resistant genotype, which aligns with our observation of increased DOX1 expression in LA1282. The role of JA in conferring resistance to *S. sclerotiorum* has been demonstrated, although the significance of longitudinal JA regulation remains inconclusive (Wei et al. 2016). While some studies do not establish a direct link between temporal gene regulation and resistance (Seifbarghi et al. 2017) or remain inconclusive (Chang et al. 2018), our findings align with prior work indicating that focal gene activity is crucial for lag-phase-mediated resistance (Westrick et al. 2019). We observed that a distinct regulatory shift at 48hpi is required to delay lesion onset on a high-QDR genotype.

Studies on *S. sclerotiorum* point to a distinct regulatory shift between the early (presymptomatic, 24-48hpi) and late (symptomatic, 96hpi) stages of infection, potentially marking the transition from biotrophy to necrotrophy (Seifbarghi et al. 2017; Westrick et al. 2019; Kabbage et al. 2015). These presymptomatic gene-expression changes align closely with our observation that a high-QDR genotype (LA1282) initiates an early regulatory response before lesion onset. Further research is needed to determine whether high-QDR genotypes actively counter the pathogen's shift in infection strategy.

A WRKY Transcription Factor might control quick QDR response to *S. sclerotiorum* inoculation.

The role of WRKY TFs in oxalic acid and *S. sclerotiorum* resistance is well documented. Multiple WRKY TFs have been identified across multiple hosts like *A. thaliana*, oil seed rape, or *Brassica juncea*, including AtWRKY28, AtWRKY75, BnWRKY8, BnWRKY33, BnWRKY61 or the WRKY25 *BjuA016484* (Chen et al. 2013; Wei et al. 2016; Yang et al. 2025; Zhao et al. 2024; Wang et al. 2014). In this study, gene regulatory network and differential gene expression analysis revealed WRKY6 (Sopen02g011350) as a putative regulator of QDR-related genes. Interestingly, WRKY6 has been characterised in *A. thaliana* for its role in abiotic stress resistance, particularly in response to phosphorus or potassium limitation (Chen et al. 2009; Niu et al. 2024). However, some studies have reported its differential expression upon *S. sclerotiorum* infection in *A. thaliana* and oil seed rape (Zhang et al. 2022; Wu et al. 2016). We speculate that the association of WRKY6 with abscisic acid (ABA) homeostasis might enable its role in defence via plant hormone signalling (Huang et al. 2016).

In tomato (*S. lycopersicum*), WRKY6 (Soly02g080890) is linked to pathogen resistance, with elevated expression reported in genotypes resistant against *Ralstonia solanacearum* and *Fusarium oxysporum* f. sp. *lycopersici* (Zhang et al. 2020; López et al. 2021). In contrast, in *S. pennellii*, however, WRKY6 has been only associated with leaf thickness development (Coneva et al. 2017).

Given its role in multiple stress responses and pathogen interactions, WRKY6 may serve as a key factor in resistance to diverse pathogens, following the observations of the typical pleiotropic nature of QDR-loci (Roux et al. 2014). We demonstrate that basal WRKY6 regulation influences complex QDR phenotypes, such as lag-phase duration, without conferring full resistance. Since WRKY6 exhibits strong regulatory connectivity to all focal genes and

shows significantly elevated basal expression in the resistant genotype, similar to the focal genes, we propose that WRKY6 is a promising candidate for further investigation within the genetic regulatory network governing QDR-associated genes.

Following the canonical model of defence response to most pathogens, TFs, like WRKYs and ERFs, act downstream of key components in the pattern-triggered immunity (PTI) signalling cascade. This includes early-response elements such as mitogen-activated protein kinases (MAPKs), as well as ROS bursts and Ca²⁺ signalling, which can contribute to QDR against *S. sclerotiorum* (Li et al. 2016; Lewis et al. 2015; Wei et al. 2016; Zhang and Klessig 2001; Lin et al. 2024; Wu et al. 2016). Unfortunately, the resolution of our time-series experiment does not capture the earliest events in the host-parasite interaction. Nevertheless, we observed clear differential regulation of several potentially PTI-associated genes in the resistant genotypes, supporting their role in QDR-associated transcriptional reprogramming.

QDR is determined by basal gene expression and defence priming.

Based on our observations, we propose that elevated basal expression of focal genes, possibly through a primed defence state, and altered pathogen perception through receptor-like proteins and -kinases determine QDR in conjunction. Consistent with this hypothesis, some of our candidate genes exhibit increased basal expression in resistant oilseed rape genotypes, resulting in stronger induction compared to susceptible backgrounds (Wu et al. 2016). We found significant variation in the basal RLK and RLP regulation across genotypes with varying QDR levels. Notably, the high-QDR genotype LA1282 shows a strong basal expression of the receptor-like kinase LIK1 (Sopen02g020810). In *A. thaliana*, LIK1 is phosphorylated by CERK1 and has been shown to enhance resistance against *S. sclerotiorum* while acting as a susceptibility factor for biotrophic pathogens (Le et al. 2014). LIK1 plays a role in chitin perception, potentially interacting with FLS2, PEPR1, and PEPR2. Interestingly, LIK1 mutants show increased sensitivity to chitin (Le et al. 2014), but fail to respond to glycans, suggesting that LIK1 mediates the recognition of carbohydrate-based elicitors, particularly mixed-link glucans (Martín-Dacal et al. 2023). Beyond RLKs, RLPs also contribute to QDR, as demonstrated by AtRLP30, AtRLP42 and AtRLP23, which mediate fungal elicitor perception (e.g., SCFE1 or nlp20), increasing QDR against multiple pathogens (Mbengue et al. 2016; Albert et al. 2015). Yet, most of the receptors identified here remain uncharacterised and appear unique to wild tomatoes. Based on our results, we raise the question of whether the QDR

phenotypes reported in most receptor-based studies are primarily attributed to delayed lesion onset.

Conclusion

In this study, we observed that subtle shifts in gene expression can significantly extend the lag-phase duration. We speculate that the fungus may be particularly vulnerable during the early stages of infection, making basal expression and fine-tuned longitudinal gene expression changes essential components of QDR.

Based on the elevated abundance of focal DEGs and PRRs, we hypothesize that LA1282 might benefit from a prime state of physiological awareness. Previously, it was shown that AtWRKY6 and PR1 are subject to trans-generational defence priming, linking transgenerational systemic acquired resistance with histone modification (Conrath et al. 2015; Luna et al. 2012). The constitutively elevated defence gene expression during the primed state might enhance QDR with a relatively low fitness cost (Ahmad et al. 2010; Li et al. 2016; Conrath et al. 2006). This study demonstrates that basal gene regulation can shape QDR by modulating the temporal dynamics of a key set of defence genes, ultimately enhancing the plant's ability to delay pathogen invasion.

Acknowledgements

We greatly acknowledge Susanne Kleingarn for her assistance during RNA isolation. Our warmest gratitude also goes to Laura Groenenberg and Theo van der Lee for providing the PlantExplorer Pro machine and the training and support for operating and conducting the experiments. We thank Hendrik Seide, who engaged in many critical discussions with us.

Publication bibliography

Ahmad, Shakoor; Gordon-Weeks, Ruth; Pickett, John; Ton, Jurriaan (2010): Natural variation in priming of basal resistance: from evolutionary origin to agricultural exploitation. In *Molecular plant pathology* 11 (6), pp. 817–827. DOI: 10.1111/j.1364-3703.2010.00645.x.

Albert, Isabell; Böhm, Hannah; Albert, Markus; Feiler, Christina E.; Imkampe, Julia; Wallmeroth, Niklas et al. (2015): An RLP23-SOBIR1-BAK1 complex mediates NLP-triggered immunity. In *Nature plants* 1, p. 15140. DOI: 10.1038/nplants.2015.140.

Barbacci, Adelin; Navaud, Olivier; Mbengue, Malick; Barascud, Marielle; Godiard, Laurence; Khafif, Mehdi et al. (2020): Rapid identification of an Arabidopsis NLR gene as a candidate conferring susceptibility to *Sclerotinia sclerotiorum* using time-resolved automated phenotyping. In *The Plant journal : for cell and molecular biology* 103 (2), pp. 903–917. DOI: 10.1111/tpj.14747.

Bi, Kai; Liang, Yong; Mengiste, Tesfaye; Sharon, Amir (2023): Killing softly: a roadmap of *Botrytis cinerea* pathogenicity. In *Trends in plant science* 28 (2), pp. 211–222. DOI: 10.1016/j.tplants.2022.08.024.

Bolger, Anthony; Scossa, Federico; Bolger, Marie E.; Lanz, Christa; Maumus, Florian; Tohge, Takayuki et al. (2014): The genome of the stress-tolerant wild tomato species *Solanum pennellii*. In *Nature Genetics* 46 (9), pp. 1034–1038. DOI: 10.1038/ng.3046.

Chang, Hao-Xun; Sang, Hyunkyu; Wang, Jie; McPhee, Kevin E.; Zhuang, Xiaofeng; Porter, Lyndon D.; Chilvers, Martin I. (2018): Exploring the genetics of lesion and nodal resistance in pea (*Pisum sativum* L.) to *Sclerotinia sclerotiorum* using genome-wide association studies and RNA-Seq. In *Plant direct* 2 (6), e00064. DOI: 10.1002/pld3.64.

Chen, Renjie; Gajendiran, Karthick; Wulff, Brande B. H. (2024): R we there yet? Advances in cloning resistance genes for engineering immunity in crop plants. In *Current opinion in plant biology* 77, p. 102489. DOI: 10.1016/j.pbi.2023.102489.

Chen, Xiaoting; Liu, Jun; Lin, Guifang; Wang, Airong; Wang, Zonghua; Lu, Guodong (2013): Overexpression of AtWRKY28 and AtWRKY75 in Arabidopsis enhances resistance to oxalic acid and *Sclerotinia sclerotiorum*. In *Plant cell reports* 32 (10), pp. 1589–1599. DOI: 10.1007/s00299-013-1469-3.

Chen, Yi-Fang; Li, Li-Qin; Xu, Qian; Kong, You-Han; Wang, Hui; Wu, Wei-Hua (2009): The WRKY6 transcription factor modulates PHOSPHATE1 expression in response to low Pi stress in Arabidopsis. In *The Plant cell* 21 (11), pp. 3554–3566. DOI: 10.1105/tpc.108.064980.

Coneva, Viktoriya; Frank, Margaret H.; Balaguer, Maria A. de Luis; Li, Mao; Sozzani, Rosangela; Chitwood, Daniel H. (2017): Genetic Architecture and Molecular Networks Underlying Leaf Thickness in Desert-Adapted Tomato *Solanum pennellii*. In *Plant physiology* 175 (1), pp. 376–391. DOI: 10.1104/pp.17.00790.

Conrath, Uwe; Beckers, Gerold J. M.; Flors, Victor; García-Agustín, Pilar; Jakab, Gábor; Mauch, Felix et al. (2006): Priming: getting ready for battle. In *Molecular Plant-Microbe Interactions®* 19 (10), pp. 1062–1071. DOI: 10.1094/MPMI-19-1062.

Conrath, Uwe; Beckers, Gerold J. M.; Langenbach, Caspar J. G.; Jaskiewicz, Michal R. (2015): Priming for enhanced defense. In *Annual review of phytopathology* 53, pp. 97–119. DOI: 10.1146/annurev-phyto-080614-120132.

Corwin, Jason A.; Kliebenstein, Daniel J. (2017): Quantitative Resistance: More Than Just Perception of a Pathogen. In *The Plant cell* 29 (4), pp. 655–665. DOI: 10.1105/tpc.16.00915.

Denton-Giles, Matthew; McCarthy, Hannah; Sehrish, Tina; Dijkwel, Yasmin; Mesarich, Carl H.; Bradshaw, Rosie E. et al. (2020): Conservation and expansion of a necrosis-inducing small secreted protein family from host-variable phytopathogens of the Sclerotiniaceae. In *Molecular plant pathology* 21 (4), pp. 512–526. DOI: 10.1111/mpp.12913.

Derbyshire, Mark; Denton-Giles, Matthew; Hegedus, Dwayne; Seifbarghy, Shirin; Rollins, Jeffrey; van Kan, Jan et al. (2017): The Complete Genome Sequence of the Phytopathogenic Fungus *Sclerotinia sclerotiorum* Reveals Insights into the Genome Architecture of Broad Host Range Pathogens. In *Genome Biology and Evolution* 9 (3), pp. 593–618. DOI: 10.1093/gbe/evx030.

Derbyshire, Mark C.; Newman, Toby E.; Khentry, Yuphin; Owolabi Taiwo, Akeem (2022): The evolutionary and molecular features of the broad-host-range plant pathogen *Sclerotinia sclerotiorum*. In *Molecular plant pathology* 23 (8), pp. 1075–1090. DOI: 10.1111/mpp.13221.

Einspanier, Severin; Tominello-Ramirez, Christopher; Hasler, Mario; Barbacci, Adelin; Raffaele, Sylvain; Stam, Remco (2024): High-Resolution Disease Phenotyping Reveals Distinct Resistance Mechanisms of Tomato Crop Wild Relatives against *Sclerotinia sclerotiorum*. In *Plant phenomics (Washington, D.C.)* 6, p. 214. DOI: 10.34133/plantphenomics.0214.

Gullner, Gábor; Komives, Tamas; Király, Lóránt; Schröder, Peter (2018): Glutathione S-Transferase Enzymes in Plant-Pathogen Interactions. In *Frontiers in plant science* 9, p. 1836. DOI: 10.3389/fpls.2018.01836.

Hamill, Philip G.; Stevenson, Andrew; McMullan, Phillip E.; Williams, James P.; Lewis, Abiann D. R.; S, Sudharsan et al. (2020): Microbial lag phase can be indicative of, or independent from, cellular stress. In *Scientific reports* 10 (1), p. 5948. DOI: 10.1038/s41598-020-62552-4.

Hathaway, Lucy J.; Brugger, Silvio D.; Morand, Brigitte; Bangert, Mathieu; Rotzetter, Jeannine U.; Hauser, Christoph et al. (2012): Capsule type of *Streptococcus pneumoniae* determines growth phenotype. In *PLoS pathogens* 8 (3), e1002574. DOI: 10.1371/journal.ppat.1002574.

Huang, Yun; Feng, Cui-Zhu; Ye, Qing; Wu, Wei-Hua; Chen, Yi-Fang (2016): Arabidopsis WRKY6 Transcription Factor Acts as a Positive Regulator of Absciscic Acid Signaling during Seed Germination and Early Seedling Development. In *PLoS genetics* 12 (2), e1005833. DOI: 10.1371/journal.pgen.1005833.

Jin, Jinpu; Tian, Feng; Yang, De-Chang; Meng, Yu-Qi; Kong, Lei; Luo, Jingchu; Gao, Ge (2017): PlantTFDB 4.0: toward a central hub for transcription factors and regulatory interactions in plants. In *Nucleic acids research* 45 (D1), D1040-D1045. DOI: 10.1093/nar/gkw982.

Kabbage, Mehdi; Yarden, Oded; Dickman, Martin B. (2015): Pathogenic attributes of *Sclerotinia sclerotiorum* : Switching from a biotrophic to necrotrophic lifestyle. In *Plant Science* 233, pp. 53–60. DOI: 10.1016/j.plantsci.2014.12.018.

Kaur, Bhavjot; Bhatia, Dharminder; Mavi, G. S. (2021): Eighty years of gene-for-gene relationship and its applications in identification and utilization of R genes. In *J Genet* 100 (2). DOI: 10.1007/s12041-021-01300-7.

Le, Mi Ha; Cao, Yangrong; Zhang, Xue-Cheng; Stacey, Gary (2014): LIK1, a CERK1-interacting kinase, regulates plant immune responses in Arabidopsis. In *PLoS one* 9 (7), e102245. DOI: 10.1371/journal.pone.0102245.

Leisen, Thomas; Werner, Janina; Pattar, Patrick; Safari, Nassim; Ymeri, Edit; Sommer, Frederik et al. (2022): Multiple knockout mutants reveal a high redundancy of phytotoxic compounds contributing to necrotrophic pathogenesis of *Botrytis cinerea*. In *PLoS pathogens* 18 (3), e1010367. DOI: 10.1371/journal.ppat.1010367.

Lewis, Laura A.; Polanski, Krzysztof; Torres-Zabala, Marta de; Jayaraman, Siddharth; Bowden, Laura; Moore, Jonathan et al. (2015): Transcriptional Dynamics Driving MAMP-Triggered Immunity and Pathogen Effector-Mediated Immunosuppression in Arabidopsis Leaves Following Infection with *Pseudomonas syringae* pv tomato DC3000. In *The Plant cell* 27 (11), pp. 3038–3064. DOI: 10.1105/tpc.15.00471.

Li, Bo; Meng, Xiangzong; Shan, Libo; He, Ping (2016): Transcriptional Regulation of Pattern-Triggered Immunity in Plants. In *Cell host & microbe* 19 (5), pp. 641–650. DOI: 10.1016/j.chom.2016.04.011.

Lin, Li; Zhang, Xingrui; Fan, Jialin; Li, Jiawei; Ren, Sichao; Gu, Xin et al. (2024): Natural variation in BnaA07.MKK9 confers resistance to *Sclerotinia* stem rot in oilseed rape. In *Nature communications* 15 (1), p. 5059. DOI: 10.1038/s41467-024-49504-6.

López, Walter Ricardo; Garcia-Jaramillo, Dora Janeth; Ceballos-Aguirre, Nelson; Castaño-Zapata, Jairo; Acuña-Zornosa, Ricardo; Jovel, Juan (2021): Transcriptional responses to *Fusarium oxysporum* f. sp. *lycopersici* (Sacc.)

- Snyder & Hansen infection in three Colombian tomato cultivars. In *BMC plant biology* 21 (1), p. 412. DOI: 10.1186/s12870-021-03187-z.
- Love, Michael I.; Huber, Wolfgang; Anders, Simon (2014): Moderated estimation of fold change and dispersion for RNA-seq data with DESeq2. In *Genome biology* 15 (12), p. 550. DOI: 10.1186/s13059-014-0550-8.
- Luna, Estrella; Bruce, Toby J. A.; Roberts, Michael R.; Flors, Victor; Ton, Jurriaan (2012): Next-generation systemic acquired resistance. In *Plant physiology* 158 (2), pp. 844–853. DOI: 10.1104/pp.111.187468.
- Madar, Daniel; Dekel, Erez; Bren, Anat; Zimmer, Anat; Porat, Ziv; Alon, Uri (2013): Promoter activity dynamics in the lag phase of Escherichia coli. In *BMC systems biology* 7, p. 136. DOI: 10.1186/1752-0509-7-136.
- Martín-Dacal, Marina; Fernández-Calvo, Patricia; Jiménez-Sandoval, Pedro; López, Gemma; Garrido-Arandía, María; Rebaque, Diego et al. (2023): Arabidopsis immune responses triggered by cellulose- and mixed-linked glucan-derived oligosaccharides require a group of leucine-rich repeat lectin receptor kinases. In *The Plant journal : for cell and molecular biology* 113 (4), pp. 833–850. DOI: 10.1111/tpj.16088.
- Mbengue, Malick; Navaud, Olivier; Peyraud, Rémi; Barascud, Marielle; Badet, Thomas; Vincent, Rémy et al. (2016): Emerging Trends in Molecular Interactions between Plants and the Broad Host Range Fungal Pathogens Botrytis cinerea and Sclerotinia sclerotiorum. In *Frontiers in plant science* 7, p. 422. DOI: 10.3389/fpls.2016.00422.
- McDowell, Ian C.; Manandhar, Dinesh; Vockley, Christopher M.; Schmid, Amy K.; Reddy, Timothy E.; Engelhardt, Barbara E. (2018): Clustering gene expression time series data using an infinite Gaussian process mixture model. In *PLoS computational biology* 14 (1), e1005896. DOI: 10.1371/journal.pcbi.1005896.
- Miao, Shuang; Liu, Jiuer; Guo, Jianhang; Li, Jian-Feng (2020): Engineering plants to secrete affinity-tagged pathogen elicitors for deciphering immune receptor complex or inducing enhanced immunity. In *Journal of integrative plant biology* 62 (6), pp. 761–776. DOI: 10.1111/jipb.12859.
- Murchie, E. H.; Lawson, T. (2013): Chlorophyll fluorescence analysis: a guide to good practice and understanding some new applications. In *Journal of experimental botany* 64 (13), pp. 3983–3998. DOI: 10.1093/jxb/ert208.
- Niu, Fangfang; Cui, Xing; Yang, Bo; Wang, Rui; Zhao, Peiyu; Zhao, Xinjie et al. (2024): WRKY6 transcription factor modulates root potassium acquisition through promoting expression of AKT1 in Arabidopsis. In *The Plant journal : for cell and molecular biology* 118 (5), pp. 1652–1667. DOI: 10.1111/tpj.16703.
- Poland, Jesse A.; Balint-Kurti, Peter J.; Wissner, Randall J.; Pratt, Richard C.; Nelson, Rebecca J. (2009): Shades of gray: the world of quantitative disease resistance. In *Trends in plant science* 14 (1), pp. 21–29. DOI: 10.1016/j.tplants.2008.10.006.
- Que, Youxiong; Su, Yachun; Guo, Jinlong; Wu, Qibin; Xu, Liping (2014): A global view of transcriptome dynamics during Sporisorium scitamineum challenge in sugarcane by RNA-Seq. In *PloS one* 9 (8), e106476. DOI: 10.1371/journal.pone.0106476.
- Ranjan, Ashish; Westrick, Nathaniel M.; Jain, Sachin; Piotrowski, Jeff S.; Ranjan, Manish; Kessens, Ryan et al. (2019): Resistance against Sclerotinia sclerotiorum in soybean involves a reprogramming of the phenylpropanoid pathway and up-regulation of antifungal activity targeting ergosterol biosynthesis. In *Plant biotechnology journal* 17 (8), pp. 1567–1581. DOI: 10.1111/pbi.13082.
- Roux, Fabrice; Voisin, Derry; Badet, Thomas; Balagué, Claudine; Barlet, Xavier; Huard-Chauveau, Carine et al. (2014): Resistance to phytopathogens e tutti quanti: placing plant quantitative disease resistance on the map. In *Molecular plant pathology* 15 (5), pp. 427–432. DOI: 10.1111/mpp.12138.
- Seifbarghi, Shirin; Borhan, M. Hossein; Wei, Yangdou; Coutu, Cathy; Robinson, Stephen J.; Hegedus, Dwayne D. (2017): Changes in the Sclerotinia sclerotiorum transcriptome during infection of Brassica napus. In *BMC genomics* 18 (1), p. 266. DOI: 10.1186/s12864-017-3642-5.
- Sperfeld, Martin; Narváez-Barragán, Delia A.; Malitsky, Sergey; Frydman, Veronica; Yuda, Lilach; Rocha, Jorge; Segev, Einat (2024): Algal methylated compounds shorten the lag phase of Phaeobacter inhibens bacteria. In *Nature microbiology* 9 (8), pp. 2006–2021. DOI: 10.1038/s41564-024-01742-6.

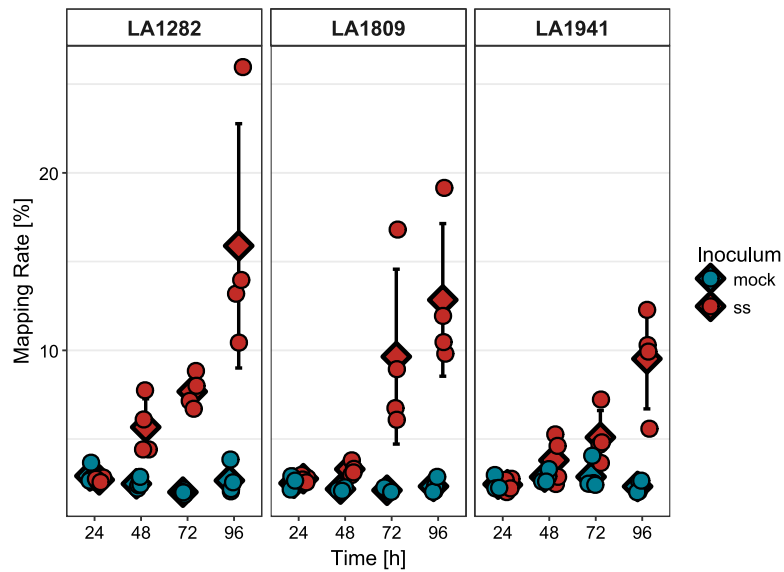
- Stam, Remco; McDonald, Bruce A. (2018): When resistance gene pyramids are not durable-the role of pathogen diversity. In *Molecular plant pathology* 19 (3), pp. 521–524. DOI: 10.1111/mpp.12636.
- Sucher, Justine; Mbengue, Malick; Dresen, Axel; Barascud, Marielle; Didelon, Marie; Barbacci, Adelin; Raffaele, Sylvain (2020): Phylotranscriptomics of the Pentapetalae Reveals Frequent Regulatory Variation in Plant Local Responses to the Fungal Pathogen *Sclerotinia sclerotiorum*. In *The Plant cell* 32 (6), pp. 1820–1844. DOI: 10.1105/tpc.19.00806.
- Supek, Fran; Bošnjak, Matko; Škunca, Nives; Šmuc, Tomislav (2011): REVIGO summarizes and visualizes long lists of gene ontology terms. In *PloS one* 6 (7), e21800. DOI: 10.1371/journal.pone.0021800.
- Tang, X.; Xie, M.; Kim, Y. J.; Zhou, J.; Klessig, D. F.; Martin, G. B. (1999): Overexpression of Pto activates defense responses and confers broad resistance. In *The Plant cell* 11 (1), pp. 15–29. DOI: 10.1105/tpc.11.1.15.
- The UniProt Consortium (2025): UniProt: the Universal Protein Knowledgebase in 2025. In *Nucleic acids research* 53 (D1), D609–D617. DOI: 10.1093/nar/gkaf1010.
- Tominello-Ramirez, Christopher S.; Muñoz Hoyos, Lina; Oubounyt, Mhaned; Stam, Remco (2024): Network analyses predict major regulators of resistance to early blight disease complex in tomato. In *BMC plant biology* 24 (1), p. 641. DOI: 10.1186/s12870-024-05366-0.
- Törönen, Petri; Holm, Liisa (2022): PANNZER-A practical tool for protein function prediction. In *Protein science : a publication of the Protein Society* 31 (1), pp. 118–128. DOI: 10.1002/pro.4193.
- Wang, Zheng; Fang, Hedi; Chen, Yu; Chen, Keping; Li, Guanying; Gu, Shoulai; Tan, Xiaoli (2014): Overexpression of BnWRKY33 in oilseed rape enhances resistance to *Sclerotinia sclerotiorum*. In *Molecular plant pathology* 15 (7), pp. 677–689. DOI: 10.1111/mpp.12123.
- Wei, Lijuan; Jian, Hongju; Lu, Kun; Filardo, Fiona; Yin, Nengwen; Liu, Liezhao et al. (2016): Genome-wide association analysis and differential expression analysis of resistance to *Sclerotinia stem rot* in *Brassica napus*. In *Plant biotechnology journal* 14 (6), pp. 1368–1380. DOI: 10.1111/pbi.12501.
- Westrick, Nathaniel M.; Ranjan, Ashish; Jain, Sachin; Grau, Craig R.; Smith, Damon L.; Kabbage, Mehdi (2019): Gene regulation of *Sclerotinia sclerotiorum* during infection of *Glycine max*: on the road to pathogenesis. In *BMC genomics* 20 (1), p. 157. DOI: 10.1186/s12864-019-5517-4.
- Wu, Jian; Zhao, Qing; Yang, Qingyong; Liu, Han; Li, Qingyuan; Yi, Xinqi et al. (2016): Comparative transcriptomic analysis uncovers the complex genetic network for resistance to *Sclerotinia sclerotiorum* in *Brassica napus*. In *Scientific reports* 6, p. 19007. DOI: 10.1038/srep19007.
- Xia, Qian; Tang, Hao; Fu, Lijiang; Tan, Jinglu; Govindjee, Govindjee; Guo, Ya (2023): Determination of Fv/Fm from Chlorophyll a Fluorescence without Dark Adaptation by an LSSVM Model. In *Plant phenomics (Washington, D.C.)* 5, p. 34. DOI: 10.34133/plantphenomics.0034.
- Xu, Shuangbin; Hu, Erqiang; Cai, Yantong; Xie, Zijong; Luo, Xiao; Zhan, Li et al. (2024): Using clusterProfiler to characterize multiomics data. In *Nature protocols* 19 (11), pp. 3292–3320. DOI: 10.1038/s41596-024-01020-z.
- Xue, Yufei; Wang, Shanshan; Zhang, Qiheng; Wu, Fangzhou; Huang, Li; Qin, Shujun et al. (2024): *Brassica napus* cytochrome P450 superfamily: Origin from parental species and involvement in diseases resistance, abiotic stresses tolerance, and seed quality traits. In *Ecotoxicology and environmental safety* 283, p. 116792. DOI: 10.1016/j.ecoenv.2024.116792.
- Yang, Xu; Guo, Shaomin; Jin, Hairun; Zhang, Jinze; Xiao, Lijing; Ouyang, Qingjing et al. (2025): Genome-wide identification and characterization of transcription factors involved in defense responses against *Sclerotinia sclerotiorum* in *Brassica juncea*. In *Scientific reports* 15 (1), p. 4341. DOI: 10.1038/s41598-025-89054-5.
- Zhang, Ming-Zhe; Sun, Chen-Hao; Liu, Yue; Feng, Hui-Qiang; Chang, Hao-Wu; Cao, Sheng-Nan et al. (2020): Transcriptome analysis and functional validation reveal a novel gene, BcCGF1, that enhances fungal virulence by promoting infection-related development and host penetration. In *Molecular plant pathology* 21 (6), pp. 834–853. DOI: 10.1111/mpp.12934.

Zhang, S.; Klessig, D. F. (2001): MAPK cascades in plant defense signaling. In *Trends in plant science* 6 (11), pp. 520–527. DOI: 10.1016/s1360-1385(01)02103-3.

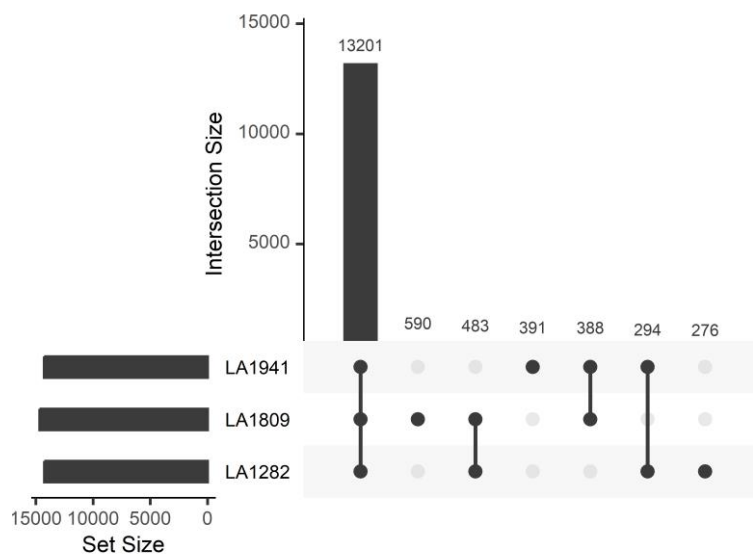
Zhang, Yu; Wang, Yuexing; Zhou, Wanying; Zheng, Shimao; Ye, Runzhou (2022): Detection of candidate gene networks involved in resistance to *Sclerotinia sclerotiorum* in soybean. In *Journal of applied genetics* 63 (1), pp. 1–14. DOI: 10.1007/s13353-021-00654-z.

Zhao, Mingzhu; Yi, Bing; Liu, Xiaohong; Wang, Dexing; Song, Dianxiu; Sun, Enyu et al. (2024): Comparative transcriptome analysis in two contrasting genotypes for *Sclerotinia sclerotiorum* resistance in sunflower. In *PloS one* 19 (12), e0315458. DOI: 10.1371/journal.pone.0315458.

Supplementary Material



Suppl. fig. 1: Mapping rate of fungal reads. Diamonds indicate the mean mapping rate per time point and treatment. Dots represent individual samples, and whiskers depict the standard deviation.



Suppl. fig. 2: Number of shared and uniquely expressed genes.

Suppl. Table 1 DEGs 48 hpi, LA1282 inf-mock

GeneID	L2FC	padj	Putative Function
Sopen08g009740	4.296	0.0004	LOX1
Sopen08g008720	4.276	0.0007	Sopen08g008720
Sopen08g008720	4.276	0.0007	Sopen08g008720
Sopen01g001520	4.228	0.0039	NAD(P)-binding Rossmann-fold superfamily protein
Sopen02g031830	3.959	0.0046	DOX1
Sopen12g023430	3.601	0.0007	Sopen12g023430
Sopen10g033140	3.365	0.0046	CytochromeP450 (Sopen10g033140)
Sopen04g012680	3.146	0.0123	Glutamatedecarboxylase
Sopen09g028060	3.115	0.0123	ERF
Sopen04g026840	3.044	0.0136	Pathogen-related protein
Sopen06g011740	3.028	0.0080	Oxalate--CoAligase
Sopen01g051340	2.927	0.0139	divinylether synthase
Sopen09g036010	2.868	0.0146	Glycosyltransferase
Sopen02g037820	2.709	0.0122	CCoAOMT1 (Sopen02g037820)
g.plus_peak_18795	2.656	0.0175	g.plus_peak_18795
Sopen01g026150	2.647	0.0080	beta-1,3-endoglucanase (Sopen01g026150)
Sopen10g028890	2.614	0.0185	CytochromeP450 (Sopen10g028890)
Sopen04g029490	2.546	0.0099	DAHPsynthase 2 precursor
Sopen03g007540	2.509	0.0122	no symbol available (Sopen03g007540)
Sopen03g007540	2.509	0.0122	no symbol available (Sopen03g007540)
Sopen12g023420	2.446	0.0080	Sopen12g023420
Sopen02g031030	2.432	0.0139	Sopen02g031030
Sopen02g031030	2.432	0.0139	Sopen02g031030
Sopen11g027650	2.373	0.0221	PUB24
Sopen10g028130	2.337	0.0122	Ammoniumtransporter
Sopen07g024910	2.305	0.0038	EF501822(Sopen07g024910)
Sopen01g002940	2.292	0.0122	syntaxin-121-like
Sopen03g029450	2.262	0.0185	Bioticcell death-associated protein
Sopen08g023280	2.227	0.0221	Polyphenoloxidase
Sopen03g041120	2.117	0.0207	CytochromeP450 (Sopen03g041120)
Sopen09g033940	2.040	0.0139	Majorallergen Pru ar.1 (Sopen09g033940)
Sopen12g034850	2.020	0.0267	Fattyacid desaturase
Sopen04g025580	2.002	0.0080	Sopen04g025580
Sopen01g026160	1.994	0.0080	Sopen01g026160
Sopen12g021540	1.909	0.0164	Sopen12g021540
Sopen03g033590	1.859	0.0221	ENO1
Sopen12g032770	1.858	0.0292	Majorallergen Pru ar.1 (Sopen12g032770)
Sopen10g032770	1.818	0.0330	AtCWIN2, AtcwINV2, CWINV2
Sopen01g046060	1.817	0.0221	Alpha/beta-Hydrolasessuperfamily protein
Sopen03g033250	1.814	0.0122	Sopen03g033250
Sopen11g009900	1.807	0.0252	Peroxidase
Sopen07g024490	1.800	0.0221	Cytochromeb5.1
Sopen04g028240	1.703	0.0340	WRKY51
Sopen10g034420	1.686	0.0102	GlutathioneS-transferase
Sopen08g028940	1.683	0.0207	Serineprotease inhibitor, potato inhibitor I-type family protein
Sopen08g022430	1.682	0.0340	aromaticamino acid decarboxylase 2
Sopen08g028950	1.675	0.0090	OSM34
Sopen08g023580	1.631	0.0340	UDP-Glycosyltransferasesuperfamily protein
Sopen05g011470	1.630	0.0292	WRKY45
Sopen05g004840	1.547	0.0221	Glycosyl transferase, family 14
Sopen01g033730	1.542	0.0357	Probable magnesium transporter
Sopen03g041450	1.541	0.0355	RING/U-boxsuperfamily protein
Sopen12g034880	1.540	0.0368	CER1-L1
Sopen01g048960	1.529	0.0340	PR-1 protein 38 (Sopen01g048960)

Sopen08g025910	1.514	0.0207	Sopen08g025910
Sopen01g040940	1.497	0.0080	PR4 (Sopen01g040940)
Sopen03g029570	1.465	0.0389	Proteinase inhibitor II
Sopen05g029280	1.457	0.0292	Phosphoglyceratemutase family protein
Sopen01g026170	1.433	0.0102	beta-1,3-endoglucanase (Sopen01g026170)
Sopen09g034580	1.415	0.0262	ABCG39
Sopen08g022500	1.366	0.0221	Tyraminen-hydroxycinnamoyl transferase
Sopen03g028580	1.348	0.0340	Phosphatecarrier protein, mitochondrial
Sopen02g037830	1.331	0.0340	CCoAOMT1 (Sopen02g037830)
Sopen10g034470	1.310	0.0357	no symbol available (Sopen10g034470)
Sopen10g034470	1.310	0.0357	no symbol available (Sopen10g034470)
Sopen01g044660	1.279	0.0340	TPS20
Sopen12g029340	1.227	0.0500	Alpha/beta-hydrolasessuperfamily protein
Sopen01g048970	1.211	0.0162	PR-1 protein 38 (Sopen01g048970)
Sopen05g004580	1.210	0.0207	Lipidphosphate phosphatase.1
Sopen05g004580	1.210	0.0207	Lipidphosphate phosphatase.1
Sopen01g034780	1.190	0.0364	Subtilisin-likeprotease
Sopen01g040950	1.168	0.0137	PR4 (Sopen01g040950)
Sopen01g040950	1.168	0.0137	PR4 (Sopen01g040950)
Sopen07g001220	1.123	0.0448	Chitinase
Sopen09g006690	1.103	0.0500	Sopen09g006690
Sopen07g024880	1.031	0.0221	EF501822(Sopen07g024880)
Sopen11g001970	1.006	0.0500	CMPG1, ATCMPG1

Suppl. Tab. 2: DEGs LA1941, 48 hpi inf vs mock

GeneID	L2FC	padj	funct_unique
Sopen03g039350	1.43	0.003	Sopen03g039350
Sopen03g040350	-1.25	0.002	beta-galactosidase3
Sopen04g001120	1.81	0.000	MYBD
Sopen04g024830	1.15	0.003	PLAT3
Sopen04g027010	2.02	0.001	EXT3
Sopen04g035160	1.81	0.001	Thaumatococcus-likeprotein.1
Sopen06g024710	-1.58	0.000	OXS3
Sopen08g022270	1.03	0.005	MFP-a
Sopen09g004270	1.21	0.002	Alpha/beta-Hydrolasessuperfamily protein
Sopen09g032860	1.05	0.003	ERF1B
Sopen10g001910	1.22	0.001	FLA2

Suppl. Tab. 3: GSEA LA1809, 48hpi

ID	Description	NES	p.adjust	setSize
GO:0006412	translation	4.050	0.0001	113
GO:0002181	cytoplasmic translation	4.033	0.0001	24
GO:0002191	cap-dependent translational initiation	3.821	0.0001	25
GO:0000028	ribosomal small subunit assembly	3.799	0.0001	161
GO:0016226	iron-sulfur cluster assembly	3.492	0.0002	22
GO:0006520	amino acid metabolic process	3.246	0.0010	13
GO:0006570	tyrosine metabolic process	3.009	0.0003	52
GO:0006414	translational elongation	2.976	0.0022	32
GO:0006112	energy reserve metabolic process	2.888	0.0016	41
GO:0006734	NADH metabolic process	2.842	0.0160	17
GO:0006457	protein folding	2.823	0.0001	103
GO:0042254	ribosome biogenesis	2.809	0.0019	60
GO:1900864	mitochondrial RNA modification	2.792	0.0207	21
GO:0006760	folic acid-containing compound metabolic process	2.676	0.0083	45
GO:0032988	protein-RNA complex disassembly	2.596	0.0307	29
GO:0006913	nucleocytoplasmic transport	2.438	0.0092	74
GO:0006227	dUDP biosynthetic process	2.324	0.0470	60

Suppl. Tab. 4: GSEA LA1941, 48hpi

ID	Description	NES	p.adjust	setSize
GO:0002181	cytoplasmic translation	3.238	0.026	21
GO:0007018	microtubule-based movement	3.104	0.026	16
GO:0006952	defense response	2.928	0.008	83

Suppl. Tab. 5: cRLP-Genes with differential expression between LA1282 and LA1809 in basal conditions (24hpi mock).

GeneID	log2FoldChange	padj
Sopen01g002540	2.425	0.0110
Sopen06g003150	2.095	0.0002
Sopen01g001720	1.466	0.0180
Sopen05g005800	-1.113	0.0135
Sopen01g001870	-1.266	0.0247
Sopen01g042220	-2.552	0.0103
Sopen06g014090	-4.597	0.0000

Suppl. Tab. 6: RLK-Genes with differential expression between LA1282 and LA1809 in basal conditions (24hpi mock).

GeneID	baseMean	log2FoldChange	padj
Sopen02g020810	17.1486	3.8109	0.0000
Sopen06g002020	9.8637	2.4009	0.0000
Sopen01g048860	19.3616	2.2068	0.0010
Sopen12g032540	9.8612	1.8516	0.0017
Sopen01g028710	9.1444	1.7339	0.0076
Sopen08g019890	69.3694	1.5467	0.0002
Sopen01g047490	94.4411	1.1532	0.0002
Sopen03g030900	32.0974	1.0801	0.0128
Sopen05g009260	10.0071	-1.0246	0.0073
Sopen05g030910	9.1162	-1.1905	0.0042
Sopen02g036420	67.9849	-1.2143	0.0000
Sopen06g030490	4.3565	-1.3392	0.0249
Sopen08g020310	27.3608	-1.3694	0.0003
Sopen10g029820	3.9187	-1.5135	0.0135
Sopen02g037670	1.9612	-1.5981	0.0368
Sopen04g003810	3.5426	-1.6662	0.0184
Sopen03g001960	5.2876	-1.9929	0.0078
Sopen08g017000	10.9703	-2.3844	0.0002
Sopen11g001980	13.4983	-2.5488	0.0001
Sopen08g020090	3.0906	-2.6146	0.0079

Suppl. Tab. 7: PTI-Genes with differential expression between LA1282 and LA1809 in basal conditions (24hpi mock).

gene	geneID	baseMean	L2FC	padj
cerk1.3	Sopen07g025160	62.3909767014575	1.091	0.000
bak.1	Sopen01g047490	94.4411297319458	1.153	0.000

Suppl. Tab. 8: Edgewise between all focal DEGs and the GRN hub WRKY6

regulatoryGene	targetGene	weight
Sopen02g011350	Sopen08g009740	0.028360696
Sopen02g011350	Sopen01g026150	0.028051527
Sopen02g011350	Sopen08g023280	0.026719102
Sopen02g011350	Sopen02g031830	0.02569113
Sopen02g011350	Sopen12g021540	0.025036
Sopen02g011350	Sopen01g044660	0.023434218
Sopen02g011350	Sopen08g023580	0.023399628
Sopen02g011350	Sopen01g046060	0.022046422
Sopen02g011350	Sopen07g024910	0.021682299
Sopen02g011350	Sopen04g025580	0.021600303
Sopen02g011350	Sopen05g029280	0.021274326
Sopen02g011350	Sopen03g033250	0.020913354
Sopen02g011350	Sopen03g041450	0.020645404
Sopen02g011350	Sopen10g034420	0.019906255
Sopen02g011350	Sopen04g029490	0.019795622
Sopen02g011350	Sopen12g034850	0.019026858
Sopen02g011350	Sopen07g024880	0.018282362
Sopen02g011350	Sopen03g028580	0.01742883
Sopen02g011350	Sopen09g036010	0.017111209
Sopen02g011350	Sopen12g032770	0.016996095
Sopen02g011350	Sopen03g029570	0.016597635
Sopen02g011350	Sopen01g040950	0.016414153
Sopen02g011350	Sopen01g001520	0.016053445
Sopen02g011350	Sopen08g008720	0.015724586
Sopen02g011350	Sopen01g048960	0.015687376
Sopen02g011350	Sopen01g040940	0.015633476
Sopen02g011350	Sopen05g004840	0.015351446
Sopen02g011350	Sopen01g034780	0.014946166
Sopen02g011350	Sopen08g022500	0.014828637
Sopen02g011350	Sopen01g033730	0.014503793
Sopen02g011350	Sopen04g012680	0.013928743
Sopen02g011350	Sopen03g007540	0.013856238
Sopen02g011350	Sopen09g028060	0.013665484
Sopen02g011350	Sopen01g026170	0.0136052
Sopen02g011350	Sopen01g026160	0.01340945
Sopen02g011350	Sopen08g028950	0.013371735
Sopen02g011350	Sopen07g024490	0.012750647
Sopen02g011350	Sopen04g026840	0.012431308
Sopen02g011350	Sopen02g031030	0.012424489
Sopen02g011350	Sopen04g028240	0.012364526
Sopen02g011350	Sopen01g048970	0.012256411
Sopen02g011350	Sopen07g001220	0.012173157
Sopen02g011350	Sopen01g002940	0.012161811
Sopen02g011350	Sopen08g025910	0.012129958
Sopen02g011350	Sopen11g027650	0.012106668
Sopen02g011350	Sopen05g011470	0.011980095
Sopen02g011350	Sopen03g033590	0.011918254
Sopen02g011350	Sopen12g034880	0.011818788
Sopen02g011350	Sopen02g037830	0.011766374
Sopen02g011350	Sopen10g028130	0.011642719
Sopen02g011350	Sopen02g037820	0.011336435
Sopen02g011350	Sopen01g051340	0.0109734
Sopen02g011350	Sopen10g033140	0.010961717
Sopen02g011350	Sopen10g032770	0.010744659

Sopen02g011350	Sopen09g034580	0.010057291
Sopen02g011350	Sopen06g011740	0.010051028
Sopen02g011350	g.plus_peak_18795	0.009756631
Sopen02g011350	Sopen11g009900	0.009656683
Sopen02g011350	Sopen09g033940	0.008887826
Sopen02g011350	Sopen08g022430	0.008757446
Sopen02g011350	Sopen03g029450	0.008587933
Sopen02g011350	Sopen12g029340	0.008311617
Sopen02g011350	Sopen12g023430	0.008074835
Sopen02g011350	Sopen10g028890	0.007815482
Sopen02g011350	Sopen12g023420	0.007661805
Sopen02g011350	Sopen05g004580	0.007359228
Sopen02g011350	Sopen11g001970	0.006641716
Sopen02g011350	Sopen03g041120	0.006346855
Sopen02g011350	Sopen08g028940	0.005798289
Sopen02g011350	Sopen10g034470	0.005191843

Suppl. Tab. 9: Focal Degs basal Expression 24 hpi mock, LA1282 vs. LA1809

GeneID	L2FC	padj	DEG	funct_unique
Sopen01g048970	7.285	2.848E-31	DEG	PR-1 protein 38 (Sopen01g048970)
Sopen03g029570	7.154	1.463E-11	DEG	Proteinase inhibitor II
Sopen08g028950	6.800	1.443E-19	DEG	OSM34
Sopen01g026150	5.878	3.160E-07	DEG	beta-1,3-endoglucanase (Sopen01g026150)
Sopen01g026170	5.835	1.093E-20	DEG	beta-1,3-endoglucanase (Sopen01g026170)
Sopen01g048960	5.388	1.213E-05	DEG	PR-1 protein 38 (Sopen01g048960)
Sopen08g009740	5.324	4.281E-06	DEG	LOX1
Sopen01g026160	5.253	8.686E-12	DEG	Sopen01g026160
Sopen12g034850	5.250	3.094E-05	DEG	Fattyacid desaturase
Sopen08g023280	5.203	1.094E-05	DEG	Polyphenoloxidase
Sopen03g033250	5.034	2.125E-11	DEG	Sopen03g033250
Sopen02g031830	4.470	9.971E-05	DEG	DOX1
Sopen04g025580	4.386	4.013E-08	DEG	Sopen04g025580
Sopen10g028890	4.361	1.105E-04	DEG	CytochromeP450 (Sopen10g028890)
Sopen08g028940	4.248	2.884E-06	DEG	Serineprotease inhibitor, potato inhibitor I-type family protein
Sopen01g040940	4.049	6.416E-13	DEG	PR4 (Sopen01g040940)
Sopen07g024490	3.691	7.150E-05	DEG	Cytochrome b5.1
Sopen09g034580	3.608	1.487E-06	DEG	ABCG39
Sopen03g028580	3.591	1.924E-05	DEG	Phosphatecarrier protein, mitochondrial
Sopen02g031030	3.439	8.870E-04	DEG	Sopen02g031030
Sopen10g034420	3.423	6.974E-09	DEG	GlutathioneS-transferase
Sopen01g034780	3.376	5.176E-07	DEG	Subtilisin-likeprotease
Sopen01g040950	3.276	8.685E-13	DEG	PR4 (Sopen01g040950)
Sopen01g051340	3.123	5.724E-03	DEG	divinylether synthase
Sopen09g028060	3.104	4.198E-03	DEG	ERF
Sopen12g029340	3.090	9.639E-04	DEG	Alpha/beta-hydrolasessuperfamily protein
Sopen03g029450	3.030	1.547E-03	DEG	Bioticcell death-associated protein
Sopen05g011470	3.013	2.269E-04	DEG	WRKY45
Sopen12g034880	2.956	2.449E-03	DEG	CER1-L1
Sopen10g032770	2.791	2.245E-03	DEG	AtCWIN2, AtcwINV2, CWINV2
Sopen08g008720	2.696	1.478E-03	DEG	Sopen08g008720
Sopen01g046060	2.692	1.659E-04	DEG	Alpha/beta-Hydrolasessuperfamily protein
Sopen04g026840	2.656	5.135E-03	DEG	Pathogen-relatedprotein
Sopen08g022430	2.564	6.495E-03	DEG	aromaticamino acid decarboxylase 2

Sopen11g009900	2.518	1.355E-03	DEG	Peroxidase
Sopen02g037830	2.410	7.291E-04	DEG	CCoAOMT1 (Sopen02g037830)
Sopen01g002940	2.301	2.944E-03	DEG	syntaxin-121-like
Sopen09g036010	2.281	1.074E-02	DEG	Glycosyltransferase
Sopen04g012680	2.205	7.548E-03	DEG	Glutamatedecarboxylase
Sopen10g033140	2.193	7.211E-03	DEG	CytochromeP450 (Sopen10g033140)
Sopen06g011740	2.179	4.220E-03	DEG	Oxalate--CoAligase
Sopen10g028130	2.160	2.367E-03	DEG	Ammoniumtransporter
Sopen05g004580	2.160	7.142E-07	DEG	Lipidphosphate phosphatase.1
Sopen03g041450	2.101	1.167E-02	DEG	RING/U-boxsuperfamily protein
Sopen03g007540	1.859	1.741E-02	DEG	no symbol available (Sopen03g007540)
Sopen12g032770	1.799	1.221E-02	DEG	Majorallergen Pru ar.1 (Sopen12g032770)
Sopen08g022500	1.782	6.362E-03	DEG	Tyraminen-hydroxycinnamoyl transferase
Sopen02g037820	1.769	1.656E-02	DEG	CCoAOMT1 (Sopen02g037820)
Sopen11g001970	1.723	1.792E-02	DEG	CMPG1, ATCMPG1
Sopen12g021540	1.604	7.014E-03	DEG	Sopen12g021540
Sopen01g044660	1.589	4.343E-02	DEG	TPS20
Sopen07g001220	1.513	2.222E-02	DEG	Chitinase
Sopen12g023420	1.437	1.756E-02	DEG	NA
Sopen09g006690	1.420	2.016E-02	DEG	Sopen09g006690
Sopen04g029490	1.343	1.350E-02	DEG	DAHPsynthase 2 precursor
Sopen07g024880	1.266	1.743E-03	DEG	EF501822(Sopen07g024880)
Sopen11g027650	1.185	5.776E-02	Not DEG	PUB24
Sopen04g028240	1.166	6.052E-02	Not DEG	WRKY51
Sopen03g041120	1.001	5.923E-02	Not DEG	CytochromeP450 (Sopen03g041120)
Sopen10g034470	0.998	4.959E-02	Not DEG	no symbol available (Sopen10g034470)
Sopen05g004840	0.912	8.509E-02	Not DEG	Glycosyl transferase, family 14
Sopen01g033730	0.854	1.083E-01	Not DEG	Probable magnesium transporter
g.plus_peak_18795	0.845	1.553E-01	Not DEG	g.plus_peak_18795
Sopen09g033940	0.825	9.174E-02	Not DEG	Majorallergen Pru ar.1 (Sopen09g033940)
Sopen08g025910	0.745	8.043E-02	Not DEG	Sopen08g025910
Sopen12g023430	0.667	1.580E-01	Not DEG	NA
Sopen01g001520	0.660	2.302E-01	Not DEG	NAD(P)-bindingRossmann-fold superfamily protein
Sopen07g024910	0.570	2.105E-01	Not DEG	EF501822(Sopen07g024910)
Sopen08g023580	0.569	2.232E-01	Not DEG	UDP-Glycosyltransferasesuperfamily protein
Sopen03g033590	0.421	3.939E-01	Not DEG	ENO1
Sopen05g029280	0.025	1.000E+00	Not DEG	Phosphoglyceratemutase family protein



Discussion

General Discussion and Outlook

The goal of this dissertation is to unravel the regulatory backbone of QDR and characterise its evolution. To achieve this, I tested three core hypotheses: a) QDR in wild tomato species emerges from species-specific defence strategies governed by independent biological mechanisms; b) high-level QDR is driven by complex gene networks subjected to lineage-specific evolutionary processes; and (c) temporal (longitudinal) variation in gene expression modulates QDR, highlighting the importance of both timing and the preformation of regulatory elements. These hypotheses were addressed through three analytical approaches, encompassing high-resolution phenotyping, gene expression profiling, and evolutionary network analyses.

QDR Diversity in Wild Pathosystems

Early modelling in plant disease epidemiology generally assumed that lesion development followed sigmoidal growth dynamics with constant expansion rates (Berger et al. 1997; Waggoner and Rich 1981; Berger and Jones 1985). Since then, most subsequent research has prioritised incidence or severity as the principal phenotypic metric in QDR. However, the increased availability of (cost-effective) high throughput phenotyping technology led to an in-depth evaluation of lesion growth dynamics or disease progression, revealing high variability in factors like expansion rates (Anderegg et al. 2024; Barbacci et al. 2020; Einspanier et al. 2024; Navarro et al. 2024). In publication 1, I studied QDR severity as the correlation of independent phenotypes: infection frequency, lag-phase duration, and lesion doubling time. I observed a wide diversity of all QDR phenotypes across the panel, with no species particularly resistant in all tested parameters. While the overarching phenotypic diversity of the wild accessions was to be expected (see previous research on similar pathosystems in Stam et al. 2017; Kahlon et al. 2021; Schmey et al. 2023), I showed that QDR parameters might function independently of each other. Moreover, I used a model-based approach to illustrate that the severity of a lesion is dependent on the interaction between lag phase duration and LDT. Accordingly, I proposed that the orchestration of both underlies significant genotype specificity.

An Extended Model of QDR

Based on those findings, I define a refined model that separates QDR into discrete functional mechanisms whose interaction determines symptom severity. These mechanisms exceed the

simplistic one- or two-step infection models commonly derived from molecular studies, often leading to imprecise QDR estimations. Specifically, QDR can be divided into three major processes: (1) inhibition of initial infection (infection frequency, IF), (2) delay of disease onset (lag-phase duration), and (3) control over lesion expansion rate (lesion doubling time, LDT). Each step likely represents distinct molecular mechanisms derived through different evolutionary trajectories driven by modular genetic factors. It is, therefore, essential to study each infection stage independently to disentangle their underlying gene clusters, elucidate temporal interactions between host and pathogen, and better understand environmental influences, ultimately offering deeper insights into host-pathogen coevolution (Hall et al. 2017).

Infection frequency

A low infection frequency is one of the most widely recognised indicators of plant resistance. IF quantifies the ratio of successful infection events and depicts a binary trait. In my analysis, I observed substantial variation in IF across all tested species, which is similar to findings on *S. chilense* resistance to *P. infestans*, *Fusarium* spp., or *A. solani* (Stam et al. 2017; Schmey et al. 2023; Kahlon et al. 2021). I did not investigate the functional basis of IF variation in this study. However, it is known that infections often fail because structural and chemical barriers effectively block the penetration of non-pathogenic fungi (Yeats and Rose 2013). Moreover, the cuticle plays an important active role in the early host-parasite interaction, as shown for *A. thaliana* CUTE plants, which exhibit complete resistance to *B. cinerea* because of increased cuticle permeability that facilitates the release of fungitoxic compounds (Chassot et al. 2007; Reina-Pinto and Yephremov 2009; Serrano et al. 2014). The composition of secondary metabolites in the wax layer, including flavonoids and triterpenoids, varies among plant species and could explain the QDR diversity in our data (Serrano et al. 2014). Notably, the antifungal alkaloid trigonelline and its precursor nicotinic acid rapidly accumulate within hours of *A. alternata* infection in a resistant tomato cultivar (*S. lycopersicum* cv. Heinz, Muñoz Hoyos et al. 2024). These structural hurdles might be involved in the interaction with appressorium formation during early pathogenesis. Since no full *R*-gene-mediated resistance is recorded for *S. sclerotiorum*, I will not address the function of *R*-genes in IF.

Lag Phase Duration

Little is known about the genetic factors controlling lag-phase duration during necrotrophic infections, partly due to analytical challenges in distinguishing long lag phases from failed

infections. Unlike IF, which is a binary measure (infected vs. non-infected), lag-phase duration assumes that infection eventually occurs but is delayed. Supporting this distinction, my results (publication 1) showed no correlation between IF and lag-phase duration. While Barbacci et al. (2020) emphasised pathogen effects on lag duration, my study provides the first functional evidence that host genotype significantly influences this phenotype. I showed that a high-QDR host controls the lag-phase duration via a WRKY6-centered gene regulatory network. I also found elevated basal expression of receptor-like proteins and kinases, potentially enabling earlier pathogen perception (fig. 3, publication 3). In contrast, susceptible genotypes display delayed longitudinal gene expression changes. I speculate that those genotypes lack the necessary receptors to detect *S. sclerotiorum*-derived molecules. The later expression of defence genes may result from secondary signalling by the perception of damage-associated molecular patterns (DAMPs). Consequently, I argue that heightened basal expression of a WRKY6-centered GRN and receptor proteins, akin to a primed state, is decisive in determining lag-phase duration (fig. 3).

I propose that additional factors, such as the *S. sclerotiorum* virulence factor OA, influence lag-phase duration. OA plays a central role during early pathogenesis by initially suppressing early plant defences like ROS bursts and later promoting cell death through increased ROS production (Cessna et al. 2000; Williams et al. 2011). Numerous reports describe the relevance of OA metabolism in *S. sclerotiorum* resistance: OA-deficient fungal strains exhibit severely reduced virulence, and enhanced resistance to *S. sclerotiorum* is achieved by introducing oxalate oxidases or by overexpressing AtWRKY28 and AtWRKY75, both known to confer OA tolerance (Kabbage et al. 2013; Williams et al. 2011; Walz et al. 2008; Chen et al. 2013). Moreover, fungal genes regulating OA homeostasis underlie finetuned longitudinal regulation (Seifbarghi et al. 2017; Liang et al. 2015). In line with these findings, rapid regulatory responses in the resistant genotype LA1282 (publication 3) correlate with enhanced OA tolerance (see suppl. fig. 1). Hence, I conclude that lag phase duration is determined by processes involving pathogen recognition, swift defence response and possibly detoxification of OA.

Lesion Growth Rate

Once the fungus successfully establishes infection (i.e., infecting a sufficient number of host cells), rapid fungal biomass accumulation begins. Previous studies have demonstrated that the host genotype significantly influences lesion expansion rates (Barbacci et al., 2020; Eizner et al., 2017; Leclerc et al., 2023). For instance, the TIR-NBS-LRR family gene LAZ5 was recently

identified as an *S. sclerotiorum* susceptibility factor affecting LDT (Barbacci et al., 2020). As the LAZ5 knockout explained only about 30% of the phenotypic variation, the authors proposed that additional genetic or regulatory factors likely contribute to the slower lesion progression. My findings in publication 2 support this hypothesis, demonstrating that highly interconnected regulatory networks govern LDT. Specifically, I identified NAC29 as a central regulator of LDT in a high-QDR *S. pennellii* genotype. This TF is not QDR-associated in any other species. Changes in TF regulation and downstream signalling determine this unique role in QDR, confirming the hypothesis of divergent GRN rewiring. Indeed, network rewiring is increasingly recognised as a crucial component of QDR development (fig. 3, Didelon et al. 2024; Delplace et al. 2024; Delplace et al. 2020).

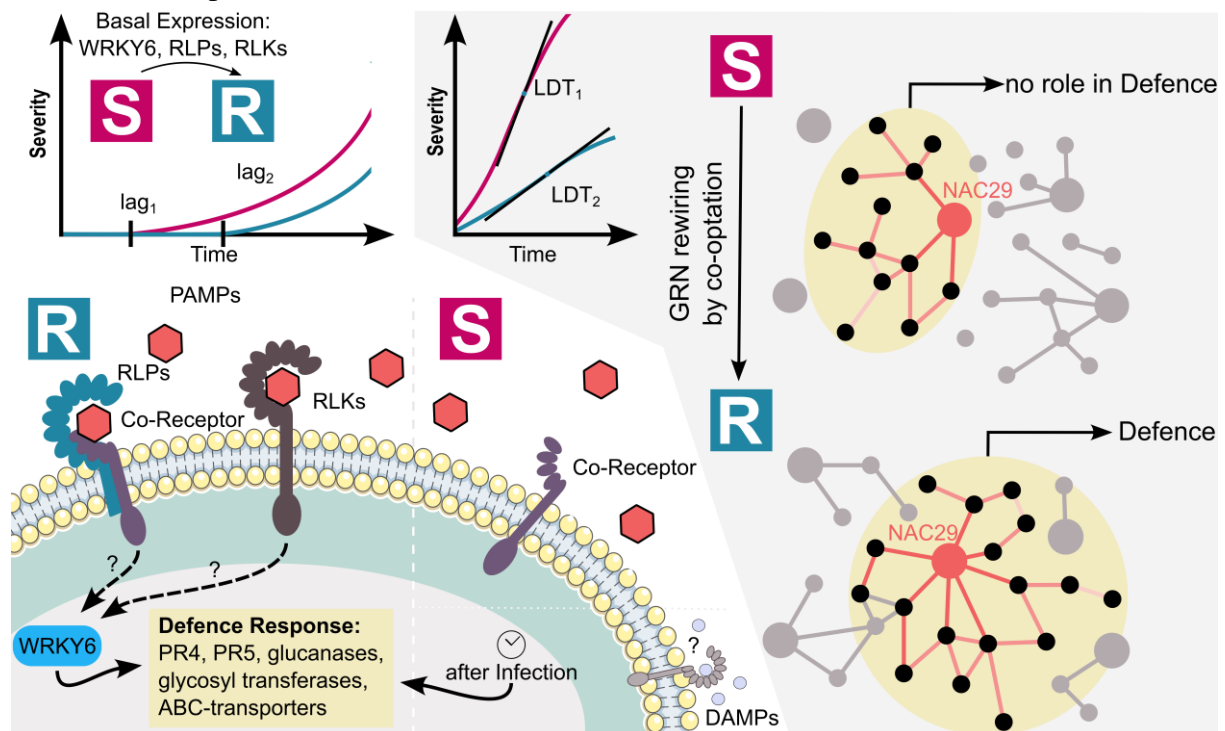


Figure 3: Overview of the main findings of this thesis. I performed gene expression profiling on genotypes with contrasting lag phase duration and LDT. A genotype characterised by a prolonged lag phase (**R**) shows a basal expression of key defence genes and rapidly induces those upon infection. These include the WRKY6 transcription factor, potentially acting as a core regulator controlling multiple defence genes. Moreover, the R-genotype is associated with basal expression of certain receptor-like proteins and kinases (RLPs and RLKs) and co-receptors. In this model, specific receptors detect pathogen-associated molecular patterns (PAMPs), triggering a finetuned defence response. By contrast, susceptible genotypes (**S**) lack specific receptors and basal expression of the core genes, leading to delayed activation of defensive pathways. This delayed activation may depend on pathways responding to damage-associated molecular patterns (DAMPs). Dashed arrows represent uncertain or hypothetical interactions. The degree of LDT-determined QDR is controlled by a complex GRN mediated by the NAC29 TF (grey shades). While susceptible genotypes (**S**) integrate the same genes into alternative network structures, resulting in neutral QDR, resistant genotypes (**R**) underwent network rewiring. Such topological changes introduce novel functional roles to the central transcription factors, exemplified by NAC29, and change the modularity of the GRN.

Implications of the QDR Model

In this study, I investigated host-plant-derived factors determining distinct QDR components. Previous research has demonstrated significant genotype-by-genotype interaction in host-pathogen dynamics (Soltis et al. 2020; Soltis et al. 2019; Caseys et al. 2021). Barbacci et al. (2020) further proved that fungus-derived QDR plasticity can surpass host diversity, particularly in lag-phase duration on *A. thaliana* and *S. sclerotiorum*. The importance of fungal diversity in shaping disease outcomes has also been emphasised in other studies (Rowe et al. 2010). Based on these findings, I propose that the discrete interaction of IF, lag, and LDT is shaped by the interaction of host genotype, pathogen genotype and environmental conditions. A systematic approach that integrates both host and pathogen diversity is needed to evaluate the stability of QDR mechanisms across different conditions and genotypes (fig. 4).

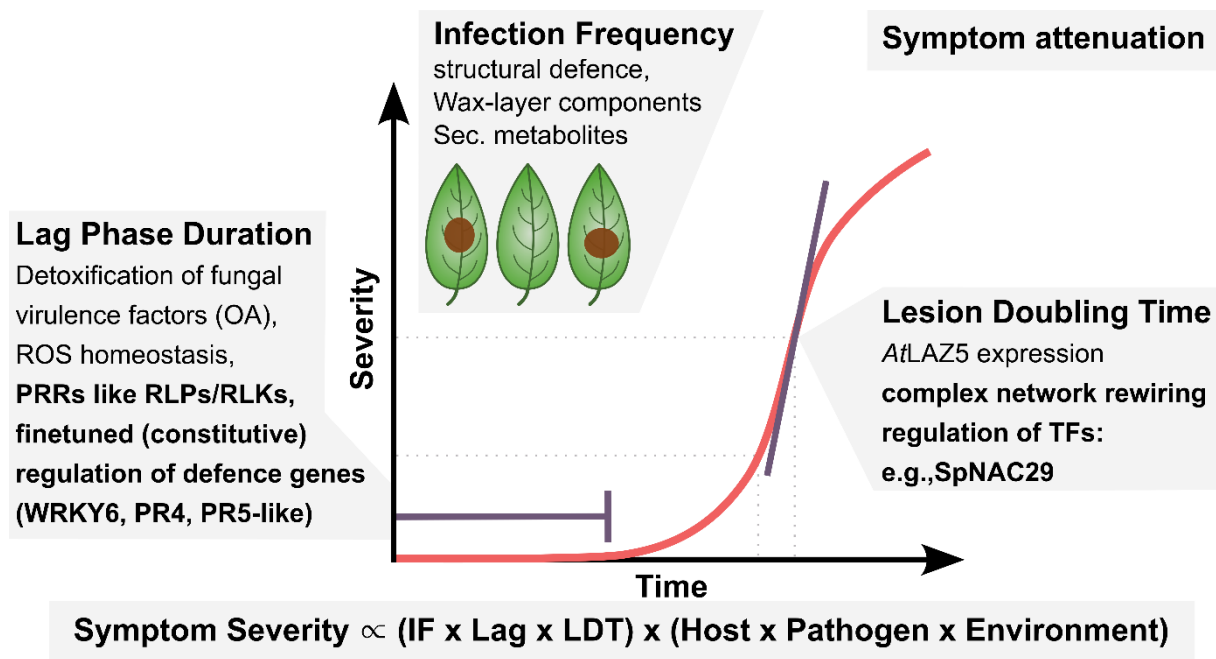


Figure 4: Extended model on factors determining QDR. The findings of this study demonstrate that lesion severity is influenced by three interacting biological parameters: infection frequency (**IF**), **lag-phase duration**, and lesion doubling time (**LDT**). Potentially underlying biological processes are added to each mechanism. Mechanisms found in this study are indicated with bold characters. Ultimately, I propose that QDR severity is governed by the combined effects of IF, lag-phase duration, and LDT, each shaped by the interplay of host genotype, pathogen genotype, and environmental conditions.

The Evolution of QDR-Networks

The preceding results raise important questions regarding the evolution of network rewiring and neofunctionalisation associated with QDR. Specifically, it remains unclear which factors govern the regulatory plasticity that enables the evolution of QDR. What roles do modularity and redundancy play in enabling this plasticity? How do selection and genetic drift shape these processes, and are hub genes subject to stronger evolutionary constraints due to pleiotropy? While the evolutionary dynamics between hosts and specialist necrotrophic pathogens are increasingly well understood, comparatively little is known about how QDR evolves in response to generalist pathogens, which may exert different and more diffuse selective pressures.

Regulatory Divergence Drives Functional Convergence

In publication 1, I found that QDR phenotypes do not reflect the genomic phylogeny of the tested *Solanum* species and accessions. This observation aligns with earlier reports in *A. thaliana* and *Brassica napus*, where phenotypes show minimal correlation with phylogenetic distance and regulatory divergence (Winkelmüller et al. 2021). More recently, Benoit et al. (2025) also highlighted the lack of a direct genotype-phenotype relationship in the context of introgression traits from wild germplasm into breeding material. This highlights that apart from single genes, even the introgression of complex polygenic loci like QTLs or complex genomic analysis cannot fully capture the regulatory network plasticity that shapes divergent phenotypes. Moreover, signs of rapid adaptation and the role of pleiotropy remain elusive (Kahlon and Stam 2021). In my study, GRNs underlie significant species-specificity (publication 2, Einspanier et al. 2025). Since NAC29 is genomically highly conserved, I proposed that *S. pennellii* has co-opted a novel function for this gene and its GRN. This finding aligns with Sucher, who showed that multiple genes, including the transporter ABCG40, have been recruited into QDR through regulatory variation (Sucher et al. 2020).

Paralog Divergence as a Driver of Convergent Evolution

Consequently, neofunctionalisation might be a central element in developing QDR against *S. sclerotiorum*. Generally, gene duplication is the primary mechanism by which novel protein functions emerge. Duplications (so the emergence of paralogs) initially lead to genomic redundancy. However, the gradual accumulation of mutations in coding or cis-regulatory regions of paralogous genes can ultimately erode redundancy through genetic drift or selection

(Gossmann and Schmid 2011; Lynch 2007). This process can lead to three distinct evolutionary outcomes: gene loss, subfunctionalisation, or neofunctionalisation (co-optation, Benoit et al. 2025; Birchler and Yang 2022; Conant and Wolfe 2008). While whole-genome duplication is the most prevalent cause of gene duplication, single-gene duplication may also occur via recombination of repetitive sequences or alternative transposition (Birchler and Yang 2022; Wang et al. 2015; Gout et al. 2023). It is important to note that most duplications are lost during speciation, and the destiny of a duplicated gene highly depends on its unique mutations and selection. Interestingly, Panchy et al. (2019) experimentally demonstrated that TF duplications can result in asymmetrical gene expression and regulation patterns, where one copy accumulates novel mutations in *cis*-regulatory regions or DNA-binding sites. At the same time, the other retains the ancestral function. Natural selection can accelerate the regulatory and functional divergence of paralogs (Lian et al. 2020; Gossmann and Schmid 2011). In publication 2, I linked a whole-genome duplication event to the duplication of NAC29, which later diverged into an *S. pennellii*-specific role in QDR. Recent examples illustrate how paralog divergence determines a wide range of agronomically relevant traits, as presented for regulating fruit size by CLAVATA3 (Benoit et al. 2025). It was shown that tandem gene duplication can lead to altered epistatic effects, removing a breeding barrier in tomatoes (Soyk et al. 2019). However, some authors mention that gene duplication might also lead to allele incompatibilities, potentially leading to loss of function (Jiao et al. 2021). In a recent study, Satterlee et al. (2024) showed how paralog diversification in *Solanum* species led to the convergent evolution of prickle-less morphology. The recent reports illustrate that paralog divergence (including their *cis*-/*trans*-sites) is a mechanism to facilitate relatively quick adaptation on a genomic and regulatory level. I, therefore, propose that regulatory polymorphism due to paralog divergence may drive phenotypic convergence of QDR phenotypes against *S. sclerotiorum*.

Functional Divergence of TF Paralogs as a Mechanism for Network Innovation and QDR

Most pioneering studies on paralog evolution have focused on mutations within single pairs of paralogs whose divergence strongly influences distinct traits, such as prickles or fruit development (Benoit et al. 2025; Yang et al. 2023; Lian et al. 2020). Although these examples effectively illustrate evolutionary mechanisms at the gene level, I propose that the implications of such divergence are likely even more profound within complex gene regulatory networks (GRNs). Whereas variation affecting individual proteins like CLAVATA3 can alter specific functions through *cis*- or *trans*-regulatory mutations, similar mutations in transcription factor (TF) paralogs could substantially reshape entire GRNs. Divergence among TF paralogs may thus drive extensive network rewiring, producing quantitatively altered phenotypes and potentially explaining the pleiotropic nature observed in QDR.

Shifts in GRN regulation typically occur through mutations either in *cis*-regulatory elements (TF binding sites at the target gene) or *trans*, so the TF itself. After duplication events, gradual divergence can drive the neofunctionalisation of transcription factors (TFs), resulting in extensive GRN rewiring via the gain or loss of regulatory interactions (edges, Voordeckers et al. 2015; Conant and Wolfe 2008; Plachetzki and Oakley 2007). In publication 2, I observed that the co-optation of a NAC29 TF paralog led to a distinctive network reconfiguration, likely involving shifts in both *cis*- and *trans*-regulatory elements. The resulting network exhibited a scale-free topology, and changes in module composition contributed to regulatory rewiring. The degree and direction of TF regulatory diversification often depend on the specific genomic context and network modularity; for instance, Winkelmüller et al. (2021) linked species-specific gene expression changes to WRKY-targeted *cis*-regulatory elements. This is further supported by findings in *Marchantia polymorpha* and *A. thaliana*, where *trans*-regulatory elements remain largely conserved while *cis*-regulatory variation drives divergent responses to salt stress (Guerrero et al. 2024). Consequently, plant TF binding motifs exhibit varying degrees of evolutionary conservation. Motifs recognised by WRKY and NAC transcription factors are typically highly conserved across plant lineages. In contrast, motifs targeted by Myb and C2H2 zinc-finger (ZF) proteins display lineage-specific expansions in *A. thaliana*, likely arising through gene duplication events (Lambert et al. 2019).

Regulatory Divergence, Genetic Drift, and the Emergence of QDR

These examples illustrate how TF divergence and neofunctionalisation underlie different evolutionary scenarios (most likely involving evolutionary constraints) possibly governed by the selection or drift of *cis/trans* mutations. Yet, it remains unclear whether and how TFs and their targets experience selection based on their position within the GRN (McDonald and Reed 2023). Notably, the gained function of a TF does not strictly imply a new function to the organism. Yet, the acquired genetic degeneracy (so independent functionally redundant functions based on independent genetic backgrounds) might be essential in the evolution of QDR (Derbyshire and Raffaele 2023). In other words, although individual mutations drive TF divergence, the cumulative effect on the molecular network's modularity could substantially enhance the host organism's ability to resist generalist pathogens. Thus, the modular organisation and inherent flexibility of regulatory networks are likely key determinants of robust resistance strategies, highlighting a potential evolutionary advantage provided by genetic degeneracy (and thus pleiotropy).

Therefore, I speculate that the co-optation of genes or gene networks might drive the convergent evolution of QDR by hub divergence (Artur and Kajala 2021). Yet, the underlying evolutionary forces remain unclear. Notably, recent modelling suggests no overlap between *S. sclerotiorum* habitat suitability and the origin of Solanum plants (Cohen 2023). This is further supported by the observation that Sclerotiniaceae expanded their host range relatively recently by host jumps rather than coevolutionary dynamics like boom-bust-cycles (Derbyshire et al. 2022; Navaud et al. 2018). Given the convergent evolution of QDR phenotypes, substantial functional divergence of transcriptional networks, and strong evidence for adaptation to abiotic habitats, it appears unlikely that directed host-pathogen coevolution was the primary driver of QDR evolution in the presented system. Lynch (2007) showed that changes in network topology rarely arise by selection but by non-adaptive processes, like genetic drift. Accordingly, I argue that either genetic drift or abiotic habitat adaptation shapes quantitative disease resistance in Solanum against *S. sclerotiorum*.

Conclusion

In this dissertation, I investigated the phenotypic and regulatory diversity underlying QDR against *S. sclerotiorum*. My results demonstrate that QDR exhibits considerable variability across multiple phylogenetic scales, showing significant diversity within and between plant species and genera. I conclude that distinct phases of infection determine QDR phenotypes influenced by host-pathogen-environment interactions. The species-specific regulatory networks observed in this study suggest that QDR evolution is likely primarily driven by convergent evolution rather than sustained directional selection. Tandem duplication events and paralog divergence might drive neofunctionalisation, most likely by mutations in *cis-/trans*-elements. Thus, I propose that genetic drift or indirect (secondary) selection (possibly through abiotic adaptation) may predominantly shape quantitative disease resistance in host plants.

Implications and Outlook

In this study, I showed that independent biological mechanisms (IF, lag phase duration, and LDT) contribute to QDR. These findings have important implications in modern breeding, providing a more nuanced framework for candidate identification and functional validation. By highlighting multiple QDR mechanisms, this work expands the toolkit for marker-assisted selection, enabling breeders to target QDR-associated genes or GRNs more precisely and trait-specific.

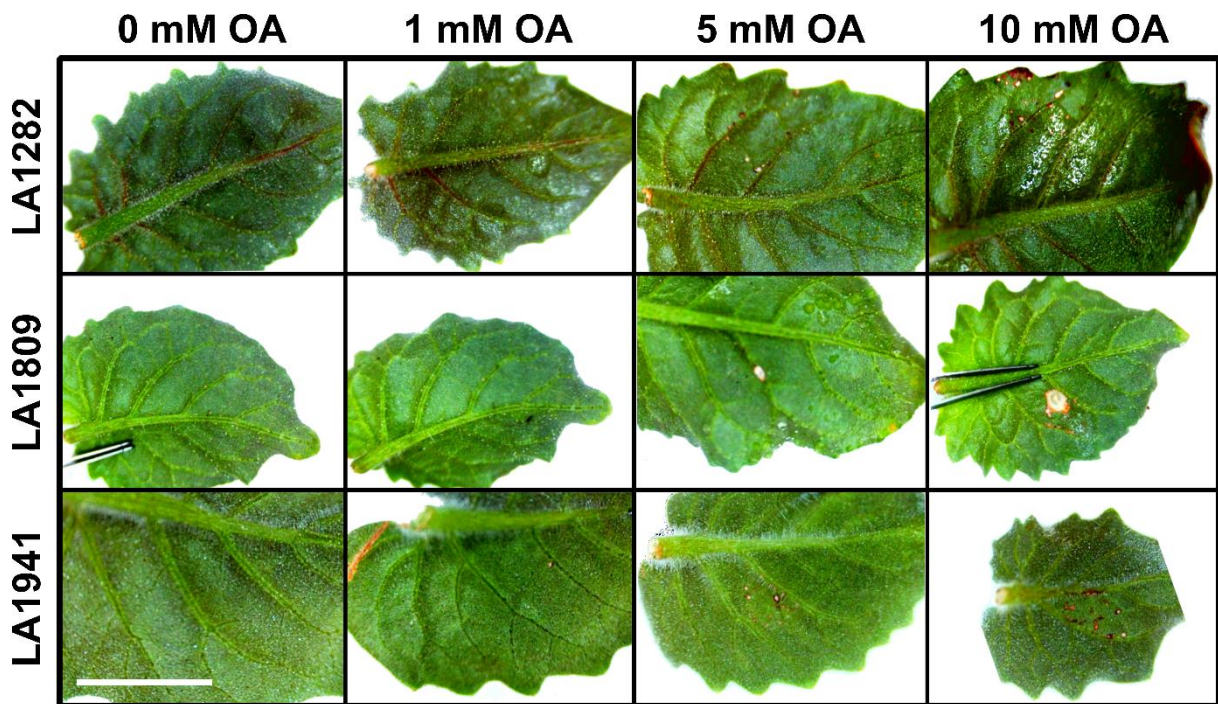
The insights on GRN topology illustrate the complex regulatory interplay of QDR. Transferring NAC29 or other QDR-associated genes into different genetic backgrounds without the regulatory context (modules) may not confer improved QDR. This also incorporates the putative interaction of RLPs/RLKs with WRKY6 and other unidentified lag phase signalling cascade components. The effectiveness of such markers relies on compatible network components in the recipient population. Future breeding efforts should validate QDR-associated markers across diverse genetic backgrounds to ensure functional effectiveness prior to large-scale deployment.

Detailed population genomic analyses are required to clarify the evolutionary forces driving QDR. Future studies should identify selection signatures across populations to differentiate between selective pressure acting on QDR-associated genes and neutral genetic drift. Investigating signatures of selection on *cis*- and *trans*-regulatory elements at a population level

will also show how gene regulatory network divergence shapes quantitative disease resistance. Ultimately answering whether or why certain networks are evolutionarily constrained while others can be co-opted for new functions (McDonald and Reed 2023). To fully understand QDR, a systems biology approach integrating multiple omics technologies (such as genomics, transcriptomics, proteomics, metabolomics, and epigenomics) is essential to bridge the gaps in genotype-to-phenotype relationships (Delplace et al. 2022).

Understanding QDR evolution in wild pathosystems is fundamental in conceptualising pre-breeding programs, helping researchers and breeders assess inter- and intraspecific variability. Therefore, informed breeding decisions will facilitate the full potential of natural diversity. Exploring the role of paralog divergence may open new perspectives in biotechnology by engineering new functions for old genes. Ultimately, the evolutionary analysis in this study contributes towards a deeper understanding of the host-pathogen coevolution. The presented insights can support the development of sustainable resistance strategies that reduce selective pressure on pathogen populations, potentially alleviating the intensity of the evolutionary arms race between crop populations and pathogens.

Supplementary Information



Suppl. Fig. 1: Oxalic acid tolerance of three *S. pennellii* accessions. A 10 μ L OA drop was inoculated on detached leaves and incubated for three days in navautron-like conditions. Images were then taken using a ProScope handheld microscope. The white bar indicates 1 cm. The experiment was repeated twice, with five leaves per treatment. A representative example per treatment is shown.

Publication bibliography

Alonge, Michael; Wang, Xingang; Benoit, Matthias; Soyk, Sebastian; Pereira, Lara; Zhang, Lei et al. (2020): Major Impacts of Widespread Structural Variation on Gene Expression and Crop Improvement in Tomato. In *Cell* 182 (1), 145–161.e23. DOI: 10.1016/j.cell.2020.05.021.

Anderegg, Jonas; Zenkl, Radek; Kirchgessner, Norbert; Hund, Andreas; Walter, Achim; McDonald, Bruce A. (2024): SYMPATHIQUE: image-based tracking of symptoms and monitoring of pathogenesis to decompose quantitative disease resistance in the field. In *Plant Methods* 20 (1), p. 170. DOI: 10.1186/s13007-024-01290-4.

Artur, Mariana A. S.; Kajala, Kaisa (2021): Convergent evolution of gene regulatory networks underlying plant adaptations to dry environments. In *Plant, Cell & Environment* 44 (10), pp. 3211–3222. DOI: 10.1111/pce.14143.

Babu, M. Madan; Luscombe, Nicholas M.; Aravind, L.; Gerstein, Mark; Teichmann, Sarah A. (2004): Structure and evolution of transcriptional regulatory networks. In *Current opinion in structural biology* 14 (3), pp. 283–291. DOI: 10.1016/j.sbi.2004.05.004.

Barbacci, Adelin; Navaud, Olivier; Mbengue, Malick; Barascud, Marielle; Godiard, Laurence; Khafif, Mehdi et al. (2020a): Rapid identification of an Arabidopsis NLR gene as a candidate conferring susceptibility to *Sclerotinia sclerotiorum* using time-resolved automated phenotyping. In *The Plant journal : for cell and molecular biology* 103 (2), pp. 903–917. DOI: 10.1111/tpj.14747.

Barbacci, Adelin; Navaud, Olivier; Mbengue, Malick; Barascud, Marielle; Godiard, Laurence; Khafif, Mehdi et al. (2020b): Rapid identification of an Arabidopsis NLR gene as a candidate conferring susceptibility to *Sclerotinia sclerotiorum* using time-resolved automated phenotyping. In *The Plant Journal* 103 (2), pp. 903–917. DOI: 10.1111/tpj.14747.

Barrett, Luke G.; Encinas-Viso, Francisco; Burdon, Jeremy J.; Thrall, Peter H. (2015): Specialization for resistance in wild host-pathogen interaction networks. In *Frontiers in Plant Science* 6, p. 761. DOI: 10.3389/fpls.2015.00761.

Bedinger, Patricia A.; Chetelat, Roger T.; McClure, Bruce; Moyle, Leonie C.; Rose, Jocelyn K. C.; Stack, Stephen M. et al. (2011): Interspecific reproductive barriers in the tomato clade: opportunities to decipher mechanisms of reproductive isolation. In *Sexual plant reproduction* 24 (3), pp. 171–187. DOI: 10.1007/s00497-010-0155-7.

Benoit, Matthias; Jenike, Katharine M.; Satterlee, James W.; Ramakrishnan, Srividya; Gentile, Iacopo; Hendelman, Anat et al. (2025): *Solanum* pan-genetics reveals paralogues as contingencies in crop engineering. In *Nature*. DOI: 10.1038/s41586-025-08619-6.

Berger, R. D.; Filho, A. B.; Amorim, L. (1997): Lesion expansion as an epidemic component. In *Phytopathology* 87 (10), pp. 1005–1013. DOI: 10.1094/PHYTO.1997.87.10.1005.

Berger, R. D.; Jones, J. W. (1985): A General Model for Disease Progress with Functions for Variable Latency and Lesion Expansion on Growing Host Plants. In *Phytopathology* 75 (7), p. 792. DOI: 10.1094/Phyto-75-792.

Birchler, James A.; Yang, Hua (2022): The multiple fates of gene duplications: Deletion, hypofunctionalization, subfunctionalization, neofunctionalization, dosage balance constraints, and neutral variation. In *The Plant Cell* 34 (7), pp. 2466–2474. DOI: 10.1093/plcell/koac076.

Bohra, Abhishek; Kilian, Benjamin; Sivasankar, Shoba; Caccamo, Mario; Mba, Chikelu; McCouch, Susan R.; Varshney, Rajeev K. (2022): Reap the crop wild relatives for breeding future crops. In *Trends in biotechnology* 40 (4), pp. 412–431. DOI: 10.1016/j.tibtech.2021.08.009.

Boland, G. J.; Hall, R. (1994): Index of plant hosts of *Sclerotinia sclerotiorum*. In *Canadian Journal of Plant Pathology* 16 (2), pp. 93–108. DOI: 10.1080/07060669409500766.

Bolger, Anthony; Scossa, Federico; Bolger, Marie E.; Lanz, Christa; Maumus, Florian; Tohge, Takayuki et al. (2014): The genome of the stress-tolerant wild tomato species *Solanum pennellii*. In *Nature Genetics* 46 (9), pp. 1034–1038. DOI: 10.1038/ng.3046.

- Broido, Anna D.; Clauset, Aaron (2019): Scale-free networks are rare. In *Nature communications* 10 (1), p. 1017. DOI: 10.1038/s41467-019-08746-5.
- Brown, James K.M. (2015): Durable Resistance of Crops to Disease: A Darwinian Perspective. In *Annual Review of Phytopathology* 53 (1), pp. 513–539. DOI: 10.1146/annurev-phyto-102313-045914.
- Caseys, Celine; Shi, Gongjun; Soltis, Nicole; Gwinner, Raoni; Corwin, Jason; Atwell, Susanna; Kliebenstein, Daniel J. (2021): Quantitative interactions: the disease outcome of *Botrytis cinerea* across the plant kingdom. In *G3 Genes\textbarGenetics* 11 (8), jkab175. DOI: 10.1093/g3journal/jkab175.
- Cessna, S. G.; Sears, V. E.; Dickman, M. B.; Low, P. S. (2000): Oxalic acid, a pathogenicity factor for *Sclerotinia sclerotiorum*, suppresses the oxidative burst of the host plant. In *The Plant Cell* 12 (11), pp. 2191–2200. DOI: 10.1105/tpc.12.11.2191.
- Chassot, Céline; Nawrath, Christiane; Métraux, Jean-Pierre (2007): Cuticular defects lead to full immunity to a major plant pathogen. In *The Plant Journal* 49 (6), pp. 972–980. DOI: 10.1111/j.1365-313X.2006.03017.x.
- Chen, Hongyu; Chen, Xiuling; Chen, Dong; Li, Jingfu; Zhang, Yi; Wang, Aoxue (2015): A comparison of the low temperature transcriptomes of two tomato genotypes that differ in freezing tolerance: *Solanum lycopersicum* and *Solanum habrochaites*. In *BMC Plant Biology* 15, p. 132. DOI: 10.1186/s12870-015-0521-6.
- Chen, Xiaoting; Liu, Jun; Lin, Guifang; Wang, Airong; Wang, Zonghua; Lu, Guodong (2013): Overexpression of AtWRKY28 and AtWRKY75 in *Arabidopsis* enhances resistance to oxalic acid and *Sclerotinia sclerotiorum*. In *Plant Cell Reports* 32 (10), pp. 1589–1599. DOI: 10.1007/s00299-013-1469-3.
- Cohen, Susan D. (2023): Estimating the Climate Niche of *Sclerotinia sclerotiorum* Using Maximum Entropy Modeling. In *Journal of fungi (Basel, Switzerland)* 9 (9). DOI: 10.3390/jof9090892.
- Conant, Gavin C.; Wolfe, Kenneth H. (2008): Turning a hobby into a job: how duplicated genes find new functions. In *Nature reviews. Genetics* 9 (12), pp. 938–950. DOI: 10.1038/nrg2482.
- Corwin, Jason A.; Kliebenstein, Daniel J. (2017): Quantitative Resistance: More Than Just Perception of a Pathogen. In *The Plant Cell* 29 (4), pp. 655–665. DOI: 10.1105/tpc.16.00915.
- Davidson, Eric H.; Erwin, Douglas H. (2006): Gene regulatory networks and the evolution of animal body plans. In *Science (New York, N.Y.)* 311 (5762), pp. 796–800. DOI: 10.1126/science.1113832.
- Davis, Joel; Yu, Daozhan; Evans, Wendy; Gokirmak, Tufan; Chetelat, Roger T.; Stotz, Henrik U. (2009): Mapping of loci from *Solanum lycopersicoides* conferring resistance or susceptibility to *Botrytis cinerea* in tomato. In *TAG. Theoretical and applied genetics. Theoretische und angewandte Genetik* 119 (2), pp. 305–314. DOI: 10.1007/s00122-009-1039-9.
- Delplace, Florent; Huard-Chauveau, Carine; Dubiella, Ullrich; Khafif, Mehdi; Alvarez, Eva; Langin, Gautier et al. (2020): Robustness of plant quantitative disease resistance is provided by a decentralized immune network. In *Proceedings of the National Academy of Sciences* 117 (30), pp. 18099–18109. DOI: 10.1073/pnas.2000078117.
- Delplace, Florent; Huard-Chauveau, Carine; Berthomé, Richard; Roby, Dominique (2022): Network organization of the plant immune system: from pathogen perception to robust defense induction. In *The Plant Journal* 109 (2), pp. 447–470. DOI: 10.1111/tpj.15462.
- Delplace, Florent; Khafif, Mehdi; Stam, Remco; Barbacci, Adelin; Raffaele, Sylvain (2024): Neutral transcriptome rewiring promotes QDR evolvability at the species level.
- Derbyshire, Mark; Mbengue, Malick; Barascud, Marielle; Navaud, Olivier; Raffaele, Sylvain (2019): Small RNAs from the plant pathogenic fungus *Sclerotinia sclerotiorum* highlight host candidate genes associated with quantitative disease resistance. In *Molecular Plant Pathology* 20 (9), pp. 1279–1297. DOI: 10.1111/mpp.12841.
- Derbyshire, Mark C.; Newman, Toby E.; Khentry, Yuphin; Owolabi Taiwo, Akeem (2022): The evolutionary and molecular features of the broad-host-range plant pathogen *Sclerotinia sclerotiorum*. In *Molecular Plant Pathology* 23 (8), pp. 1075–1090. DOI: 10.1111/mpp.13221.

- Derbyshire, Mark C.; Raffaele, Sylvain (2023): Till death do us pair: Co-evolution of plant-necrotroph interactions. In *Current Opinion in Plant Biology* 76, p. 102457. DOI: 10.1016/j.pbi.2023.102457.
- Didelon, Marie; Sucher, Justine; Carvalho-Silva, Pedro; Zaffuto, Matilda; Barbacci, Adelin; Raffaele, Sylvain (2024): Acclimation to high daily thermal amplitude converts a defense response regulator into susceptibility factor. In *BioRxiv*. DOI: 10.1101/2024.08.22.609129.
- Ding, Li-Na; Li, Teng; Guo, Xiao-Juan; Li, Ming; Liu, Xiao-Yan; Cao, Jun; Tan, Xiao-Li (2021): Sclerotinia Stem Rot Resistance in Rapeseed: Recent Progress and Future Prospects. In *Journal of Agricultural and Food Chemistry* 69 (10), pp. 2965–2978. DOI: 10.1021/acs.jafc.0c07351.
- Doehlemann, Gunther; Ökmen, Bilal; Zhu, Wenjun; Sharon, Amir (2017): Plant Pathogenic Fungi. In *Microbiology spectrum* 5 (1). DOI: 10.1128/microbiolspec.FUNK-0023-2016.
- Egli, Lukas; Schröter, Matthias; Scherber, Christoph; Tschardtke, Teja; Seppelt, Ralf (2020): Crop asynchrony stabilizes food production. In *Nature* 588 (7837), E7-E12. DOI: 10.1038/s41586-020-2965-6.
- Einspanier, S.; Tominello-Ramirez, C.; Delplace, F.; Stam, R. (2025): Co-optation of Transcription Factors Drives Evolution of Quantitative Disease Resistance Against a Necrotrophic Pathogen. In *BioRxiv*. DOI: 10.1101/2025.02.26.640262.
- Einspanier, Severin; Tominello-Ramirez, Christopher; Hasler, Mario; Barbacci, Adelin; Raffaele, Sylvain; Stam, Remco (2024): High-Resolution Disease Phenotyping Reveals Distinct Resistance Mechanisms of Tomato Crop Wild Relatives against *Sclerotinia sclerotiorum*. In *Plant Phenomics* 6, Article 0214. DOI: 10.34133/plantphenomics.0214.
- Erwin, Douglas H.; Davidson, Eric H. (2009): The evolution of hierarchical gene regulatory networks. In *Nature reviews. Genetics* 10 (2), pp. 141–148. DOI: 10.1038/nrg2499.
- Espinosa-Soto, Carlos (2018): On the role of sparseness in the evolution of modularity in gene regulatory networks. In *PLOS Computational Biology* 14 (5), e1006172. DOI: 10.1371/journal.pcbi.1006172.
- Finkers, Richard; van Heusden, Adriaan W.; Meijer-Dekens, Fien; van Kan, Jan A. L.; Maris, Paul; Lindhout, Pim (2007): The construction of a *Solanum habrochaites* LYC4 introgression line population and the identification of QTLs for resistance to *Botrytis cinerea*. In *TAG. Theoretical and applied genetics. Theoretische und angewandte Genetik* 114 (6), pp. 1071–1080. DOI: 10.1007/s00122-006-0500-2.
- Gopalan-Nair, Rekha; Jardinaud, Marie-Françoise; Legrand, Ludovic; Landry, David; Barlet, Xavier; Lopez-Roques, Céline et al. (2021): Convergent Rewiring of the Virulence Regulatory Network Promotes Adaptation of *Ralstonia solanacearum* on Resistant Tomato. In *Molecular Biology and Evolution* 38 (5), pp. 1792–1808. DOI: 10.1093/molbev/msaa320.
- Gossmann, Toni I.; Schmid, Karl J. (2011): Selection-driven divergence after gene duplication in *Arabidopsis thaliana*. In *Journal of Molecular Evolution* 73 (3-4), pp. 153–165. DOI: 10.1007/s00239-011-9463-2.
- Gout, Jean-Francois; Hao, Yue; Johri, Parul; Arnaiz, Olivier; Doak, Thomas G.; Bhullar, Simran et al. (2023): Dynamics of Gene Loss following Ancient Whole-Genome Duplication in the Cryptic *Paramecium* Complex. In *Molecular Biology and Evolution* 40 (5). DOI: 10.1093/molbev/msad107.
- Guerrero, Sara; Roces, Víctor; García-Campa, Lara; Valledor, Luis; Meijón, Mónica (2024): Proteomic dynamics revealed sex-biased responses to combined heat-drought stress in *Marchantia*. In *Journal of Integrative Plant Biology*. DOI: 10.1111/jipb.13753.
- Hall, Matthew D.; Bento, Gilberto; Ebert, Dieter (2017): The Evolutionary Consequences of Stepwise Infection Processes. In *Trends in Ecology & Evolution* 32 (8), pp. 612–623. DOI: 10.1016/j.tree.2017.05.009.
- Hatleberg, William L.; Hinman, Veronica F. (2021): Modularity and hierarchy in biological systems: Using gene regulatory networks to understand evolutionary change. In *Current topics in developmental biology* 141, pp. 39–73. DOI: 10.1016/bs.ctdb.2020.11.004.

- Hill, Mark S.; Vande Zande, Pétra; Wittkopp, Patricia J. (2021): Molecular and evolutionary processes generating variation in gene expression. In *Nature reviews. Genetics* 22 (4), pp. 203–215. DOI: 10.1038/s41576-020-00304-w.
- Houle, David; Rossoni, Daniela M. (2022): Complexity, Evolvability, and the Process of Adaptation. In *Annu. Rev. Ecol. Evol. Syst.* 53 (1), pp. 137–159. DOI: 10.1146/annurev-ecolsys-102320-090809.
- Jiao, Wen-Biao; Patel, Vipul; Klasen, Jonas; Liu, Fang; Pecinkova, Petra; Ferrand, Marina et al. (2021): The Evolutionary Dynamics of Genetic Incompatibilities Introduced by Duplicated Genes in *Arabidopsis thaliana*. In *Molecular Biology and Evolution* 38 (4), pp. 1225–1240. DOI: 10.1093/molbev/msaa306.
- Jones, D. A.; Thomas, C. M.; Hammond-Kosack, K. E.; Balint-Kurti, P. J.; Jones, J. D. (1994): Isolation of the tomato Cf-9 gene for resistance to *Cladosporium fulvum* by transposon tagging. In *Science* 266 (5186), pp. 789–793. DOI: 10.1126/science.7973631.
- Kabbage, Mehdi; Williams, Brett; Dickman, Martin B.; Tyler, Brett (2013): Cell Death Control: The Interplay of Apoptosis and Autophagy in the Pathogenicity of *Sclerotinia sclerotiorum*. In *PLoS Pathogens* 9 (4), e1003287. DOI: 10.1371/journal.ppat.1003287.
- Kahlon, Parvinderdeep S.; Seta, Shallet Mindih; Zander, Gesche; Scheikl, Daniela; Hückelhoven, Ralph; Stam, Remco (2020): Population studies of the wild tomato species *Solanum chilense* reveal geographically structured major gene-mediated pathogen resistance, p. 9.
- Kahlon, Parvinderdeep S.; Stam, Remco (2021): Polymorphisms in plants to restrict losses to pathogens: From gene family expansions to complex network evolution. In *Current Opinion in Plant Biology* 62, p. 102040. DOI: 10.1016/j.pbi.2021.102040.
- Kahlon, Parvinderdeep S.; Verin, Melissa; Hückelhoven, Ralph; Stam, Remco (2021): Quantitative resistance differences between and within natural populations of *Solanum chilense* against the oomycete pathogen *Phytophthora infestans*. In *Ecology and Evolution* 11 (12), pp. 7768–7778. DOI: 10.1002/ece3.7610.
- Krug, Aubrey Streit; B M Drummond, Emily; van Tassel, David L.; Warschefsky, Emily J. (2023): The next era of crop domestication starts now. In *Proceedings of the National Academy of Sciences of the United States of America* 120 (14), e2205769120. DOI: 10.1073/pnas.2205769120.
- Lambert, Samuel A.; Yang, Ally W. H.; Sasse, Alexander; Cowley, Gwendolyn; Albu, Mihai; Caddick, Mark X. et al. (2019): Similarity regression predicts evolution of transcription factor sequence specificity. In *Nature Genetics* 51 (6), pp. 981–989. DOI: 10.1038/s41588-019-0411-1.
- Li, Ning; He, Qiang; Wang, Juan; Wang, Baiké; Zhao, Jiantao; Huang, Shaoyong et al. (2023): Super-pangenome analyses highlight genomic diversity and structural variation across wild and cultivated tomato species. In *Nature Genetics* 55 (5), pp. 852–860. DOI: 10.1038/s41588-023-01340-y.
- Lian, Shuaibin; Zhou, Yongjie; Liu, Zixiao; Gong, Andong; Cheng, Lin (2020): The differential expression patterns of paralogs in response to stresses indicate expression and sequence divergences. In *BMC Plant Biology* 20 (1), p. 277. DOI: 10.1186/s12870-020-02460-x.
- Liang, Xiaofei; Moomaw, Ellen W.; Rollins, Jeffrey A. (2015): Fungal oxalate decarboxylase activity contributes to *Sclerotinia sclerotiorum* early infection by affecting both compound appressoria development and function. In *Molecular Plant Pathology* 16 (8), pp. 825–836. DOI: 10.1111/mpm.12239.
- Liao, Chao-Jan; Hailemariam, Sara; Sharon, Amir; Mengiste, Tesfaye (2022): Pathogenic strategies and immune mechanisms to necrotrophs: Differences and similarities to biotrophs and hemibiotrophs. In *Current Opinion in Plant Biology* 69, p. 102291. DOI: 10.1016/j.pbi.2022.102291.
- Lin, Li; Zhang, Xingrui; Fan, Jialin; Li, Jiawei; Ren, Sichao; Gu, Xin et al. (2024): Natural variation in BnaA07.MKK9 confers resistance to *Sclerotinia* stem rot in oilseed rape. In *Nature communications* 15 (1), p. 5059. DOI: 10.1038/s41467-024-49504-6.
- Lynch, Michael (2007): The evolution of genetic networks by non-adaptive processes. In *Nature reviews. Genetics* 8 (10), pp. 803–813. DOI: 10.1038/nrg2192.

- Mackay, Trudy F. C.; Anholt, Robert R. H. (2024): Pleiotropy, epistasis and the genetic architecture of quantitative traits. In *Nature reviews. Genetics* 25 (9), pp. 639–657. DOI: 10.1038/s41576-024-00711-3.
- Madriñán, Santiago; Cortés, Andrés J.; Richardson, James E. (2013): Páramo is the world's fastest evolving and coolest biodiversity hotspot. In *Frontiers in genetics* 4, p. 192. DOI: 10.3389/fgene.2013.00192.
- Mazumdar, Purabi (2021): Sclerotinia stem rot in tomato: a review on biology, pathogenicity, disease management and future research priorities. In *Journal of Plant Diseases and Protection* 128 (6), pp. 1403–1431. DOI: 10.1007/s41348-021-00509-z.
- Mbengue, Malick; Navaud, Olivier; Peyraud, Rémi; Barascud, Marielle; Badet, Thomas; Vincent, Rémy et al. (2016): Emerging Trends in Molecular Interactions between Plants and the Broad Host Range Fungal Pathogens *Botrytis cinerea* and *Sclerotinia sclerotiorum*. In *Frontiers in Plant Science* 7. DOI: 10.3389/fpls.2016.00422.
- McCouch, Susan (2004): Diversifying selection in plant breeding. In *PLOS Biology* 2 (10), e347. DOI: 10.1371/journal.pbio.0020347.
- McDonald, Jeanne M. C.; Reed, Robert D. (2023): Patterns of selection across gene regulatory networks. In *Seminars in cell & developmental biology* 145, pp. 60–67. DOI: 10.1016/j.semcdb.2022.03.029.
- Miao, Shuang; Li, Fengshuo; Han, Yang; Yao, Zhongtong; Xu, Zeqian; Chen, Xiuling et al. (2022): Identification of OSCA gene family in *Solanum habrochaites* and its function analysis under stress. In *BMC Genomics* 23 (1), p. 547. DOI: 10.1186/s12864-022-08675-6.
- Munir, Shoaib; Liu, Hui; Xing, Yali; Hussain, Saddam; Ouyang, Bo; Zhang, Yuyang et al. (2016): Overexpression of calmodulin-like (ShCML44) stress-responsive gene from *Solanum habrochaites* enhances tolerance to multiple abiotic stresses. In *Scientific Reports* 6, p. 31772. DOI: 10.1038/srep31772.
- Muñoz Hoyos, Lina; Anisha, Wan Petra; Meng, Chen; Kleigrew, Karin; Dawid, Corinna; Hückelhoven, Ralph; Stam, Remco (2024): Untargeted metabolomics reveals PTI-associated metabolites. In *Plant, Cell & Environment* 47 (4), pp. 1224–1237. DOI: 10.1111/pce.14794.
- Nakazato, Takuya; Warren, Dan L.; Moyle, Leonie C. (2010): Ecological and geographic modes of species divergence in wild tomatoes. In *American Journal of Botany* 97 (4), pp. 680–693. DOI: 10.3732/ajb.0900216.
- Navarro, Barbara Ludwig; Streit, Sebastian; Nogueira Júnior, Antonio Fernandes; Tiedemann, Andreas von (2024): Photosynthetic Costs and Impact on Epidemiological Parameters Associated with Ht Resistance Genes in Maize Lines Infected with *Exserohilum turcicum*. In *Phytopathology* 114 (4), pp. 760–769. DOI: 10.1094/PHYTO-07-23-0247-R.
- Navaud, Olivier; Barbacci, Adelin; Taylor, Andrew; Clarkson, John P.; Raffaele, Sylvain (2018): Shifts in diversification rates and host jump frequencies shaped the diversity of host range among Sclerotiniaceae fungal plant pathogens. In *Molecular Ecology* 27 (5), pp. 1309–1323. DOI: 10.1111/mec.14523.
- Newman, Toby E.; Derbyshire, Mark C. (2020): The Evolutionary and Molecular Features of Broad Host-Range Necrotrophy in Plant Pathogenic Fungi. In *Frontiers in Plant Science* 11, p. 591733. DOI: 10.3389/fpls.2020.591733.
- Nicolau, Miguel; Schoenauer, Marc (2009): On the evolution of scale-free topologies with a gene regulatory network model. In *Bio Systems* 98 (3), pp. 137–148. DOI: 10.1016/j.biosystems.2009.06.006.
- Nosenko, Tetyana; Böndel, Katharina B.; Kumpfmüller, Gabriele; Stephan, Wolfgang (2016): Adaptation to low temperatures in the wild tomato species *Solanum chilense*. In *Molecular Ecology* 25 (12), pp. 2853–2869. DOI: 10.1111/mec.13637.
- Oliver, Richard P.; Hückelhoven, Ralph; Del Ponte, Emerson M.; Di Pietro, Antonio; Agrios, George N. (Eds.) (2024): *Agrios' plant pathology*. Sixth edition. London, San Diego, Cambridge, MA: Academic Press.
- Ouma, Wilberforce Zachary; Pogacar, Katja; Grotewold, Erich (2018): Topological and statistical analyses of gene regulatory networks reveal unifying yet quantitatively different emergent properties. In *PLOS Computational Biology* 14 (4), e1006098. DOI: 10.1371/journal.pcbi.1006098.

- Panchy, Nicholas L.; Azodi, Christina B.; Winship, Eamon F.; O'Malley, Ronan C.; Shiu, Shin-Han (2019): Expression and regulatory asymmetry of retained *Arabidopsis thaliana* transcription factor genes derived from whole genome duplication. In *BMC evolutionary biology* 19 (1), p. 77. DOI: 10.1186/s12862-019-1398-z.
- Peralta, Iris E.; Spooner, David M.; Knapp, Sandra (2008): Taxonomy of wild tomatoes and their relatives (*Solanum* sect. *Lycopersicoides*, sect. *Juglandifolia*, sect. *Lycopersicon*; Solanaceae). Ann Arbor, Mich: American Soc. of Plant Taxonomists (Systematic botany monographs).
- Petit, Apolline (2024): Theoretical and empirical study of the evolution of gene regulatory networks. Dissertation. Universite Paris-Saclay, Paris.
- Plachetzki, David C.; Oakley, Todd H. (2007): Key transitions during the evolution of animal phototransduction: novelty, “tree-thinking,” co-option, and co-duplication. In *Integrative and comparative biology* 47 (5), pp. 759–769. DOI: 10.1093/icb/icm050.
- Poland, Jesse A.; Balint-Kurti, Peter J.; Wissner, Randall J.; Pratt, Richard C.; Nelson, Rebecca J. (2009): Shades of gray: the world of quantitative disease resistance. In *Trends in Plant Science* 14 (1), pp. 21–29. DOI: 10.1016/j.tplants.2008.10.006.
- Powell, Adrian F.; Feder, Ari; Li, Jie; Schmidt, Maximilian H-W; Courtney, Lance; Alseekh, Saleh et al. (2022): A *Solanum lycopersicoides* reference genome facilitates insights into tomato specialized metabolism and immunity. In *The Plant journal : for cell and molecular biology* 110 (6), pp. 1791–1810. DOI: 10.1111/tpj.15770.
- Purugganan, Michael D.; Fuller, Dorian Q. (2009): The nature of selection during plant domestication. In *Nature* 457 (7231), pp. 843–848. DOI: 10.1038/nature07895.
- Ray, Deepak K.; Gerber, James S.; MacDonald, Graham K.; West, Paul C. (2015): Climate variation explains a third of global crop yield variability. In *Nature communications* 6, p. 5989. DOI: 10.1038/ncomms6989.
- Reina-Pinto, José J.; Yephremov, Alexander (2009): Surface lipids and plant defenses. In *Plant Physiology and Biochemistry* 47 (6), pp. 540–549. DOI: 10.1016/j.plaphy.2009.01.004.
- Renard, Delphine; Tilman, David (2019): National food production stabilized by crop diversity. In *Nature* 571 (7764), pp. 257–260. DOI: 10.1038/s41586-019-1316-y.
- Rick, Charles M.; Butler, L. (1956): Cytogenetics of the Tomato. In, vol. 8: Elsevier (Advances in Genetics), pp. 267–382.
- Roux, Fabrice; Voisin, Derry; Badet, Thomas; Balagué, Claudine; Barlet, Xavier; Huard-Chauveau, Carine et al. (2014): Resistance to phytopathogens e tutti quanti : placing plant quantitative disease resistance on the map: Quantitative disease resistance in plants. In *Molecular Plant Pathology* 15 (5), pp. 427–432. DOI: 10.1111/mpp.12138.
- Rowe, Heather C.; Kliebenstein, Daniel J. (2007): Elevated genetic variation within virulence-associated *Botrytis cinerea* polygalacturonase loci. In *Molecular Plant-Microbe Interactions®* 20 (9), pp. 1126–1137. DOI: 10.1094/MPMI-20-9-1126.
- Rowe, Heather C.; Kliebenstein, Daniel J.; Rall, Glenn F. (2010): All Mold Is Not Alike: The Importance of Intraspecific Diversity in Necrotrophic Plant Pathogens. In *PLoS Pathogens* 6 (3), e1000759. DOI: 10.1371/journal.ppat.1000759.
- Sackton, Timothy B.; Hartl, Daniel L. (2016): Genotypic Context and Epistasis in Individuals and Populations. In *Cell* 166 (2), pp. 279–287. DOI: 10.1016/j.cell.2016.06.047.
- Satterlee, James W.; Alonso, David; Gramazio, Pietro; Jenike, Katharine M.; He, Jia; Arrones, Andrea et al. (2024): Convergent evolution of plant prickles by repeated gene co-option over deep time. In *Science (New York, N.Y.)* 385 (6708), eado1663. DOI: 10.1126/science.ado1663.
- Schluter, Dolph; Pennell, Matthew W. (2017): Speciation gradients and the distribution of biodiversity. In *Nature* 546 (7656), pp. 48–55. DOI: 10.1038/nature22897.

Schmey, Tamara; Small, Corinn; Einspanier, Severin; Hoyoz, Lina Muñoz; Ali, Tahir; Gamboa, Soledad et al. (2023): Small-spored *Alternaria* spp. (section *Alternaria*) are common pathogens on wild tomato species. In *Environmental Microbiology*, 1462-2920.16394. DOI: 10.1111/1462-2920.16394.

Scott, J. W.; Jones, J. P. (1989): Monogenic resistance in tomato to *Fusarium oxysporum* f. sp. *lycopersici* race 3. In *Euphytica* 40 (1-2), pp. 49–53. DOI: 10.1007/BF00023296.

Seifbarghi, Shirin; Borhan, M. Hossein; Wei, Yangdou; Coutu, Cathy; Robinson, Stephen J.; Hegedus, Dwayne D. (2017): Changes in the *Sclerotinia sclerotiorum* transcriptome during infection of *Brassica napus*. In *BMC Genomics* 18 (1), p. 266. DOI: 10.1186/s12864-017-3642-5.

Serrano, Mario; Coluccia, Fania; Torres, Martha; Lâ€™Haridon, Floriane; MÃ©traux, Jean-Pierre (2014): The cuticle and plant defense to pathogens. In *Frontiers in Plant Science* 5. DOI: 10.3389/fpls.2014.00274.

Silva-Arias, Gustavo A.; Gagnon, Edeline; Hembrom, Surya; Fastner, Alexander; Khan, Muhammad Ramzan; Stam, Remco; Tellier, Aurélien (2025): Patterns of presence-absence variation of NLRs across populations of *Solanum chilense* are clade-dependent and mainly shaped by past demographic history. In *The New phytologist* 245 (4), pp. 1718–1732. DOI: 10.1111/nph.20293.

Soltis, Nicole E.; Atwell, Susanna; Shi, Gongjun; Fordyce, Rachel; Gwinner, Raoni; Gao, Dihan et al. (2019): Interactions of Tomato and *Botrytis cinerea* Genetic Diversity: Parsing the Contributions of Host Differentiation, Domestication, and Pathogen Variation. In *The Plant Cell* 31 (2), pp. 502–519. DOI: 10.1105/tpc.18.00857.

Soltis, Nicole E.; Caseys, Celine; Zhang, Wei; Corwin, Jason A.; Atwell, Susanna; Kliebenstein, Daniel J. (2020): Pathogen Genetic Control of Transcriptome Variation in the *Arabidopsis thaliana* - *Botrytis cinerea* Pathosystem. In *Genetics* 215 (1), pp. 253–266. DOI: 10.1534/genetics.120.303070.

Soyk, Sebastian; Lemmon, Zachary H.; Sedlazeck, Fritz J.; Jiménez-Gómez, José M.; Alonge, Michael; Hutton, Samuel F. et al. (2019): Duplication of a domestication locus neutralized a cryptic variant that caused a breeding barrier in tomato. In *Nature plants* 5 (5), pp. 471–479. DOI: 10.1038/s41477-019-0422-z.

St.Clair, Dina A. (2010): Quantitative Disease Resistance and Quantitative Resistance Loci in Breeding. In *Annual Review of Phytopathology* 48 (1), pp. 247–268. DOI: 10.1146/annurev-phyto-080508-081904.

Stam, Remco; Scheikl, Daniela; Tellier, Aurélien (2017): The wild tomato species *Solanum chilense* shows variation in pathogen resistance between geographically distinct populations. In *PeerJ* 5, e2910. DOI: 10.7717/peerj.2910.

Stern, David L.; Orgogozo, Virginie (2009): Is genetic evolution predictable? In *Science (New York, N.Y.)* 323 (5915), pp. 746–751. DOI: 10.1126/science.1158997.

Stukenbrock, Eva H.; McDonald, Bruce A. (2009): Population genetics of fungal and oomycete effectors involved in gene-for-gene interactions. In *Molecular Plant-Microbe Interactions*® 22 (4), pp. 371–380. DOI: 10.1094/MPMI-22-4-0371.

Sucher, Justine; Mbengue, Malick; Dresen, Axel; Barascud, Marielle; Didelon, Marie; Barbacci, Adelin; Raffaele, Sylvain (2020): Phylotranscriptomics of the *Pentapetalae* Reveals Frequent Regulatory Variation in Plant Local Responses to the Fungal Pathogen *Sclerotinia sclerotiorum*. In *The Plant Cell* 32 (6), pp. 1820–1844. DOI: 10.1105/tpc.19.00806.

Szymański, Jędrzej; Bocobza, Samuel; Panda, Sayantan; Sonawane, Prashant; Cárdenas, Pablo D.; Lashbrooke, Justin et al. (2020): Analysis of wild tomato introgression lines elucidates the genetic basis of transcriptome and metabolome variation underlying fruit traits and pathogen response. In *Nature Genetics* 52 (10), pp. 1111–1121. DOI: 10.1038/s41588-020-0690-6.

Tanksley, Steven D.; McCouch, Susan R. (1997): Seed Banks and Molecular Maps: Unlocking Genetic Potential from the Wild. In *Science* 277 (5329), pp. 1063–1066. DOI: 10.1126/science.277.5329.1063.

Tellier, A.; Fischer, I.; Merino, C.; Xia, H.; Camus-Kulandaivelu, L.; Städler, T.; Stephan, W. (2011): Fitness effects of derived deleterious mutations in four closely related wild tomato species with spatial structure. In *Heredity* 107 (3), pp. 189–199. DOI: 10.1038/hdy.2010.175.

- Thomas, C. M.; Dixon, M. S.; Parniske, M.; Golstein, C.; Jones, J. D. (1998): Genetic and molecular analysis of tomato Cf genes for resistance to *Cladosporium fulvum*. In *Philosophical transactions of the Royal Society of London. Series B, Biological sciences* 353 (1374), pp. 1413–1424. DOI: 10.1098/rstb.1998.0296.
- Thomas, C. M.; Jones, D. A.; Parniske, M.; Harrison, K.; Balint-Kurti, P. J.; Hatzixanthis, K.; Jones, J. D. (1997): Characterization of the tomato Cf-4 gene for resistance to *Cladosporium fulvum* identifies sequences that determine recognitional specificity in Cf-4 and Cf-9. In *The Plant Cell* 9 (12), pp. 2209–2224. DOI: 10.1105/tpc.9.12.2209.
- Thompson, Dawn; Regev, Aviv; Roy, Sushmita (2015): Comparative analysis of gene regulatory networks: from network reconstruction to evolution. In *Annual review of cell and developmental biology* 31, pp. 399–428. DOI: 10.1146/annurev-cellbio-100913-012908.
- Voordeckers, Karin; Pougach, Ksenia; Verstrepen, Kevin J. (2015): How do regulatory networks evolve and expand throughout evolution? In *Current opinion in biotechnology* 34, pp. 180–188. DOI: 10.1016/j.copbio.2015.02.001.
- Waggoner, Paul E.; Rich, Saul (1981): Lesion distribution, multiple infection, and the logistic increase of plant disease. In *Proceedings of the National Academy of Sciences* 78 (6), pp. 3292–3295. DOI: 10.1073/pnas.78.6.3292.
- Walz, A.; Zingen-Sell, I.; Loeffler, M.; Sauer, M. (2008): Expression of an oxalate oxidase gene in tomato and severity of disease caused by *Botrytis cinerea* and *Sclerotinia sclerotiorum*. In *Plant Pathology* 57 (3), pp. 453–458. DOI: 10.1111/j.1365-3059.2007.01815.x.
- Wang, Dafang; Yu, Chuanhe; Zuo, Tao; Zhang, Jianbo; Weber, David F.; Peterson, Thomas (2015): Alternative Transposition Generates New Chimeric Genes and Segmental Duplications at the Maize p1 Locus. In *Genetics* 201 (3), pp. 925–935. DOI: 10.1534/genetics.115.178210.
- Wang, Zheng; Ma, Lu-Yue; Cao, Jun; Li, Yu-Long; Ding, Li-Na; Zhu, Ke-Ming et al. (2019): Recent Advances in Mechanisms of Plant Defense to *Sclerotinia sclerotiorum*. In *Frontiers in Plant Science* 10, p. 1314. DOI: 10.3389/fpls.2019.01314.
- Wei, Kai; Sharifova, Saida; Zhao, Xiaoyun; Sinha, Neelima; Nakayama, Hokuto; Tellier, Aurélien; Silva-Arias, Gustavo A. (2024): Evolution of gene networks underlying adaptation to drought stress in the wild tomato *Solanum chilense*. In *Molecular Ecology*, Article e17536. DOI: 10.1111/mec.17536.
- Wilkins, Adam S. (2007): Between “design” and “bricolage”: genetic networks, levels of selection, and adaptive evolution. In *Proceedings of the National Academy of Sciences* 104 Suppl 1 (Suppl 1), pp. 8590–8596. DOI: 10.1073/pnas.0701044104.
- Williams, Brett; Kabbage, Mehdi; Kim, Hyo-Jin; Britt, Robert; Dickman, Martin B.; Tyler, Brett (2011): Tipping the Balance: *Sclerotinia sclerotiorum* Secreted Oxalic Acid Suppresses Host Defenses by Manipulating the Host Redox Environment. In *PLoS Pathogens* 7 (6), e1002107. DOI: 10.1371/journal.ppat.1002107.
- Winkelmüller, Thomas M.; Entila, Frederickson; Anver, Shajahan; Piasecka, Anna; Song, Baoxing; Dahms, Eik et al. (2021): Gene expression evolution in pattern-triggered immunity within *Arabidopsis thaliana* and across Brassicaceae species. In *The Plant Cell* 33 (6), pp. 1863–1887. DOI: 10.1093/plcell/koab073.
- Yang, Yixuan; Xu, Tanchumin; Conant, Gavin; Kishino, Hirohisa; Thorne, Jeffrey L.; Ji, Xiang (2023): Interlocus Gene Conversion, Natural Selection, and Paralog Homogenization. In *Molecular Biology and Evolution* 40 (9). DOI: 10.1093/molbev/msad198.
- Yeats, Trevor H.; Rose, Jocelyn K.C. (2013): The Formation and Function of Plant Cuticles. In *Plant Physiology* 163 (1), pp. 5–20. DOI: 10.1104/pp.113.222737.

Declarations of co-authorship

Anlage 3

C	A	U	Christian-Albrechts-Universität zu Kiel	Agrar- und Ernährungs- wissenschaftliche Fakultät
----------	----------	----------	---	--

Declaration of co-authorship

If a dissertation is based on co-authored articles, a declaration from each of the authors regarding the part of the work done by the doctoral candidate must be enclosed when submitting the dissertation.

1. Doctoral candidate

Name: Severin Einspanier




2. This co-author declaration applies to the following article:


High-Resolution Disease Phenotyping Reveals Distinct Resistance Mechanisms of Tomato Crop Wild Relatives against *Sclerotinia sclerotiorum*

The extent of the doctoral candidate's contribution to the article is assessed on the following scale:

- A. Has contributed to the work (0-33%)
- B. Has made a substantial contribution (34-66%)
- C. Did the majority of the work independently (67-100%)

3. Declaration on the individual phases of the scientific work (A,B,C)		Extent
Concept: Formulation of the basic scientific problem based on theoretical questions which require clarification, including a summary of the general questions which, it is assumed, will be answerable via analyses or concrete experiments/investigations		C
Planning: Planning of experiments/analyses and formulation of investigative methodology, including choice of method and independent methodological development, in such a way that the scientific questions asked can be expected to be answered		C
Execution: Involvement in the analysis or the concrete experiments/investigation		C
Manuscript preparation: Presentation, interpretation and discussion of the results obtained in article form		C

4. Signature of all co-authors		
Date	Name	Signature
17/02/2025	Sylvain Raffaele	
17/02/2025	Adelin Barbacci	
17/02/2025	Christopher Tominello-Ramirez	

5. Signature of doctoral candidate		
Date	Name	Signature
25.03.25	Severin Einspanier	

Anlage 3

C A U	Christian-Albrechts-Universität zu Kiel	Agrar- und Ernährungs- wissenschaftliche Fakultät
------------------	---	--

Declaration of co-authorship

If a dissertation is based on co-authored articles, a declaration from each of the authors regarding the part of the work done by the doctoral candidate must be enclosed when submitting the dissertation.

1. Doctoral candidate

Name: Severin Einspanier



2. This co-author declaration applies to the following article:


High-Resolution Disease Phenotyping Reveals Distinct Resistance Mechanisms of Tomato Crop Wild Relatives against *Sclerotinia sclerotiorum*

The extent of the doctoral candidate's contribution to the article is assessed on the following scale:

- A. Has contributed to the work (0-33%)
- B. Has made a substantial contribution (34-66%)
- C. Did the majority of the work independently (67-100%)

3. Declaration on the individual phases of the scientific work (A,B,C)	Extent
Concept: Formulation of the basic scientific problem based on theoretical questions which require clarification, including a summary of the general questions which, it is assumed, will be answerable via analyses or concrete experiments/investigations	C
Planning: Planning of experiments/analyses and formulation of investigative methodology, including choice of method and independent methodological development, in such a way that the scientific questions asked can be expected to be answered	C
Execution: Involvement in the analysis or the concrete experiments/investigation	C
Manuscript preparation: Presentation, interpretation and discussion of the results obtained in article form	C

4. Signature of all co-authors		
Date	Name	Signature
19.02.2025	Mario Hasler	
27.02.25	Remco Stam	

5. Signature of doctoral candidate		
Date	Name	Signature
25.03.25	Severin Einspanier	

Anlage 3

C A U	Christian-Albrechts-Universität zu Kiel	Agrar- und Ernährungs- wissenschaftliche Fakultät
------------------	---	--

Declaration of co-authorship

If a dissertation is based on co-authored articles, a declaration from each of the authors regarding the part of the work done by the doctoral candidate must be enclosed when submitting the dissertation.

1. Doctoral candidate

Name: Severin Einspanier

2. This co-author declaration applies to the following article:

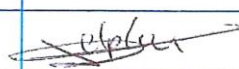
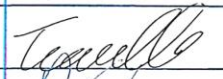

Co-optation of Transcription Factors Drives Evolution of Quantitative Disease Resistance Against a Necrotrophic Pathogen

The extent of the doctoral candidate's contribution to the article is assessed on the following scale:


- A. Has contributed to the work (0-33%)
- B. Has made a substantial contribution (34-66%)
- C. Did the majority of the work independently (67-100%)

3. Declaration on the individual phases of the scientific work (A,B,C)	Extent
Concept: Formulation of the basic scientific problem based on theoretical questions which require clarification, including a summary of the general questions which, it is assumed, will be answerable via analyses or concrete experiments/investigations	C
Planning: Planning of experiments/analyses and formulation of investigative methodology, including choice of method and independent methodological development, in such a way that the scientific questions asked can be expected to be answered	C
Execution: Involvement in the analysis or the concrete experiments/investigation	C
Manuscript preparation: Presentation, interpretation and discussion of the results obtained in article form	C

4. Signature of all co-authors

Date	Name	Signature
18/2/2025	Delplace Florent	
18/02/2025	Christopher Tominello-Ramirez	
27.2.25	Remco Stam	

5. Signature of doctoral candidate

Date	Name	Signature
25.03.25	Severin Einspanier	

Anlage 3

C A U	Christian-Albrechts-Universität zu Kiel	Agrar- und Ernährungs- wissenschaftliche Fakultät
------------------	---	--

Declaration of co-authorship

If a dissertation is based on co-authored articles, a declaration from each of the authors regarding the part of the work done by the doctoral candidate must be enclosed when submitting the dissertation.

1. Doctoral candidate

Name: Severin Einspanier

2. This co-author declaration applies to the following article:

Temporal Shifts in Gene Expression Drive Quantitative Resistance to *Sclerotinia sclerotiorum* in *Solanum pennellii*

The extent of the doctoral candidate's contribution to the article is assessed on the following scale:

- A. Has contributed to the work (0-33%)
- B. Has made a substantial contribution (34-66%)
- C. Did the majority of the work independently (67-100%)

3. Declaration on the individual phases of the scientific work (A,B,C)	Extent
Concept: Formulation of the basic scientific problem based on theoretical questions which require clarification, including a summary of the general questions which, it is assumed, will be answerable via analyses or concrete experiments/investigations	C
Planning: Planning of experiments/analyses and formulation of investigative methodology, including choice of method and independent methodological development, in such a way that the scientific questions asked can be expected to be answered	C
Execution: Involvement in the analysis or the concrete experiments/investigation	C
Manuscript preparation: Presentation, interpretation and discussion of the results obtained in article form	C

4. Signature of all co-authors

Date	Name	Signature
25.03.2025	Remco Stam	

5. Signature of doctoral candidate

Date	Name	Signature
25.3.25	Severin Einspanier	